UNIVERSITÀ DEGLI STUDI DI FIRENZE

Dipartimento di Scienze Biochimiche

DOTTORATO DI RICERCA IN BIOCHIMICA E BIOLOGIA APPLICATA (XXII CICLO)

-settore disciplinare BIO/10-

Tesi di dottorato

"THE MOLECULAR BASIS OF AMYLOID AGGREGATE CYTOTOXICITY
New S-acyl-glutathione derivatives prevent amyloid oxidative attack"

Il Coordinatore del Corso
Chiar.mo Prof. Gianni Cappugi

Il Docente Guida
Chiar.mo Prof. Gianfranco Liguri

Il Candidato
Dr.ssa Mariagioia Zampagni

DEDICATION

To my parents and Carlo…..

CONTENTS

SUMMARY

A wide range of human pathologies arises from the failure of a specific peptide or protein to adopt, or remain in, its native functional conformational state. These pathological conditions are generally referred to as protein misfolding diseases and range from neurodegenerative disorders to systemic amyloidoses. The largest group of misfolding diseases is associated with the conversion of specific peptides or proteins from their soluble functional states into insoluble highly organized fibrillar aggregates often called amyloid fibrils. It is increasingly evident that the oligomeric assemblies, kinetic intermediates in fibrillization process, are the primary pathogenic species in many protein deposition diseases. It has recently been found that prefibrillar aggregates from proteins not involved in amyloid diseases can impair cell viability when added to cultured cell media. It follows that the cross-β fold is not only the structural feature common to all amyloid aggregates, but is also the structural determinant of cytotoxicity of any amyloid aggregate. These data have led to propose that the prefibrillar assemblies share basic structural features that, at least in most cases, seem to underlie common biochemical mechanisms of cytotoxicity. The toxicity of these early oligomers appears to result from an intrinsic ability to impair fundamental cellular processes by interacting with cellular membranes and disassembling the lipid bilayer. The resulting impairment of membrane permeability would lead to an imbalance of the intracellular redox status and ion levels, together with other modifications such as mitochondria injury and lipid peroxidation. The N-terminal domain of the prokaryotic hydrogenase maturation factor (HypF-N) is a valuable model system for investigating the structural basis of the cellular impairment caused by misfolded protein oligomers. In fact, it can rapidly be converted into stable oligomers under conditions that promote its unfolding into partially folded species and can generate a cascade of events, resulting in cytoxicity and death, when added to cells.

Alzheimer's disease (AD) is the most common senile neurodegenerative disease characterized by progressive dementia, extracellular amyloid plaques and intracellular neurofibrillary tangles. The amyloid hypothesis postulates that Aβ peptide, the major component of senile plaques, may play a causative role in the development and progression of AD. Aβ peptides derived from the proteolytic cleavage of the amyloid

precursor protein (APP) carried out by β- and γ-secretase in the amyloidogenic pathway, and prefibrillar Aβ oligomers, rather than mature fibrils, have been indicated as the main responsible of cytotoxicity and synapse failure.

Among the mechanisms involved in Aβ-mediated neurotoxicity, oxidative stress has largely been implicated as a major cause of neurotoxicity in AD and it has been established a strong link between lipid peroxidation and amyloid plaques within the AD brain. Moreover, there is a rising consensus on major role of membranes as initial triggers of the biochemical modifications culminating with neuronal death. In fact, Aβ oligomers can readily insert into plasma membrane and compromise its integrity, resulting in a prompt impairment of fundamental cellular processes by causing oxidative stress and increasing free Ca^{2+} that eventually lead to apoptotic or necrotic cell death.

Considerable attention has been focused on the possible association between cholesterol metabolism in the central nervous system (CNS) and AD pathogenesis. Clinical evidence suggests that reducing circulating and brain cholesterol protects against AD by reducing Aβ production and secretion, however a growing body of evidence implicates low membrane cholesterol in the pathogenesis of AD. The content of membrane cholesterol can modulate Aβ production, aggregation and clearance in various ways, particularly by affecting the stability of lipid rafts, or detergent resistant membrane domains (DRMs), which are discrete cholesterol-rich microdomains of the cell membrane involved in a wide range of biological processes, such as cellular trafficking and signalling events.

Recently, lipid rafts have been proposed to function as platforms where neurotoxic oligomers of proteins, including the Aβ peptides are assembled. Remarkably, increasing evidence supports the idea that the initial events of Aβ oligomerization and cytotoxicity in AD involve the interaction of amyloid Aβ-derived diffusible ligands (ADDLs) with the cell membrane. Increasing evidence now shows that Aβ can tightly associate with GM1 ganglioside (a component of lipid rafts), and it was originally postulated that this may act as a seed for its accumulation and aggregation. These findings, together with the presence, in the raft domains, of ligand-gated calcium channels (the AMPA and NMDA glutamate receptors) involved in Ca^{2+} influx into neuronal synaptic ends and in Ca^{2+} permeabilization of amyloid-exposed cells has implicated lipid rafts as likely primary interaction sites for ADDLs.

CNS is physiological protected from oxidative damage by antioxidant molecules. Glutathione (GSH) is one of the most abundant intracellular non-protein thiols in the CNS, where it plays a major antioxidant role within both neurons and non-neuronal cells. Some brain regions of AD patients show a decrease in free radical defences or an increase in free radical formation, or both. Aβ can fragmentate and generate free radical peptides with potent lipoperoxidizing effects on the synaptosomal membranes in the neocortex. Indeed, cells experiencing amyloid toxicity usually exhibit impaired viability, oxidative stress, and mitochondrial dysfunction. Reactive oxygen species (ROS) and peroxynitrite accumulation result in chemical modification of cell components including lipids, proteins, and nucleic acids. It has therefore been proposed that lipid peroxidation and the weakening of cell antioxidant defenses may contribute to AD pathogenesis. In particular, GSH metabolism is altered and its levels are decreased in affected brain regions and peripheral cells from AD patients and in experimental models of AD. The alteration of GSH homeostasis impairs neuronal viability, leaving neurons vulnerable to oxidative stress injury. In the past decade, interest in the protective effects of various antioxidants aimed at increasing intracellular GSH content has been growing. Finally, much experimental evidence suggests a possible protective role of unsaturated fatty acids in age-related diseases. Indeed, it has been found a reduction in the risk of cognitive impairment in population-based samples with a high intake of monounsaturated fatty acids (MUFA) and polyunsaturated fatty acids (PUFA).

Taking into account these observations, the aim of the present study is to get clues into the molecular basis of amyloid cytotoxicity with particular interest in the interaction of different types of oligomers, related or not with diseases, with cell membrane (or its subfractions, as lipid rafts) and the resulting cascade of events, culminating in cellular dysfunction and death. We also focused our attention to the role of membrane cholesterol as a possible modulator of the interaction between amyloid aggregates and the plasma membrane of exposed cells. Finally, considering the importance of developing new antioxidant compounds and the relevance of their application in the treatment of neurodegenerative diseases, we aimed to synthesize new S-acylglutathione (acyl-SG) derivatives, and to test their protective effect on cells experiencing amyloid aggregate oxidative insult.

The present studies provide evidence that:

I) Two types of oligomers formed by the HypF-N protein, both possessing a hydrophobic core, showed a different degree of flexibility of the exposed hydrophobic surfaces, which is essential to determine the different ability of aggregates to exert a toxic function. In particular, only the oligomers exposing hydrophobic surface, and endowed with sufficient structural plasticity, are able to penetrate the plasma membrane of human SH-SY5Y neuroblastoma cells and to increase cytosolic Ca^{2+} levels, intracellular ROS production and lipid peroxidation, resulting in the activation of the apoptotic pathway. In contrast, cellular stress markers and viability were unaffected in culture and neuronal cells exposed to HypF-N oligomers with a higher degree of packing and lower structural flexibility. Our results support the rising consensus on the role of plasma membranes as primary targets of toxic protein oligomers, suggesting that the ability to form amyloid-like structures is generic to polypeptide chains, whether or not such species are pathogenic will depend on their structural features, notably the extent to which hydrophobic residues are flexible and exposed on their surfaces within the environment of a living organism.

II) Cell resistance to amyloid toxicity is strictly related to plasma membrane cholesterol content in SH-SY5Y cells and in Familial Alzheimer's Disease (FAD) fibroblasts. In particular, in our model cells, membrane cholesterol modulation was achieved by supplementing the cell culture media with water soluble cholesterol (PEG-chol or Chol) to increase the levels of membrane cholesterol; on the other hand, cholesterol levels were diminished by using methyl-β-cyclodextrin (β-CD) or mevastatin. Under these conditions, membrane cholesterol enrichment readily prevent the interaction of Aβ42 oligomers with the cell membrane, thus reducing cell damage and oxidative stress. Therefore, membrane cholesterol enrichment significantly decreases intracellular ROS production and membrane lipoperoxidation with respect to cholesterol-depleted cells. Finally, the higher resistance to amyloid-induced oxidative stress in cholesterol-enriched cells matched an improved cell viability. These results identify membrane cholesterol as being key to Aβ42 oligomer accumulation at the cell surfaces and to the following Aβ42-induced cell dysfunction and death in AD neurons.

III) Lipid rafts/DRMs are chronic targets of Aβ-induced lipid peroxidation in SH-SY5Y human neuroblastoma cells overexpressing amyloid precursor protein APPwt and

APPV717G genes and in fibroblasts bearing the APPV717I gene mutation. Therefore, Aβ-oxidized rafts recruit more ADDLs than corresponding domains in control cells, triggering a further increase in raft lipid peroxidation and loss of membrane integrity. Moreover, amyloid pick up at the oxidative-damaged domains was prevented by enhanced cholesterol levels, anti-ganglioside (GM1) antibodies and the B subunit of cholera toxin binding to GM1. The increase of the structural rigidity of the DRMs, isolated from cells and exposed to ADDLs, indicates a specific perturbation of raft physicochemical features in cells facing increased amyloid assembly at the membrane surface. This data identifies lipid rafts as specific targets of oxidative damage and membrane degeneration in APP-mutated neurons as a result of their ability to recruit aggregates to the cell surface.

IV) The new synthesized acyl-SG derivatives can easily cross the plasma membrane and be internalized in cellular compartments; due to their lipophilic nature, acyl-SGs act as GSH carriers, allowing GSH to enter the cell and, once internalized in the cytoplasm, to be converted back to the corresponding free fatty acid and GSH by cellular thioesterases. Moreover, acyl-SG thioesters prevent Aβ42-induced oxidative stress by a significant decrease in intracellular ROS production, a large inhibition of membrane lipoperoxidation and apoptotic pathway activation in SH-SY5Y cells, and prevent amyloid oxidative injury in primary fibroblasts from FAD patients. Moreover, an increase in antioxidant and neuroprotective effects with the presence of the double bond and the lengthening of the chain in these compounds occurred. Therefore, our results put forward acyl-SG derivatives as new antioxidants with neuroprotective effects against Aβ-induced oxidative injury, which could be useful in the treatment of AD and other oxidative stress-related disorders.

CHAPTER I – INTRODUCTION

-PROTEIN FOLDING, MISFOLDING AND AMYLOID AGGREGATION-

Protein folding

Proteins are involved in virtually every biological process in a living system. They are synthesized on ribosomes as linear chains of typically several hundred aminoacid residues in a specific order from information encoded within the cellular DNA. One of the most remarkable characteristics of a living system is the ability of its molecular components to self-assemble into their functional states. The most fundamental example of biological self-assembly is protein folding, the process through which disordered polypeptide chains convert into the tightly packed protein structures through which they exert their biological functions [1]. In addition to generating biological activity, however, the folding is coupled to many other biological processes, including the trafficking of molecules to specific cellular locations and the regulation of cellular growth and differentiation [2]. Most of the newly synthesized polypeptide chains usually fold into their functional and compact "native states". Native states of proteins generally correspond to the structures that are most thermodynamically stable under physiological conditions and are characterized by a well-defined, persistent secondary and tertiary structure [3]. Nevertheless, the total number of possible conformations of a polypeptide chain is so large that it would take an astronomical length of time to find this particular structure by means of a systematic search of all conformational space [2]. The folding process of proteins can be reproduced *in vitro*, and has been extensively investigated with a variety of experimental and computational methods [4, 5]. It is now clear that this process consists in a stochastic search of the conformations accessible to a given polypeptide, targeted at finding the most energetically favourable conformation [3, 6]. Inherent fluctuations in the conformation of unfolded or incompletely folded states enable different portions of the amino acid sequence to come into contact with one other. Because the correct (native-like) interactions between different residues are on average more stable than the incorrect (nonnative) ones, such a search mechanism is in principle able to find the lowest energy structure [7]. In fact, when the fluctuations trigger the formation of stable native-like interactions a folding nucleus forms, reducing

the number of conformations that need to be sampled by a protein molecule during its transition from a random coil state to the native structure [3, 8-10]. This stochastic description of protein folding involves the concept of an "energy landscape" for each protein, describing the free energy of the polypeptide chain as a function of its conformational properties. To enable a protein to fold efficiently, the landscape required has been likened to a funnel because the conformational space accessible to the polypeptide chain is reduced as the native state is approached [7]. The shape of the energy landscape is encoded by the amino acid sequence, thus natural selection has enabled proteins to fold rapidly and efficiently. Small single domain proteins (e.g. < 100 amino acids in length), in general, fold to the native state on a sub-second timescale and have been the focus of many experimental and theoretical studies of folding [11]. For small proteins, typically of 60-100 residues, this landscape appears to be rather "smooth" as these proteins have been found to convert rapidly into their native states, without populating partially folded intermediates [2]. The highly cooperative folding observed for naturally occurring small proteins has been proved to be the product of natural selection [12]. On the other hand, larger polypeptide sequences have "rougher" energy landscapes, allowing the population of partially folded species that may be on- or off-pathway to the native fold [13]. In figure 1 is shown the energy landscape for the folding of a highly simplified model of a small protein. The critical region on a simple surface such as this one is the saddle point corresponding to the transition state, the barrier that all molecules must cross if they are to fold to the native state. In figure 1, applied to this schematic surface, are ensembles of structures corresponding to different steps of the folding process. The transition state ensemble was calculated by using computer simulations controlled by experimental data from mutational studies of acylphosphatase [14]. The results of many studies suggest that the fundamental mechanism of protein folding involves the interaction of a relatively small number of residues, 'key residues', to form a folding nucleus, about which the rest of the structure rapidly condenses [10]. In this scheme, the yellow spheres represent the three 'key residues' in the structure: when these residues have formed their native-like contacts the general topology of the native fold is established. At the top are indicated some contributors to the distribution of unfolded species that represent the starting point for folding, while the structure of the native state is shown at the bottom of the surface.

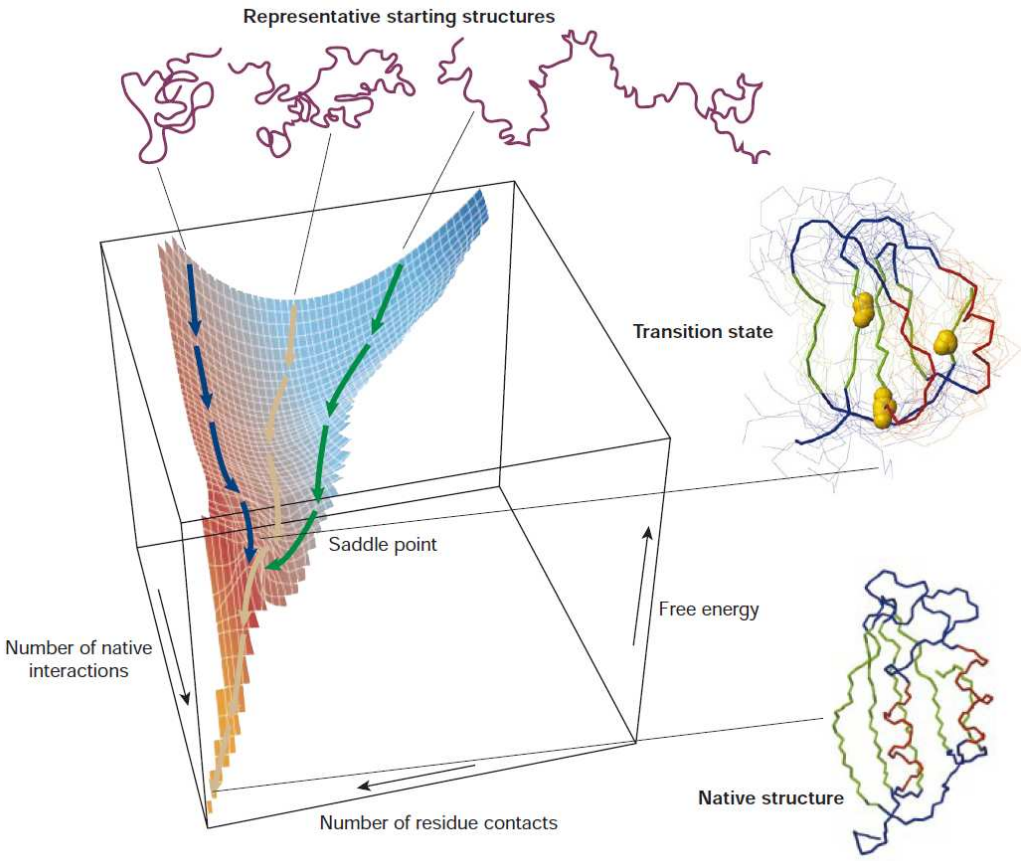

Figure 1. A schematic energy landscape for protein folding. The surface is derived from a computer simulation of the folding of a highly simplified model of a small protein. The surface 'funnels' the multitude of denatured conformations to the unique native structure. From [2].

Theoretical studies, particularly involving simulation techniques, have been used to complement experimental data, and *vice versa*, allowing a complete view of folding from the earliest steps to conformational transitions as the native structure ultimately forms [15]. One approach incorporates experimental measurements directly into the simulations as restraints limiting the regions of conformational space that are explored in each simulation; this strategy has enabled rather detailed structures to be generated for transition states [14]. The results suggest that, despite a high degree of disorder, these structures have the same general topology as the native fold. In essence, interactions involving the key residues force the chain to adopt a rudimentary native-like architecture. Once the correct topology has been achieved, the native structure will then almost invariably be generated during the final stages of folding [14]. Conversely,

if these key interactions are not formed, the protein cannot fold to a stable globular structure; this mechanism therefore acts also as a 'quality control' process by which misfolding can generally be avoided. Although it is not yet clear exactly how the sequence encodes such characteristics, the essential elements of the fold are likely to be determined primarily by the pattern of hydrophobic and polar residues that favours preferential interactions of specific residues as the structure becomes increasingly compact [16]. Another important parameter is "the contact order" which describes the average separation in the sequence between residues that are in contact with each other in the native structure. The existence of such a correlation can be rationalized by the argument that a stochastic search process will be more time consuming if the residues that form the nucleus are further away from each other in the sequence. [17]. Experiments show that the *in vitro* folding of proteins with more than about 100 residues involves a larger number of species than the fully unfolded and the fully folded states found to be populated in the simplest systems [18]. Experiments have shown that the folding intermediates that result from larger proteins, sometimes correspond to species in which segments of the protein have become highly native-like, whilst others have yet to achieve a folded state [3]. In particular, they suggest that these proteins generally fold in modules, in other words, folding can take place largely independently in different segments or domains of the protein [9]. The fully native structure is only acquired when all the native-like interactions have been formed both within and between the domains; this happens in a final cooperative folding step when all the side chains become locked in their unique close-packed arrangement and water is excluded from the protein core [19]. This modular mechanism is attractive because it suggests that highly complex structures might be assembled in manageable pieces. Folding *in vivo* is more complex and can occur before the completion of protein synthesis, particularly for multidomain proteins where individual domains fold separately after the end of their synthesis. Folding can occur in the cytoplasm after release from the ribosome, or in specific compartments, such as mitochondria or the endoplasmic reticulum (ER) [20-22]. The details of the folding mechanism of a given sequence *in vivo* depend on the peculiar environment in which this process takes place. However, the fundamental principles of protein folding are thought to be the same *in vivo* and *in vitro*. The key difference is that living cells have evolved mechanism of control and

regulation of the process [2]. Examples are molecular chaperones [21, 22], folding catalysts [23] and the quality-control and protein degradation mechanisms present in eukaryotic cells for proteins taking the secretory pathway [24].

Protein misfolding in the cell

Within the past two decades it has been recognized that the inability of a protein to adopt, or remain in, its native conformation is often referred to as protein misfolding. Indeed, in the misfolding process a protein adopts an alternative conformation, either a partially or totally unfolded monomeric state or an aggregated state. Protein misfolding is a common and intrinsic propensity of proteins that occurs continuously. Misfolding is influenced by the amino acid composition, and certain mutations are known to accelerate the process. Moreover, it also depends on environmental conditions, because once proteins are exposed to specific environmental changes such as increased temperature, high or low pH, agitation, elevated glucose, or oxidative agents, they can lose their native conformation more rapidly. Because of the lack of arrangement, unfolded proteins are nonfunctional. Importantly, the unfolded state is thermodynamically unfavorable and unstable, thus, seeking lower energy levels and more stability, unfolded proteins have a tendency to aggregate [25]. Protein misfolding often results in the formation of aggregates because misfolded proteins are more prone than native proteins to undergo aberrant self-association. The native state of a protein has indeed minimal propensity to aggregate, because most of its hydrophobic moieties and a large portion of the backbone amide and carboxylic groups are sequestered inside the protein; while the regions on the protein surface that may potentially retain a residual ability to trigger undesired intermolecular association are protected by structural adaptations developed during evolution [26]. By contrast, partially or fully unfolded states expose to the solvent some regions of the protein that might have a high propensity to form interchain interactions with other molecules. It is in fact well known that the first event that generally triggers the aggregation process of a globular protein is the adoption of a non-native, partially or fully unfolded state [27, 28]. Living cells have developed different strategies to avoid the occurrence of aberrant aggregation. Of particular importance are the many molecular chaperones that are present in all types of cells and cellular compartments. [29]. Despite their similar general role in enabling

efficient folding and assembly, their specific functions can differ substantially and it is evident that many types of chaperone work in tandem with one other [22]. Some molecular chaperones have been found to interact with nascent chains as they emerge from the ribosome, and bind rather non-specifically to protect aggregation-prone regions rich in hydrophobic residues. Others are involved in guiding later stages of the folding process, particularly for complex proteins including oligomeric species and multimolecular assemblies. The best characterized of the chaperones studied in this manner is the bacterial complex involving GroEL, a member of the family of 'chaperonins', and its 'co-chaperone' GroES. [21, 22]. Of particular interest is that GroEL, and other members of this class of molecular chaperone, contains a cavity in which incompletely folded polypeptide chains can enter and undergo the final steps in the formation of their native structures while sequestered and protected from the outside world [30]. Molecular chaperones increase the efficiency of the folding process by reducing the probability of competing reactions, particularly aggregation. However, there are several classes of folding catalyst that accelerate potentially slow steps in the folding process. [23]. Clear evidence that molecular chaperones are needed to prevent misfolding and its consequences comes from the fact that the concentrations of many of these species are substantially increased during cellular stress. Indeed, many chaperones were found in such situations, and their nomenclature as Hsps (heat shock proteins) reflects this fact [31]. Some molecular chaperones are able to rescue misfolded and even aggregated proteins, enable them to fold correctly, for example solubilising some forms of aggregates [32]. Such active intervention in the folding process requires energy, and ATP is required for most of the molecular chaperones to function with full efficiency [22]. In eukaryotic systems, many of the proteins that are synthesized are translocated into the ER, where folding takes place before secretion through the Golgi apparatus. The ER contains a wide range of molecular chaperones, folding catalysts and the proteins that fold here must satisfy a 'quality-control' check before being exported (Fig. 2) [24].

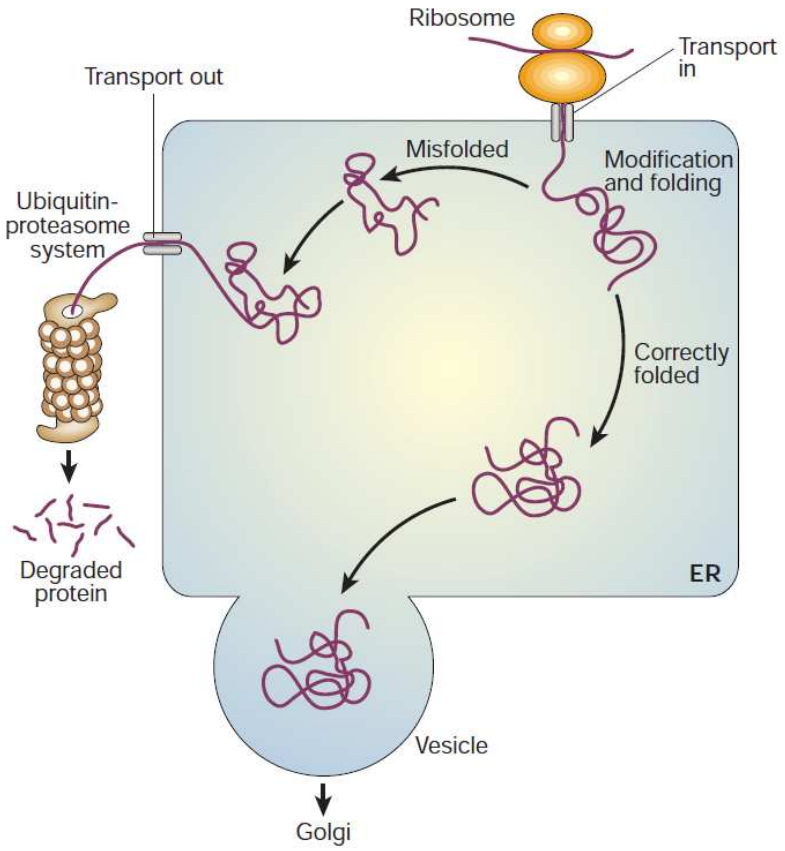

Figure 2. Regulation of protein folding in the ER. Many newly synthesized proteins are translocated into the ER, where they fold into their three-dimensional structures with the help of a series of molecular chaperones and folding catalysts. Correctly folded proteins are then transported to the Golgi complex and then delivered to the extracellular environment. Incorrectly folded proteins are detected by a quality-control mechanism and sent along another pathway in which they are ubiquitinated and then degraded in the cytoplasm by proteasomes. From [2].

This quality-control mechanism involves a complex series of glycosylation and deglycosylation reactions that prevents misfolded proteins from being secreted from the cell. In addition, unfolded and misfolded proteins are recognized and targeted for degradation through the ubiquitin–proteasome pathway [24]. Folding and unfolding are the ultimate ways of generating and abolishing cellular activities. It is not surprising therefore that failure to fold correctly, or to remain correctly folded, will give rise to the malfunctioning of living systems and hence to disease [30, 33, 34]. The details of how these incredible regulatory systems operate represent astonishing examples of the rigorous mechanisms that biology has established to ensure that misfolding, and its consequences, are minimized. Some diseases, such as cystic fibrosis [33] and some

types of cancer [31] is associated with aberrations in the folding process [33]. In other cases, proteins with a high propensity to misfold escape all the protective mechanisms and form intractable aggregates within cells or (more commonly) in extracellular space. An increasing number of pathologies, including Alzheimer's and Parkinson's diseases, the spongiform encephalopathies and type II diabetes, are directly associated with the deposition of such aggregates in tissues, including the brain, heart and spleen [27, 30, 34]. Diseases of this type are among the most debilitating, socially disruptive and costly diseases in the modern world, and they are becoming increasingly prevalent as our societies age and become more dependent on new agricultural, dietary and medical practices [35].

Amyloid aggregation and diseases

Protein misfolding can be at the basis of some of the most important disorders that affect humans including cancer, metabolic pathologies and degenerative diseases [36]. Indeed, protein misfolding and aggregation are often coupled, with over 40 human diseases associated with formation of fibrillar aggregates [37]. Subsequent to protein unfolding, aggregation, starts with the nucleation, when proteins reversibly attach to a growing core. Then, further protein molecules attach irreversibly to the core, developing a large aggregate. Protein aggregation can result in various different structural appearances with intermediates (oligomers) varying from unordered amorphous aggregates to highly ordered fibrils that are called amyloid (Fig. 3) [25]. They are generally enriched in cross-β structure [38], yet fluctuate in sequence, time, and conditions [39].

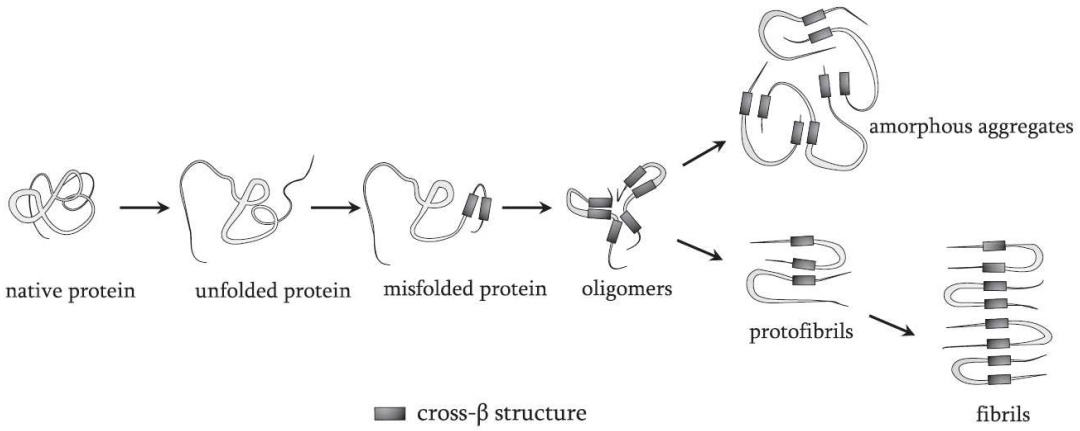

Figure 3. Protein misfolding and aggregation. Under certain circumstances such as pH or temperature change, mechanical stress, glycation, or oxidation, proteins undergo conformational changes that result in unfolding and partial misfolding that is associated with the tendency to aggregate. During aggregation, proteins can obtain a range of different structural appearances, which are generally enriched in cross-β structure, including intermediates varying from unordered amorphous aggregates to ordered fibrils that are called amyloid. From [25].

Considerable attention is presently focused on a group of protein misfolding diseases known as amyloidoses. These disease are characterized by the deposition in organs and tissues of specific peptides or proteins, incorrectly folded or unfolded, which aggregate intra- or extracellularly into polymeric assemblies (amyloid fibrils) rich in β-sheet [7, 40]. The deposits in strictly defined amyloidoses are extracellular and can often be observed as thread-like fibrillar structures, sometimes assembled further into larger aggregates or plaques. Some of these diseases are sporadic, familial or transmissible degenerative pathologies affecting either the central nervous system (Alzheimer's and Creutzfeldt-Jakob diseases,) or a variety of peripheral tissues and organs (systemic amyloidoses and type II diabetes) [40]. In addition, there are others diseases (Parkinson's and Hungtington's diseases) characterized by the presence of intracellular, rather then extracellular, deposits localized in the cytoplasm, in the form of specialized aggregates known as Lewy bodies, or in the nucleus (Table 1). These structures are generally described as "amyloid fibrils" or "amyloid plaques" when they accumulate extracellularly, whereas the term "intracellular inclusions" is used when fibrils with the same morphological and structural properties form inside the cell [41].

Table 1: peptides and proteins associated with known amyloid diseases

Disease	Main aggregate component
Alzheimer's disease	Aβ peptides (plaques); tau protein (tangles)
Spongiform encephalopathies	Prion (whole or fragments)
Parkinson's disease	α-synuclein (wt or mutant)
Primary systemic amyloidosis	Ig light chains (whole or fragments)
Secondary systemic amyloidosis	Serum amyloid A (whole or 76-residue fragment)
Fronto-temporal dementias	Tau (wt or mutant)
Senile systemic amyloidosis	Transthyretin (whole or fragments)
Familial amyloid polyneuropathy I	Transthyretin (over 45 mutants)
Hereditary cerebral amyloid angiopathy	Cystatin C (minus a 10-residue fragment)
Haemodialysis-related amyloidosis	β_2-microglobulin
Familial amyloid polyneuropathy III	Apolipoprotein AI (fragments)
Finnish hereditary systemic amyloidosis	Gelsolin (71 amino acid fragment)
Type II diabetes	Amylin (fragment)
Medullary carcinoma of the thyroid	Calcitonin (fragment)
Atrial amyloidosis	Atrial natriuretic factor
Hereditary non-neuropathic systemic amyloidosis	Lysozyme (whole or fragments)
Injection-localised amyloidosis	Insulin
Hereditary renal amyloidosis	Fibrinogen α-A chain, transthyretin, apolipoprotein AI, apolipoprotein AII, lysozyme, gelsolin, cystatin C
Amyotrophic lateral sclerosis	Superoxide dismutase 1 (wt or mutant)
Huntington's disease	Huntingtin
Spinal and bulbar muscular atrophy	Androgen receptor [whole or poly(Q) fragments]
Spinocerebellar ataxias	Ataxins [whole or poly(Q) fragments]
Spinocerebellar ataxia 17	TATA box-binding protein [whole or poly(Q) fragments]

From [40].

Each amyloid disease involves the aggregation of a specific protein although a range of other components, including other proteins and carbohydrates, is also incorporated into the deposits when they form *in vivo*. The characteristics of the soluble forms of the proteins involved in the well-defined amyloidoses are varied - they range from intact globular proteins to largely unstructured peptide molecules - but the aggregated forms have many common characteristics [42]. The various peptides and proteins associated with amyloid diseases have no obvious similarities in size, amino acid composition, sequence or structure. Nevertheless, the amyloid fibrils into which they convert are very similar in their external morphology (Fig. 4) and in their internal structure (Fig. 5) [40]. The fibrils can be imaged *in vitro* using transmission electron microscopy (TEM) or atomic force microscopy (AFM). These experiments reveal that amyloid fibrils usually consist of a number (typically 2–6) of protofilaments, each about 2–5 nm in diameter that are often twisted around each other to form supercoiled rope-like structures that are typically 7–13 nm wide [42, 43] or associate laterally to form long ribbons that are 2–5 nm thick and up to 30 nm wide [44, 45]. Circular dichroism, Fourier transform infra-red spectroscopy and X-ray fibre diffraction data have shown that in each individual protofilament the protein or peptide molecules are arranged so that the polypeptide chain forms β-strands that run perpendicular to the long axis of the fibril to generate what is described as a cross-β structure [42]. The latter confers to the amyloid fibrils specific biophysical characteristics and a variety of tinctorial properties, notably

staining with thioflavin T (ThT) and Congo red (CR) [46, 47]. The cross-β structure can be therefore considered as the main structural hallmark of the amyloid aggregates.

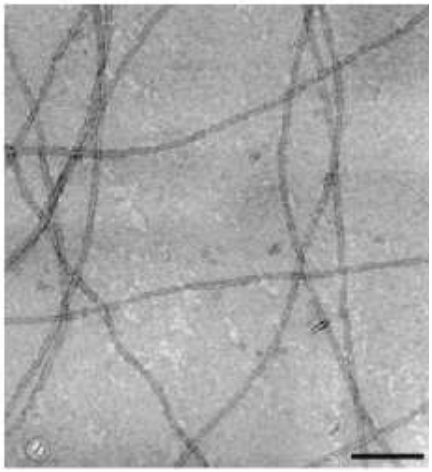

Figure 4. Transmission electron microscopy of a mesh of amyloid fibrils assembled from human lysozyme negatively stained with uranyl acetate. Scale bar, 400 nm. From [48].

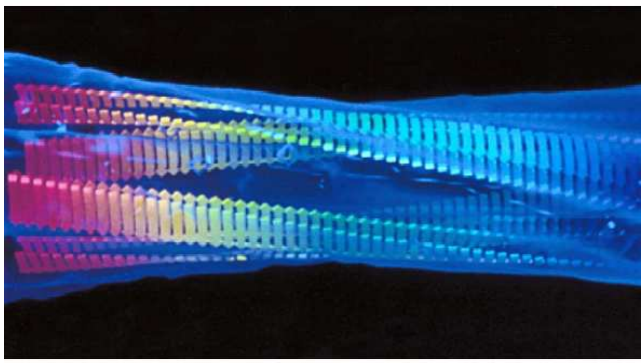

Figure 5. Schematic drawing of the structural organization of insulin fibrils. From [49].

The ability of polypeptide chains to form amyloid structures is not restricted to the relatively small number of proteins associated with recognized clinical disorders, but it now seems to be a generic feature of polypeptide chains [28, 34]. The core structure of the fibrils seems to be stabilized primarily by interactions, particularly hydrogen bonds, involving the polypeptide main chain. Because the main chain is common to all polypeptides, this observation explains why fibrils formed from polypeptides of very different sequence seem to be so similar [28, 42]. The generic amyloid structure contrasts strongly with the highly unique globular structures of most natural proteins. In these latter structures the interactions associated with the very specific packing of the side chains seem to ignore the main-chain preferences [28, 50]. Even though the ability to form amyloid fibrils seems to be generic, the propensity to do so, under given circumstances, can vary markedly between different sequences. The relative aggregation rates for a wide range of peptides and proteins correlates with the physicochemical features of the molecules such as charge, secondary-structure propensities and hydrophobicity [51]. In a globular protein the polypeptide main chain

and the hydrophobic side chains are largely hidden within the folded structure. Only when they are exposed, for example when the protein is partly unfolded (for example, at low pH) or fragmented (for example, by proteolysis), will conversion into amyloid fibrils be possible.

A general mechanism of amyloid formation: common characteristic of polypeptide chains

The observation that proteins associated with amyloid diseases, thought displaying in their soluble native state a very different nature, are able to generate similar fibrillar forms, encouraged the proposal that there are strong similarities in the intrinsic structure of the amyloid fibrils and in the mechanism by which they are formed [34]. Amyloid fibril formation follows a "nucleated growth" mechanism similar to that observed in protein crystallization [52]. The aggregation pathways of different systems have been extensively investigated. At the beginning of the aggregation process small soluble oligomers can be found to be in rapid equilibrium with the monomer. This is the case for example of Aβ peptides, widely studied for its links with Alzheimer's disease, whose small oligomers have been trapped by protein cross-linking and have been found to be relatively disordered and composed by 2-4 and 5-6 molecules for Aβ40 and Aβ42, respectively [53]. In particular, during the pathway of fibril formation, Aβ exists as soluble oligomers in rapid equilibrium with the corresponding monomeric forms. These species, also termed as Aβ-derived diffusible ligands (ADDLs) [54], precede the formation of the so called "protofibrils", a series of metastable, nonfibrillar species that can be visualized using AFM and TEM [55]. Insights into the structure of Aβ protofibrils are emerging; the exciting finding that a specific antibody can bind to protofibrillar species from different protein sources, but not their corresponding monomeric or fibrillar states, suggests that such soluble amyloid oligomers have some important common structural elements [56]. Some of these aggregates appear to be spherical beads of 2-5 nm in diameter, others appear to be beaded chains with the individual beads again having a diameter of 2-5 nm and seeming to assemble in linear and curly chains. Yet, others appear as annular structures, apparently formed by the circularization of the beaded chains. At longer aggregation times, curvilinear fibers form with a beaded appearance and an extensive β-sheet structure [37]. Analogous

spherical and chain-like protofibrillar structures have been observed for many other systems, including α-synuclein [57], amylin [58], the immunoglobulin light chain [59], transthyretin [60] and polyQ-containing proteins [58]. Similar aggregated structures can also be formed by proteins unrelated to disease, such as the N-terminal domain of HypF from *Escherichia coli* (HypF-N) [61, 62], the *Sulfolobus solfataricus* acylphosphatase [63] and an SH3 domain from bovine phosphatidyl-inositol-3'-kinase (PI3-SH3) [64]. Actually, for the first time in 1998, two independent groups reported the observation that a protein unrelated to any amyloid disease aggregated *in vitro* into structures indistinguishable from the amyloid fibrils produced by disease-associated peptides and proteins. Indeed, it was reported that two proteins, particularly the PI3-SH3 and fibronectin type III, aggregated *in vitro* to form structures indistinguishable from those formed *in vivo* by the proteins associated with the known amyloid diseases [65]. It was presently shown that a similar conversion could be achieved deliberately for other proteins by a rational choice of appropriate solution conditions [66, 67]. These proteins have different secondary and tertiary structure contents, different functions and belong to different organisms. In most cases, aggregation of full-length proteins was found to require solution conditions that destabilize the native structure but do not inhibit the formation of hydrogen bonds, such as low pH, lack of specific ligands, high temperature, high pressure and moderate concentrations of salts or co-solvents such as trifluoroethanol (Fig. 6). By contrast, many peptides that were unable to fold into stable globular structures readily formed fibrils [68]. The reduced physicochemical stability of the partially unfolded monomers leads them to organize into the oligomeric assemblies seen in the path of fibrillization and eventually into stable mature fibrils.

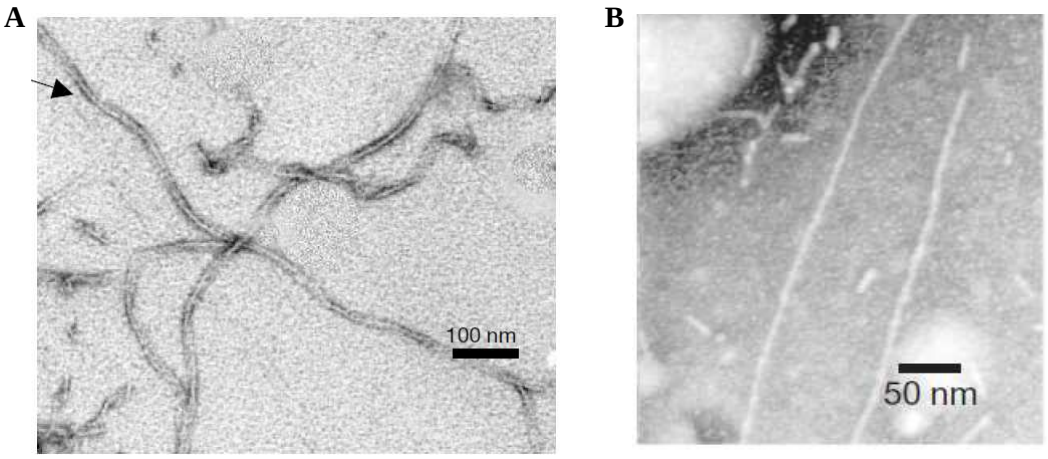

Figure 6. Electron micrographs of amyloid fibrils from **A,** PI3-SH3 and **B,** the N-terminal domain of the bacterial hydrogenase maturation factor HypF (HypF-N), a protein unrelated to any amyloid disease. The formation of these fibrillar aggregates was obtained by incubating 10 mg/ml PI3-SH3 in H_2O/HCl mixture, pH 2.0 at 37 °C for 1 month and 0.3 mg/ml HypF-N in 50mM acetate buffer, pH 5.5, in the presence of 30% (v/v) TFE at room temperature for 20 days, respectively. From [69].

The demonstration that peptides and proteins that are unrelated to disease have a generic ability to form amyloid fibrils has incited a more general discussion of the various states that can be adopted by polypeptides following their synthesis *in vivo*. It is now clear that the native state of a polypeptide chain is in dynamic equilibrium with other states including aggregates and their precursors (Fig. 7) [2, 37, 40]. Moreover, the proposal that amyloid fibrils are a generic structure of polypeptide chains allowed the researchers to suggest that the conformational properties of all proteins should be considered in terms of the multiple conformational states that are accessible and into wich they interconvert on a wide range of timescales [37].

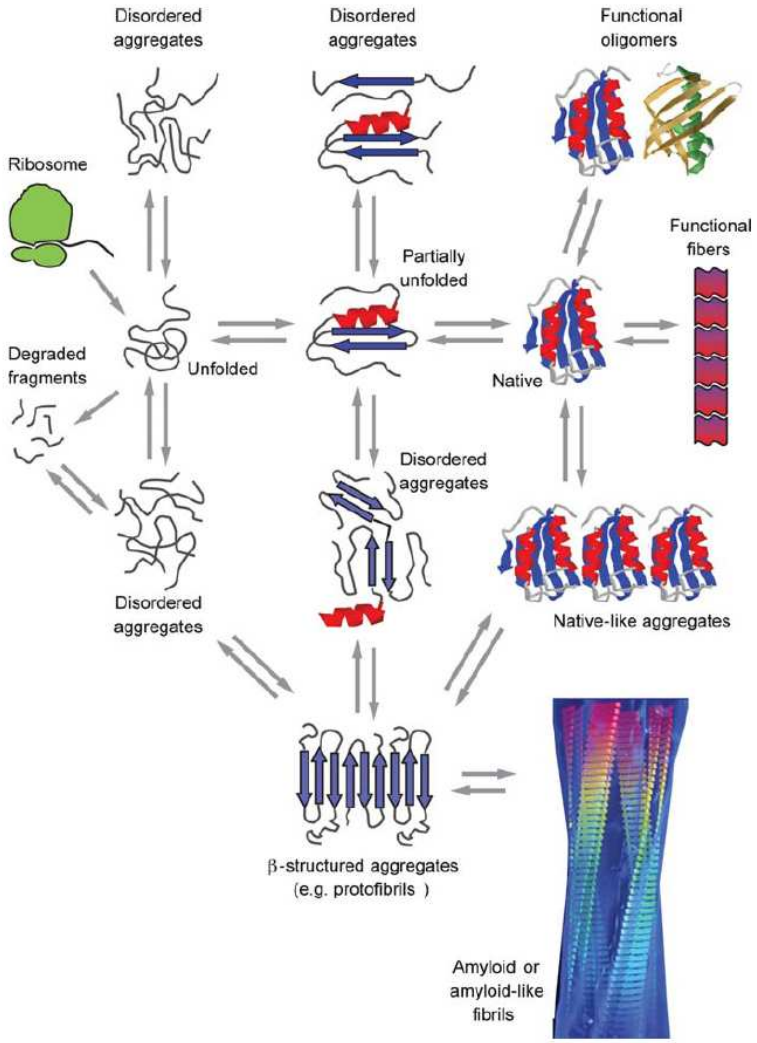

Figure 7. A schematic representation of some of the many conformational states that can be adopted by polypeptide chains. All of these different conformational states and their interconversions are carefully regulated in the biological environment, but conformational diseases will occur when such regulatory systems fail. From [37].

Following biosynthesis on a ribosome, a polypeptide chain is initially unfolded and can then remain unfolded, or fold into a unique compact structure, often through one or more partially folded intermediates. Moreover, natively unfolded proteins and peptides can also aggregate under some circumstances. Some of the initial amorphous aggregates simply dissociate, but others may reorganize to form oligomers with amyloid structure, including the spherical, chain-like, and annular amyloid protofibrils observed for many systems [2, 37]. The structured polypeptide aggregates can then sometimes grow into mature fibrils by further self-association or through the repetitive addition of monomers

(Fig. 7). Indeed, to understand the determinants of protein folding and aggregation a full characterization of the multitude of non-native conformational states populated on the folding energy landscape is crucial. [70, 71]. The idea that amyloid is a generic form of protein structure rises the question of why it is only associated with diseases [34]. One possible explanation is that the formation of amyloid fibrils is difficult to control, and once formed it is often extremely hard or impossible to degrade. Recent data have shown that general physicochemical features, such as mean hydrophobicity, net charge and propensity to α and β structure formation, affect the tendency of an unfolded or partially folded polypeptide chain to aggregate [72]. This may explain the higher propensity to aggregation of peptides and natively unfolded proteins such as α-synuclein (involved in Parkinson's disease) and tau (involved in Alzheimer's disease) carrying specific mutations enhancing their mean hydrophobicity or reducing their mean net charge. Finally, protein aggregation may be favoured under conditions resulting in the impairment or overwhelming of the molecular machineries (i.e. chaperones) responsible for the quality control of protein folding [40]. Despite much recent work in this area, many questions about the amyloid aggregation remain open, and considerable efforts are currently devoted to the study of the phenomenon of protein aggregation because of its association with a wide variety of human diseases and of its potential applications in biotechnology.

Role of prefibrillar aggregates as causative agents of neurodegenerative diseases

The data reported in the past few years have considerably improved the knowledge of the molecular basis of protein misfolding and aggregation, as well as of the relationship between structure and toxicity of the amyloid aggregates, even if the specific nature of the pathogenic species, and their ability to damage cells, are however, the subject of intense debate [40]. Recent findings indicate that the protein assemblies preceding the formation of mature amyloid fibrils, such as low-molecular-weight disordered oligomers and/or structured protofibrils, are the pathogenic species in neuropathic diseases. The severity of cognitive impairment in Alzheimer's disease correlates with the levels of low-molecular-weight species of Aβ rather than with the amount of fibrils [73]. Abundant data show that also the prefibrillar species of other amyloidogenic proteins such as α-synuclein or transthyretin, which are formed early in the process of

fibrillogenesis, are neurotoxic, whereas the mature fibrils are much less toxic [40, 50, 74]. Pre-fibrillar aggregates formed by transthyretin can also be toxic to neuronal cells or perturb their function [75]. Protofibril appearance in tissues precedes the expression of the clinical phenotype thus explaining the lack of relationship found in most cases between extent of amyloid deposits and severity of the clinical symptoms [76]. In addition, transgenic mice show deficits in cognitive impairment, cell function, and synaptic plasticity before the accumulation of significant quantities of amyloid plaques [77]. Importantly in this context, pre-fibrillar forms of the proteins that have no link with amyloid-associated disease, such as HypF-N, the PI3-SH3 and apomyoglobin from sperm whale, are also highly toxic to cultured fibroblasts and neurons, whereas the monomeric native states and the amyloid-like fibrils (all formed *in vitro*) displayed very little, if any, toxicity [69]. This result implies that the ability of pre-fibrillar aggregates to cause cell dysfunction arises from common characteristics of the supramolecular structure of the aggregates rather than from specific features of the amino acid sequences of the polypeptides. A wide variety of biochemical, cytological, and physiological perturbations has been identified following the exposure of neurons to such species, both *in vivo* and *in vitro*. It can be hypothesized that protofibrillar aggregates impair cell function because they expose on their surface an array of groups that are normally hidden in globular proteins or dispersed in highly unfolded peptides or proteins. Indeed the exposed regions could be rich in hydrophobic groups able to stick onto cell membranes. Pre-fibrillar assemblies have indeed been shown to interact with synthetic phospholipid bilayers and with cell membranes [78, 79], possibly destabilising them and impairing the function of specific membrane-bound proteins [80]. The precise molecular mechanism of toxicity of these aggregates is still unclear and it is also possible that different types of pre-fibrillar aggregates exert their toxicities in different ways. However, it is clear that the presence of toxic aggregates inside or outside cells can impair a number of cell functions that ultimately lead to cell death by an apoptotic mechanism [81]. Many evidence points to a central role of aggregate interaction with cell membrane and subsequent intracellular redox status modifications with free Ca^{2+} levels alterations [69, 78, 80], suggesting a mechanism of cell death possibly shared among prefibrillar aggregates of most peptides and proteins [82]. In conclusion, prefibrillar aggregates, although originated from different peptides and proteins, seems

to have common structural features. These characteristics are different from those of their precursors (not aggregated) or mature fibrils. The results obtained in the last few years suggest the idea that exists a distinct mechanism of pathogenesis, inherently associated with the aforementioned common structure.

-HypF-N: A MODEL OF AMYLOID AGGREGATION UNRELATED TO DISEASE-

Function, structure and aggregation of HypF-N

An increasing number of proteins with no link to protein deposition diseases has been found to form, under various conditions *in vitro*, fibrillar aggregates that have the morphological, structural, and tinctorial properties that allow them to be classified as amyloid fibrils [40]. One example is HypF, a large protein of about 82 KDa that assists the folding of [NiFe]-hydrogenases, key enzymes in the hydrogen metabolism of prokaryotes [83]. In their fully functional forms, the iron atoms of the active sites of these [NiFe]-hydrogenases are stabilized in the low oxidation state (Fe^{2+}) by binding to the carbon monoxide (CO) and cyanide (CN^-) ligands [84]. Both molecules have been shown to originate from the processing of carbamoylphosphate [85]. Thus, the assembly of the complex hydrogenase system requires the coordinated action of different maturation and regulatory factors. Indeed, hydrogenase operons contain a number of accessory genes (HypA-F) encoding maturation and regulatory proteins, including the essential maturation factor HypF [86]. *E. coli*, as any other prokaryote, expresses a HypF protein, that contains an N-terminal acylphosphatase-like domain (residues 1-91) (HypF-N). The HypF-N displays sequence and structural homology with other members of the acylphosphatase-like structural family. Acylphosphatases (AcPs) are small enzymes specifically catalysing the hydrolysis of carboxyl-phosphate bonds in acylphosphates such as carbamoylphosphate, succinylsphosphate and 1,3-bisphosphoglycerate [87]. Recent experiments shed light on the role of *E. coli* HypF in the conversion of carbamoylphosphate into CO and CN^-, and on the coordination of these ligands to the assembled hydrogenase metal cluster [88]. According to these results, HypF-N acts as a carbamoyltransferase that transfers the carbamoyl moiety of

carbamoyladenylate to the C-terminal cysteine of the partner protein HypE, forming an enzyme-thiocarbamate. HypE dehydrates the S-carbamoyl moiety in an ATP-dependent process to yield the enzyme thiocyanate. Finally, the cyano group can be nucleophically transferred to an iron complex [88]. The structure of HypF-N has been resolved by X-ray crystallography and is well defined for residues 5-91 (Fig. 8) [89]. The domain has a ferredoxin-like fold, which consists in a α/β sandwich, with βαββαβ topology. Following the sequence identity with AcPs, it has been assigned to the acylphosphatase-like structural family. The five β-strands of the domain form a slightly twisted β-sheet (β4-β1-β3-β2-β5 strand arrangement), which faces on one side two antiparallel α-helices; the other side is instead fully solvent-exposed. Overall, the domain has a size of about 43x28x27 Å. This compact globular state displays the main structural strategies exploited by all-β and α/β proteins to escape amyloid aggregation [26].

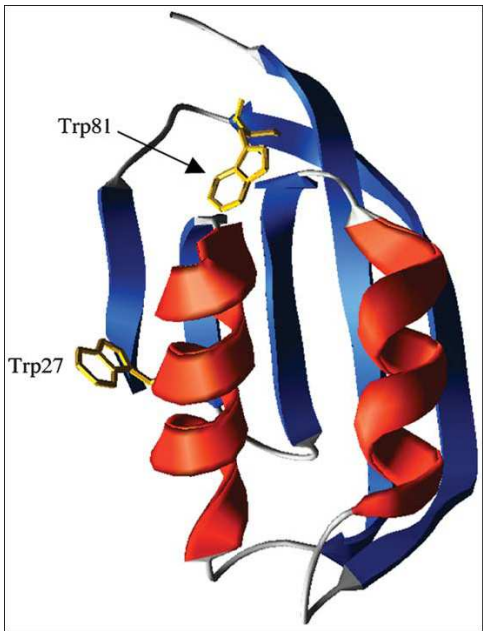

Figure 8. Three-dimensional structure of native HypFN from X-ray crystallography. The red and blue colours indicate α-helices and β-strands, respectively. From [90].

HypF-N forms amyloid-like fibrils under conditions that promote its partial unfolding, such as in the presence of trifluoroethanol (TFE) or following a decrease of pH. Formation of amyloid-like fibrils has been obtained initially at pH 5.5 with 30% (v/v) TFE or at pH 3.0 in citric acid [66]. The formation of a partially folded state is a key

event in the aggregation pathway of this protein *in vitro*, even under mild destabilising conditions in which the folded state is by far the predominant species. Indeed, under mild denaturing conditions generated by moderate concentrations of trifluoroethanol [6–12% (v/v)], the native state of HypF-N is in rapid equilibrium with a partially unfolded state, whose population is about 1–2%; a kinetic analysis has shown that amyloid aggregation under these conditions arises from molecules accessing this amyloidogenic state [90]. Recently, new aggregation conditions for HypF-N, enabling the characterization of the partially folded state populated prior undergoing aggregation, have been described, such as at pH 5.5 in the presence of 12% (v/v) TFE, or at pH 1.7 in the presence of salts (NaCl). A detailed structural investigation of this partially folded state has also been performed and achieved by means of different biophysical and biochemical techniques. [91]. The resulting species have been imaged with tapping mode atomic force microscopy (TM-AFM), have been shown to increase the fluorescence of thioflavin T (ThT), indicating the presence of intermolecular β-sheet structure typical of amyloid aggregates. In general, the data obtained suggest that the aggregation process of this protein starts from a partially folded state that can be either fully populated or in rapid equilibrium with the native state when the latter is destabilized by mutations and/or mild unfolding conditions [90]. The results support an aggregation pathway in which the native protein first converts into a partially folded state separated from the native state by an energy barrier comparable to that of (un)folding. This monomeric state converts into globular small aggregates and small beaded fibrils that further associate into ring-like structures. Finally, the ring-like structures convert into ribbon-like fibrils that associate into fibrillar tangles [61]. As many disease-involved systems aggregate following similar pathways, HypF-N represents a useful model system to determine the common principles underlying amyloid formation.

HypF-N protofibrils interact with cell membranes originating a cytotoxic cascade

It is increasingly suggested that the oligomers formed by proteins that are not related to any human disease can be toxic when added to the extracellular medium of cultured cells, whereas the same proteins in monomeric or fibrillar forms are not [69]. The observation that the oligomers formed from such a heterogeneous group of proteins

impair cell viability suggests that these species share the ability to "misinteract" with the macromolecular components of living organisms, such as membranes and proteins, and interfere with their normal function. The early prefibrillar aggregates of HypF-N formed in 30% TFE were shown to be able to interact with, insert into, and eventually disassemble synthetic membranes and supported phospholipid bilayers [61, 92]. Moreover, these species can interact with the plasma membrane of cultured cells and be internalized inside the cytoplasm, resulting in cell impairment and death [93, 94]. Recently, it was found that their interaction with cell membranes is disfavoured by a high membrane cholesterol content [95, 96]. Similarly to the protofibrillar aggregates of disease-related proteins and peptides, treatment of the cells with HypF-N protofibrils leads to an increase of reactive oxygen species (ROS) and free Ca^{2+} levels inside the cells, which ultimately die by apoptosis or necrosis [93, 94]. Moreover, the increase of intracellular Ca^{2+} levels is associated with both the activation of plasma membrane receptors with Ca^{2+} channel activity, such as AMPA and NMDA, and unspecific membrane permeabilization, with the former effect being more important at early times [97]. The susceptibility of different cells to HypF-N aggregates was shown to depend on their ability to counteract these early impairments, which increases during cell differentiation [94, 96]. Remarkably, HypF-N protofibrils can also induce a loss of cholinergic neurons when injected into rat brains, demonstrating that these species can act as toxins even in higher organisms [98]. These data strongly support the hypothesis that a common mechanism of cytotoxicity exists, which is related to the misfolded nature and oligomeric state of a protein rather than to its sequence. In spite of this advancement, a structural characterization of the conformational properties of the oligomers finalized to an understanding of the relationship with their toxic effect is still lacking, mainly due to the fact that the transient formation of these species and their structural heterogeneity have hampered considerably their investigation. The structural determinants of the protein oligomers that are responsible for cell dysfunction are starting, only these days, to be elucidated. Recently, the functional and structural properties of the spherical aggregates formed by HypF-N in two distinct environmental conditions can be compared. It is therefore nowadays essential to determine in detail the structure of the toxic oligomeric species in order to identify new therapeutical targets,

and to understand whether it represents a single common fold or rather exhibits some polymorphism.

A causative link between the structure of HypF-N oligomers and their ability to cause cellular dysfunction

It is well known that incubation of the same protein/peptide under different experimental conditions causes the formation of oligomers or fibrils with different morphologies and that such differences result in different degrees of toxicity [99-101]. Similarly, mutations or covalent modifications result in different levels of oligomers or different fibrillar structures with completely different toxicities [102]. However, little experimental information is available on the structural features of oligomers grown under different conditions and on the relationship between their structure and their ability to cause cell dysfunction. Recently, it has been found that oligomers formed from the same protein (HypF-N) under different conditions (pH 5.5 in the presence of 12%(v/v) TFE or pH 1.7 in the presence of 330 mM NaCl) exhibited similar morphological and tinctorial properties, yet differed in their molecular structure. Comparisons of the two types of aggregates, indicated that their structural differences resulted from different degrees of packing of the hydrophobic residues within their cores with a consequent different level of structural flexibility and solvent-exposure of such residues [91]. Thus, whilst the ability to form amyloid-like structures is generic to polypeptide chains, whether or not such species are pathogenic will depend on their structural features, notably the extent to which hydrophobic residues are flexible and exposed on their surfaces within the environment of a living organism. These findings, however, do not seem to be limited to the HypF-N aggregates, and could indeed explain the toxic properties of the oligomers formed by disease-related systems. In fact, several studies indicated a correlation between the size and surface hydrophobicity of Aβ40 aggregates and their ability to decrease the bilayer fluidity of model membranes [103], suggesting that the exposure to the solvent of hydrophobic surfaces determines the ability of these species to interact with cell membranes. A correlation between hydrophobicity, tendency to form aggregates and aggregate cytotoxicity has also been observed in comparative studies where the behavior of different homopolymeric amino acid (HPAA) stretches was investigated [104]. It has been recently reported that

expanded huntingtin-exon1 forms fibrillar aggregates at two different temperatures that have different structural and physical properties as well as different cytotoxicities [99]. The structures and toxicities of both forms of the aggregates are comparable with those extracted from regions of mouse brains affected to different extents by huntingtin deposition. In both pairs of structures a direct relationship between structural flexibility and cytotoxicity of amyloid assemblies was found, supporting the generality of previous conclusions [99]. Finally, all these data lend support to the idea that a key feature in the generation of toxicity is the conversion of a species of aggregates where stability is associated with extreme burial of hydrophobic residues to one where such residues are substantially exposed and disorganized [105]. Recently, it has been suggested that for therapeutic purposes the toxicity can be dramatically reduced if the hydrophobic residues are incorporated to a greater extent within the interior of the oligomeric assemblies, even in the absence of an effective change in morphology [91]. Approaches of this type will facilitate the elucidation of the causative link between the molecular structure of aberrant protein oligomers and their ability to cause cell dysfunction, with the aim of understanding the pathogenesis of protein deposition diseases and identifying therapeutic strategies to combat them. Moreover, a detailed understanding of the forces that determine the structure of amyloid-like oligomers will also enable to identify the factors that can modulate it, and eventually alter the biological activities of these species.

-ALZHEIMER'S DISEASE-

APP processing and Aβ formation

Alzheimer's disease (AD) is a progressive neurodegenerative disorder characterized by irreversible cognitive and physical deterioration and affects 5–15% of the population over the age of 65 years [106]. Causes involve multiple genetic and environmental factors. The pathology of AD is characterized by progressive accumulation of intraneuronal fibrillary tangles composed of abnormally phosphorylated tau protein, and by senile neuritic plaques composed of aggregated amyloid β-protein (Aβ), often surrounded by proliferating activated microglia and astrocytes [107]. Neurofibrillary

tangles (NFT) are predominantly composed of paired helical filaments (PHF), but straight 15-nm filaments, 10-nm intermediate filaments, dense granules of various sizes, and other structures are also present [108]. Tau is a multifunctional microtubule-associated protein that regulates cytoskeleton structure. In normal brain, the equilibrium between phosphorylations and dephosphorylations of tau modulates the stability of the cytoskeleton and consequently axonal morphology [109]. In contrast, when highly phosphorylated, tau is sequestered into paired helical filaments [110] and causes disruption of microtubules that ultimately leads to cell death. Several kinases have been involved in the anomalous hyperphosphorylation of tau protein. Tau kinase I or GSK3 phosphorylates tau but also interacts with other proteins, like presenilin-1, that are important in the onset of AD pathology. Tau kinase II or cdk5 also modifies tau protein and this kind of phosphorylation could be deregulated in a neurodegenerative disorder like AD due to proteolytic cleavage of the regulatory subunit, p35, of the kinase [111]. Additionally, it has been suggested that another kinase, cdc2, that is mainly present in proliferating cells, is abnormally upregulated in AD [112] and that it could phosphorylate tau protein. The consequences of this phosphorylation could be a conformational change that prevents the binding of phosphotau to microtubules. Tau phosphorylation by protein kinases precedes the formation of paired helical filaments that cause neurodegeneration [113]. In AD, the lack of binding to microtubules and the formation of aberrant aggregates, NFT, has been correlated with the level of dementia. In addition, the development of filamentous tau pathology in specific neural cells has been described. It has been suggested that the defects in a single cell, start with a modification of tau by phosphorylation, giving place to a “pre-tangle” stage [114]. After this stage, filamentous polymers (PHF) are assembled and the aberrant aggregation of these PHF results in the formation of cytoplasmic (intracellular) NFT. As a consequence of this, it has been suggested that neurons degenerate and die, thus leaving NFT in the extracellular space [115]. Aβ deposits in AD patients are almost exclusively composed of the highly amyloidogenic 1-42 form (Aβ42), which is normally produced by cells in much lower quantities than the 40 residues form (Aβ40). Aβ42 is more prone to aggregation *in vitro* than Aβ40, and its cytotoxicity is considered to be the main cause of neuronal impairment in AD. Aβ peptides arise from sequential proteolysis of the transmembrane amyloid precursor protein (APP), a type I membrane protein, expressed

in a wide variety of tissue and cell types, and whose main function has been clearly defined. APP is characterized by a large N-terminal extracellular/luminal domain and a small intracellular/cytosolic C-terminal domain [116]. Presently, the overproduction and/or the reduced clearance of Aβ peptides are considered key factors underlying their fibrillar polymerization. Recent studies have suggested that soluble Aβ oligomers correlate better than plaque load with cognitive impairment and neuronal dysfunction and may be the principal toxic species of Aβ involved in AD [117, 118]. APP is proteolytically processed following two different pathways, the so-called amyloidogenic and non-amyloidogenic processing, respectively (Fig. 9). These mechanisms are carried out by several different proteases called secretases in at least three main cleavages sites (known as the α, β and γ sites) in and around the transmembrane encompassing region [119]. The non-amyloidogenic pathway involves the activity of α-secretase (a metalloprotease) at a plasma membrane level, which cleaves APP within the Aβ domain to produce secreted sAPPα and the non-amyloidogenic C-terminal fragment C83. C83 can undergo further processing mediated by γ-secretase cleavage at the C-terminal end of the Aβ domain to yeild non-amyloidogenic P3. The APP amyloidogenic processing results in the generation of Aβ peptides in AD and involves the combined activity of β- and γ-secretase [120, 121]. β-secretase has been identified as the beta-site APP-cleaving enzyme (BACE)-1, cleaving APP at the N-terminal end of the Aβ domain generate an extracellular soluble fragment called sAPPβ and an intracellular C-terminal amyloidogenic fragment C99 (βCTF). Subsequent, γ-secretase cleavage of C99 at residues 40/42/43 of the Aβ domain gives rise to the highly amyloidogenic Aβ peptides. Indeed, the γ-cleavage site is unusually located within the transmembrane domain itself. Sequential processing of APP in the extracellular domain by β-secretase followed by γ-secretase cleavage within the transmembrane domain generates Aβ peptides and the APP intracellular domain (AICD).

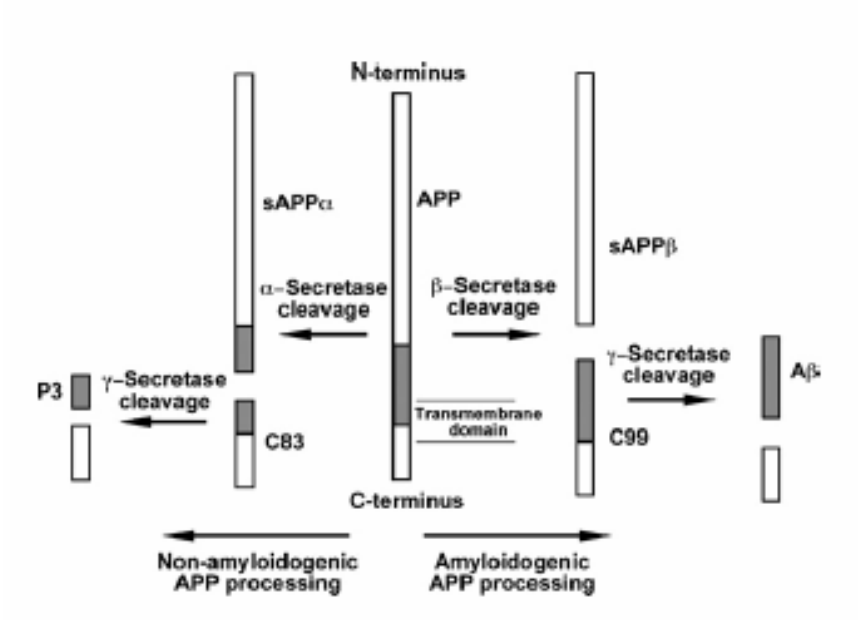

Figure 9. Secretase mediated processing of APP. **Non amyloidogenic APP processing**. α-Secretase mediated processing cleaves APP within Aβ domain to produce secreted sAPPα and the nonamyloidogenic C-terminal fragment C83. C83 can undergo further processing mediated by γ-secretase cleavage at the C-terminal end of the Aβ domain to yeild non-amyloidogenic P3. **Amyloidogenic APP processing**. Alternate APP processing initiated by β-secretase cleavage at the N-terminal end of the Aβ domain gives rise to sAPPβ and the amyloidogenic C99 fragment. Subsequent γ-secretase cleavage of C99, at the C-terminal end of the Aβ domain gives rise to the highly amyloidogenic Aβ. From [120].

Missense mutations in APP itself were the first genetic cause of AD to be identified, and these mutations are principally located at or near either the β- or γ-secretase cleavage sites [122]. The mutations enhance both cleavages, resulting in overproduction of the highly amyloidogenic and more neurotoxic Aβ42. Further genetic analysis of families with early-onset familial AD led to the identification of Presenilin-1 (PS-1) and Presenilin-2 (PS-2) as the causative genes. Missense mutations in PS increase the cellular production of Aβ42 by slightly altering the γ-secretase cleavage site and thus the protease specificity. Deletion of PS-1 in mice significantly lowers Aβ production and increases the C-terminal fragments of APP that are substrates for γ-secretases [123]. Evidence for the relationship between the development of AD and abnormal Aβ production also comes from the familial forms of AD (FAD). FAD only accounts for about 5% of all AD cases, but the most significant FAD mutations are all associated with APP processing to yield Aβ. Autosomal dominant forms of FAD are often characterized by specific mutations in the APP gene located on chromosome 21, or in

the genes mapped on chromosomes 14 and 1, encoding PS-1 and PS-2, respectively [124]. Mutations in these three different genes appear to affect very similar pathological mechanisms, which at the end accelerate Aβ aggregation, deposition and neurotoxicity [125]. These evidences point to a pathogenetic role for the metabolism of APP and for the deposition of Aβ, suggesting a role for Aβ in the non-genetic AD forms, since the pathological endpoint and hallmarks of familial and sporadic AD are very similar.

APP alternative functions in AD and its relationship with specialized membrane regions

Research efforts over the last two decades have clearly elucidated the fundamental role of APP and its proteolytic processing in the pathology of AD. This is also highlighted by the fact that 50% of familial AD forms (FAD) are caused by mutations in the APP gene itself or in the presenilin genes which encode components of the γ-secretase complex [126]. The ubiquitous expression of APP in many tissues as well as the presence of homologues in a variety of species, including mammals and invertebrates, argue for an important physiological function of APP. Some biological properties have been attributed to APP, including adhesion, neuronal development, synaptogenesis, neurite outgrowth, neuroprotection, and stimulation of proliferation of neuronal progenitor cells [127]. However, beside amyloidogenic APP processing, other involvement of APP in direct or indirect neurotoxicity in AD is still unclear. Recent studies have proposed that the content of membrane cholesterol can modulate Aβ peptide production by affecting the stability of lipid rafts (ganglioside- and cholesterol-enriched dynamic membrane microdomains) and other membrane domains where APP and some APP processing secretases are located. In particular, membrane cholesterol can affect the cellular localization and the activity of the APP and the secretases modulating APP processing through the amyloidogenic or the non-amyloidogenic pathway [128]. Moreover, membrane cholesterol can affect the way Aβ peptides interact with the plasma membrane favouring or disfavouring aggregate nucleation and it can hinder the interaction of Aβ oligomers with the cell membrane thus avoiding their cytotoxic effects [128]. Conflicting results have highlighted that altered cholesterol content in neuronal membranes could favour the amyloidogenic or the non-amyloidogenic pathway of APP processing with increased or reduced Aβ40/42

production, respectively [128]. Several reports indicate that α-secretase and BACE1 compete for APP and that such competition depends on APP compartmentalization in the cell membrane [130]; in addition, recent findings support the idea that the way APP is processed by the cell depends on the membrane localization of the APP itself and the various secretases. However, conflicting data have been reported on the effect of membrane cholesterol on APP processing. Several data indicate that in peripheral and neuronal cell lines low membrane cholesterol and increased membrane fluidity stimulate the non-amyloidogenic pathway (α/γ-secretase cleavage); this could result from reduced activity of BACE1, the enzyme starting the amyloidogenic pathway, and from increased α-secretase activity and APP content in the cell membrane, where it can undergo α-secretase cleavage [131]. The proposed model postulates that two pools of APP do exist in the cells, one associated with membrane rafts and another out of rafts, where α-cleavage occurs, suggesting that only the raft-localized APP processing results in Aβ generation [132]. According to this model, lipid raft clustering would bring into close contact APP and BACE1, with increased β-cleavage in the amyloidogenic pathway. Such a scenario would be favoured by high levels of brain cholesterol. According another theory, BACE1, but not APP, is localized to lipid rafts [128], as a consequence, a moderate loss of membrane cholesterol would result in raft disassembly and increased BACE1-APP colocalization in non-raft membrane domains, with increased β-cleavage and consequent Aβ generation. Such a scenario would be favoured by low levels of brain cholesterol. Gangliosides (GM1, GD1a, GD1b, GT1b etc.), mainly found in the outer leaflet of mammalian plasma membranes, are glycosylated sphingolipids enriched in membranes of the nervous system. Further studies pointed out that in AD brain tissue the total ganglioside pattern is significantly altered [133]. Micropathological analysis of amyloid plaques has revealed that GM1, like cholesterol, binds to Aβ and it was suggested that the GM1/Aβ complex might initiate amyloid fibril formation [133]. In addition, it has been demonstrated that GM1 is the most effective natural compound that increases Aβ production. In the presence of GM1, increased γ-secretase and decreased α-secretase activity resulted in up to a 10-fold increase in Aβ levels [134]. The effect of gangliosides on Aβ production supports the notion that cholesterol is not the only lipid that mediates APP processing. Indeed, both cholesterol homeostasis and glycosphingolipids, especially the ganglioside GM1, can cause

significant alterations in Aβ production. Interestingly, both lipid classes, gangliosides and cholesterol, are major components of lipid rafts. The dynamic nature of lipid rafts means that both proteins and lipids can move in and out of raft domains with different partitioning kinetics, and there is evidence to indicate that lipid rafts influence the processing of membrane-anchored proteins [132]. Pertinent to AD, the proteins that could partition to lipid rafts include the secretases and APP, and changes in raft composition may result in altered APP processing. Findings such as these could provide the basis for novel AD therapeutics that specifically target the membrane. The processing of APP in membranes can be influenced by many factors, each of which can be important determinants of APP-mediated toxicity. Evidence from these studies further highlights the dynamic nature of the interactions between membrane proteins and cholesterol enriched membrane domains such as rafts in regulating both physiological and pathological processes at this site, and the implications of this for AD are becoming increasingly obvious. However, it is unknown whether APP is involved in the mechanism of neuronal degeneration in AD, apart from its role as the precursor of Aβ. It has been shown that the toxic fibrillar form of Aβ binds with high affinity to a subset of neuronal membrane proteins that includes APP. In particular, Aβ interacts with holo-APP and, to a much lesser extent, with the secreted soluble form of APP. Aβ neurotoxicity is significantly reduced in cortical cultures established from APP-null mice, suggesting that APP can modulate Aβ toxicity [135]. Thus an interaction of Aβ with its normal cellular precursor may lead to neuronal degeneration in a manner reminiscent of the pathogenic mechanism of prions. It has been seen that Aβ may also interact with APP at the level of APP processing. For example, Aβ can induce its own expression [136] and alter the metabolism of APP [137]. Several reports indicated that the over-expression of APP in neurons or neuronal cell lines is toxic in several studies [138, 139]. Over-expression of APP in differentiated NT2 cells activates caspase-3 and induces apoptosis [140]. APP could potentially transduce a pro-apoptotic signal through its interaction with the adapter proteins Fe65 and X11 or through an interaction with G proteins [141], suggesting that the binding of Aβ to APP resulted in a toxic gain of function, possibly by inducing an APP conformational change that triggered cell death. Different cell phenotypes over-expressing APP were shown to undergo an intense amyloidogenic metabolism with elevated Aβ peptide production [142]. In line with

these data, a higher resistance threshold to cytotoxicity has been found in some APP over-expressing cell lines, such as B103 cells that exhibited rescue features against ultraviolet irradiation and staurosporine toxicity [143]. Thus, Aβ toxicity and APP biology may be linked. These mechanisms of toxicity involve anomalous processing/expression of APP or interaction between Aβ and APP either at the cell surface or in the secretory pathway, where the two proteins are in proximity.

Peripheral cells as an investigational tool for Alzheimer's disease

To identify those cellular and molecular abnormalities that cause the neuropathological lesions characteristic of AD, autopsied brains and extraneural tissues have been used. The use of peripheral cells is based on the hypothesis that AD might be a systemic disease that affects several tissues in the body. The specific brain damage could be the expression of a greater sensitivity to injury in postmitotic cells of the brain. Furthermore, a potential genetic defect underlying the disease may be manifest in several body tissues that express the gene involved. Peripheral tissues suitable for exploring pathophysiological hypotheses and possibly for providing a useful biological marker for diagnosis of AD comprise skin fibroblasts, platelets, lymphocytes, as well as body fluids such as plasma or cerebrospinal fluid (CSF) [144]. Among extraneural tissues, cultured skin fibroblasts have been used successfully to elucidate the molecular and biochemical bases of a large number of inborn errors of metabolism which cause neurological disease i.e. Refsum's disease, Lesch-Nyhan disease and Tay-Sachs disease [145]. Moreover, fibroblasts are an appropriate model for studies on those genetic diseases of the nervous system with late clinical onset, including familial Alzheimer' s disease (FAD), because they can be cultured and amplified, and contain the complete genomic information of the organism from which they are derived. A number of abnormalities in metabolic and biochemical processes have been found in cultured FAD [146-149]. Some of the described alterations reflect events that have also been demonstrated to occur in the AD brain [147, 148]. Another piece of evidence in support of speculation that AD is not confined to the brain and that justifies the use of fibroblasts in AD research, is the finding that β-amyloid can accumulate in non neural tissues and blood vessels of AD patients, including skin, subcutaneous tissues and intestine [150] although it should be stressed that this finding has only been confirmed

by one group. When using cultured skin fibroblasts, some technical variables should also be considered. Growth properties and *in vitro* aging of AD and control fibroblast cultures have been shown to differ by some Authors [151] but not by others [152]. Since growth properties and biological age in culture can have profound effects on the properties of cells cultured from skin, including the expression of genes (which could be related to AD), this point is critical and requires reexamination in a larger population [153]. Accordingly, reproducible and interpretable results with the AD fibroblasts model require attention to the replicability of culture conditions including, but not limited to, matching AD and control cells for age, sex of the donors, and biological age in culture. Different growth conditions, aging of cultures *in vitro* and state of confluency of the cells at the time of the experiment may well account for discrepancies between data from different laboratories. Only abnormalities which replicate in larger series across different laboratories or characterize subgroups of AD patients are likely to be interesting in diagnosing AD. Alzheimer's disease diagnosis appears to be the major challenge posed by AD in its sporadic late-onset form, which still represents the vast majority of all cases. On the other hand, data obtained using fibroblasts from individuals with known gene defects, although representing only a small proportion of all AD cases, could be very informative about the cellular pathophysiology of AD. Recent advances in understanding the genetics of AD allow identification of families bearing mutations in APP, presenilin-1 (PS-1), or presenilin-2 (PS-2) genes coded on chromosomes 21, 14 and 1, respectively [154]. Fibroblast lines from FAD patients can therefore be classified according to the specific gene defect to see whether a particular genetic abnormality alters cellular function in a unique manner (Table 2).

Table 2: Genetic defects and functional consequence in cultured human FAD fibroblasts

Chromosome	Gene involved	Age at onset, in years (range)	Functional consequence in fibroblasts
Chromosome 1	Presenilin 2	50–65	Increased $A\beta_{1-42}$ secretion Increased $A\beta_{1-40}$ secretion
Chromosome 14	Presenilin 1	33–52	Increased $A\beta_{1-42}$ secretion Increased $A\beta_{1-40}$ secretion
Chromosome 21	APP	43–59	Increased Aβ secretion No PKC activity alterations (Swedish kindred)

Modified from [152]

In spite of these drawbacks, peripheral cells can be used to identity and to test hypothesis on the primary pathophysiological mechanisms leading to AD avoiding variables derived from a *postmortem* state. Studies of autopsied brain tissue cannot clarify whether abnormal oxidative processes are inherent properties of AD cells or are secondary to neurodegeneration [2], while studies on cultured skin fibroblasts from FAD patients bearing either APP or PS-1 gene mutations could reveal the early biochemical anomalies induced by various forms of Aβ aggregates, approaching to the identification of early modifications in living cells having a genetic drawback in tissues where AD lesions occur. On the other hand, peripheral cells can not be used to answer other clinically relevant questions that require a behaving organism, or intact brains. Low or absent expression of neuronal proteins by peripheral cells cultured under standard conditions is an important limiting factor. In the study of AD and other neurological diseases, peripheral cells are indeed an adjunct for studies of the brain and other clinically affected tissues, providing the tools to study *in vitro* the dynamic alteration of metabolic processes that neuropathological examination indicates might be targets of the disease [144].

-THE MOLECULAR BASIS OF AMYLOID CYTOTOXICITY-

The data reported in the last few years showing that protein aggregation into assemblies of amyloid type can be considered a generic property of the polypeptide chains suggest that protein aggregation in cells can be a more common phenomenon than previously believed. Furthermore, the findings that aggregates of disease-unrelated proteins display the same cytotoxicity as those formed by proteins and peptides associated with disease suggest that toxicity is a consequence of the common structure of aggregates and that, at least in most cases, it proceeds by impairing common cellular parameters such as free calcium (Ca^{2+}) and reactive oxygen species (ROS) levels [155]. An increasing body of evidence supports the idea that the most highly cytotoxic aggregates are the early prefibrillar assemblies or, possibly in some cases, the individual misfolded molecules [156] rather than mature fibrils. In addition, the cascade of biochemical modifications triggered by the exposure of cells to any aggregated polypeptide chain ultimately leading to cell death, at least in most cases, starts with the

alteration of the same cellular parameters, such as the disruption of the integrity of cell membranes, the imbalance of ion homeostasis, the impairment of mitochondrial activity, the alteration of lipid metabolism [157].

Cell membranes as key sites of amyloid interaction and cytotoxicity

A leading theory on the molecular basis of amyloid toxicity suggests that amyloid unstable assemblies interact with cell membranes destroying their ordered structure, eventually leading to membrane permeabilization with subsequent alteration of ion homeostasis and intracellular redox status [40, 58]. Indeed cell surfaces can catalyze aggregate nucleation and self-assembly on the bilayer surface is critical for membrane disruption [158]. However, in spite of the remarkable research efforts spent in the last years, the molecular basis of Aβ–membrane interaction and the ensuing structural modifications of the latter remains substantially elusive. Indeed, the question as to whether oligomer receptors or preferential interaction sites on the cell membrane do exist still awaits a convincing answer. The question is made even more intriguing by the increasing data indicating that amyloids grown from different peptides and proteins could behave similarly in their cytotoxic effects and, conversely, that structurally different amyloids grown under differing conditions from the same peptide/protein can display different cytotoxicities [159]. These evidences support the idea that amyloid cytotoxicity results from aggregate interaction with the cell membrane, with non-specific permeabilization of the latter [40, 56, 58, 160]. Because amyloid oligomers share a common structure and they are all intrinsically toxic to cells, this suggests that they also share a common mechanism of toxicity. If soluble oligomers have a common mechanism of toxicity, it implies that they act on the same primary target. This fundamental unity restricts number of potential targets to ones that are plausible of all of the different types of soluble amyloid oligomers. Additionally, some amyloids are cytosolic, whereas others are luminal or extracellular, suggesting that the target of oligomers must be accessible to both compartments. The obvious target that satisfies this criterion is the plasma membrane, because it forms the interface between the two compartments [161]. It has also been reported that all types of oligomers specifically permeabilize cell membranes. The addition of amyloid oligomers to cell cultures causes a rapid and large increase in cytosolic free Ca^{2+} and leads to liberation of Ca^{2+} from

intracellular stores. This is consistent with reports that oligomers may subsequently penetrate into cells where they similarly disrupt intracellular membranes to cause leakage of sequestered Ca^{2+}, but it could also result as a consequence of altered intracellular signaling [157] Amyloid oligomers also caused the leakage of the membrane impermeant dye calcein from cells, indicating that a variety of molecules diffuse across the membrane after oligomer treatment. This is in good agreement with previous reports of oligomer induced release of dye from phospholipid vesicles. [61, 162]. Even though soluble oligomers may not be acutely toxic *in vivo* as they are *in vitro*, the chronic leakage of ions across the plasma membrane may be sufficient to disrupt normal neuronal function and serve as a source of chronic stress in maintaining a normal membrane potential [161]. The neurotoxicity of Aβ is exhibited in many fields. One of the potential mechanisms for inducing the neurotoxicity of Aβ is direct interaction with the membranes. It has been reported that Aβ–membrane interaction event may be followed by the insertion of Aβ into the membrane in a structural configuration which forms ionic pores [163]. Aβ can destroy the structure of brain membranes [164] and may stimulate free radical production by interfering with the regulation of Ca^{2+} homeostasis and cell enzymatic activity [165]. Aβ can also alter the physical-chemical properties of neuronal membranes, including membrane fluidity, membrane lipid dynamics, and the activity of various membrane-bound proteins [166]. The interaction of Aβ with non-protein components of the plasma membrane, such as monosialoganglioside GM1 and cholesterol, has been a subject of intense investigation. These studies have addressed the fundamental question about the conversion of elemental units of Aβ into its toxic aggregates. Indeed, a series of findings indicate that the lipid composition of the membrane governs the outcome of Aβ interactions with cell membranes and the effectiveness of this interaction closely correlates with Aβ secondary structure [167]. It has been shown that the ability of Aβ to insert into lipid bilayer is critically controlled by the *ratio* of cholesterol to phospholipids. Altering this *ratio*, by lowering the concentration of cholesterol, results in Aβ staying on the membrane surface region, mainly in a β-sheet structure. In contrast, as the *ratio* of cholesterol to phospholipids rises Aβ can insert spontaneously into lipid bilayer by its C terminus, generating α-helix and removing almost all β-sheet structure [168]. Moreover, increasing evidence reported that Aβ selectively recognizes GM1 clusters in membranes

and binds to, and accumulates on, GM1-rich domains in a time- and concentration-dependent manner by adopting an altered conformation which could act as a seed for the assembly of soluble Aβ [169]. A recent paper has shown that annular protofibrils grown from Aβ peptides are relatively stable and harmless to cultured neuronal cells and do not permeabilize synthetic lipid vesicles, contrary to similar protofibrils grown from prefibrillar oligomers at the lipid surface [101]. These data, together with immunological evidence, led to suggest that the toxic annular protofibrils may form pore structures into the membrane resembling those arising from pore-forming toxins. In conclusion, the interaction of Aβ with the surface of the cell membrane may results in the activation of a chain of processes that, when large enough, become cytotoxic and induce cell death by apoptosis. However, the studies on membrane permeabilization have been carried out mainly on synthetic lipid vesicles lacking the complex lipid and protein structure of the cell membrane. Therefore, any conclusion that amyloids are endowed by themselves with non-specific lipid membrane permeabilizing behaviour, although of value, cannot be directly extrapolated to cells, both in culture and in tissue, mainly as far as the specificity of the permeabilization effect is concerned.

Dysregulation of calcium homeostasis in Alzheimer's disease

Rising evidence suggests that soluble amyloid oligomers, sharing common structural features and the ability to permeabilize membranes, may also share a common primary mechanism of pathogenesis in degenerative diseases. Indeed, membrane permeabilization by amyloid oligomers may initiate a common group of downstream pathologic processes, including intracellular Ca^{2+} dyshomeostasis, production of ROS, altered signaling pathways, and mitochondrial dysfunction that represent key effectors of cellular dysfunction and cell death in amyloid-associated degenerative disease [161]. The mechanism by which Aβ oligomer interaction with the membrane results in the generation of a subsequent Ca^{2+} influx remains elusive, and a variety of mechanisms have been proposed [161, 170]. Numerous studies have first showed that Aβ increases the level of cytoplasmic Ca^{2+} rendering neurons more susceptible to glutamate-induced neurotoxicity and that this increase in cytoplasmic Ca^{2+} is principally due to an influx of extracellular Ca^{2+} across the cell membrane [171, 172]. Another mechanism by which Aβ can disrupt calcium homeostasis is related to its ability to form ROS that may induce

membrane lipid peroxidation, which causes alterations in membrane properties and affects the function of membrane transporters and ion channels leading to an elevation of intracellular Ca^{2+} levels [173]. Interactions of Aβ oligomers and Fe^{2+} and Cu^{+} generate hydrogen peroxide and hydroxyl radicals [174]. A third mechanism by which Aβ disrupts Ca^{2+} homeostasis [163] suggests that Aβ may bind to the plasma membrane to form artificial membrane pores. The ability of Ab oligomers to form Ca^{2+}-permeable channels in neuronal plasma membranes is consistent to recent *in vivo* Ca^{2+}-imaging experiments performed with APP transgenic mice, by showing that resting Ca^{2+} levels were significantly elevated in approximately 35% of neurites located in the immediate vicinity of Aβ plaques [175]. Moreover, electrophysiological and atomic force microscopy (AFM) studies have shown that Aβ oligomers can form small annular structures on lipid membranes which resemble membrane pores [78]. Indeed, similar structures have also been seen using another neurotoxic protein α-synuclein [176]. Other studies also support the notion that Aβ peptides can disrupt lipid membranes. However, in these studies the investigators suggest that Aβ may cause weakening or thinning of the plasma membrane [160, 177]. Despite the large number of studies suggesting that Aβ may directly disrupt lipid membranes, most of the evidence for the membrane pore hypothesis comes from *in vitro* studies using purified Aβ and artificial lipid membranes. In contrast to the artificial pore hypothesis, there is abundant evidence both from cell culture and *in vivo* studies to indicate that Aβ can trigger Ca^{2+} influx through endogenous membrane ion channels. Several studies indicate that Aβ may trigger the opening of NMDA receptors. It has been observed that Aβ-induced toxicity in HEK293 cells expressing NMDA receptor subunits was blocked by a non-competitive NMDA receptor antagonist [178]. It has also been proposed that effects of Aβ on NMDA receptors may be mediated by a direct action on a7nicotinic acetylcholine receptors (a7nAChR) [179]. Furthermore, it was reported that Aβ can block a fast-inactivating K^{+} current, potentially leading to prolonged cell depolarization and increased Ca^{2+} influx and intracellular accumulation [180]. Studies using other amyloidogenic proteins support the notion that oligomers stimulate Ca^{2+} influx via voltage-gated Ca^{2+} channels (VGCCs). Other studies showed that prion protein (PrP) and Aβ raised intracellular Ca^{2+} through L-type channels [181]. In addition other reports show that amyloidogenic transthyretin can induce Ca^{2+} influx through both L- and N-

type channels in SH-SY5Y neuroblastoma cells [182]. Other studies suggest that Ca^{2+} may enter through a non-selective cation channel in response to Aβ [183]. Finally, it has been found that changes in the lipid composition of the neuronal membranes may have regulatory consequences for interactions of Aβ with cells in the brain. The presence of cholesterol in artificial lipid bilayers inhibits the channel-forming activity of human amylin [184] and reduces the insertion and formation of ion channels by Aβ25–35 [185]. It has also been suggested that cholesterol controls the incorporation of Aβ into cell membranes by modifying the fluidity of the neuronal membranes. This incorporation consequently results in formation of Aβ Ca^{2+} channels, and thus cell death. If the Aβ oligomer encounters a membrane with increased fluidity due to a lower than normal level of cholesterol, the insertion process occurs and a Aβ Ca^{2+} channel is formed. When the level of cholesterol in the membrane is higher than normal, the insertion process is prevented by the enhanced stiffness of the membrane [186]. In conclusion, it has been demonstrated that the magnitude of the toxicity expressed by Aβ on cells is modulated by the amount of cholesterol in the surface membrane. By affecting the physical properties of the membrane, cholesterol modulates the interaction and possibly the incorporation of Aβ ion channel protein into the cell membrane. Recent studies indicate that genetic factors could also play a role in the dysregulation of Ca^{2+} homeostasis in AD. It is now well established that mutations in the genes encoding presenilins-1 or 2 (PS-1or PS-2) cause familial AD (FAD) [187]. In the case of the PS-1 gene, more than 150 FAD mutations have now been identified, and, 10 FAD mutations have been identified in the PS-2 gene. It seems very likely that all FAD mutations cause AD via a similar mechanism, i.e., by increasing the relative proportion of Aβ species that aggregate readily. Presenilin mutations have been found to increase release of intracellular Ca^{2+} from ryanodine or inositol 1,4,5-trisphosphate (IP3) channels [188]. It is possible that there is a link between γ-secretase activity and intracellular Ca^{2+} stores. In fact, it has been found that presenilin mutant-induced enhancement of Aβ secretion was abolished in IP3 receptor knockout cells [189]. The finding suggests that γ-secretase cleavage must be downstream of IP3 signalling, but how this occurs is still very unclear. Recently, a polymorphism in a gene encoding a novel Ca^{2+} conducting channel was found to have linkage to AD [190]. This channel is called Ca^{2+} homeostasis modulator 1 (CALHM1) and is a conserved three transmembrane domain containing

glycoprotein. It localizes to both the ER and the plasma membrane. Overexpression of this channel induces a cytosolic Ca^{2+} influx pathway, which is unaffected by conventional Ca^{2+} channel blockers, but prevented by the removal of extracellular Ca^{2+} and non-specific ion channel pore blockers. The induction of this particular Ca^{2+} influx route into the cytosol results in an increase in APPα production, with a concomitant reduction in Aβ, suggesting an effect on one of the α-secretase enzymes. Notably, knockdown of this channel, or the presence of the identified polymorphism for AD (rs2986017 encoding P86L substitution) decreases Ca^{2+} permeability and increases Aβ production. These data provide strong evidence that Ca^{2+} signalling and influx can contribute to the initiation of AD pathology in the aged brain, and that specific Ca^{2+} pathways can affect APP metabolism. While further studies are required to replicate the linkage of the CALHM1 rs2986017 polymorphism to AD, this important finding shows how changes in Ca^{2+} influx pathways can alter APP processing and Aβ production [190].

Oxidative stress and Alzheimer's disease

All aerobic organism are susceptible to oxidative stress simply because semireduced oxygen species, superoxide and hydrogen peroxide are produced by mitochondria during respiration [191]. The brain is particularly vulnerable to oxidative processes because: (I) glucose is the major nutrient and, therefore, the brain has a high glucose metabolism and respiratory turnover; (II) it has only low levels of antioxidant defense enzymes compared to other tissues; (III) it contains high concentrations of polyunsaturated fatty acids, which are potential substrates for lipid peroxidation; and (IV) it is rich in enzymatically active transition metals, which can potentially catalyze radical formation [192]. In addition to the oxidative phosphorylation in the mitochondria, numerous other enzymatic and non-enzymatic cellular mechanisms exist that can generate O^{2-} or H_2O_2 [192]. The AD brain is under intense oxidative stress [193]. Among the mechanisms involved in Aβ-mediated neurotoxicity, oxidative stress (lipid peroxidation, protein oxidation, DNA and RNA oxidation) has largely been proposed to play a pivotal role in the development of AD (Fig. 10) [194-198].

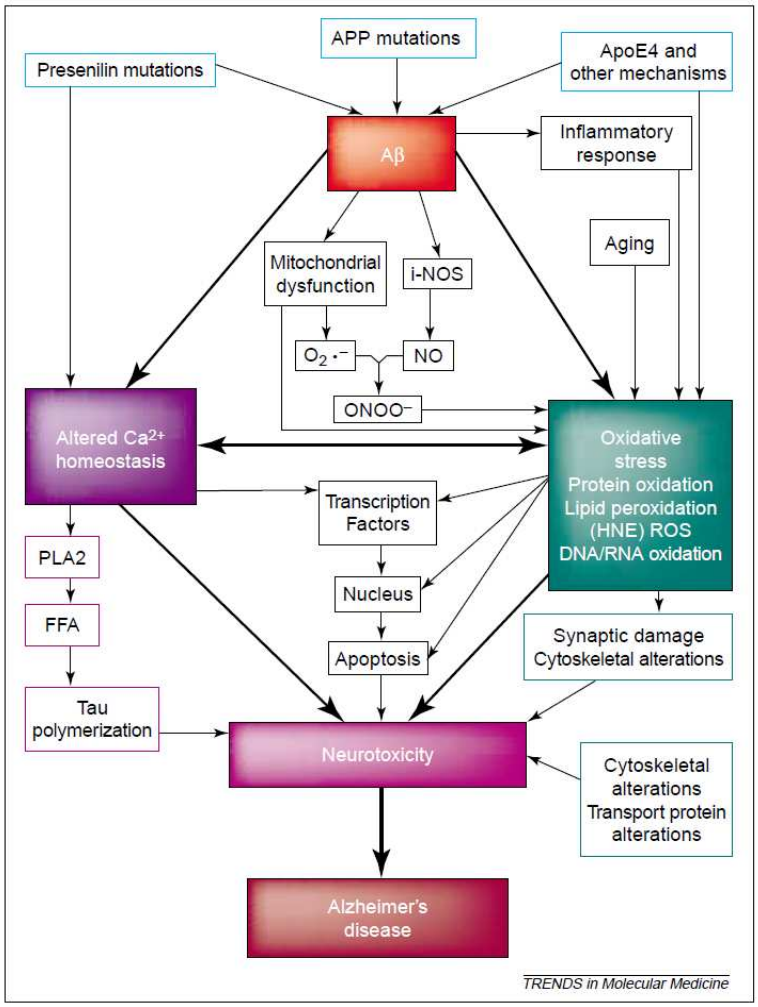

Figure 10. Central role of Aβ in the oxidative stress in, and toxicity to, neurons in AD brain. The oxidative stress is manifested by ROS formation, lipid peroxidation and subsequent modification of proteins by the reactive lipid peroxidation products HNE and acrolein. Other consequences of Aβ-associated oxidative stress are free fatty-acid release, protein oxidation, Ca^{2+} dyshomeostasis (with subsequent alterations in mitochondrial function, oxidative stress, and induction of apoptosis pathways), mitochondrial impairment, peroxynitrite formation, inflammatory response, apoptosis and other cellular responses. Ultimately, the neuron dies. Antioxidants are able to interfere with most, if not all, of these processes, including the neurotoxicity. From [193].

Aβ can fragmentate and generate free radical peptides with potent lipoperoxidizing effects on the synaptosomal membranes in the neocortex [199]. Indeed, cells experiencing amyloid toxicity usually exhibit impaired viability, oxidative stress, and mitochondrial dysfunction. Reactive oxygen species (ROS) and reactive nitrogen species (RNS) accumulation result in chemical modification of cell components including lipids, proteins, and nucleic acids leading to oxidative damage of these

biomolecules [200, 201]. Oxidative stress may be defined as an imbalance between the production of free radicals and the ability of the cell to defend against them through a set of antioxidants and detoxifying enzymes that include superoxide dismutase, catalase and glutathione peroxidase. When this imbalance occurs, oxidatively modified molecules (lipids, proteins, nucleotides) accumulate in the cellular compartment causing dysfunction [202]. It is well known that membrane destabilization by the insertion of Aβ aggregates into the lipid bilayer, and the subsequent early modifications of ion balance and intracellular redox status may trigger subsequent modifications eventually leading to cell death [56, 93, 157]. Small-angle X-ray studies showing the insertion of Aβ into the lipid domain of membranes [203], and electron microscopic immunolocalization of Aβ to the neuronal plasma membrane of cultured cells [204], confirm membranes as the target for Aβ damage. Moreover, it has recently described that amyloid oligomers exogenously added to the culture medium of fibroblasts bearing APPV717I gene mutation, obtained from familial AD (FAD) patients, can readily insert into oxidative-damaged surfaces where the membrane integrity is compromised, resulting in a prompt increase in the production of ROS [205]. These findings compel evidence that cells bearing increased membrane lipoperoxidation are more susceptible to aggregate toxicity as a result of their reduced ability to counteract amyloid oligomeric attack. These data support the rising consensus on major role of membranes as initial triggers of the biochemical modifications culminating with neuronal death [40]. Loss of membrane integrity leads to cellular dysfunction, such as inhibition of ion-motive ATPases, loss of Ca^{2+} homeostasis, inhibition of glial cell Na^{+}-dependent glutamate uptake system with consequences on neuronal excitatory NMDA receptors, loss of protein transporter function, disruption of signaling pathways, and activation of nuclear transcription factors and apoptotic pathways [206]. Usually, in cells, the rise of free Ca^{2+} is associated with a marked increase in ROS. This is a result of the activation of oxidative metabolism following the increased need for ATP required by the Ca^{2+} pumps to clear the excess free Ca^{2+} [93]. In turn, ROS increase may reinforce the rise of free Ca^{2+} by inhibiting the Ca^{2+} pumps. In addition, ROS trigger mitochondrial impairment and consequent intrinsic or extrinsic apoptotic pathways [93], or in some cases lead to cell death by necrosis [93]. Several studies have shown that the role of methionine 35 (Met-35), in conjunction with the secondary structure of the Aβ42 itself, is critical for

the oxidative and neurotoxic properties of the peptide [207]. Mutagenesis studies on the C-terminal helical region of the peptide suggest that presence of Aβ42 in the lipid bilayer is necessary for induction of Met-35 lipid peroxidation and subsequent neurotoxicity. The lipoperoxidation process could influence the pathogenesis of AD [201]. Lipid peroxidation can lead to changes in the membrane fluidity, formation of conjugated dienes, multiple aldehydes, and isoprostanes, the release of free fatty acids, and a consequent decrease in levels of polyunsaturated fatty acids (PUFA), *etc*. [206]. Indeed, 4-hydroxynonenal (4-HNE), which is one of the most reactive end products of lipoperoxidation, appears to induce neuronal death upon binding to proteins by altering important transporter proteins, such as the ATPases involved in Ca^{2+} homeostasis and the glutamate transporter EAAT2 [207, 208]. The healthy brain is protected from oxidative injury by antioxidant defences that include antioxidant enzymes and free radical scavengers. It has therefore been proposed that the weakening of cell antioxidant defenses (TAC) may contribute to AD pathogenesis [208]. This hypothesis agrees with data indicating that lymphoblasts and fibroblasts from FAD patients carrying mutations in the APP and PS-1 genes display a significant TAC impairment, with altered glutathione (GSH) levels and a marked increase in membrane lipoperoxidation compared to the same cells from age-matched healthy controls [205, 209, 210].

-CHOLESTEROL IN THE CENTRAL NERVOUS SYSTEM-

Sterols are essential components of eukaryote membranes. Their incorporation enhances the packing of the acyl chains of phospholipids in the hydrophobic phase of the bilayer, increases its mechanical strength, and reduces its permeability [211]. Cholesterol is an essential component of the plasma membrane of all cells (nearly 90% of total cellular cholesterol), where it increases membrane rigidity reducing lipid disorder. Cholesterol determines the biophysical properties of cell membranes by its unique structure, lowers the permeability of membranes, possibly by compacting phospholipids, and regulates their fluidity in a temperature-dependent manner by changing the order of fatty acyl chains. Importantly, cholesterol also determines the functional properties of membrane-resident proteins like ion channels and transmitter receptors [212, 213]. Mammals and other vertebrates can either make sterols *de novo* or

get cholesterol from the diet. The homoeostasis of cholesterol in the brain is maintained by a series of interdependent processes that include synthesis, storage, transport, and catabolism. Glial cells and neurons can synthesize cholesterol *de novo*, while cholesterol can also be recycled from extracellular locations within the Central Nervous System (CNS). Essentially all the cholesterol used in the brain appears predominantly synthesized *de novo* in the CNS, where it enhances the production of pre-synaptic components and synaptic vesicles, whereas statins block dendrite outgrowth and axonal branching [214]. Neuronal cells appear to synthesize most of the cholesterol needed for their growth and synaptogenesis during development, whereas mature neurons progressively lose such ability, getting cholesterol from glial cells, particularly astrocytes, possibly as a consequence of the large metabolic requirement in the biosynthesis of cholesterol, and the need for optimal energy efficiency within the CNS [215]. The brain synthesizes essentially all of its cholesterol and does not appear to depend on the circulating pool of the steroid; actually, the plasma lipoproteins do not cross the blood brain barrier (BBB) and do not deliver significant amounts of cholesterol to the CNS [216]. In the adult brain, the astrocytes not only synthesize, but also internalize and recycle the cholesterol released from degenerating nerve terminals to deliver it back to neurons [217]; this transport requires cholesterol binding to one of the variants of apolipoprotein E (ApoE), a major lipoprotein in the CNS that is synthesized by astrocytes [218]. ApoE is a ligand for cell surface lipoprotein receptors such as the LDL receptor and the LDL receptor-related proteins (LRP); ApoE also regulates lipid transport to neurons and clears cholesterol from the extracellular space [219]. ApoE-cholesterol complexes internalized by endocytosis are then hydrolyzed in the neuronal lysosomes allowing the intracellular release of free cholesterol, with reduction of endogenous synthesis, by 3-hydroxy-3-methylglutarylCoA reductase (HMGCoAR) inhibition, and storage upon fatty acid esterification by acyl-coenzyme A cholesterol acyltransferase (ACAT) [219]. As neuronal membranes must be kept with a reasonably constant amount of cholesterol, so to guarantee proper function, a mechanism for cholesterol elimination is required. Because there is no degradation mechanism for this sterol any excess must exit the brain into the circulation. Cholesterol exchanges between the CNS and the circulating blood imply the participation of the BBB, that hinders the direct passage to the CNS of the blood cholesterol and limits the

reverse passage of cholesterol from the CNS to the venous circulation. Hydroxylation of the side chain of cholesterol by the cholesterol 24-hydroxylase allows the sterol molecule to cross the BBB freely [220]. In fact, the main product of brain cholesterol metabolism is the 24-hydroxy derivative that is translocated to the circulating blood through the BBB. This mechanism is responsible for the catabolism of most of the cholesterol that is turned over in the brain. In conclusion, the cholesterol content of cellular membranes is tightly controlled by elaborate mechanisms that balance the level of cholesterol synthesis, uptake, transport and release, allowing neurons and glial cells maintain proper sterol levels.

Lipid rafts

Cholesterol is not uniformly distributed in biological membranes, but it is found mainly in the cytofacial leaflet, where together with other lipids like sphingomyelin is concentrated in microdomains or rafts, and plays key roles in neuronal development as well as in the maintenance of neuronal plasticity and function [221]. The plasma membrane displays a complex structure with different regions coexisting in dynamic equilibrium. Among these, caveolae and lipid rafts – purified as detergent-resistant membrane fractions (DRMs) – appear to be involved in many cellular processes as well as endocytosis, signalling, oxidative stress, apoptosis, ion homeostasis and membrane protein trafficking and turnover [222, 223]. DRMs are cholesterol-, sphingolipid- and ganglioside-rich dynamic ordered microdomains freely diffusible throughout the cell membrane, which display very short half-lives and persistence times of the molecules embedded within them [224]. In lipid rafts, cholesterol is thought to act as a spacer between the hydrocarbon chains of the sphingolipids and as a dynamic glue that holds together rafts upon assembly. Cholesterol removal results in raft disassembly with dissociation, deregulation and/or inactivation of most raft proteins [225]. Many experimental data suggest that by means of raft formation, cholesterol contributes to the dynamic compartmentalization of molecules, allowing the fine-tuned modulation of signaling and proteolysis events [226], and it serves as a precursor or cofactor of several signaling molecules [226]. As the main constituent of rafts, cholesterol also contributes to raft molecule endocytosis [227], it is required for the formation of synapses [228] and it is a major component of the myelin sheath essential for an efficient electrical

transmission [229]. In particular, cholesterol is decisive for the ability of neurons to communicate. For that reason the brain posses a most robust mechanism to maintain the levels of cholesterol, in the neurons and their supporting cells, as independent as possible from the variations that occur in the circulation [215]. Due to the highly ordered nature of lipid rafts, glycosyl-phosphatidylinositol (GPI) anchored and doubly acylated proteins tend to cluster in these microdomains. Additionally, other proteins have shown the ability to move in and out of membrane rafts in response to ligand binding or oligomerization. Lipid rafts contain a variable set of membrane proteins and their clustering is thought to provide a spatial and temporal meeting point for signalling molecules, as well as for molecules involved in processing and trafficking of membrane proteins. This includes the APP and at least some of the proteases carrying on its cleavage [129, 230]. In particular, lipid rafts have been proposed to function as platforms where neurotoxic oligomers of proteins and peptides, including the prion protein (PrP) and the Aβ peptides, are assembled [231]. Actually, lipid rafts appear directly involved in prion protein stabilization and in the pathological conversion of the cellular (PrPc) to the scrapie (PrPsc) form [232]. Moreover, the PrPc conformation can be stabilized upon association with lipid rafts in the secretory pathway [233]. Increasing evidence shows that Aβ can also associate with lipid rafts and components of DRMs isolated from human and rodent brain as well as from cultured cells. Aβ was found to be tightly associated with monosialotetrahexosylganglioside (GM1), and it was originally postulated that this may act as a seed for its accumulation and aggregation [234]. Accordingly, it has been proposed that soluble Aβ peptide and PrP aggregation can be raft-associated processes [132] and that any alteration of cholesterol (as well as sphingolipid) homeostasis can be a shared primary cause of a number of neurodegenerative diseases [235]. All these findings, together with the presence, in the raft domains, of ligand-gated calcium channels (the AMPA and NMDA glutamate receptors) involved in Ca^{2+} influx into neuronal synaptic ends [236, 237] and in Ca^{2+} permeabilization of amyloid-exposed cells [238] has implicated lipid rafts also in functional impairment of cells exposed to β-amyloid [239]. However, no clear mechanistic evidence is presently available concerning the molecular and biochemical features of the relation between lipid rafts, their lipid content and dynamics, the generation of the aggregate precursors, as well as amyloid growth and toxicity. A recent

study aimed at providing information on the proteins involved in extracellular Aβ internalization inside primary neuronal cells has suggested a caveolae-independent, raft-mediated mechanism. This implies lipid rafts as contributors not only to Aβ biogenesis and accumulation [132] but also to extracellular Aβ translocation [240] and aggregation [239]. A recent report highlights a Fyn-dependent mechanism as a possible molecular basis of membrane-bound Aβ oligomer recruitment to lipid rafts [241], even if the relation between the preferential amyloid recruitment and physicochemical modifications of lipid rafts is currently unclear.

A protective role for lipid raft cholesterol against amyloid-induced membrane damage

Several reports showed that the disruption of cholesterol homeostasis can be detrimental to cells because toxic Aβ aggregates interact more easily with cholesterol-poor membranes [94, 186, 242]. It has been recently demonstrated that membrane cholesterol can influence ADDL cytotoxicity to human neurotypic SH-SY5Y cells by modulating either the physical state of the cell membrane, mainly at the lipid raft level, or oligomer binding to the membrane itself, in most cases a key step in amyloid cytotoxicity. In particular, it seems that the cholesterol content of the cell membrane is inversely correlated with the membrane perturbing effects of Aβ42 oligomers [243]. Many reports suggest that Aβ binding and aggregation, as detected by ThT or Congo Red staining, occur in lipid raft domains where it is favoured by clusters of the key component GM1 ganglioside [241, 244]. It has also been hypothesized that Aβ42 adopts an altered conformation upon binding to GM1 and that in such an altered conformation it can act as a seed for Aβ fibrillogenesis in AD brain [244]. Moreover, numerous findings indicate that GM1 clusters are affected by membrane cholesterol depletion [245]. There are several reported findings on the effect of cholesterol on amyloid aggregate binding to the cell membrane [186, 242], in particular, in neuroblastoma cells, a mild loss of neuronal membrane cholesterol results in an increased binding of ADDLs to neuronal lipid rafts, while cholesterol-enriched membranes exhibited a significantly reduced ADDL-rafts colocalization [243]. There is no consensus on the steady-state fraction of rafts in the cell membranes, their size, location and lipid/protein composition, which might reflect rapid raft dynamics accounting for intrinsic raft

heterogeneity in different cultured or tissue cells. In fact, whether, and to what extent, these isolated DRMs reflect the physical, chemical and biochemical organization of lipid rafts *in vivo* remains to be elucidated. The ability of ADDLs to interact with purified DRMs and the effect of such interaction on physical and morphological features of the latter has been recently investigated [243]. The use of fluorescent probes to monitor the structural order and dynamics within the acyl chain region of liposome lipid bilayers is a technique abundantly used nowadays. The linear probe 1,6-diphenyl-1,3,5-hexatriene (DPH) is the more widely and easily used and is seen as particularly useful when quantitative interpretation of observations in terms of details of bilayer dynamics and order are critical [246]. The DPH probe partitions equally between the ordered and the disordered phases of membrane lipid domains [247]. It is evenly distributed throughout all the lipidic regions in the plasma membrane of a living cell [246] and its location is similar in membranes with different content of cholesterol [248]. Anisotropy fluorescence measurements of DRMs purified from neuroblastoma cells confirmed that there is an inverse relation between cholesterol content and membrane perturbing effects of ADDLs. In particular, the DRMs microdomains purified from cholesterol-enriched cells are less susceptible to the decrease of fluidity caused by Aβ oligomers, conversely, the loss of cholesterol resulted in a higher susceptibility of disassembled lipid rafts, not only to Aβ42 oligomers but also to the Aβ42–1 monomeric peptide. This suggests that the more fluid the lipid raft membrane, the greater its ability to bind non-specifically Aβ42 and, possibly, other peptides [243]. The presence of β-sheet structure appears to be required for the membrane perturbing properties of Aβ oligomers only in DRMs mimicking raft microdomains with basal cholesterol content, but not in DRMs purified from cholesterol depleted plasma membranes, in agreement with previously reported evidences in synaptosomal plasma membranes [249]. In a recent study, rafts purified from the plasma membrane of neurotypic model cells previously enriched or depleted in cholesterol were for the first time imaged by atomic force microscopy (AFM) in liquid and it was shown that treatment of DRMs with ADDLs resulted in the formation of large cavities, or hollows. The size and depth of these cavities were significantly reduced in DRMs purified from cholesterol-enriched cells, suggesting cholesterol may protect against amyloid-induced cell membrane damage at the lipid raft level. The ADDL–lipid interaction may result in

lipid depletion from the bilayer, with the formation of steps reflecting differences between the thickness of a standard bilayer and that of a thinner phase [243]. Similar effects have been observed previously in supported lipid bilayers exposed to prefibrillar amyloid aggregates [92]. A thinner phase may result from lipid interdigitation, as observed in supported lipid bilayers interacting with transmembrane peptides [250]. Alternatively, oligomer interaction with the bilayer may induce trans–gauche conformational changes of the lipids, giving rise to a reduced bilayer thickness [251]. The formation of cavities was observed also in DRMs purified from cells pre-treated with Aβ42 oligomers [243]. However, in this case the depth and size of the cavities were significantly reduced, suggesting that living cells are able to resist, at least in part, ADDL-induced membrane damage. A typical feature of DRM samples observed by AFM was the presence of domains protruding from the lipid surface. These domains were shown to consist of fluid protein or lipoprotein complexes. In fact, they disappeared in the presence of proteases and displayed higher adhesion forces than the background [243]. Furthermore, it has been found that the domain size inversely correlates with the cholesterol content, reflecting increased environment fluidity, on the contrary, domain height directly correlates with the cholesterol content, as the result of an increased compliance of the cholesterol-depleted DRM environment. In addition, treatment of DRMs with ADDLs induced changes in domain morphology that appeared to depend on the content of cholesterol and suggested domain disassembly [243]. Overall, these data on DRM domains provide information on the structural and morphological features of the cell plasma membrane and its cholesterol- and GM1 ganglioside-enriched raft domains. In particular, they suggest that the cholesterol content affects the ability of ADDLs to interact with the cell membrane by modulating membrane physical features at the raft level.

Role of cholesterol in AD

There is growing evidence that a link between cholesterol and the pathogenesis of AD exists [252]. ApoE is one of the major apolipoproteins in the plasma and the principal cholesterol carrier in the brain. In humans there are three common allele of APOE gene: ε2, ε3, ε4. Numerous independent studies have consistently confirmed that the ε4 allele of the APOE is the most prevalent risk factor for sporadic AD [253]. The risk for AD

conferred by APOE ε4 increases in a dose-dependent manner; however APOE ε4 is neither necessary nor sufficient to cause AD [254]. A key role of membrane cholesterol as a modulator of Aβ peptide production and clearance [128] as well as aggregation and neurotoxicity [186, 242, 255, 256] has recently been described. High cholesterol levels as risk factor for AD were first proposed in the early 1990s and since then considerable biochemical and clinical research has claimed the existence of a link between cholesterol, statin therapy and AD development [257-259]. Indeed, it was reported that lowering membrane cholesterol by statins and a cholesterol extracting drug (methyl-β-cyclodextrin) resulted in the drastic reduction of amyloid production both *in vitro* and *in vivo* [257, 258]. Presently, the question of whether statins can lower the incident rate of AD remains unresolved [260]. In general, these observations lead to hypothesize that lowering the levels of cellular cholesterol would be a therapeutic target in the treatment of AD. On the other hand, high dietary cholesterol was shown to increase Aβ levels [258] and increased content of cholesterol in the brain appeared to correlate with an increased risk of developing AD. However, not all studies sustain this vision and epidemiological studies on the association between plasma cholesterol levels and the development of AD have produced contradictory conclusions [261]. Indeed, it is known that hydrophilic statins do not cross the BBB and that brain cholesterol progressively reduces with increasing age (the main risk factor for sporadic AD), such decrease appearing considerably accelerated in AD people [262, 263]. Two alternative scenarios involving lipid rafts, based on conflicting experimental results have been proposed to describe the effect of cholesterol in Aβ generation and aggregation in AD. The high neuronal membrane cholesterol model for AD claims that high cholesterol favours APP processing with increased Aβ generation and aggregation through lipid raft clustering bringing into close contact the resident populations of APP and its processing enzyme BACE-1 [264]. The alternative low neuronal membrane cholesterol model claims that most of the APP is normally located in non-raft membrane domains. Accordingly, low membrane cholesterol would favour raft disassembly and BACE-1 translocation to non-raft domains supporting its contact with APP and enhancing cleavage of the latter with Aβ generation and aggregation (Fig. 11) [264]. Taken together, the findings reported in the last decade depict lipid rafts both as key domains where APP processing occurs and as primary interaction sites of ADDLs (and, possibly, other amyloid aggregates).

However, much must still be learnt about the effective specificity and the biochemical, molecular and biological significance of such interaction.

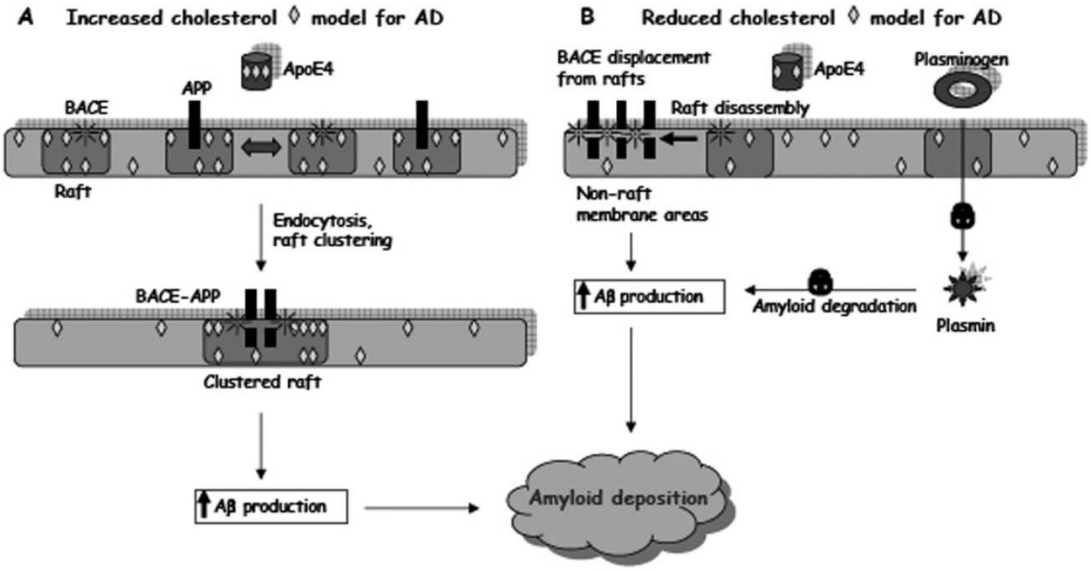

Figure 11. The high (**A**) and low (**B**) neuronal membrane cholesterol models of AD pathogenesis. The high cholesterol model assumes that low neuronal membrane cholesterol is protective against AD. In fact, high membrane cholesterol would result in increased lipid raft co-clustering and APP-BACE1 co-localization thus favouring the amyloidogenic pathway of APP processing with increased Aβ production. On the contrary, the low membrane cholesterol model envisages a protective role of relatively high amounts of membrane cholesterol assuming that APP is located in non-raft membrane domains. From [225].

The changes in the lipid composition of the neuronal membranes may have regulatory consequences for interactions of Aβ aggregates with cells in the brain. The presence of cholesterol in neuronal membranes is known to induce large changes in membrane physical features such as fluidity and density of lipid packing resulting in alterations of aggregate recruitment to the membrane and membrane permeabilization [184, 186]. In particular, it has been reported that the presence of cholesterol in artificial lipid bilayers inhibits the channel-forming activity of human amylin and reduces the insertion and formation of ion channels by Aβ40, Aβ42, and Aβ25–35 peptides [184-186]. Membrane cholesterol also interferes with neuronal apoptosis induced by soluble oligomers of Aβ peptide [256]. On the other hand, reducing membrane cholesterol makes the cell more vulnerable to the action of amyloid aggregates [186]. Accordingly, it has previously reported a significant correlation between resistance to amyloid toxicity and membrane

cholesterol content in various cultured cell types [94]. It has recently been shown that selective Alzheimer's disease indicator-1 (seladin-1) gene, whose proteic product catalyzes the last steps of cholesterol biosynthesis, appears to be down-regulated in brain areas affected by AD [265]. Seladin-1 overexpression appears to protect neuroglioma H4 cells against Aβ-mediated toxicity by reducing oxidative stress and caspase-3 activity [265]. Some recent findings also indicate that seladin-1-induced membrane cholesterol enrichment protects SH-SY5Y cells against amyloid toxicity by reducing the interaction of Aβ42 oligomer with cell membrane, featuring seladin-1 as a susceptibility gene candidate for sporadic AD [266]. These data support a link between AD pathogenesis and loss of brain cholesterol suggesting that a fine modulation of the levels of this membrane sterol plays a crucial role in neuronal viability.

-PROTECTIVE EFFECT OF GLUTATHIONE IN AD-

Intracellular sources of reactive oxygen species

The observation that biomolecules, which consist primarily of carbon, hydrogen, oxygen, nitrogen and sulfur, are disrupted by the presence of oxygen (O_2) is an evolutionary paradox for aerobic life [267]. A wide variety of reactive oxygen species (ROS) can be found in biological systems. These ROS differ in their site of formation, their physiological function, their reactivity and their biological half-life. Mitochondria, nitric oxide synthase, arachidonic acid metabolism, xanthine oxidase, monoamine oxidase and P450 enzymes are sources of ROS in the brain. Correspondingly, healthy brain cells possess high concentrations of both enzymatic and small molecule antioxidant defenses (Fig. 12). The enzymes include CuZn-superoxie dismutase and Mn-superoxide dismutase, GSH-Peroxidase (GSH-Px) and catalase, as well as the small molecules glutathione (GSH), ascorbic acid, vitamin E and a number of dietary flavonoids. Thus, under normal physiological conditions cells manage with the flux of ROS. Oxidative stress describes a condition in which cellular antioxidant defenses are insufficient to keep the levels of ROS below a toxic threshold. This may be either due to excessive production of ROS, loss of antioxidant defenses or both (Fig. 12).

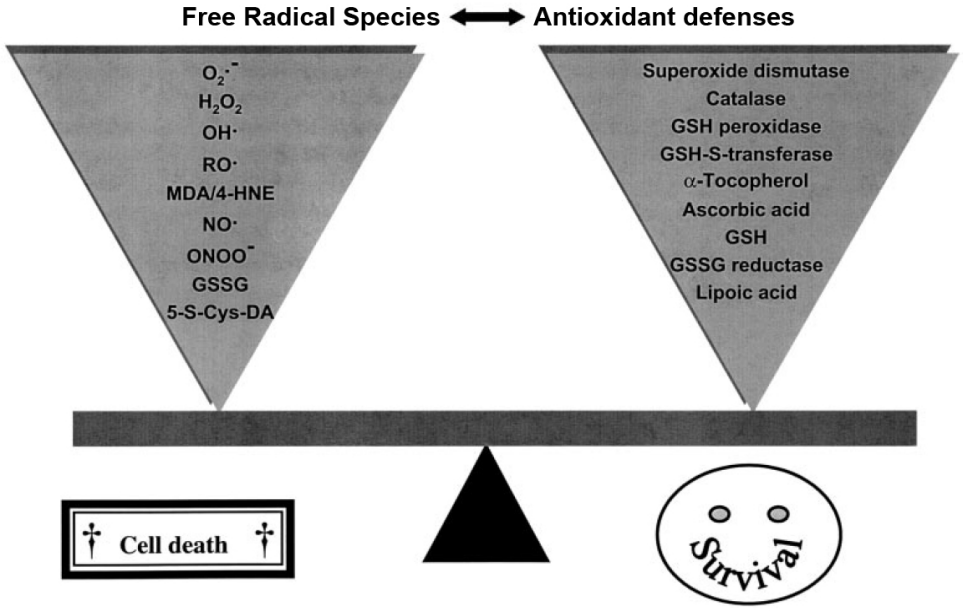

Figure 12. Balance of ROS generation and antioxidative systems. An imbalance of both systems due to either excessive production of ROS (left) or reduced antioxidant defense (right) leads to oxidative stress Modified from [268].

Glutathione homeostasis

GSH is a tripeptide (L-γ-glutamyl-L-cysteinyl-glycine) that serves several essential functions within the cell [269-271]. It is the most abundant nonprotein thiol in almost all aerobic species, occurring at intracellular concentrations of 0.5 to 10 mM. In contrast, extracellular GSH concentrations are usually 3 to 4 orders of magnitude lower. Under physiological conditions, GSSG reductase maintains more than 98% of intracellular GSH in the reduced, thiol form (GSH). The rest is present within the cell as mixed disulfides (mainly GS-S-protein), as the disulfide (GSSG), and as thioethers. The key functional element of the GSH molecule is the cysteinyl moiety, which provides the reactive thiol group and is responsible for the many functions of GSH. These functions include (*I*) the maintenance of protein structure and function by reducing the disulfide linkages of proteins, (*II*) the regulation of protein synthesis and degradation, (*III*) the maintenance of immune function, (*IV*) protection against oxidative damage, and (*V*) detoxification of reactive chemicals. Moreover, GSH contributes as a storage and transport form of the cysteine moiety and it functions in leukotriene and prostaglandin metabolism [269-272]. The key structural elements of GSH are the γ-carboxyl peptide

linkage of glutamate and the presence of the C-terminal glycine, which directly determine its metabolism and function. The N-terminal glutamyl and cysteinyl moieties are linked through the γ-carboxyl group of glutamate instead of the more common α-carboxyl peptide linkage, restricting cleavage to γ-glutamyl transpeptidase (γGT), which occurs on the external surface of certain cell membranes. Therefore, GSH is resistant to intracellular degradation and can only be cleaved by cell types that have γGT on the cell membrane. The presence of the C-terminal glycine protects the peptide against cleavage by intracellular γ-glutamylcyclotransferase.

Glutathione biological functions

GSH is predominantly involved in regulation of cellular sulfhydryl status *via* redox reactions. All aerobic organisms are subject to physiological oxidative stress as a consequence of aerobic metabolism. The intermediates that are formed, including superoxide and hydrogen peroxide, lead to the further production of toxic oxygen radicals that can cause lipid peroxidation and disrupt metabolic processes. GSH is the predominant defense against these toxic products of oxygen, particularly in the mitochondria, a major site for the synthesis of reactive oxygen intermediates [269]. Mitochondrial GSH is critical in the defense against both physiologically and pathologically generated oxidative stress. Mitochondria do not have the enzymes necessary for GSH synthesis, and they import cytosolic GSH. Endogenously produced hydrogen peroxide is reduced by GSH in the presence of selenium-dependent GSH peroxidase (GSH–Px) (Fig. 13). As a consequence, GSH is oxidized to GSSG, which in turn is rapidly reduced back to GSH by GSSG reductase at the expense of reduced nicotinamide adenine dinucleotide phosphate (NADPH), thereby forming a closed system (redox cycle) as illustrated in figure 13. Under normal conditions, GSSG reductase is quite effective at maintaining most cellular GSH in its reduced state (more than 98% GSH). However, under severe oxidative stress or where GSSG reductase activity is impaired, the ability of the cell to reduce GSSG may be overwhelmed, leading to its accumulation within the cytosol. To protect itself from a shift in redox equilibrium, the cell can actively transport GSSG out of the cell. However, GSSG may also react with cellular protein sulfhydryls *via* a mixed disulfide reaction, a process that can result in impaired protein function. Furthermore, GSH is implicated in regulation of

cellular sulfhydryl status *via* thiol-disulfide exchange. As oxygen tension in the environment increased during evolution, aerobic organisms needed a system to restore key sulfhydryl groups to their reduced state after exposure to oxidative stress [273, 274]. Without a process to reduce protein disulfides, vulnerable cysteinyl residues of essential enzymes might remain oxidized, leading to changes in catalytic activity.

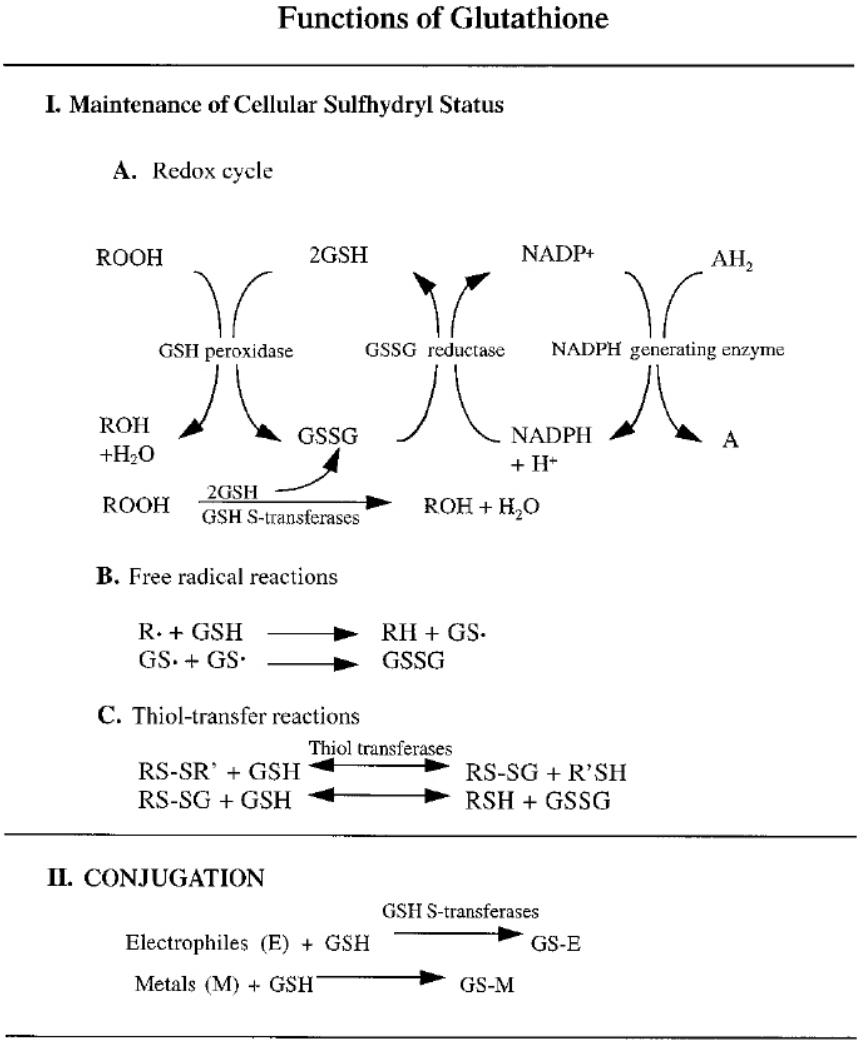

Figure 13. The detoxification functions of GSH include the conjugation of electrophilic chemicals and reactive metals and the maintenance of the cellular thiol redox status. AH2 and A, reduced and oxidized forms, respectively, of compounds that participate in the synthesis of NADPH; RH and R, reduced and oxidized forms, respectively, of some organic molecules; ROOH, a hydroperoxide; ROH, an alcohol; RS-SG, a glutathione thioester; RS-SR', a mixed disulfide of two organic molecules. From [275].

This function is fulfilled by the thiol-disulfide exchange catalyzed by thiol-transferases in the presence of GSH, and may be essential to aerobic life (Fig. 13). The

thiol-disulfide equilibrium within the cell may regulate certain metabolic pathways by activating or inactivating key enzymes. Whereas many proteins are active when the key sulfhydryls are in the thiol form, others require them to be in the oxidized, disulfide form. Because the thiol-transferase reaction is bidirectional, the equilibrium will be determined by the redox state of the cell. Moreover, GSH regulates the cellular sulfhydryl status *via* storage and transfer of cysteine. Cysteine autooxidizes rapidly to cystine, producing potentially toxic oxygen radicals [276]. To avoid the toxicity of the autooxidation reaction, most of the nonprotein cysteine is stored as GSH. The liver and kidney play a major role in the homeostasis of GSH and cysteine [269]. Finally, GSH is implicated in conjugation of electrophiles and metals. GSH plays a major role in detoxifying many reactive metabolites by either spontaneous conjugation or by a reaction catalyzed by the GSH S-transferases [272, 277, 278]. GSH S-transferases have broad and overlapping substrate specificities, which allow them to participate in the detoxification of a chemically diverse group of compounds. The most common reactions involve nucleophilic attack by GSH on an electrophilic carbon: saturated carbon atoms (e.g., alkyl halides, lactones and epoxides), unsaturated carbon atoms (e.g., α, β-unsaturated compounds, quinones and quinonimines, and esters), or aromatic carbon atoms (e.g., aryl halides and aryl nitro compounds [279]. The substrates have in common a degree of hydrophobicity and possess electrophilic centers that undergo nucleophilic substitution, nucleophilic addition to α, β-unsaturated ketones or epoxides or, in the case of hydroperoxides, nucleophilic attack on electrophilic oxygen, resulting in reduction. GSH S-transferases are a family of multifunctional enzymes present in the cytosol of most cells as homodimeric or heterodimeric proteins, with subunit molecular weights ranging from 24,000 to 27,500 [278, 280]. GSH also forms metal complexes *via* nonenzymatic reactions [281]. GSH is one of the most versatile and pervasive metal binding ligands and plays an important role in metal transport, storage, and metabolism. GSH works (*I*) in the mobilization and delivery of metals between ligands, (*II*) in the transport of metal across cell membranes, (*III*) as a source of cysteine for metal binding, and (*IV*) as a reductant or cofactor in redox reactions involving metals. The sulfhydryl group of the cysteine moiety of GSH has a high affinity for metals, forming thermodynamically stable but kinetically labile mercaptides with several metals, including mercury, silver, cadmium, arsenic, gold, zinc, and copper. Conjugation with

GSH is not always protective but may actually activate compounds. For example, the GSH conjugation of dibromoethane, which is used as a lead scavenger in leaded gas, forms a 2-bromo-thioether, which is subsequently transformed into a highly reactive, mutagenic, and carcinogenic intermediate, possibly an episulfonium [282]. Sulfur mustards are capable of alkylating nucleophilic sites in proteins and DNA. Other classes of compounds, including nephrotoxic haloalkenes, quinones, and isothiocyanates, are also converted by GSH conjugate formation to toxic metabolites [283, 284].

Glutathione and aging

The aging process represents various morphological and biochemical changes that occur from maturity to senescence, rendering the organism more vulnerable to disease and toxicity and eventually leading to death [285]. According to the oxidative stress hypothesis of aging, the senescence-associated loss of functional capacity is due to the accumulation of molecular oxidative damage [286] by toxic free radicals produced during normal respiration. The defenses evolved to limit the rate of production of free radicals and to scavenge those that are produced. The most reliable and robust risk factor for neurodegenerative diseases is normal aging. Aging results in the increased formation and release of ROS with consequent biochemical and functional alterations, increased protein oxidation, and DNA damage [287]. There is substantial evidence that mitochondrial function declines with age. Direct evidence for age-dependent increase in oxidative damage to mitochondrial DNA comes from measurements of 8-hydroxy-20-deoxyguanosine (8OH20dG), which is an oxidized form of deoxyguanosine that occurs following attack by a variety of free radicals [288]. An involvement of oxidative stress in aging has been further strengthened by reports of increases in tissue lipid peroxidation with age. Therefore, antioxidant defenses may play a major role during normal aging. In particular, GSH may contribute to longevity in various ways. The protective capacity of GSH is due to the reactive sulfhydryl cysteine moiety which can bind to electrophilic sites on xenobiotics and endogenous toxins. The resulting highly water soluble conjugate is excreted through the kidney [289]. In addition, free radical scavenging by GSH can occur either non-enzymatically or in conjunction with GSH–Px [290]. An age-related decline in GSH has been observed in a number of senescent organisms including mosquitoes, adult houseflies, fruit flies, mice, rats and humans

[286]. Glutathione concentrations in the cerebral spinal fluid (CSF) of humans decrease during aging [291], while the forced ectopic expression of GSH prolongs the life span [286]. Such studies suggest that age-related decreases in GSH may represent a key factor in the aging process and may underlie a number of changes occurring in normal aging and the onset of various diseases.

Glutathione in the nervous system

The GSH system plays a central role in thiol status control in the brain. GSH, as free radical scavenger, is particularly effective against the $^{\cdot}OH$ radical. The ability of GSH to non-enzymatically scavenge both singlet oxygen and $^{\cdot}OH$ [292] provides a first line of antioxidant defense. Glutathione is synthesized and degraded in most cell types by a series of well characterized enzymatic reactions [293]. Reduced GSH strongly modulates the redox state (*ratio* of oxidizing to reducing equivalents) of the cell, a role which is critical for cell survival [191]. In addition to antioxidative actions, GSH is involved in a number of other essential tasks including DNA synthesis and repair, protein synthesis, amino acid transport, enhancement of immune function, and enzyme activation [294]. Roles specific to the nervous system appear to include actions as a redox modulator of some ionotropic receptor currents [295] and as a potential neurotransmitter [296]. Due to such multiple roles in normal tissue, there is a considerable potential for alterations in GSH to be causally associated with disease. Lowered levels of GSH have been reported in aging, e.g., in the human lens [297] and decreased GSH status is associated with various diseases, including a number of neurological disorders [298]. Free radicals can be generated in neural cells by oxidative phosphorylation, the breakdown of neurotransmitters such as dopamine and serotonin, the over-activation of neurons by Ca^{2+} or EAAs, and Aβ production. Oxidative stress arising from free radical formation can affect the *ratio* of reduced to total GSH and the GSH status of the cell as GSH is depleted to combat such radicals. It has been suggested that GSH depletion caused nerve cell death [299]. In particular, using immature cortical neurons and a neuronal cell line, it has been shown that a decrease in GSH triggered the activation of neuronal 12-lipoxygenase (12-LOX) which leaded to the production of peroxides, the influx of Ca^{2+} and ultimately cell death. Others concluded that astrocytes in the CNS counteract oxidative stress due to their higher content of GSH as compared

to neurons [300, 301]. In addition, GSH appears to provide neuroprotection against excitatory amino acid excitotoxicity in stroke, ischemia and epilepsy [302]. GSH modulates ionotropic receptor action [303], thus, controlling transmembrane currents, and may also have excitatory neurotransmitter/neuromodulator actions in some neural pathways [296]. All of these actions together suggest that alterations in GSH status may be deleterious to normal neuronal function.

GSH: oxidative stress, mitochondrial damage and cell death

Approximately 90% of total cellular glutathione is localized in the cytosolic fraction, the rest being compartmentalized within mitochondria [304]. The mitochondrial pool of GSH is likely to be involved in maintaining intra-mitochondrial protein thiols in a reduced state. These mitochondrial protein thiols are essential for a number of functions, such as the regulation of selective membrane permeability to Ca^{2+}. A clear example of the relationship between GSH status, oxidative stress, mitochondrial damage and neuronal dysfunction/death due to excess free Ca^{2+} is shown by the effects of excessive production of H_2O_2 within mitochondria leading to depletion of mitochondrial GSH, in turn causing the oxidation of protein thiols and impairment of mitochondrial function. This relationship may have relevant implications in terms of the degeneration of dopaminergic neurons. Monoamine oxidase acts on monoamines including dopamine, producing H_2O_2 within mitochondria which may lead to a decrease in mitochondrial GSH [305]. It is clear that the loss of GSH may cause mitochondrial damage [306] and it was demonstrated that the converse situation is also true, namely, that impairment of mitochondrial function may lead to a decrease in cytosolic GSH. As GSH synthesis requires ATP, a deficiency of energy supplied by mitochondria is likely to affect the cellular turnover of GSH. Such situation may be particularly crucial for neurons and it is notable that it has provided evidence that mitochondria in *substantia nigra* in cat and rat show higher immunoreactivity for GSH [307]. In fact, these data lend further support to the hypothesis that the oxidative stress and neuronal damage observed in the *substantia nigra* of patients with Parkinson disease could be caused by a mitochondrial defect in GSH. Loss of glutathione and oxidative damage have been suggested to constitute early, possibly signaling events in apoptotic cell death [308]. In thymocytes, a decrease of GSH and disruption of the mitochondrial transmembrane potential preceded the onset of

apoptosis [309]. Moreover, a direct depletion of mitochondrial and cytoplasmic GSH in cerebellar granule neurons and PC12 cells, resulted in increased generation of ROS, disruption of the mitochondrial transmembrane potential and rapid loss of mitochondrial function [310].

GSH depletion in neurodegenerative disorders

Oxidative stress may be initiated by a decline in the antioxidative defense system. The most robust and significant alteration in the antioxidant defense is a decrease in GSH concentration. Reduced GSH is one of the most abundant intracellular non-protein thiols present in the central nervous system where it acts as a major cellular antioxidant within both neurons and non-neuronal cells [271]. GSH plays an important role in the adult brain by removing reactive oxygen and nitrogen species (ROS/RNS) formed during normal cellular metabolism such as during oxygen utilization by the mitochondria. GSH is synthesized in the cytosol and transported into the mitochondria via energy-dependent transporters [311]. Decreases in GSH availability in the brain promotes morphological mitochondrial damage most likely *via* increases in levels of oxidative or nitrosative stress in this organelle [312]. GSH metabolism is reported to be altered in affected brain regions from AD patients and its levels are decreased in experimental models of AD [313, 314]. Application of exogenous Aβ fibrils to neurons in culture leads to intracellular GSH depletion [315]. Recent data directly test the hypothesis that GSH is part of the cellular response to stressors associated with either intraneuronal aggregation or exogenous addition of Aβ peptide, and not simply a marker of oxidative damage, which could merely act as a downstream radical scavenger [316]. GSH, as a critical component of antioxidant defense, has been linked directly to oxidative stress, and evidence that alterations in GSH status may play a role in neurological diseases is growing. However, the oxidative stress may be only one way that changes in GSH status could affect neural function and survival. In addition to its critical role as an antioxidant/free radical scavenger, GSH may act as redox modulator of ionotropic receptors, serve as neuroprotectant against the effects of glutamatergic excitotoxicity, and may also be a unique neurotransmitter. These roles are summarized in figure 14.

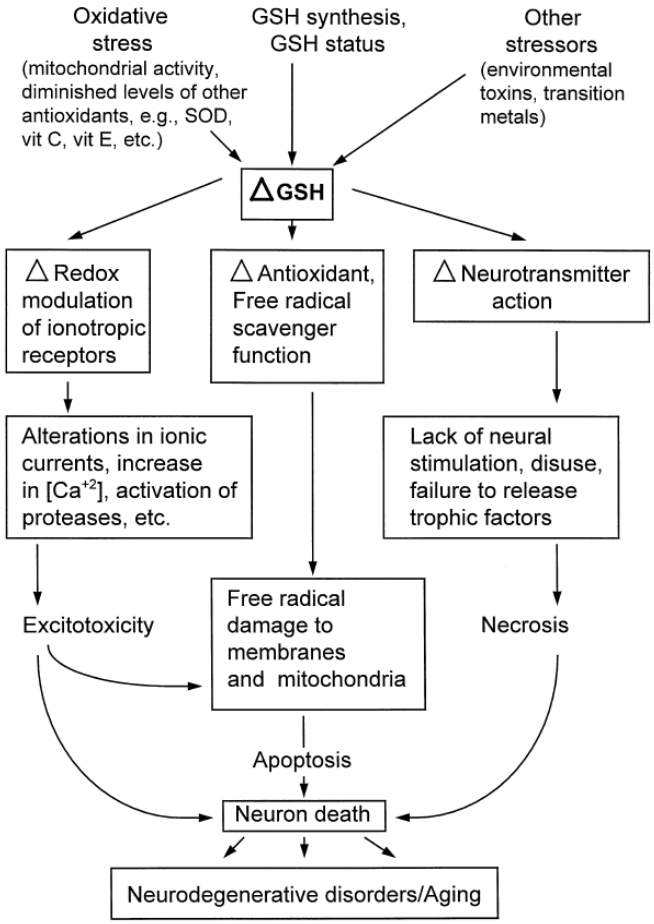

Figure 14. GSH-depletion model for neurodegenerative disorders. From [285].

The hypothesis that oxidative damage may be causal to some forms of neural degenerative diseases is not novel [287]. A specific role for GSH in such diseases has also been previously proposed [294, 317-319]. Several account for a GSH depletion model of neural disease which is constituted of many possible elements: (I) factors which determine the site of degeneration, such as selective alterations in GSH status due to abnormalities in synthesis (precursor pools or synthetic enzyme levels); GSH degradation (production of excessive glutamate or cysteine); GSH recovery from GSSG via GSH reductase; or alterations in local transport of GSH; (II) secondary stressors which increase free radical production (transition metals, H_2O_2, increased neural activity, an abnormal metabolic rate, or a defect in mitochondrial function); (III) specific neuronal vulnerability, such as the presence of 'stressors' (e.g., transition metals and/or aluminium), age, compensation by other antioxidant defenses, *etc.*

Depending on the above factors, the type of neural degeneration may be either necrotic or apoptotic and may strike more than one neural subset [285].

Glutathione in Alzheimer's disease

The brain is particularly vulnerable to oxidative damage due to the high utilization of inspired O_2, the abundance of redox-active transition metal ions, and the relative dearth of antioxidant defense systems. Free radicals are produced from a number of sources, among which are enzymatic, mitochondrial, and redox metal ion-derived sources [320]. Aging, the major risk factor for AD, leads to loss of free radical scavenging ability by endogenous mechanisms [320]. Hence, the normal balance between free radical generation and free radical scavenging is disrupted with aging and other oxidative stress conditions [321]. Strong evidence that oxidative stress was involved in the pathogenesis of AD come from a clinical study showing that oral vitamin E intake delayed progression in patients with moderately severe impairment from AD [322]. A role of oxidative stress in AD is further supported by increased levels of thiobarbituric acid-reactive substances, a measure of lipid peroxidation [323]. However, studies reporting a disturbance of GSH homeostasis are less clear. The total brain levels of GSH appeared to be unaffected in AD [324], whereas GSH peroxidase and GSSG reductase were found to be elevated in different brain regions [323] Transcription of GSH peroxidase and GSSG reductase was elevated in hippocampus and inferior parietal lobule, but not in cerebellum of AD patients, which may reflect the protective gene response to the increased peroxidation in the brain regions showing severe AD pathology [325]. In fact, in AD, oxidized GSH is increased [326], while the activity of glutathione S-transferase is decreased [327], consistent with the known increase in oxidative stress in this pathology [193, 206, 328]. In particular, among the mechanisms involved in Aβ-mediated neurotoxicity, oxidative stress has largely been proposed to play a pivotal role in the development of AD [194-198]. Aβ can fragmentate and generate free radical peptides with potent lipoperoxidizing effects on the synaptosomal membranes in the neocortex [199, 329]. It has therefore been proposed that lipid peroxidation and the weakening of cell antioxidant defenses (TAC) may contribute to AD pathogenesis [208]. This hypothesis correlates with recent data indicating that lymphoblasts and fibroblasts from familial AD (FAD) patients carrying mutations in the APP and PS-1

genes display a significant TAC impairment, with altered GSH levels and a marked increase in membrane lipoperoxidation compared to the same cells from age-matched healthy controls [205, 209, 210]. Various reactive aldehydes, including 4-hydroxynonenal (4-HNE), malondialdehyde (MDA), and 2-propenal (acrolein) [320], distinctive markers of lipid peroxidation, are neurotoxic in neuronal culture and have been detected immunochemically in AD brain, particularly in neurofibrillary tangles, one of the major hallmarks of AD [330, 331]. The levels of glutathione transferase, a protective enzyme against aldehydes and especially 4-HNE, were decreased in the brain and ventricular CSF of autopsied AD and normal control subjects [327]. Nonreactive iso- and neuroprostanes, two other typical markers of lipid peroxidation, have been found in excess in AD brain and induced by Aβ [332]. In addition to protection against ROS, GSH is an excellent scavenger of lipid peroxidation products. In fact, GSH plays an important role in protecting neurons against oxidative damage and metabolic insults by detoxifying 4-HNE [285], which levels are increased in AD [333]. It has been shown that GSH protects cultured neurons against oxidative damage resulting from Aβ peptide, iron, HNE and other oxidative insults. [333, 334]. It is interesting to note that level of HNE is increased in association with degenerating neurons in brains of subjects with AD. Coupled to the loss of glutamine synthetase (GS) activity in AD brain [335], excess glutamate-induced NMDA receptor-facilitated excitotoxicity could occur in AD brain with resultant neurodegeneration. GSH also forms metal complexes via nonenzymatic reactions. The sulfhydryl group of the cysteine moiety of GSH has a high affinity for metal ions such as Hg, Ar, Cd, As, Au, Zn, and Cu, forming a thermodynamically stable complex that can be eliminated. Redox metal ions can catalyze free radical reactions and may contribute to oxidative damage observed in AD brain. Fe(II) and Cu(I) induce the Fenton reaction, producing an abundance of hydroxyl free radicals for lipid peroxidation. GSH protects against oxidative damage [333] and lipid peroxidation caused by iron toxicity [336]. A significant decrease in Cu, and significant increases in Zn and Fe, were found in AD hippocampus and amygdala, areas showing severe histopathologic alterations in AD [337]. In contrast, copper, iron, and zinc are all elevated in senile plaques of AD [338]. Together these data imply that oxidative stress plays an important role in the pathogenic process but that alterations in the glutathione system are secondary to other events leading to neurodegeneration. Since oxidative

stress may underlie some, if not all, aspects of AD neurodegeneration, and since Aβ appears central to the disease [193], considerable research has been aimed at reducing the effects of oxidative stress by use of free radical scavengers. GSH as essential cellular antioxidant plays a key role in the defense of brain cells against oxidative stress [339, 340].

Therapeutic approaches for neurodegenerative diseases

One hallmark of AD is the accumulation of Aβ peptide, which invokes a cascade of oxidative damage to neurons that can eventually result in neuronal death. Aβ is the main component of senile plaques and generates free radicals ultimately leading to neuronal damage of membrane lipids, proteins and nucleic acids. The mechanisms involved in Aβ-mediated neurotoxicity are unknown, but there is evidence suggesting that oxidative stress plays a key role [193, 194, 196]. Growing attention has been focused to investigate the oxidative mechanism of Aβ toxicity and as well in the search for novel neuroprotective agents. Previous studies reported that Aβ peptide induces *in vitro* ROS production, protein oxidation, DNA and RNA oxidation and lipid peroxidation [195]. Because of the involvement of oxidative stress-mediated toxicity in neurodegenerative events and neuronal cell death [341, 342], various experimental approaches for effective protection by antioxidants have emerged. GSH is one of the major intracellular defense systems, and depletion of GSH is known to be involved in several neurodegenerative disorders [195, 328]. Moreover, if alterations in GSH metabolism play an important role in the pathogenesis of several neurodegenerative diseases, treatments that lead to enhanced synthesis of GSH or that inhibit its degradation may result in a slowing of disease progression. Numerous potential free-radical scavengers have been tested in different experimental paradigms of oxidative stress-induced cell death, natural antioxidants such as Vitamin E [343], vitamin C, melatonin [344], ginkgo biloba [345], steroid hormones [346], *N*-acetylcysteine [347], etc. However, many clinical trials are still unsuccessful because all the antioxidants tested are poorly active in crossing the blood brain barrier (BBB). Moreover GSH itself is poorly transported into most cells or tissues. For this reason many attempts to develop GSH derivatives able to easily cross the membranes of many cell types, mimicking GSH antioxidant properties, have been made. For instance, endogenous GSH levels have been increased by dietary or

pharmacological intake of GSH precursors or GSH mimetics or "thiol-delivering" compounds [348-350]. Moreover, because GSH itself penetrates the BBB only poorly and cannot be taken up by neurons directly, treatments with GSH monoethyl ester, glutathione precursors or other glutathione analogs have been used in patients or animal models. The GSH analog YM 737 provides protection against cerebral ischemia in rats by inhibiting lipid peroxidation [319]. Because glutathione synthesis in neurons is limited by the availability of cysteine [340], compounds that can be metabolized to cysteine could be used as pro-drugs to increase neuronal GSH concentrations. In the murine mutant wobbler, treatment with the glutathione precursor N-acetyl-l-cysteine resulted in a significant reduction of motor neuron loss and elevated glutathione peroxidase levels within the cervical spinal cord [351]. Treatment with l-2-oxothiazolidine-4-carboxylate, a cysteine precursor, stimulates growth and normalizes tissue glutathione concentrations in rats fed a sulfur amino acid deficient diet [352]. Unfortunately, the therapeutic window for treatment with substances that increase brain cysteine may be narrow, because cysteine is potentially toxic for neurons [276]. Alternatively, GSH in brain can be increased by intracerebroventricular administration of the dipeptide γ-glutamylcysteine [353]. Neurons can utilize either γ-glutamylcysteine or cysteinylglycine for the synthesis of GSH [354]. In a study on 13 subjects with Amyotrophic Lateral Sclerosis, the safety and pharmacokinetic properties of procysteine, a cysteine prodrug that increases levels of intracellular glutathione was found. Procysteine entered the CSF after both intravenous and oral dosing and accumulated to significant levels in CSF [291]. However, no increase of CSF GSH concentrations were found at 4 h after i.v. infusion of procysteine. Furthermore, esters of GSH can increase cellular GSH in a variety of tissue types [355] and are particularly effective in restoring mitochondrial GSH [356]. A GSH mimetic, such as the xanthate D609 [357], protects primary neuronal culture against Aβ42-induced oxidative stress and neurotoxicity *in vitro* [358] and against Aβ42 *in vivo* [350]. D609 has the ability to scavenge hydrogen peroxide and hydroxyl free radicals. D609 can bind to reactive alkenals and detoxify their effect, thereby preventing these alkenals from damaging mitochondria [357, 359]. Although a disturbance of GSH homeostasis has been implicated in the pathogenesis of several neurodegenerative diseases it remains open to debate whether, at least in some illnesses, this is a primary defect or only a consequence

of ROS generation; brain GSH can be increased safely using different treatment strategies; and an increase of brain GSH will result in clinical benefit and/or neuroprotection in animal models or in human diseases [360]. The modulation of free radicals generated by Aβ might represent an efficient therapeutic strategy for treatment of Alzheimer's disease and other oxidative-stress related disorders. A large number of natural antioxidants have been used; nevertheless, many clinical trials are still unsuccessful because all the compounds tested have difficulty in crossing the BBB and do not readily enter the brain in the adult [348]. Considering that Aβ42 is a potent inducer of oxidative stress and that the deposition of this peptide can induce the cascade of pathological changes occurring in AD, many attempts to test effective protection by antioxidants are currently under investigation. However, many clinical trials are unsuccessful due to a low brain-accessible capability of the antioxidant compounds tested. Based on these notions, searches for new potential antioxidant compounds could be of relevance for future directions of AD treatments.

Role of dietary fatty acids in cognitive decline

Recent attention has been paid to the possible role of dietary fatty acids in age-related cognitive impairment of degenerative diseases [361]. Fatty acids can be categorized briefly into saturated fatty acids (SFA) and unsaturated fatty acids (UFA). SFA, such as stearic acid, are present in products such as meat, dairy products, cookies and pastries. Monounsaturated fatty acids (MUFA) are most frequently consumed in olive oil. The principal series of polyunsaturated fatty acids (PUFA) are n-6 (i.e. linoleic acid) and n-3 (i.e. a-linolenic acid, docosahexaenoic acid, and eicosapentaenoic acid). In the Mediterranean dietary pattern the main sources of n-6 PUFA are vegetable oils, while the principal sources of n-3 PUFA are fatty fish (salmon, tuna, and mackerel). In fact, olive oil contains 70–80% MUFA (oleic acid) and 8–10% PUFA (6–7% linoleic acid and 1–2% a-linolenic acid). Several studies suggested that an increase in SFA could have negative effects on cognitive functions. On the other hand, a reduction in the risk of cognitive impairment in population-based samples with a high intake of MUFA and PUFA has been found [361]. Higher SFA intake was associated with an increased risk of impairment in memory function, psychomotor speed, and cognitive flexibility by 15–19%. Whereas, an inverse relationship between MUFA intake selective attention and

cognitive decline was found. Moreover, fatty fish and marine n-3 PUFA consumption were significantly associated with a decreased risk of global cognitive function impairment and psychomotor speed by 19–28% [362]. Finally, recent studies increased the evidence of a strict linkage between dementia and fatty acid intake [363, 364]. A high intake of saturated fat and trans-unsaturated fat may be associated with a higher risk of AD; while a high intake of n-6 PUFA and MUFA may be protective against AD [363]. Furthermore, a higher intake of n-3 PUFA and weekly fish consumption may reduce the risk of incident AD. The protective effect of dietary UFA could be related to their ability to maintain the structural integrity of neuronal membranes on which neuronal transmission depends [365, 366]. Furthermore, essential fatty acids can modify the activity of certain membrane-bound enzymes (phospholipase A2, protein kinese C), as well as the function of membrane proteins and ion channels [365]. Finally, an increase in MUFA and a decrease in PUFA content in aged neuronal membranes has been demonstrated, suggesting that during aging there is an increasing demand for MUFA [367]. In rats, dietary oleic acid deficiency leads to a reduction of the oleic acid concentration in many tissues, including the sciatic nerve, but not in the brain [368]. In many organs, endogenous synthesis therefore, does not compensate for the absence of oleic acid in food [369]. This fatty acid is therefore, not synthesized in sufficient quantities, at least in rats and especially during pregnancy-lactation, implying a need for dietary intake. It must be remembered that organization of the neurons is almost complete several weeks before birth, and that these neurons remain for the subject's life time. Consequently, any disturbance of these neurons, an alteration of their connections, and impaired turnover of their constituents at any stage of life, will tend to accelerate aging [368]. Several studies confirmed that high intakes of n-6 PUFA, n-3 PUFA, and MUFA appear to be protective against the risk of AD. High MUFA intake may be a marker for other dietary factors responsible for the protection against cognitive disorders, i.e. the great amount of tocopherol and polyphenols, the antioxidant compounds of olive oil, and the low intake of SFA. Elevated UFA intake (MUFA and PUFA), high levels of antioxidant compounds, and very low SFA intake could act synergistically in improving cognitive performance. In conclusion, epidemiological studies on the association between diet and cognitive decline suggested a possible role of fatty acids intake in maintaining adequate cognitive functioning and possibly in

preventing or delaying the onset of dementia, both of degenerative or vascular origin. Appropriate dietary measures or supplementation with specific macronutrients might open new ways for the prevention and management of cognitive decline and dementia.

-AIM OF THE STUDY-

Recent remarkable findings of protein aggregation as a common key feature in several neurodegenerative diseases represent notable progress in understanding the basic mechanism of the "amyloid hypothesis" of Alzheimer's disease (AD). A deeper knowledge of the modifications underlying the different cell vulnerability to death, following exposure to toxic aggregates, appears mandatory to improve our information on the chain of events eventually leading exposed cells to die. To better address this issue, in the present research, the molecular basis of cell damage induced by prefibrillar forms of different aggregates after the interaction with plasma membrane was investigated in depth. In particular, oxidative stress markers and either apoptotic or necrotic pathway activation in human SH-SY5Y neuroblastoma cells and fibroblasts from familial AD (FAD) patients in comparison to healthy cells were checked. In addition, the role of membrane cholesterol as a modulator of Aβ peptide interaction with cell membrane and the following neurotoxicity was investigated. Additionally, considering the importance of developing new antioxidant compounds and the relevance of their application in the treatment of neurodegenerative diseases, new S-acylglutathione (acyl-SG) derivatives were synthesized, and their protective effect on cells experiencing amyloid aggregate oxidative insult was tested.

Peptides or proteins can adapt from their soluble forms into highly ordered fibrillar aggregates, giving rise to pathological conditions ranging from neurodegenerative disorders to systemic amyloidoses. The N-terminal domain of the prokaryotic hydrogenase maturation factor (HypF-N) can quickly be converted into stable oligomers under conditions that promote its unfolding into partially folded species. In this study, we investigated in depth the cascade of events, resulting in cellular dysfunction and death, triggered by two HypF-N oligomer species that are morphologically and tinctorially similar, but possess distinct structural features, such as a different degree of flexibility of the exposed hydrophobic surfaces. In particular, the different interaction with and internalization into the cell membrane of these aggregates, and the various

downstream effects that these aggregates causes on SH-SY5Y cells were studied. Our results support the rising consensus on the role of plasma membranes as primary targets of toxic protein oligomers (Results I). The comparison between the biological properties of these protein aggregates shed light into the molecular basis of aggregate toxicity in protein deposition diseases.

A link between AD pathogenesis and loss of brain cholesterol is increasingly recognized, suggesting that a fine modulation of the levels of this membrane sterol plays a crucial role in neuronal viability. Therefore this study also investigated the influence of membrane cholesterol modulation on cell vulnerability to amyloid toxicity, by checking the extent of amyloid aggregate interaction with the cell membrane, the oxidative stress and the cell death markers both in human SH-SY5Y neuroblastoma cells and in fibroblasts from FAD patients compared to cells from healthy subjects. In particular, membrane cholesterol levels modulation was achieved by cell culture media supplementation with water soluble cholesterol (PEG-chol and Chol), to increase the content of membrane cholesterol. On the other hand, cholesterol levels were reduced by exposing the cells to the cholesterol extracting drug methyl-β-cyclodextrin (β-CD) or mevastatin (Mev). Membrane cholesterol enrichment significantly slows the recruitment, and reduces the interaction, of Aβ42 oligomers with the cell membranes, thus preventing the cell damage associated to amyloid-induced imbalance of cytosolic Ca^{2+} and oxidative stress in our cell models (Results II). Our data suggest a key role of cholesterol in modulating Aβ42 oligomer accumulation at the cell surfaces and to the following Aβ42-induced cell death in AD neurons. In conclusion, these results support the idea that neuronal resistance to Aβ toxicity requires the maintenance of a proper steady-state level of membrane cholesterol.

It has recently been reported that Aβ binding and aggregation to the cell surfaces occurs in lipid raft, cholesterol- and sphingolipids-rich ordered membrane microdomains, where it is mediated by clusters of the ganglioside GM1. To shed further light on the ability of lipid rafts to recruit Aβ-derived diffusible ligands (ADDLs) and on the resulting structural modifications induced by aggregate binding, we carried out a study on SH-SY5Y cells overexpressing the wilde-type amyloid precursor protein (APPwt) and a FAD mutated form of amyloid precursor protein (APPV717G) and on fibroblasts bearing the APPV717I gene mutation. We found that, in our model cells,

lipid rafts are chronic targets of Aβ-induced lipid peroxidation and physicochemical perturbation on the cell surface, leading to disruption of selective permeability of plasma membrane (Results III). Accordingly, membrane lipid peroxidation positively correlates with the perturbing effects of Aβ42 oligomers on detergent resistant microdomains (DRMs). Moreover, amyloid recruitment at the oxidative-damaged domains was prevented by enhanced cholesterol levels, anti-GM1 antibodies and the binding of B subunit of cholera toxin to GM1. This data identifies lipid rafts as primary target of oxidative injury and membrane degeneration as a result of their ability to recruit amyloid aggregates to the cell surfaces.

Recent data support the role of oxidative stress in the pathogenesis of AD. In particular, glutathione (GSH) metabolism is altered and its levels are decreased in affected brain regions and peripheral cells from AD patients and in experimental models of AD. Therefore, therapeutic strategies based on intracellular increase in GSH levels by dietary or pharmacological intake of GSH precursors or substrates for GSH synthesis to protect the brain against oxidative stress have been developed. Because much experimental evidence suggests a possible protective role of unsaturated fatty acids in age-related diseases and considering the importance of developing new antioxidant compounds for the treatment of neurodegenerative diseases, we designed the synthesis of new S-acylglutathione (acyl-SG) thioesters with protective effects on cells experiencing amyloid aggregate oxidative insult. These acyl-SG derivatives were easily internalized into the cells and they significantly reduced Aβ42-induced oxidative attack in SH-SY5Y cells and primary fibroblasts from FAD patients (Results IV). In particular, acyl-SG coniugates can prevent the impairment of intracellular scavengers of reactive oxygen species (ROS), intracellular ROS accumulation, lipid peroxidation, and apoptotic pathway activation. Indeed, the observed increase in antioxidant and neuroprotective effects with the presence of the double bond and the lengthening of the chain suggests that, the partial lipophilic nature of such compounds might account for their intracellular uptake of these compounds. Therefore, our results present these acyl-SG thioesters as new antioxidants with neuroprotective effects against Aβ-induced oxidative injury and put forward these derivatives as new compounds which could be excellent candidates for therapeutic treatment of AD and other oxidative stress-related diseases.

CHAPTER II - MATERIALS & METHODS

-MATERIALS-

Chemicals

All reagents were of analytical grade or the highest purity available. Tissue plastic-ware was obtained from PBI international (Milan, Italy). Acetonitrile, methyl-β-cyclodextrin (β-CD), Bradford reagent and *N*,*O*-bis(trimethylsilyl)-trifluoroacetamide (BSTFA), cholesterol, cholesterol oxidase, water-soluble cholesterol balanced with methyl-β-cyclodextrin (Chol), Congo Red (CR), N-[N-(3,5-difluorophenacetyl)-l-alanyl]-S-phenylglycine t-buthyl ester (DAPT), dimethylsulfoxide (DMSO), 1,6-diphenyl-1,3,5-hexatriene (DPH), ethylenediaminetetraacetic acid (EDTA), fetal bovine serum (FBS), filipin III, geneticin (G418), glutathione (GSH), hexafluoro-2-isopropanol (HFIP), lauroyl-CoA, media for cell cultures, mevastatin (Mev), palmitoleoyl-CoA, phosphate buffer saline (PBS), polyoxyethyl-cholesteryl sebacate (PEG-cholesterol), phospholipase C, propidium iodide (PI), pluronic acid F-127, Vitamin E (Vit E) and other chemicals were from Sigma (Milan, Italy). D-Threo-1-phenyl-2-decanoylamino-3-morpholino-1-propanol (PDMP) (Matreya, LLC, PA, USA).

Fluorescent probes

Alexa Fluor 647-conjugated cholera toxin subunit B (CTX-B), 4,4-difluoro-3a,4adiaza-s-indacene (BODIPY 581/591 C_{11}), calcein-acetoxymethyl (Calcein-AM), 2',7'-dichlorodihydrofluorescein diacetate, acetyl ester (CM-H_2,DCFDA), fluo3-acetoxymethyl ester (Fluo3-AM) and wheat germ agglutinin-conjugated with fluorescein or with Alexa Fluor 633 were purchased from Molecular Probes (Eugene, OR, USA). All the fluorescent probes were prepared as stock solutions in DMSO, purged with nitrogen and stored in light-protected vessels at −20 °C until use.

Antibodies

Mouse monoclonal anti-Aβ antibodies 6E10 were purchased from (Signet, DBA, Italy). Fluorescein-conjugated and Texas Red-conjugated anti-mouse secondary antibodies were from Vector Laboratories (DBA, Italy). Rabbit polyclonal A11 anti-Aβ oligomer antibodies and Alexa Fluor 488-conjugated anti-rabbit antibodies were from Invitrogen

(Milan, Italy). Rabbit anti-HypF-N polyclonal antibodies were provided from Primm S.r.l. (Milan, Italy). Mouse anti-flotillin-1 monoclonal antibodies were from BD Biosciences (San Diego, CA). Goat polyclonal sc-1615 antibodies against β-actin and peroxidase-conjugated anti-goat antibodies were obtained from Santa Cruz Biotechnology Inc. (CA, USA). Peroxidase-conjugated anti-mouse and anti-rabbit antibodies were purchased from Pierce (Rockford, IL, USA). Rabbit polyclonal anti-GM1 antibodies were from Calbiochem EMD Chemicals Inc. (Darmstadt, Germany).

Synthesis and purification of acyl-SG thioesters

Acyl-SG thioesters, consisting of the tripeptide GSH linked by its sulfhydryl group to the carboxylic group of the SFA lauric acid (C12:0) and the MUFA palmitoleic acid (C16:1), were obtained by incubating 25 mM reduced GSH with 5 mM acyl-CoA thioesters of lauric acid or palmitoleic acid, in 50 mM sodium phosphate buffer, pH 7.5, at 37°C as previously described [370]. To determine the time-dependent acyl-SG thioester formation, aliquots of the reaction mixtures were withdrawn at various incubation times (0, 1, 2, 3, and 24 h) and injected onto a reversephase high-pressure liquid chromatography (HPLC) Shimadzu system equipped with an LC-10AD pump and an SPD-10A UV–Vis detector using a Vidac C18 column (5 μm, 4.6 mm × 25 cm). The kinetic of conjugate synthesis was monitored by UV detection of HPLC peaks at 228 nm at various time points. Lauroyl-SG and palmitoleoyl-SG derivatives were purified from the water phase with solvent A (0.1%TFA, v/v, in water). A gradient elution of 20–60% B (0.1% TFA, v/v, in acetonitrile) in 60 min for lauroyl-SG derivative and of 20–70% B in 70 min for palmitoleoyl-SG derivative was performed at a flow rate of 0.7 ml/min. Fractions containing acyl-SG derivatives were collected, frozen, lyophilized to dryness, and stored at −80°C until use. The identity and the purity of acyl-SG derivatives dissolved in water/acetonitrile (50/50) in the presence of formic acid were analyzed by matrix-assisted laser desorption/ionization time-of-flight (MALDI/TOF) on a OmniFlex-NT (Bruker Daltronics) instrument. Acyl-SG thioester synthesis yield was indirectly determined by a quantitative analysis of the respective reduced GSH released after acidic hydrolysis in 50 mM HCl at 80°C for 48 h, according to the Ellman test for the detection of free thiols with minor modifications [371, 372]. Briefly, the samples were dissolved in 15% 5,5′-dithio-bis(2-nitrobenzoic acid) (DTNB)

stock solution (50 mM sodium acetate, 2 mM DTNB in H2O), 20% Tris buffer (1M Tris, pH 8.0), 50% H_2O_2, and 15% 50 mM HCl solution and incubated 5 min at 37°C. Upon oxidation, the colorless DTNB conversion to yellow TNB, in the presence of thiol compounds, was optically measured at 412 nm until it reached a plateau at 5–20 min. The results were calculated using a calibration curve with GSH as an internal standard.

Peptides and aggregation protocols

HypF-N protein, expressed and purified as previously reported [91], was converted into stable oligomers by incubation to 48 μM for 4 h or for 3 and 9 days at 25 °C in two different experimental conditions: 50 mM acetate buffer, 12% (v/v) trifluoroethanol (TFE), 2 mM dithiothreitol (DTT), pH 5.5 (condition A) and 20 mM trifluoroacetic acid (TFA), 330 mM NaCl, pH 1.7 (condition B). Both types of HypF-N oligomers were centrifuged at 16100 g, dried under N_2 to remove the TFE and TFA when necessary, dissolved in the appropriate culture media at 48 μM concentration and immediately added to cultured cells at differing final concentrations. Native HypF-N was tested by diluting the protein stock solution in the same cell media. Tapping-mode atomic force microscopy revealed the presence of spherical bead-like aggregates with heights in the range of 2-6 nm and 2-7 nm under conditions A and B, respectively [91]. Aβ42 and Aβ42-1 reverse peptides were purchased from Sigma (Milan, Italy), Aβ42 amine-reactive succinimidyl esters of carboxyfluorescein (Aβ42-FAM) was from AnaSpec (San Jose, CA) [373]. Lyophilized Aβ42, Aβ42-FAM and Aβ42-1 were initially incubated in 1 mM in hexafluoro-2-propanol (HFIP) at least for 1 h at room temperature to allow complete peptide monomerization. Then, aliquots of peptide solutions were dried under nitrogen and stored at −80 ◦C. Prefibrillar aggregates of the Aβ42 peptide were obtained according to Lambert's protocol [374]. Briefly, aliquots of Aβ42 were dissolved in DMSO to a final concentration of 5.0 mM, incubated in ice-cold F12 medium to a concentration of 100 μM at 4°C for 24 h and then centrifuged at 14,000 x g for 10 min to remove insoluble structures. The supernatant, defined as the amyloid β-derived diffusible ligand (ADDL) preparation, consisted of a fibril-free solution of globular assemblies, as routinely assessed by atomic force microscopy [243]. Fluorescein-labeled Aβ42-FAM aggregates were prepared as described above, except that the aggregation mixture contained a combination of Aβ42-FAM peptide with 2

molar equivalents of unlabeled Aβ42 peptide (at a 1:2 *ratio*) to minimize possible interference of the fluorophore with the aggregation, while retaining sufficient fluorescence signal [373]. For fibrillar conditions, 10mM HCl was added to bring the peptide to a final concentration of 100 µM, and the peptide was incubated for 24 h at 37 ◦C [375]. Lyophilized amylin 1–37 (Sigma, Milan, Italy) was stored as powder at −20 °C until reconstitution in HFIP at a concentration of 1.25 mM. The reconstituted peptide was stored as 10 µl aliquots at -80 °C until used.

-CELL CULTURES-

Human SH-SY5Y neuroblastoma cells (A.T.C.C., Manassas, VA, USA) were cultured in DMEM/F-12 Ham with 25 mM N-2-hydroxyethylpiperazine-N-2-ethanesulfonic acid (HEPES) and $NaHCO_3$ (1:1) supplemented with 10% FBS, 1.0% glutamine and 1.0% antibiotics. The cell culture was maintained in a 5.0% CO_2 humidified atmosphere at 37 °C and grown until 80% confluence for a maximum of 20 passages. The SY5Y clones over-expressing wild-type APP gene (APPwt) and FAD-like mutant valine 717 to glycine APP gene (APPV717G) were prepared by transfecting 80% confluent cells with 1 µg/well of the pcDNA-APPwt or with pcDNA-APPV717G constructs using LipofectamineTM 2000 reagent (Invitrogen, Milan, Italy). A SY5Y clone transfected with an empty pcDNA vector (SY5Y) was used as control cells. Then, G418 was added at a concentration of 800 µg/ml and drug resistant cells were collected after 2–3 weeks for single cell cloning, in which cells were seeded in 96-well plates. After 4–6 weeks, surviving clones reached confluence and were expanded for banking. Stable transfected cells expressing the APP constructs or an empty pcDNA vector were maintained in 300 µg/ml G418. Fibroblasts were obtained from three patients belonging to Italian families bearing the APP Val717Ile mutation (mean ± SD age = 53.3 ± 7.1 years) and from three patients belonging to other Italian families bearing the PS-1 Leu392Val and Met146Leu mutations (mean ± SD age = 56.7 ± 8.6 years), respectively. They underwent clinical assessment according to published guidelines and the AD diagnosis fulfilled the Diagnostic and Statistical Manual of Mental Disorders criteria (DSM-IV) [376, 377]. Primary fibroblasts were also obtained from three age-matched healthy subjects (mean ± SD age = 49.7 ± 8.3 years), carrying neither APP or PS-1 mutations nor diagnosis of neurological disorders. The local ethical committee approved the protocol and written

consent was obtained from all subjects or, where appropriate, their caregivers. Skin biopsies of 3 mm punch were obtained from the volar side of the upper arm of FAD patients and healthy controls. The cells were grown in Dulbecco's Modified Eagle's Medium (DMEM), supplemented with 10% FBS, 1% L-Gln and 1% antibiotics and harvested in T-25 flasks until confluence, 7 days after previous subculture [205]. All nine fibroblast lines were subjected to an equal number of passages (ranging from 10 to 18) and analyzed in three different experiments before confluence.

-METHODS-

Western blotting analysis

Aβ42 soluble oligomers

Western blotting analysis of Aβ42 soluble oligomers was performed on a Criterion XT Precast gel 4–12% Bis–Tris SDS/PAGE (Bio-Rad, Milan Italy), blotted onto a PVDF Immobilio-P Transfer Membrane (Millipore Corporation, Bedford, MA). The membrane was blocked in 1.0% (w/v) BSA in TBS-Tween (0.1% Tween 20 in 20mM Tris–HCl, pH 7.5, containing 100mM NaCl) and incubated with 1:1000 diluted mouse monoclonal 6E10 anti-Aβ antibodies and then with 1:5000 diluted peroxidase-conjugated anti-mouse antibodies. The immunolabeled bands were detected using a Super Signal West Dura (Pierce, Rockford, IL, USA).

APP expression

Immunoblot analysis of APP expression in cell lysates and APP distribution in sucrose gradient fractions were carried out on a 12% (w/v) SDS/PAGE, blotted onto a PVDF Immobilio-P Transfer Membrane and incubated with 1:1000 diluted mouse monoclonal 6E10 antibodies or with 1:5000 diluted goat polyclonal sc-1615 antibodies against β-actin and with 1:5000 diluted peroxidase-conjugated anti-mouse antibodies or with 1:5000 diluted peroxidase-conjugated anti-goat antibodies, respectively. The immunolabelled bands were detected using a Super Signal West Dura.

Detection of Aβ peptides

Human Aβ42 peptides were quantified both in the cell extracts and in the media of SH-SY5Y, APPwt and APPV717G clones (neuroblastoma cells) using a commercial ELISA kit (Invitrogen, Milan, Italy).

Inhibition of enzymes

In a series of experiments, inhibition of γ-secretase activity of neuroblastoma cells was achieved by cell treatment with 100 nM DAPT in fresh culture medium for 24 h [378]. In another set of experiments, inhibition of glucosylceramide synthase was realized by treatment with 25 μM PDMP in fresh culture medium for 48 h [379].

Cholesterol content modulation

The increase in the content of membrane cholesterol was achieved in FAD fibroblasts by supplementing cell culture media with 0.5 mM PEG-cholesterol for 2 h at 37 °C, whereas human SH-SY5Y cells were exposed to 0.1 mM PEG-cholesterol for 1 h at 37 °C, before peptide aggregate treatments. The increase in membrane cholesterol content was also achieved by supplementing SH-SY5Y cell and FAD fibroblasts culture media with 200 μg/ml soluble cholesterol (Chol) for 3 h at 37 °C. Membrane cholesterol depletion was obtained by incubating SH-SY5Y cells and FAD fibroblasts with 1 mM β-CD for 30 min and 2 h, respectively, at 37 °C in the presence of 1 % FBS. Membrane cholesterol depletion was also performed by incubating the cells with 10 μM mevastatin (Mev) for 48 h at 37 °C in the presence of 1% FBS. Cells were then extensively washed with PBS and exposed to peptide oligomers.

Separation processes

Cell lysis

Total cell lysates were obtained from cells by three freeze–thaw cycles followed by 5 s ultrasonication in ice in 20 mM Tris–HCl buffer, pH 8.0, containing 1.0% Triton X100, 137 mM NaCl, 10% glycerol, 6.0 M urea, 0.1 mM PMSF, 10 μg/ml leupeptin, 10 μg/ml aprotinin and by centrifugation at 14,000×g for 10 min at 4 °C. Protein content was measured in cytosolic and nuclear fractions according to the colorimetric method of Bradford [380]. Briefly, the method involves the binding of Coomassie Brilliant Blue to

protein and it is based on the observation that Coomassie Brilliant Blue exists in two different color forms, red and blue. The red form is converted to the blue form upon binding of the dye to protein. This binding causes a shift in the absorption maximum of the dye from 365 to 595 nm, and it is the increase in absorption at 595 nm which is monitored [380].

Membrane purification

The cells were homogenized in PBS containing 9.0% sucrose with three freeze-thaw cycles, 5 s sonication in ice and centrifugation at 700 × g for 10 min at 4.0 °C [266]. The membrane fractions were pelleted by a further supernatant centrifugation at 110,000 × g for 1 h at 4.0 °C. Protein content was measured by the method of Bradford [380].

Purification of DRMs

The cells were washed twice with ice-cold PBS, scraped, and collected by centrifugation at 1000 × g. To purify detergent-resistant membrane fractions (DRMs), the cells were dispersed in a 10 mM Tris-HCl buffer, pH 7.5, containing 150 mM NaCl, 5.0 mM EDTA, 1.0 mM Na_3VO_4, 1.0% Triton X-100 (TNE), protease inhibitors (10 µg/ml leupeptin and 10 µg/ml aprotinin) and incubated in ice for 20 min [381]. The cells were disrupted in a Dounce homogenizer (80 strokes) and centrifuged at 1500 × g for 5 min at 4.0 °C to obtain the post-nuclear fraction. The post-nuclear lysate was adjusted to 40% (w/v) sucrose by 1:1 addition of 80% sucrose prepared in TNE buffer, placed at the bottom of an ultracentrifuge tube and overlaid with two layers of 30% and 5.0% sucrose in TNE buffer. The sucrose gradient was centrifuged at 170,000 × g for 22 h at 4.0 °C using a Beckman SW50 rotor. Fractions were then collected from the top of the gradient as follow: 0.5 ml for fraction 1, 0.25 ml for fractions 2 to 11, 1 ml for fractions 12 and 13, while the pellet was dissolved in 0.08 ml of TNE buffer (fraction 14) [243]. A representative amount of each fraction was subjected to immunoblot analysis of flotillin-1 marker on a 12% (w/v) SDS/PAGE, blotted onto a PVDF Immobilio-P Transfer Membrane, incubated with 1:500 diluted mouse monoclonal anti-flotillin-1 antibodies (BD Biosciences, San Diego, CA) and 1:5000 anti-mouse antibodies. The flotillin-1-rich fractions were pooled as DRMs and extensively dialyzed against TNE buffer to remove sucrose. The amount of sphingomyelin in lipid rafts was

assayed using a photometric method with the Sphingomyelin Assay Kit (Cayman Chemical, Ann Arbor, MI, USA). Briefly, sample sphingomyelin was hydrolyzed by sphingomyelinase to phosphorylcholine and ceramide for 60 min at 37 °C. The choline resulting from the subsequent incubation of phosphorylcholine with alkaline phosphatase was oxidized by choline oxidase with production of H_2O_2. The latter was reacted in the presence of peroxidase with N-ethyl-N-(2-hydroxy-3-sulfopropyl)-3,5-dimethoxyaniline (DAOS) and 4-aminoantipyrine, yielding a blue color product with an optimal absorption at 595 nm [382]. Sphingomyelin was quantified by comparison with a reference curve built by assaying known amounts of sphingomyelin (25–800 ng).

Cholesterol content measurements

Microscope analysis

A labeling of membrane cholesterol was achieved using the fluorescent probe filipin III. The cells seeded on glass coverslips were fixed in 4.0% buffered paraformaldehyde for 20 min at 0 °C and then were incubated with 0.25 mg/ml cholesterol binding agent (filipin III) in PBS for 24 h at 37 °C. After washing, the cells were fixed again in 4.0% buffered paraformaldehyde for 20 min at 0 °C. Cell fluorescence was analyzed by inverted epifluorescence microscopy (Nikon, Diaphot TMD-EF) with a Ph 2-20DL 40 x oil immersion objective and using an UV filter for filipin excitation. To quantify the fluorescence intensity of filipin III, a variable number of cells ranging from 10 to 22 were analyzed in each experiment. Fluorescence signals are expressed as fractional changes above the resting baseline, $\Delta F/F$, where F is the average baseline fluorescence in control cells (assumed as 100%) and ΔF represents the fluorescence changes over the baseline in cells exposed to cholesterol modulation.

Enzymatic assay

The amount of cholesterol in membrane fractions and in purified lipid rafts was assessed using the sensitive fluorimetric Amplex Red Cholesterol Assay Kit (Molecular Probes, Eugene, OR, USA). Sample cholesterol was oxidized by 1.0 U/ml cholesterol oxidase for 30 min at 37 °C to yield H_2O_2 and the corresponding ketone product. In the presence of 1.0 U/ml horseradish peroxidase (HRP), H_2O_2 reacted with 150 μM 10-acetyl-3,7-dihydroxyphenoxazine (Amplex Red reagent) with a 1:1 stoichiometry to

generate the highly fluorescent resorufin [383]. At the end of the incubation, sample fluorescence was measured at 544 nm excitation and at 590 nm emission. Cholesterol content was determined by comparison with a reference curve built by assaying various cholesterol amounts (0.01-1.0 µg) [384].

Dot blot analysis

To detect ganglioside GM1 in the membrane fractions of SY5Y, APPwt and APPV717G cells, 2 µg of protein from each fraction was spotted onto PVDF Immobilio-P Transfer Membranes, incubated with 1:500 diluted rabbit polyclonal anti-GM1 antibodies and with 1:5000 diluted peroxidase-conjugated anti-rabbit antibodies. The immunolabelled bands were detected using a Super Signal West Dura.

Thioester cell treatment

Lyophilized lauroyl-SG or palmitoleoyl-SG were dissolved in 0.1% DMSO, diluted in cultures and then added to cell culture media at various final concentrations and for various incubation times. Then, SH-SY5Y cells and fibroblasts were exposed to 5.0 µM Aβ42 aggregates obtained as above described.

Determination of intracellular GSH uptake

In order to verify cellular incorporation of acyl-SG thioesters and intracellular release of free GSH after thioester hydrolysis by cellular thioesterases. GSH uptake was stopped by washing the cell plates twice with ice-cold PBS, followed by addition of $HClO_4$ 5%. Then, the cells were collected by scraping and were lysed by twice sonication for 5 s after the addition of 1.0 mM γ-glutamylglutamate (internal standard). The homogenate was centrifuged at 12,000 x g for 5 min. The supernatant was neutralized with 2 M K_2CO_3, centrifuged again, and used to assay GSH content by HPLC as previously described [209]. The supernatants were derivatized with 5% fluorodinitrobenzene and then analyzed by liquid chromatography on a Bio-Sil NH_2 90±5 S Bio-Rad column. The 2,4-dinitrophenyl derivatives were detected at 365 nm. GSH was quantified by chromatogram integration using the internal standard. The precipitate was solubilized in 0.5 M NaOH and used for protein determination by Bradford's method [380].

Cell exposure to peptide aggregates

Aliquots of solutions containing native or aggregated HypF-N in prefibrillar forms (condition A and B) were centrifuged, dried under N_2 to remove the TFE or TFA when necessary, dissolved in the appropriate cell media at 48 µM concentration and immediately added to SH-SY5Y cultured cells at differing final concentrations. The cells were incubated in the presence of the aggregates for differing lengths of time. Previous AFM data confirmed that, under conditions A and B, HypF-N prefibrillar aggregates are mainly present as spherical bead-like aggregates [91].

SH-SY5Y cells, APPwt and APPV717G clones, or FAD and wild-type fibroblasts were exposed to 1 µM Aβ42 and Aβ42-FAM prefibrillar aggregates obtained according to Lambert's protocol as above reported [374]. In some experiments, the oligomers were added to cell culture media to appropriate final concentrations for differing lengths of time. Neither disassembly nor microscopic differences in the aggregate structure were observed following dilution in the cell culture media. Aggregate concentration was calculated as monomeric peptide concentration. In some experiments cells were also exposed to Aβ42-1 reversed sequence peptide, as negative control, processed as reported for Aβ42 peptides. For cell culture treatments with amylin, aliquots of 1.25 mM stock solution were dried under N_2 to remove HFIP and immediately dissolved in the cell culture media at a final concentration of 4 µM.

Analysis of aggregate interaction with the cells

Congo Red staining

The quantitation of aggregate adsorption to the surface of our different cell models - with basal or increased/diminished membrane cholesterol - was performed using the specific Congo Red dye as previously described [266]. The same number of cells was treated for differing times with 1.0 µM Aβ42 prefibrillar aggregates in a 96-well plate and washed twice with PBS. The residual aggregate-cell complex was stained with 100 µl of 1:1 Congo Red to aggregate concentration in PBS for 20 min. The Congo Red content was measured photometrically at 490 nm (free Congo Red) and 550 nm (bound Congo Red) by an ELISA plate reader. Under these conditions, the optical density at 550 nm of aggregate-Congo Red complex is a measure of the amount of prefibrillar

aggregates adsorbed to the cell membrane [385]. Congo Red values are reported as % increases with respect to corresponding untreated cells (assumed as 100%).

Flow cytometric analysis

The aggregate adsorption to the cell surface of neuroblastoma cells and fibroblasts was quantified using flow cytometric analysis. Briefly, cells were incubated in culture medium containing 3.0 μM Aβ42-FAM aggregates, containing a mixture of Aβ42-FAM and Aβ42 peptide at 1:2 *ratio*, for differing times and then analyzed by a FACSCanto (Beckton Dickinson Bioscences, San Jose, CA, USA).

Confocal microscope analysis

The interaction of different HypF-N and Aβ42 aggregates with plasma membranes was monitored in SH-SY5Y cells, APP overexpressing clones, FAD and wild-type fibroblasts by confocal scanning microscopy, as previously described [91]. Briefly, cells were incubated for 60 min with HypF-N aggregates formed under conditions A or B, at differing final protein concentrations or for different periods at 12 μM final protein concentrations. Neuroblastoma cells were then counterstained for 10 min with 5.0 μg/ml Alexa Fluor 633-conjugated wheat germ agglutinin and fixed in 2% buffered paraformaldehyde for 10 min at room temperature. After plasma membrane permeabilization with a 3% glycerol solution for 5 min, the coverslips were incubated for 60 min with 1:1000 diluted rabbit polyclonal anti-HypF-N antibodies and then for 90 min with 1:1000 diluted Alexa Fluor 488-conjugated anti-rabbit antibodies. In another set of experiments, SH-SY5Y cells - pre-treated or not with DAPT or PDMP - and fibroblasts were exposed to 1.0 μM ADDLs for differing length of times. Then, the cells were counterstained with 5.0 μg/ml fluorescein-conjugated wheat germ agglutinin for 10 min to detect plasma membrane profiles and fixed in 2% buffered paraformaldehyde for 10 min at room temperature. After plasma membrane permeabilization with a 3% glycerol solution, the coverslips were incubated for 60 min with 1:1000 diluted mouse monoclonal 6E10 anti-Aβ antibodies. The immunoreaction was revealed by incubation for 90 min with 1:1000 diluted Texas Red-conjugated anti-mouse antibodies. Negative controls were obtained by substituting the blocking solution for the primary antibody. Aggregate adsorption to the cells was also analyzed by cell treatment with 3.0 μM Aβ42-FAM oligomers, counterstaining the plasma membranes

with Alexa Fluor 633-conjugated wheat germ agglutinin and fixing in 2% buffered paraformaldehyde, without plasma membrane permeabilization or using antibodies. In another set of experiments, the cells were incubated for 60 min with 1:300 diluted rabbit polyclonal A11 anti-oligomer antibodies and revealed by incubation for 90 min with 1:1000 diluted Alexa Fluor 488-conjugated anti-rabbit antibodies. The colocalization of Aβ42 aggregates with the monosialotetrahexosylganglioside (GM1), marker of lipid rafts, was monitored in neuroblastoma cells seeded on glass coverslips using mouse monoclonal 6E10 anti-Aβ antibodies and with 1:1000 diluted fluorescein-conjugated anti-mouse antibodies and 4.5 µg/ml Alexa Fluor 647-conjugated cholera toxin subunit B. The cell fluorescence was analyzed by a confocal Leica TCS SP5 scanning microscope (Mannheim, Germany) equipped with an argon laser source for fluorescence measurements using excitation lines at 488 nm, 568 nm, 633 nm, and 647 nm for fluorescein and Alexa Fluor 488-conjugated anti-rabbit secondary antibodies, Texas Red, Alexa Fluor 633-conjugated wheat germ agglutinin and Alexa Fluor 647-conjugated CTX-B, respectively. A series of optical sections (1024 x 1024 pixels) 1.0 µm in thickness was taken through the cell depth for each examined sample using a Leica Plan Apo 63 x oil immersion objective and projected as a single composite image by superimposition. GM1 colocalization with Aβ42 aggregates on the cell membrane was estimated on areas of interest (12–13 cells) using the ImageJ (NIH, Bethesda, MD, USA) and JACOP plugin (rsb.info.nih.gov) softwares [386].

Analysis of membrane permeability

In order to assess whether Aβ42 or HypF-N aggregates disrupt cell membrane integrity, neuroblastoma cells and fibroblasts were pre-treated for 20 min at 37°C with 2.0 µM calcein-AM, dissolved in DMSO and resuspended in cell culture medium [266]. The decay in fluorescence was analyzed by confocal microscopy at 488 nm excitation wavelength after cell exposure to 1.0 µM Aβ42 aggregates or to 12 µM HypF-N aggregates at 37°C for differing length of times.

In another set of experiments, the cells were exposed to calcein-AM and then incubated for 20 min in the absence or in the presence of 4.5 µg/ml Alexa Fluor 647-conjugated CTX-B or 1:100 diluted rabbit polyclonal anti-GM1 antibodies, before treatment with 1.0 µM Aβ42 aggregates for 60 min.

Analysis of cytosolic Ca^{2+} dyshomeostasis

The effect of Aβ42 or HypF-N aggregates on cytosolic free Ca^{2+} levels was analyzed in SH-SY5Y cells, cholesterol-enriched, cholesterol-depleted and basal fibroblasts, plated on glass coverslips and loaded with Fluo3-AM, a Ca^{2+}-specific fluorescent probe. The cells were first exposed to 1.0 μM Aβ42 aggregates or to12 μM HypF-N aggregates for differing length of times at 37°C. Cytosolic Ca^{2+} levels were also examined in SH-SY5Y cells exposed to HypF-N aggregates in Ca^{2+}-free medium, including 5 mM Mg^{2+} and 10 mM EGTA, according to Demuro [160] or in cells pre-treated for 24 h with 100 μM vitamin E prior to aggregate exposure in Ca^{2+}-containing medium. The cells were then loaded for 30 min at 37°C with 10 μM Fluo3-AM, 0.01% (w/v) pluronic acid F-127 in Hank's Balanced Salt Solution (HBSS) and subsequently fixed in 2.0% buffered paraformaldehyde for 10 min at room temperature. Fluorescence was detected at 488-nm excitation by collecting the emitted fluorescence with the confocal scanning system described above.

Evaluation of ROS production

Confocal microscope analysis

Intracellular ROS production was detected by using CM-H_2,DCFDA, a ROS-sensitive fluorescent dye. CM-H_2,DCFDA esterified derivative is loaded more effectively within the cytoplasm of the cells because it is more cell permeant before ester groups are hydrolyzed by the cellular esterases. Only a negligible leakage of the probe occurred, since chloromethyl-DCF is negatively charged at physiological intracellular pH. SH-SY5Y cells, cholesterol-enriched, cholesterol-depleted and basal fibroblasts were first cultured on glass coverslips and exposed to Aβ42 or HypF-N aggregates for different times at 37°C. Cells were also exposed to aggregates in a Ca^{2+}-free medium or pre-treated for 24 hours with 100 μM vitamin E prior to aggregate exposure in Ca^{2+}-containing medium. The cells were then incubated with 5 μM CM-H_2,DCFDA, dissolved in 0.1% DMSO and Pluronic acid F-127 (0.01% w/v), in the final 10 min of aggregate exposure. The cells were then fixed in 2.0% buffered paraformaldehyde for 10 min at room temperature and the emitted CM-H_2,DCFDA fluorescence was detected at 488-nm excitation by a Leica Plan Apo 63 x oil immersion objective.

Spectrofluorimetric analysis

Intracellular ROS levels were detected in SH-SY5Y cells cultured in 6-well plates, exposed to 1.0 μM acyl-SG thioesters for 3 h and then treated with 5.0 μM Aβ42 aggregates or 250 μM H_2O_2 for differing length of times. Then, the cells were loaded with 5 μM CM-H_2DCFDA for 20 min, washed twice with PBS and lysed with RIPA buffer (50mM Tris–HCl, 150 mM NaCl, 1.0% Triton X-100, 100 mM NaF, 2.0 mM EGTA, 1.0 mM vanadate, pH 7.5) containing 0.1 mM PMSF, 10 μg/ml leupeptin, and 10 μg/ml aprotinin. CM-H_2DCFDA fluorescence was measured using a Perkin–Elmer LS 55 spectrofluorimeter at 485 nm excitation and 538 nm emission wavelengths. The fluorescence of the oxidized probe was also read directly on intact cells using a fluorescence multiwell plate reader. Untreated cells were used for background readings.

Cellular redox status

Total antioxidant capacity (TAC) assay

The total antioxidant capacity (TAC), accounting for non-enzymatic hydrophilic ROS scavengers, was assayed in cytosolic fractions of SH-SY5Y cell lysates by a competition-based chemiluminescence assay using the photoprotein Pholasin (ABEL Antioxidant Test Kit, Knight Scientific Ltd., UK) as previously reported [205]. In particular, this test assesses the capacity of a sample to scavenge superoxide and other free radicals. If the sample has already been exposed to superoxide and/or other free radicals then its complement of antioxidants will be very much reduced, leaving the sample with a diminished capacity to deal with free radicals that are generated in the assay. In a series of experiments, the time course of intracellular scavengers after cell exposure to 1.0 μM acyl-SG thioesters for differing times was evaluated. Moreover, the time course of cellular antioxidant defense was evaluated after cell incubation with 1.0 μM acyl-SG thioesters for 180 min and then with 5.0 μM Aβ42 aggregates or 250 μM H_2O_2 for different length of times. In another set of experiments, intracellular hydrophilic ROS scavengers were measured in cell lysates of FAD and healthy fibroblasts exposed to 1.0 μM Aβ42 aggregates for 3 h. The results were calculated from a standard curve based on the soluble antioxidant L-ascorbic acid. 100 μM Vit E

cell exposure for 24 h at 37 °C, before cholesterol content modulation and aggregate treatments of FAD fibroblasts, was used as negative control for oxidative stress.

Analysis of lipid peroxidation

Measurement of lipid peroxidation products

To assess the rate of lipid peroxidation after Aβ42 or HypF-N cell treatment, the levels of 8-OH isoprostane were measured photometrically in the neuroblastoma and fibroblasts cell lysates and in the neuroblastoma raft fractions at 405 nm using the 8-isoprostane EIA kit (Cayman Chemical Company, Ann Arbor, MI). In addition, to confirm the protective effect of acyl-SG thioesters on lipid peroxidation in our experimental models, isoprostane levels were measured in the cytosolic fraction of cells incubated or not with 1.0 μM acyl-SG thioesters and then with 5.0 μM Aβ42 aggregates. Alternatively, the levels of typical end products of the process such as malonaldehyde (MDA) and hydroxyalkenals (4-HNE) were determined in the raft fractions of SH-SY5Y using a colorimetric method at 586 nm, according to the reaction of the chromogen N-methyl-2-phenylindole with MDA and 4-HNE in the presence of methanesulfonic acid at 45 °C [387].

Confocal microscope analysis

Lipid peroxidation after cell exposure to Aβ42 or HypF-N aggregates was also investigated in neuroblastoma cells and fibroblasts by confocal scanning microscope analysis, using the fluorescent probe BODIPY 581/591 C_{11}, which is intrinsically lipophilic thus mimicking the properties of natural lipids [388]. In particular, BODIPY 581/591 C_{11} can be used to measure antioxidant activity in lipid environments since it behaves as a fluorescent lipid peroxidation reporter that shifts its fluorescence from red to green when challenged with oxidizing agents [389]. FAD and wild-type fibroblasts with differing cholesterol content were cultured on glass coverslips and exposed to 1 μM Aβ1-42 aggregates for 3 h at 37 °C. As a negative control, fibroblasts were pretreated with 100 μM Vit E for 24 h at 37 °C, before membrane cholesterol modulation and aggregate exposure. In another set of experiments, neuroblastoma cells, cultured on glass coverslips, were pre-incubated for 20 min in the absence or in the presence of 4.5 μg/ml Alexa Fluor 647-conjugated CTX-B or 1:100 diluted rabbit

polyclonal antibodies against GM1 and then exposed to 1.0 μM Aβ42 aggregates for 60 min. Parallel experiments were also performed on cells pre-treated with acyl-SG thioesters to investigate their protective effects against aggregate- or H_2O_2-induced lipid peroxidation. Neuroblastoma cells were exposed to 1.0 μM acyl-SG thioesters for 3 h and then to 5.0 μM Aβ42 aggregates or 250 μM H_2O_2 treatments for 3 h at 37°C. Dye loading was achieved by adding 5.0 μM fluorescent BODIPY, dissolved in 0.1% DMSO, to the cell culture media for 30 min at 37 °C. The cells were fixed in 2% buffered paraformaldehyde for 10 min and the BODIPY fluorescence was measured by simultaneous acquisition of the green (ex 485nm/em 520nm) and red signal (ex 581nm/em 591nm), by confocal microscope analysis, as described above.

Flow cytometric analysis

The lipid peroxidation was also quantified in SH-SY5Y cells by flow cytometric analysis using the fluorescent probe BODIPY 581/591 C_{11}. Briefly, cells were incubated for 24 h at 37°C in culture medium containing 12 μM native or aggregated HypF-N. Then, the cells were loaded with 2.5 μM fluorescent BODIPY dissolved in 0.1% DMSO as above reported. After labeling, cells were washed and resuspended in PBS and analyzed using a FACSCanto flow cytometer (Beckton Dickinson Bioscences, San Jose, CA, USA).

Mitochondrial status

Cytotoxicity assay

The toxic effect of the differing aggregates on metabolic cell functions was assessed in cell models by the 3-(4,5-dimethylthiazol-2-yl)-2,5-diphenyltetrazolium bromide (MTT) assay in 96-well plates [205]. Native or aggregated HypF-N were added to the SH-SY5Y cell culture media at differing final concentrations for 24 h at 37 °C. The cells were also treated with 12 μM HypF-N species grown for different times of aggregation (4h, 3 and 9 days). In another set of experiments, cholesterol-enriched, cholesterol-depleted and basal fibroblasts were exposed to 1.0 μM Aβ42 monomers, oligomers or fibrils or to Aβ42-1 reversed peptide or amylin for 24 h at 37 ◦C. As a negative control, fibroblasts were pre-treated with 100 μM vitamin E for 24 h at 37 ◦C, before membrane cholesterol modulation and aggregate exposure. Moreover, the protective effects of

acyl-SG derivatives against amyloid aggregate or H_2O_2 cytotoxicity were also assessed by MTT assay. In a series of experiments, cells were incubated or not with acyl-SG thioesters for differing lengths of time. In another set of experiments, various final concentrations of acyl-SG thioesters were added to cell culture media for 3 h at 37°C. Comparative experiments with 1.0 μM acyl-CoA thioesters of lauric and palmitoleic acids and GSH alone were performed.

After cell treatments, 100 μl of 0.5 mg/ml MTT solution in PBS was added to the cell cultures and the samples were incubated for 4 h at 37°C. Finally, 100 μl of cell lysis buffer (20% SDS, 50% N,N-dimethylformamide, pH 4.7) was added to each well and the samples were incubated for at least 3 h at 37°C in a humidified incubator, before determination of absorbance value of blue formazan at 590 nm with an ELISA plate reader. Cell viability was expressed as a percentage of MTT reduction in aggregate or H_2O_2-exposed cells compared to untreated cells (assumed as 100%).

Cell death analysis: apoptotic and necrotic markers

Caspase-3 activity

The extent of the apoptotic program activation in SH-SY5Y cells was evaluated by confocal microscope and flow cytometric analyses of caspase-3 activity, which is the main effector caspase in apoptosis. For flow cytometric analysis, the cells were exposed to 12 μM native or aggregated HypF-N aggregates for 24 h at 37 °C. For confocal experiments, cells cultured on glass coverslips were exposed to 1.0 μM acyl-SG thioesters for 3 h and then to 5.0 μM Aβ42 aggregates or 250 μM H_2O_2 for 6 h at 37°C. After the appropriate treatment, the culture media were removed and replaced with FAM-FLICA Caspases 3&7 solution (Caspase 3&7 FLICA kit; FAM-DEVD-FMK; Immunochemistry Technologies, LLC, Bloomington, MN, USA) for 30 min, following the manufacturer's instructions. Cells were then washed three times with a wash buffer provided by the kit. For flow cytometric analysis, fluorescence was analyzed by a FACSCanto (Beckton Dickinson Bioscences, San Jose, CA, USA). For confocal experiments, the cells were fixed on glass coverslips in 2.0% buffered paraformaldehyde for 10 min at room temperature and then fluorescence was detected at 488 nm excitation.

Hoechst staining

Nuclear alterations eventually induced by the amyloid aggregates were investigated by Hoechst 33342 dye staining. Briefly, cholesterol-enriched cholesterol-depleted and basal fibroblasts were exposed to 1.0 µM Aβ42 monomers, oligomers or fibrils or to Aβ42-1 reversed sequence peptide or amylin for 24 h at 37 ◦C. As a negative control, fibroblasts were pre-treated with 100 µM vitamin E for 24 h at 37 ◦C, before membrane cholesterol modulation and aggregate exposure. Then, the cells were incubated with 20 µg/ml Hoechst for 15 min at 37 °C and fixed in 2% buffered paraformaldehyde for 10 min at room temperature. Blue fluorescence micrographs of cells were obtained under UV illumination in an epifluorescence inverted microscope (Nikon, Diaphot TMD-EF) with an appropriate filter set.

LDH release

The presence of necrotic cells was assessed by measuring the activity of lactate dehydrogenase (LDH), a typical necrotic marker released into the cell culture medium after plasma-membrane rupture. LDH activity was measured in the culture media of SH-SY5Y cells and fibroblasts after exposure to 12 µM native or aggregated HypF-N for differing times, or to 1.0 µM Aβ42 aggregates, or to Aβ42-1 reversed sequence peptide for 48 h at 37 ◦C using the LDH assay kit (Roche Diagnostics, Mannheim, Germany) at 490 nm, after blank subtraction at 595 nm.

Steady-state fluorescence anisotropy

Fluorescence anisotropy (r) of DPH was used to measure the structural order of the hydrophobic region of the purified lipid rafts under steady-state conditions [243]. Anisotropy measurements were performed at 37 °C by a Perkin-Elmer LS 55 luminescence spectrometer equipped with manual polarisers with excitation and emission wavelengths set at 360 nm and 425 nm, and with a slit-width of 2.5 nm and 4 nm, respectively. Our system was initially calibrated using DPH in mineral oil, which should give an anisotropy value of 1.0. The g factor was calculated using horizontally polarized excitation and subsequent comparison of the horizontal and vertical emissions. Lipid rafts were incubated for 10 min in the absence or in the presence of Aβ42 aggregates at differing final concentrations and then further incubated for 30 min

with DPH at a 1:250 probe-to-lipid *ratio*. In another set of experiments, lipid rafts were incubated for differing times in the presence of 1.0 μM Aβ42 aggregates before dye loading. Fluorescence intensity was measured with the excitation polariser in the vertical position and the analysing emission polariser in both the vertical (I_{VV}) and the horizontal (I_{VH}) positions; the anisotropy constant, r, was calculated using the equation:

$$r = \frac{I_{VV} - gI_{VH}}{I_{VV} + 2gI_{VH}}$$

Statistical analysis

All data are expressed as mean ± standard deviation (SD). Comparisons between the different groups were performed by ANOVA followed by Bonferroni's t-test. A p value less than 0.05 was accepted as statistically significant.

CHAPTER III – RESULTS

-RESULTS I-

RELATIONSHIP BETWEEN CELLULAR IMPAIRMENT AND OLIGOMER STRUCTURE IN PROTEIN DEPOSITION DISEASES

Peptides or proteins can convert from their soluble forms into highly ordered fibrillar aggregates, giving rise to pathological conditions ranging from neurodegenerative disorders to systemic amyloidoses. The N-terminal domain of the prokaryotic hydrogenase maturation factor (HypF-N) can rapidly be converted into stable oligomers under conditions that promote its unfolding into partially folded species. In the first part of the result section, the different abilities to cause cell dysfunction of two types of HypF-N oligomers with distinct structural features were shown. In particular, only the oligomers exposing hydrophobic surface and endowed with sufficient structural plasticity are able to penetrate the plasma membrane and to increase cytosolic Ca^{2+} levels, intracellular ROS production and lipid peroxidation, resulting in the activation of the apoptotic pathway. In contrast, cellular stress markers and viability were unaffected in cultured neuronal cells exposed to HypF-N oligomers with a higher degree of packing and lower structural flexibility. The comparison between the biological properties of these protein aggregates shed light into the molecular basis of aggregate toxicity in protein deposition diseases.

Differential cytotoxic effects of two distinct types of HypF-N oligomers

Several studies report that early prefibrillar aggregates can interact with the plasma membrane of cultured cells, resulting in cell impairment and death [40, 58, 94, 160]. Two types of stable oligomeric species of HypF-N were obtained by incubation for 4 h at 48 μM, 25°C in (i) 50 mM acetate buffer, 12% (v/v) trifluoroethanol (TFE), 2 mM DTT, pH 5.5 (condition A) and (ii) 20 mM trifluoroacetic acid (TFA), 330 mM NaCl, pH 1.7 (condition B) [91]. These species did not resolubilize when placed under physiological conditions and preserved their ability to bind the amyloid specific dye ThT [91]. Both HypF-N types of oligomers were able to bind to SH-SY5Y cells; but only aggregates formed under condition A could penetrate cell membranes. Indeed, the ability to cross the hydrophobic bilayer of the cell membrane appeared to correlate with a higher flexibility and solvent-exposure of the hydrophobic regions in the oligomers formed under condition A (Fig. 15).

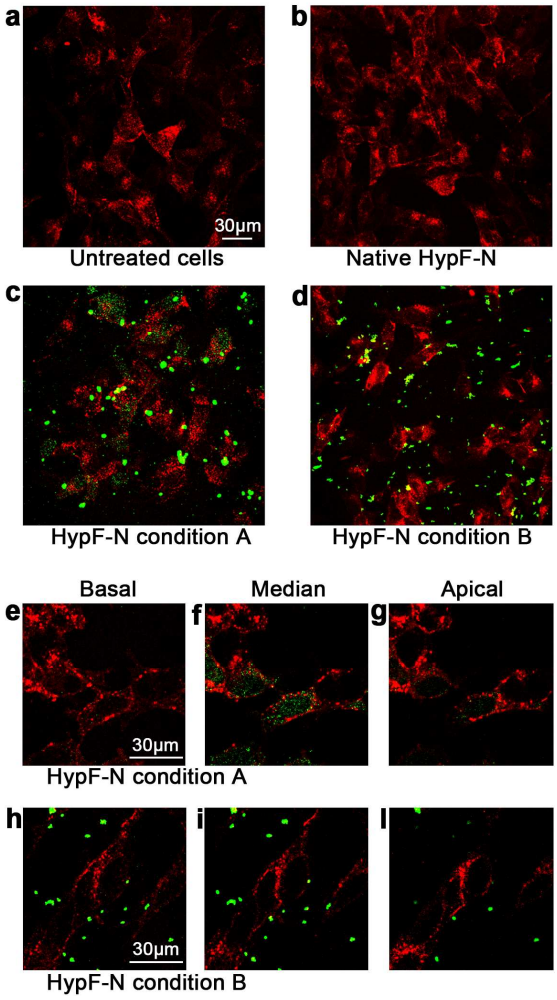

Figure 15. Interaction of the aggregates formed under conditions A and B with cells. **a-d**, Confocal scanning microscopy images of SH-SY5Y cells untreated (**a**), or treated with 12 µM native HypF-N (**b**), 12 µM HypF-N pre-incubated under condition A (**c**) and 12 µM HypF-N preincubated under condition B (**d**). **e-l**, Optical sections taken through the cells after treatment with 12 µM HypF-N pre-incubated under conditions A (**e-g**) and B (**h-l**) at basal (**e, h**), median (**f, i**) and apical (**g, l**) focal lengths. In all images red and green fluorescence indicate cell profiles and HypFN, respectively.

Then, we investigated by confocal microscopy whether the different ability of the oligomeric species to penetrate cell membranes was dependent on different concentrations of HypF-N aggregates (0.12, 1.2, 12 and 48 µM). HypF-N aggregates formed in condition A were able to cross cell membranes and be internalized in the cytoplasm, reaching maximal internalization at 12 µM concentration (Fig. 16). By contrast, although HypF-N oligomers formed in condition B could accumulate near the plasma membrane, none of the investigated concentrations allowed aggregate

internalization. Moreover, cytotoxicity tests on cultured cells indicated that only the aggregates formed in condition A are able to impair the cell viability (Fig. 16). In particular, a strict correlation between the impairment in SH-SY5Y cell viability and the amount of aggregates formed in condition A was observed. By contrast, no inhibition of MTT reduction was detected when cells where treated with various concentrations of HypF-N aggregates formed under condition B. Taken together, these results indicate that only oligomers able to cross the cell membrane and reach the interior of the cell, rather than the outer species, cause cell dysfunction.

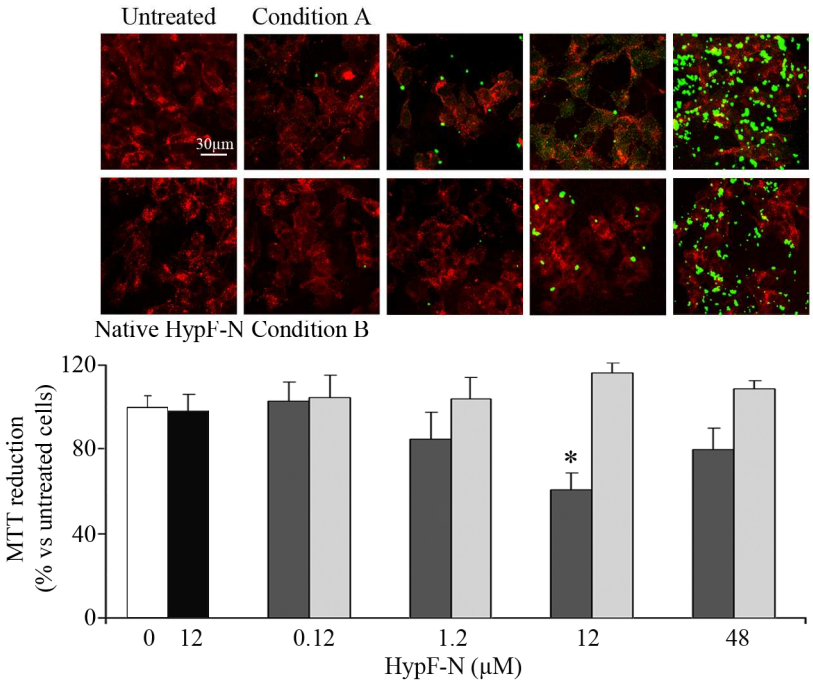

Figure 16. Representative confocal microscope images showing HypF-N aggregates in contact with, or penetrating into, the plasma membrane and cytoplasm of SH-SY5Y cells after exposure to 12 µM native protein or with differing concentrations (0.12, 1.2, 12 and 48 µM) of HypF-N oligomers grown under condition A or B. After plasma membrane permeabilization with a 3% glycerol solution, counterstaining was performed with Alexa Fluor 633-conjugated wheat germ agglutinin to detect plasma membrane profile (red) and with 1:1000 diluted rabbit polyclonal anti-HypF-N antibodies and 1:1000 diluted Alexa Fluor 488-conjugated anti-rabbit antibodies (green) to detect the oligomers. Cell viability was checked by the 3-(4,5-dimethylthiazol-2-yl)-2,5-diphenyltetrazolium bromide (MTT) reduction test in SH-SY5Y cells treated for 24 h at 37 °C with 12 µM native protein or with varying amounts of HypF-N oligomers formed under condition A and B. Cell cultures were incubated with 0.5 mg/ml MTT solution for 4 h and with cell lysis buffer (20% SDS, 50% N,N-dimethylformamide, pH 4.7) for 3 h. Absorbance values of blue formazan were determined at 590 nm using an ELISA plate reader. Cell viability was expressed as percent of MTT reduction in treated cells with respect to untreated cells (assumed as 100%). The values shown are means ± SD of three independent experiments carried out in triplicate. *Significant difference ($p \leq 0.05$) *vs* untreated cells.

Differential membrane interaction of two distinct types of HypF-N oligomers

The idea that the most highly cytotoxic species are the early prefibrillar aggregates whereas mature fibrils are substantially armless is currently gaining increasing support [40, 55]. In the present study, we investigated whether changes in HypF-N aggregate maturation affected the interaction with cell membranes and consequently internalization and cytotoxicity. In particular, the two types of HypF-N oligomers were grown for different times (4, 24 and 60 h) in conditions A and B, and then added to SH-SY5Y cell culture media. As revealed by the MTT assay, the aggregates formed in condition B maintained their benign effect after prolonged incubation up to 2 weeks, while the initially toxic aggregates formed in condition A decreased their toxicity with time until they reach, after 60 h, a value of MTT reduction similar to that of untreated cells (Fig. 17a). The observed decrease in cytotoxicity correlates with a reduction of oligomers internalization into the cells. In fact, when cells were exposed for 60 min to HypF-N species formed in condition A and B upon prolonged aggregation times (3 and 9 days), only few aggregates in the proximity of cell membranes were found (Fig. 17a). These results indicate that HypF-N species, grown -at longer times-in both aggregation conditions, are less able to penetrate plasma membranes, enter the cells and trigger cytotoxicity. Then, we evaluated whether the period of SH-SY5Y cell exposure to HypF-N aggregates could affect the ability of the membrane to bind and internalize HypF-N oligomers. Thus, a time course of aggregate binding to the plasma membranes was performed by exposing cells to HypF-N aggregates formed under condition A or B for 5, 10, 30, 60 and 180 min. Toxic HypF-N aggregates accumulated quickly (see 10 min) at the plasma membrane, showing a rapid kinetic of interaction with cell surfaces and internalization to a considerable extent in cell model (Fig. 17b). On the other hand, non-toxic HypF-N aggregates assembled outside the plasma membrane without entering the cytoplasm even at longer times of incubation. Our findings suggest that the absence of internalization in cells treated with aggregates formed in condition B is not determined by the period of cell incubation with these oligomers.

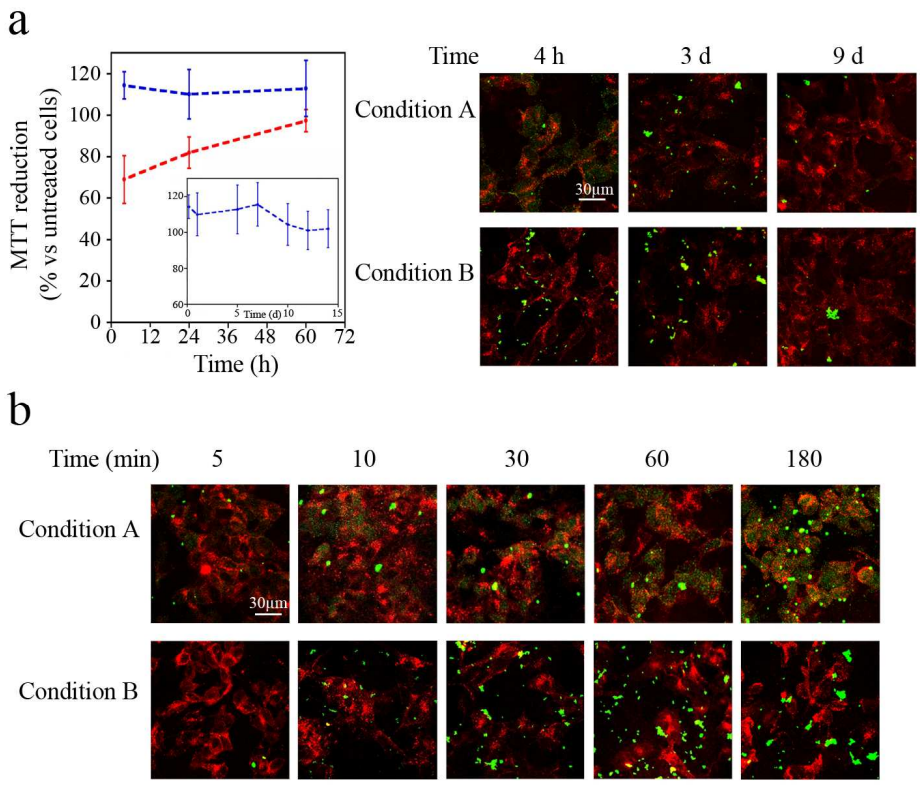

Figure 17. a, Cell viability was checked by the MTT reduction assay in SH-SY5Y cells treated for 24 h at 37 °C with 12 µM HypF-N pre-incubated in condition A (red) and in condition B (blue) for the lengths of time reported in the x axis. The inset shows the data corresponding to the aggregates formed in condition B on a time scale of up to 2 weeks. On the right, representative confocal microscope images showing cells exposed for 60 min to 12 µM HypF-N species aged for 4h, 3 and 9 days in conditions A or B. **b,** Representative confocal images showing time course analysis of HypF-N aggregates, grown in conditions A and B, in contact with, or penetrating into, the plasma membrane and cytoplasm of SH-SY5Y cells. In all images red and green fluorescence indicate cell profiles and HypF-N protein, respectively.

Toxic oligomers disrupt plasma membrane integrity and trigger a cytosolic Ca^{2+} spike

Several studies suggest that cell membranes play an important role in determining amyloid aggregate cytotoxicity, not only because the interaction of amyloidogenic proteins with the membrane favours aggregation, but also because aggregates are thought to permeabilize the lipid bilayer, resulting in unregulated calcium influx into the cells [92, 160, 390, 391]. Accordingly, SH-SY5Y cells loaded with calcein-AM exhibited a marked decrease in intracellular fluorescence when exposed for 60 minutes to HypF-N oligomers formed under condition A (Fig. 18). The decay in calcein

fluorescence was less marked when SH-SY5Y cells were treated with aggregates formed under condition A for only 10 minutes, which suggests that greater membrane permeabilization occurred at longer periods of aggregate exposure. By contrast, any decrease in calcein fluorescence was observed in cells treated with HypF-N oligomers formed under condition B or with the native protein for 60 minutes.

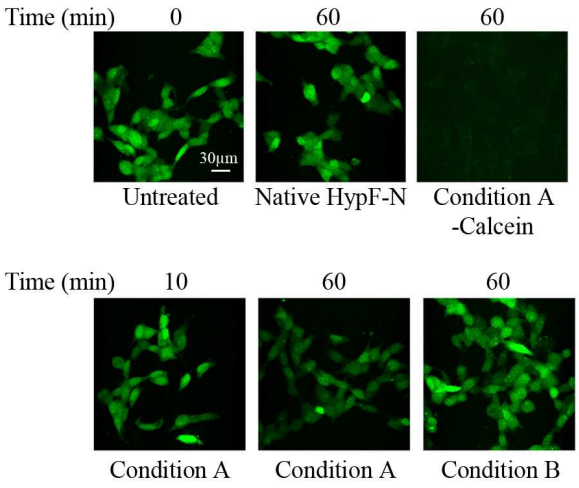

Figure 18. Representative confocal images showing plasma membrane permeabilization in SH-SY5Y cells treated with or without 12 µM native HypF-N or HypF-N aggregates formed under condition A or condition B for the lengths of time reported up the figure. The cells were pre-loaded with 2.0 µM calcein-AM (green fluorescence) for 20 min at 37°C, then exposed to HypF-N aggregates and, fixed in 2.0% buffered paraformaldehyde for 10 min at room temperature.

Then, a time course of intracellular Ca^{2+} levels was performed in SH-SY5Y cells by confocal microscope analysis. Oligomers formed under condition A induced an early and sharp increase in cytosolic free Ca^{2+} (Fig. 19a). The cytosolic Ca^{2+} spike is marked after only 5 min of cell exposure to aggregates and increases over the time course, peaking after 60 min. By contrast, cells treated with HypF-N oligomers formed under condition B didn't exhibit any increase in intracellular fluorescence over the time course, even at longer periods. No increase in intracellular Ca^{2+} was also observed in cells exposed to native HypF-N (Fig. 19b). The sharp increase in cytosolic free Ca^{2+} was inhibited when cells were treated with toxic oligomers in a Ca^{2+}-free medium, suggesting that ion influx from the extracellular medium is responsible for this effect. The vitamin E pre-treatment also prevented the cytosolic Ca^{2+} spike.

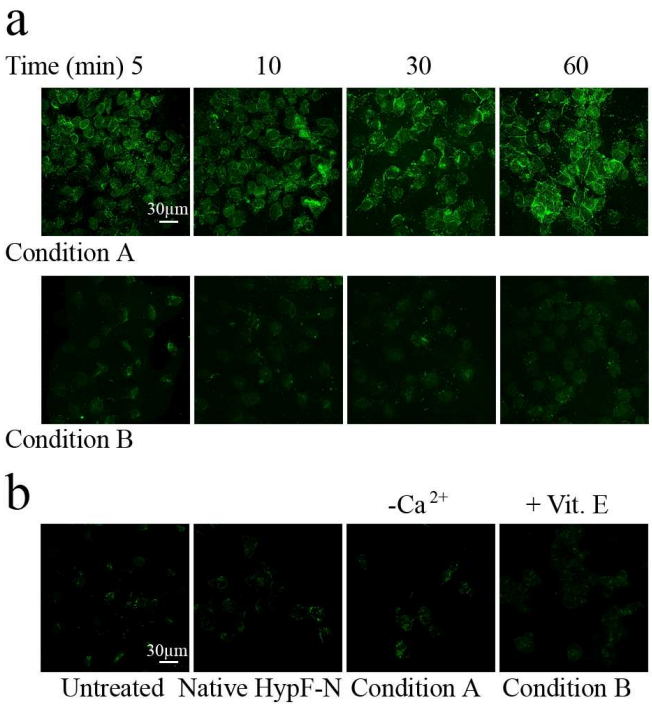

Figure 19. a, Representative confocal microscope images showing time course analysis of cytosolic Ca^{2+} dysregulation in SH-SY5Y cells exposed to 12 μM oligomers formed under conditions A and B. The cells were treated with 10 μg/ml Fluo-3-AM for 30 min, resuspended in HBSS in a 1:1 *ratio* with Pluronic acid F-127 (0.01% w/v) and subsequently fixed in 2.0% buffered paraformaldehyde for 10 min at room temperature. **b**, SH-SY5Y cells were treated for 60 min with or without native HypF-N protein or with 12 μM oligomers formed under condition A in a Ca^{2+}-free medium or following a pre-incubation with 100 μM vitamin E for 24 h.

Toxic oligomers induce ROS production and membrane lipid peroxidation

The generation of intracellular ROS is one of the earliest biochemical changes that cells exposed to amyloid aggregates undergo [95, 196, 392]. ROS production in SH-SY5Y cells exposed to both types of oligomers as well as to the native protein was also investigated. A time course analysis revealed that HypF-N oligomers formed under condition A triggered a ROS increase after only 5 min, peaking after 30-60 min of cell exposure to aggregates (Fig. 20a). By contrast, the cells treated with oligomers formed under condition B showed an intracellular redox status similar to that found in untreated cells. Treating the cells with native HypF-N for 60 min also failed to induce ROS production. Almost complete inhibition of ROS production was achieved by pre-incubating cells with 100 μM vitamin E for 24 h or exposing cells to oligomers formed under condition A in a Ca^{2+}-free medium. Then, membrane lipid peroxidation after cell

exposure to oligomers was evaluated by flow cytometric analysis using the fluorescent probe BODIPY. The fluorescence curves detected in native and condition B-oligomer treated cells was similar to that obtained in untreated cells. By contrast, a fluorescence shift toward higher intensity levels was evident in SH-SY5Y cells, suggesting an increase in membrane lipid peroxidation after 24 h of cell exposure to oligomers formed under condition A (Fig. 20b).

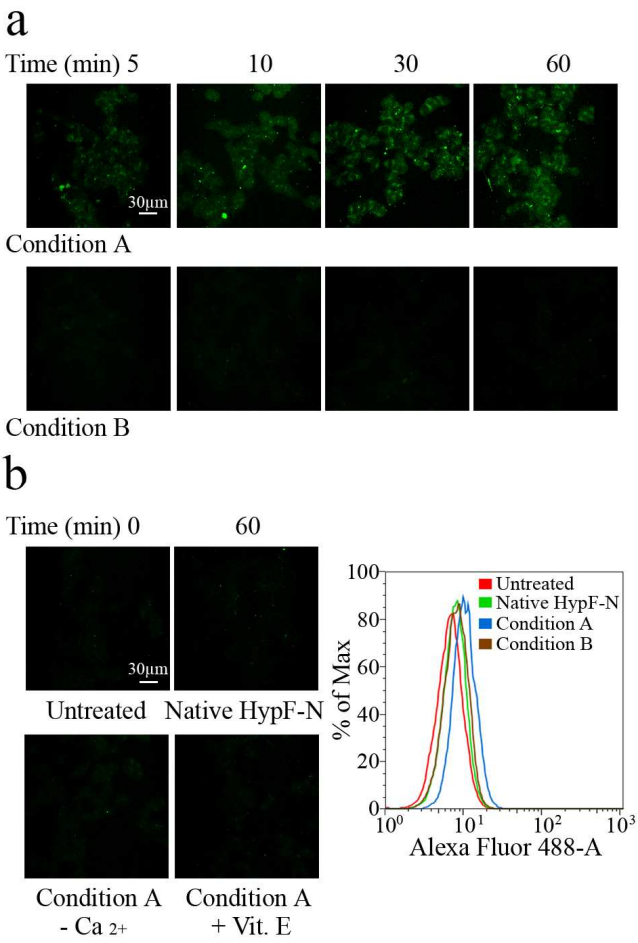

Figure 20. a, Representative confocal microscope images showing time course analysis of intracellular ROS production in SH-SY5Y cells exposed to 12 µM HypF-N oligomers formed in conditions A and B. **b**, Cells were treated for 60 min with or without native HypF-N protein or with 12 µM oligomers formed under condition A in a Ca^{2+}-free medium or following a pre-incubation with 100 µM vitamin E for 24 h. All images were acquired by simultaneously incubating aggregate-exposed cells with 10 µM CM-H_2,DCFDA resuspended in culture medium in a 1:1 *ratio* with Pluronic acid F-127 (0.01% w/v), in the last 10 min of aggregate exposure. Representative histograms illustrate the flow cytometric analysis of lipid peroxidation in SH-SY5Y cells treated or not for 24 h with 12 µM native HypF-N or 12 µM HypF-N aggregates grown under conditions A or B. Then, single-cell suspensions were washed with PBS and incubated, in the dark, for 30 minutes at 37°C with 2.5 µM BODIPY. After labeling, the cells were washed, resuspended in PBS and analyzed using a FACSCanto flow cytometer.

Differential apoptotic and necrotic effects of two distinct types of HypF-N oligomers

Finally, we evaluated whether the different ability of HypF-N oligomers to induce cytosolic ROS and Ca^{2+} increases resulted in a different apoptotic outcome by flow cytometric analysis of caspase-3 activity. In agreement with our aforementioned results, a marked increase in caspase-3 activity was apparent in SH-SY5Y cells treated for 24 h with oligomers formed under condition A, whereas a negligible caspase-3 activation by native HypF-N or oligomers formed under condition B was detected (Fig. 21a). Then, we investigated whether cells exposed to HypF-N aggregates for longer times (48 h) also underwent a necrotic cell death. A significant LDH release, supporting the presence of a necrotic outcome, was observed only in the culture media of cells exposed to oligomers formed under condition A (Fig. 21b).

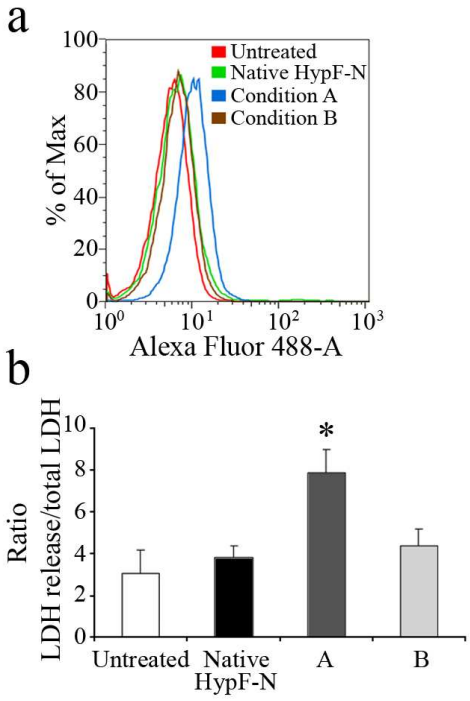

Figure 21. a, Caspase-3 activity was quantified in SH-SY5Y exposed or not for 24 h to 12 µM native HypF-N or to oligomers formed under conditions A and B by flow cytometric analysis. Single-cell suspensions were incubated with FAM-FLICA™ Caspases 3 solution for 60 min at 37°C, washed with PBS and analyzed using a FACSCanto flow cytometer. **b,** Cell viability was checked by LDH release into the culture medium after 48 h exposure at 37 °C to 12 µM native HypF-N or to aggregates formed under conditions A and B. The values shown are means ± S.D. of three independent experiments, each performed in triplicate. *Significant difference ($p \leq 0.05$) *vs* untreated cells.

-RESULTS II-

MEMBRANE CHOLESTEROL ENRICHMENT PREVENTS Aβ-INDUCED OXIDATIVE STRESS IN ALZHEIMER'S FIBROBLASTS

Cell degeneration in Alzheimer's disease is mediated by a toxic mechanism that involves Aβ peptide interaction with the plasma membrane of the target cells. A growing body of evidence implicates low membrane cholesterol in the pathogenesis of Alzheimer's disease (AD). In the second part of the result section, Aβ42 soluble oligomers are shown to accumulate more slowly and in reduced amount at the plasma membranes of PS-1L392V (PS-1) and APPV717I (APP) fibroblasts from familial AD (FAD) patients enriched in cholesterol content than at the counterpart membranes. The permeabilization of the cell membranes and the early cytosolic Ca^{2+} rise following exposure to Aβ42 aggregates were reduced by increasing membrane cholesterol whereas the opposite effects were found in cholesterol-depleted cells. Moreover, the Aβ42-induced production of reactive oxygen species (ROS) and the increase in membrane lipoperoxidation were also prevented by high membrane cholesterol, thus resulting in a higher resistance to amyloid toxicity with respect to control fibroblasts. On the other hand, the recruitment of amyloid assemblies to the plasma membrane of cholesterol-depleted fibroblasts was significantly increased, thus triggering an earlier and sharper production of ROS and a higher membrane oxidative injury. These results identify membrane cholesterol as being key to Aβ42 oligomer accumulation at the cell surfaces and to the following Aβ42-induced cell death in AD neurons.

Membrane cholesterol enrichment reduces Aβ aggregate binding to the cell membrane

Cell degeneration in amyloid diseases appears to be mediated by a toxic mechanism involving some interaction of the aggregated species with the plasma membrane of the affected cells [40, 58, 393]. Moreover, Aβ42 aggregates accumulate quicker near the plasma membrane in FAD fibroblasts than in wild-type cells possibly as a result of increased membrane lipoperoxidation [205]. Here, the dependence of the membrane binding capacity of Aβ42 soluble oligomers (Fig. 22a) on membrane cholesterol content in PS-1, APP and wild-type fibroblasts was investigated. In particular, we induced modifications of membrane cholesterol content by incubating FAD and healthy fibroblasts in the presence of either PEG-cholesterol or β-CD followed by extensive washing with PBS. As shown in Fig. 22b, a morphological evaluation of FAD and healthy fibroblasts by confocal microscopy revealed a clear modulation of membrane cholesterol content under our experimental conditions. Quantitative analysis confirmed that cell exposure to soluble cholesterol resulted in a significant increase in membrane cholesterol (about 20%) *vs* respective control cells in all investigated fibroblast lines (Fig. 22b). Conversely, fibroblasts treated with β-CD underwent a significant reduction in membrane cholesterol (about 25%) *vs* counterpart fibroblasts.

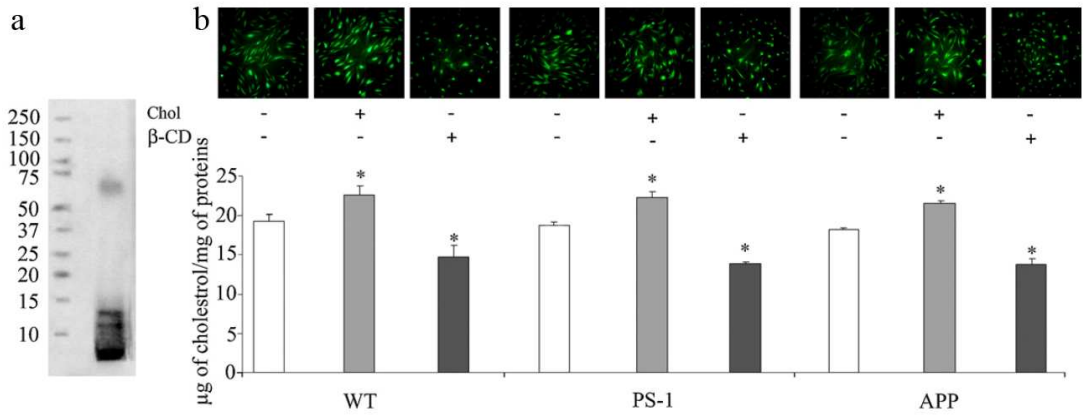

Figure 22. Modulation of membrane cholesterol in FAD and healthy fibroblasts. **a,** Representative Western blotting analysis of Aβ42 soluble oligomers separated by SDS/PAGE on a 4–12% criterion XT Precast Bis–Tris gel and probed with monoclonal mouse 6E10 antibodies and with peroxidase-conjugated anti-mouse antibodies. **(b)** Representative confocal microscope analysis of membrane cholesterol in WT, PS-1 and APP fibroblasts probed by the fluorescent dye filipin. Membrane cholesterol enrichment was achieved by incubating WT, PS-1 and APP fibroblasts with 0.5 mM PEG-cholesterol (Chol) for 2 h at 37 ◦C; membrane cholesterol depletion was performed by adding 1.0 mM β-CD for 2 h at 37 ◦C in the culture media. The reported values are representative of three independent experiments. *Significant difference ($p \leq 0.05$) vs relative control cells with basal cholesterol levels.

The increase in plasma membrane cholesterol resulted in a reduced amyloid-binding capacity to the plasma membrane of FAD fibroblasts with respect to relative cells, as assessed by confocal microscope analysis of cells exposed for 30, 60 and 180 min to Aβ42 aggregates (Fig. 23a). Accordingly, the Congo Red assay showed that cell media supplementation with soluble cholesterol resulted in a significant reduction of Aβ42 aggregate binding to the cell plasma membranes with respect to controls (Fig. 23b). On the other hand, in fibroblasts from healthy subjects just few aggregates following longer time of protein exposure can be observed (Fig. 23a). Conversely, the same amyloid oligomers added to the cell culture medium appear to accumulate more rapidly and to a greater extent at the plasma membrane in β-CD treated cells characterized by a reduced content of cholesterol than in counterpart cells (Fig. 23a and 23b). Furthermore, Aβ42 assemblies share a more rapid kinetic of interaction with cell surfaces in APP than in PS-1 fibroblasts. No significant difference in Congo Red absorbance values between wild-type and FAD groups of Aβ42-untreated cells was observed. An equal cell number from cultures with a comparable division rate from different donors were exposed to the aggregates in order to exclude the influence of these factors on the amount of Aβ

bounded to the cell surface. The ability of exposed cells to bind Aβ aggregates appeared saturable, reaching its limit in the first 30–60 min (Fig. 23b).

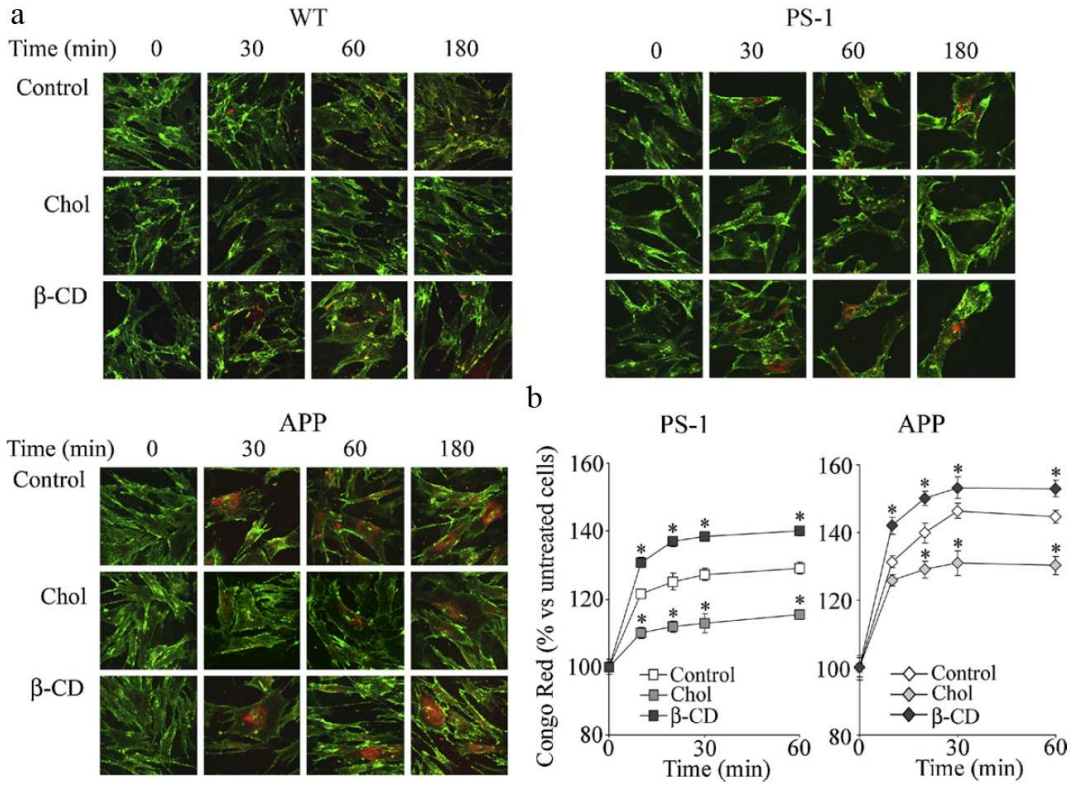

Figure 23. Increasing cell cholesterol reduces Aβ aggregate binding to the cell membrane. **a,** Confocal microscope images show aggregates penetrating into the plasma membrane of wild-type, PS-1 and APP fibroblasts under different experimental conditions. After treatment for 0, 30, 60 and 180 min with 1.0 μM Aβ42 aggregates, counterstaining was performed with fluorescein-conjugated wheat germ agglutinin to detect plasma membrane profile (green). The aggregates were labeled with monoclonal mouse 6E10 anti-Aβ antibodies and Texas Red-conjugated anti-mouse antibodies after plasma membrane permeabilization with glycerol. **b,** Time-course of amyloid aggregate binding to PS-1 and APP fibroblasts. After the exposure to 1.0 μM Aβ42 aggregates for 0, 10, 20, 30, 60 min, cells were washed and the residual aggregate-cell complex was stained with 1.0 μM Congo Red for 20 min. Under these conditions, Congo Red-staining is a measure of the amount of Aβ42 aggregates adsorbed to cell membrane surface. The reported values (means ± SD) are representative of three independent experiments each carried out in triplicate. *Significant difference ($p \leq 0.05$) *vs* relative control cells with basal cholesterol levels.

Moreover, the red fluorescence signals related to 6E10 antibody, that recognizes also the full length human APP, are negligible in all the analyzed conditions before Aβ treatment (see time 0). This evidence let us to rule out the possibility that the differences in the accumulation of exogenous Aβ at the cell surface were due to different levels of

APP expression or to the presence of APP mutant forms in these cells. In order to exclude the contribute of intracellular Aβ to 6E10 red signals, a set of experiments was carried out in the same experimental conditions with fluorescein-labeled Aβ42-FAM aggregates. Confocal microscope images of fibroblasts treated with Aβ42-FAM aggregates also confirmed the idea that the ability of Aβ42 aggregates to bind to the plasma membrane is significantly affected by its content in cholesterol (Fig. 24a). The staining profile of APP fibroblasts exposed to Aβ42-FAM aggregates retained a less fluorescent signal compared to images shown in Fig. 23a, since to minimize fluorophore interference with the aggregation process, the oligomers were prepared by mixing just one Aβ42-labeled molecule with two equivalents of Aβ42-unlabeled peptide. Amyloid binding to APP fibroblasts, as a function of membrane cholesterol content, was also quantified by flow cytometric analysis. Histograms illustrating the distribution for Aβ42-FAM-positive fibroblasts are shown in Fig. 24b. A higher percentage of fluorescent positive cells (+42%) in fibroblasts with low membrane cholesterol with respect to controls was evident, as indicated by the shift of the distribution curve toward higher intensity levels. On the other hand, the increase in membrane cholesterol resulted in a lower percentage of fibroblasts (−39%) with surface-binding affinity toward fluorescent Aβ42-FAM aggregates.

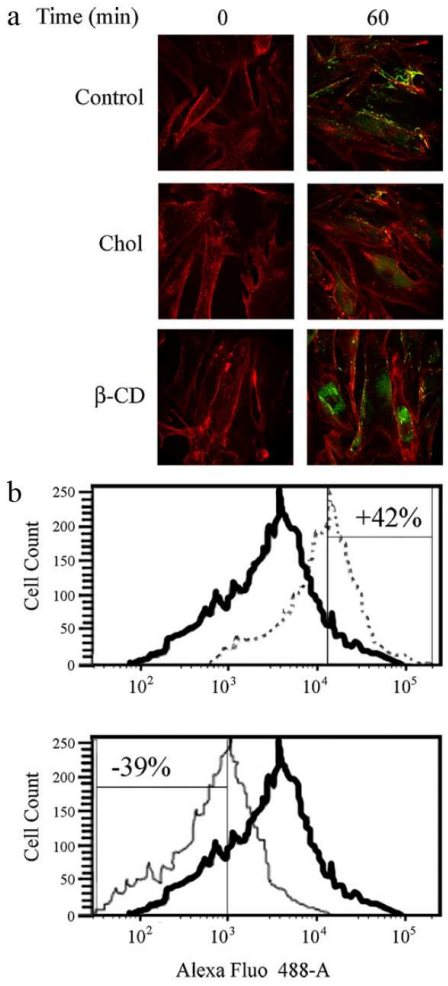

Figure 24. Aβ aggregate binding inversely correlates with membrane cholesterol content. **a,** Confocal microscope images show fluorescein-labeled Aβ42-FAM aggregates (green) penetrating into the plasma membrane of APP fibroblasts with different membrane cholesterol content. Membrane profile was counterstained with Alexa Fluor 633-conjugated wheat germ agglutinin (red). **b,** Flow cytometric analysis of Aβ42-FAM binding to APP fibroblasts after treatment for 60 min with 1.0 µM Aβ42 aggregates in basal (solid line), in cholesterol-depleted (dotted line) and in cholesterol-enriched conditions (thinner solid line). Histograms of the number of cells *vs* Aβ42-FAM fluorescence. Fluorescent gates were used to separate cells with lower Aβ42-FAM binding affinity and cells with higher Aβ42-FAM binding affinity with respect to control cells.

To make these data more relevant, we extended our study to human SH-SY5Y neuroblastoma cells in basal condition (10.84±0.54 µg membrane cholesterol/mg of protein), in cells significantly enriched in cholesterol content (13.55±0.68 µg membrane cholesterol/mg of protein; $p \leq 0.01$) and in cells significantly depleted in cholesterol content (8.26±0.73 µg membrane cholesterol/mg of protein; $p \leq 0.01$). According to fibroblast data, the increase in plasma membrane cholesterol resulted in a reduced Aβ

oligomer binding to the plasma membrane in human neuroblastoma cells as detected by confocal microscope analysis using monoclonal anti-Aβ antibodies (Fig. 25). On the other hand, the same oligomers added to the neuroblastoma culture medium appeared to accumulate to a greater extent at the plasma membrane in β-CD treated cells characterized by reduced membrane cholesterol content.

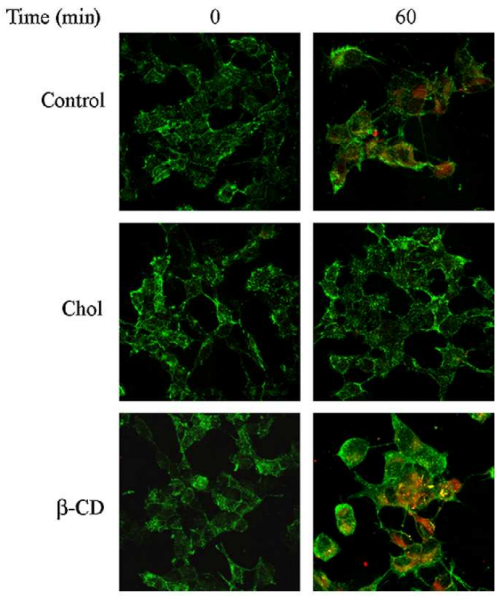

Figure 25. Membrane cholesterol modulates Aβ aggregate binding to human SH-SY5Y neuroblastoma cells. Representative confocal microscope images showing aggregates penetrating into the plasma membrane of neuroblastoma cells after cell treatment for 0 or 1 h with 1.0 μM Aβ42 aggregates in basal conditions, in cholesterol enriched cells (Chol) and in cholesterol-depleted cells (β-CD).

Membrane cholesterol enrichment reduces Aβ42-induced membrane permeabilization and alteration of intracellular Ca^{2+} levels

A leading theory on the molecular basis of amyloid toxicity is that pore-like pre-fibrillar aggregates interact with the cell membranes leading to membrane permeabilization and free Ca^{2+} imbalance [40, 58, 390]. The alteration in membrane integrity, upon exposure to Aβ42 aggregates, on membrane cholesterol content in PS-1 and APP fibroblasts was investigated (Fig. 26). FAD fibroblasts loaded with calcein-AM exhibited a marked decrease in intracellular fluorescence when exposed for 30 minutes to Aβ42 oligomers. In particular, the higher decline of calcein fluorescence was

observed in FAD fibroblasts depleted in membrane cholesterol and exposed to Aβ42 aggregates (Fig. 26). Additionally, a greater calcein leakage in APP than in PS-1 fibroblasts was evident (Fig. 26), suggesting an extensive alteration of membrane permeability induced by Aβ42 aggregates in the former. Moreover, the lower calcein fluorescence in APP fibroblasts compared to PS-1 fibroblasts, before exogenously addition of Aβ42 aggregates, indicated a chronic amyloid-induced membrane damage in cell facing a higher Aβ production.

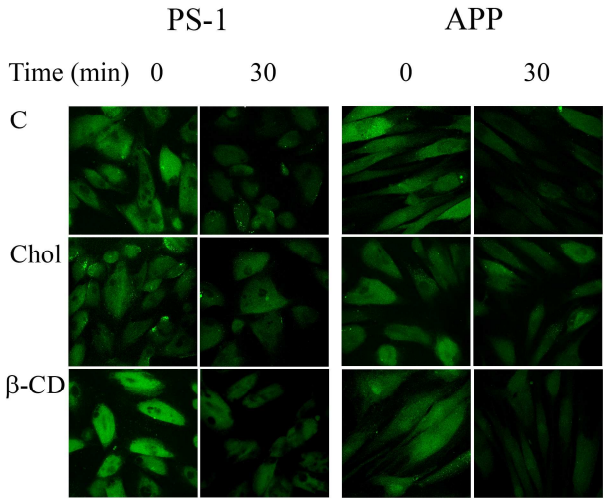

Figure 26. Cholesterol enrichment reduces the Aβ-induced increase in membrane permeability. Representative confocal microscope images of PS-1 and APP fibroblasts loaded with 2.0 μM calcein-AM for 20 minutes and then exposed to aggregates for 0 and 30 minutes in basal conditions, in cholesterol enriched fibroblasts (Chol) and in cholesterol depleted fibroblasts (β-CD).

Then, a time course of intracellular Ca^{2+} levels was performed in PS-1 and APP fibroblasts enriched or depleted in membrane cholesterol by confocal microscope analysis. A higher membrane cholesterol content prevented the early and sharp increase in cytosolic free Ca^{2+} levels induced by Aβ42 aggregates in FAD fibroblasts with basal cholesterol content (Fig. 27). Conversely, loss in membrane cholesterol, resulting from cell treatment with β-CD, triggered an accelerated and greater increase of cytosolic free Ca^{2+}. Notably, the free Ca^{2+} increase was earlier, higher and more prolonged in APP than in PS-1 fibroblasts under the same experimental conditions.

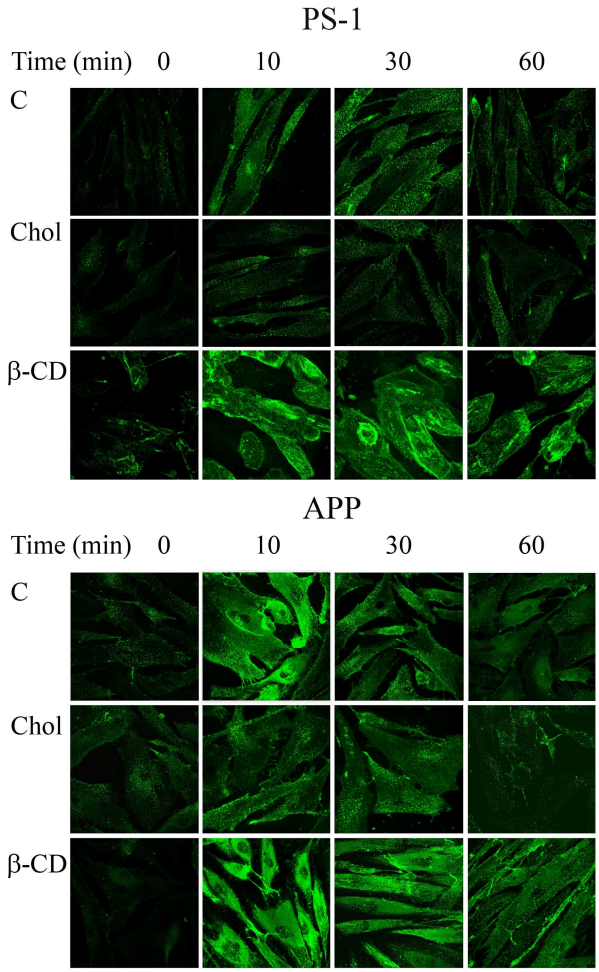

Figure 27. Cholesterol enrichment reduces the Aβ42-induced increase in cytosolic free Ca^{2+}. Representative confocal microscope images of cytosolic Ca^{2+} levels in PS-1 and APP fibroblasts treated with 1.0 μM Aβ42 prefibrillar aggregates for 0, 10, 30 and 60 min. Cells were then treated for 30 minutes with 10 μg/ml Fluo-3-AM, resuspended in HBSS in a 1:1 *ratio* with Pluronic acid F-127 (0.01% w/v) and subsequently fixed in 2.0% buffered paraformaldehyde for 10 min at room temperature.

Membrane cholesterol enrichment reduces ROS production and ROS scavenger impairment

There is strong experimental evidence that oxidative stress is an early biochemical modification in cells facing amyloid aggregates [394]. Therefore, we investigated the dependence of ROS production on membrane cholesterol content in human fibroblasts exposed to amyloid aggregates. A time-course analysis showed that in APP and, to a lesser extent, in PS-1 fibroblasts an earlier and sharper increase in intracellular ROS

content than in wild type fibroblasts (Fig. 28a). The reduced ability of APP cells to counteract Aβ42 aggregate oxidative attack was also confirmed by a significant impairment in intracellular ROS scavengers with respect to that observed in PS-1 and wild type fibroblasts. Indeed, ROS scavengers were significantly different among the investigated fibroblast lines with basal cholesterol content (1500±52 nmol ascorbate/mg of proteins in wild-type, 1170±39 nmol ascorbate/mg of proteins in PS-1, and of 821±49 nmol ascorbate/mg of proteins in APP fibroblasts), according to our previous reported data [210]. Interestingly, PEG-cholesterol addition to the cell culture media was as effective as vitamin E in reducing ROS production induced by Aβ aggregates with respect to relative cells with basal cholesterol content (Fig. 28a). Moreover, the impairment of ROS scavengers was less in cholesterol-enriched FAD cells, matching the almost complete prevention of aggregate-induced oxidative stress obtained by pre-incubating the cells with 100 μM vitamin E. Conversely, loss in membrane cholesterol, resulting from cell treatment with β-CD, induced a greater increase in intracellular ROS production and consumption of ROS scavengers (Fig. 28a and 28b). Notably, PEG-cholesterol and β-CD exposure do not induce ROS production in amyloid untreated fibroblasts, as we can see at time 0 (Fig. 28a).

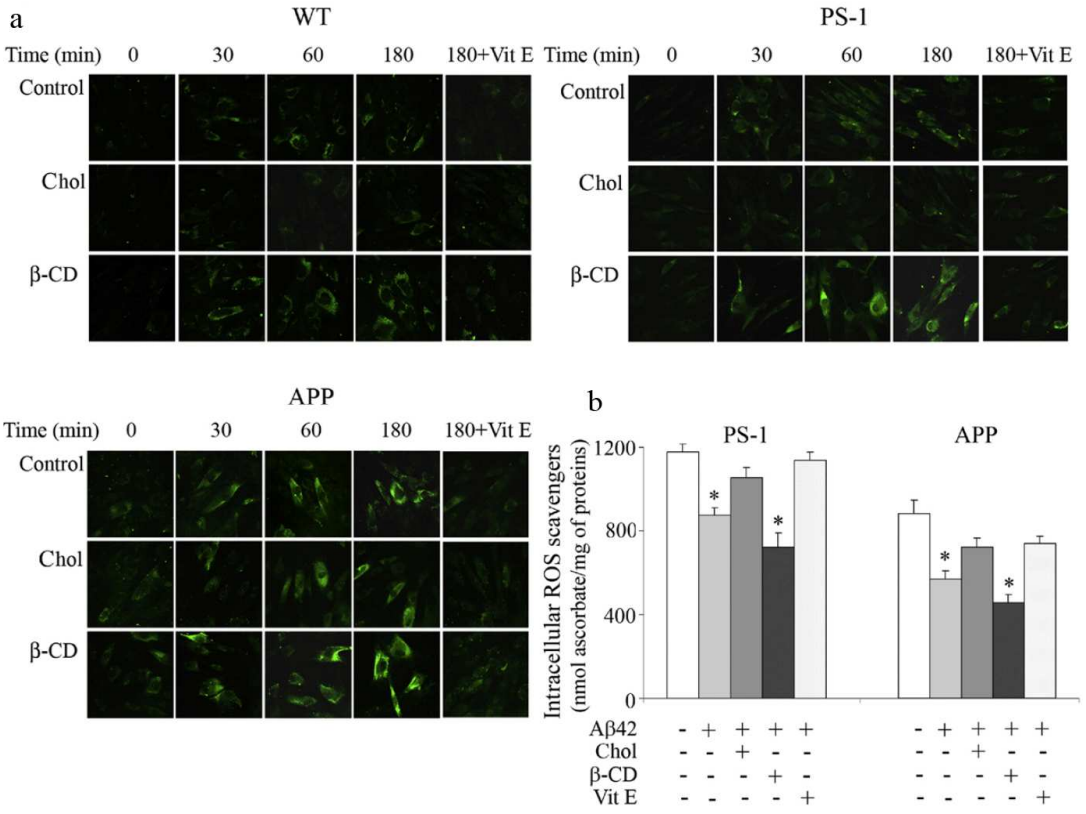

Figure 28. Cholesterol enrichment reduces Aβ42-induced ROS production and ROS scavenger weakening. **a,** Representative confocal images of intracellular ROS levels in WT, PS-1 and APP fibroblasts under different experimental conditions. After treatment for 0, 30, 60 and 180 min with 1.0 μM Aβ42 prefibrillar aggregates, cells were incubated for 10 min in the presence of the redox fluorescent probe CM-H2DCFDA and then fixed. Vitamin E (Vit E) was used as negative control. For details see Materials and Methods. **b**, Intracellular ROS scavengers were assessed in cell lysates, after 3 h of exposure to 1.0 μM Aβ42 aggregates by a chemiluminescent assay and expressed in ascorbate-equivalent units. The reported values (means ± SD) are representative of three independent experiments each carried out in triplicate. *Significant difference ($p \leq 0.05$) *vs* relative untreated cells.

Membrane cholesterol enrichment reduces Aβ aggregate-induced lipoperoxidation

Membrane lipoperoxidation after aggregate exposure was analyzed by confocal microscope analysis using the fluorescent probe BODIPY. The red fluorescence observed in basal cholesterol and in β-CD cholesterol-depleted fibroblasts from healthy subjects shifted to green after 3 h of amyloid aggregate exposure (Fig. 29a). According to previous reported data [210], PS-1 and, to a greater extent, APP fibroblasts showed a basal oxidative-stressed condition, as revealed by the orange fluorescence in untreated fibroblasts. Anyway, the fluorescence signals observed in membrane cholesterol-

enriched cells exposed toAβ42 aggregates did not significantly differ from their respective in untreated cells, confirming a fair protective role of membrane cholesterol in FAD cells. Similar experiments carried out in the presence of vitamin E on all investigated fibroblast lines confirmed the specificities of the fluorescence signals. Moreover, we measured the levels of 8-OH isoprostanes, as quantitative lipoperoxidation marker. As shown in figure 29b, isoprostanes were significantly higher in APP than in PS-1 fibroblasts, since at a basal level. Cellular isoprostane levels were further increased following Aβ42 exposure both in cells with basal and, to a greater extent, with reduced membrane cholesterol content. Conversely, membrane cholesterol enrichment was effective in reducing isoprostane production like as vitamin E in FAD fibroblasts treated with Aβ42 aggregates compared to relative control cells.

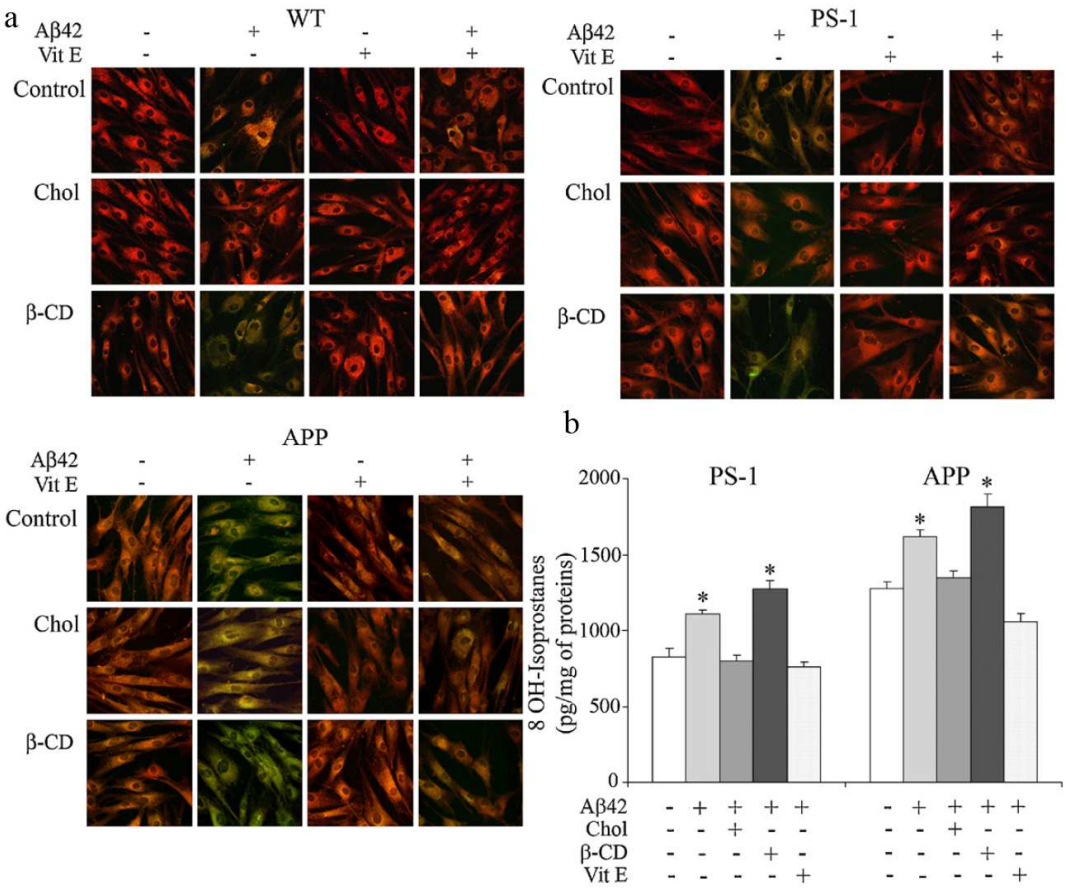

Figure 29. Cholesterol enrichment protects FAD fibroblasts from Aβ42 peptide-induced lipoperoxidation. **a,** Representative confocal microscope images of lipid peroxidation in WT, PS-1 and APP fibroblasts under different experimental conditions. Cells were treated with 1.0 μM Aβ42 for 3 h, with or without vitamin E (Vit E), and lipid peroxidation was measured using the fluorescent probe BODIPY as a probe according to Materials and Methods. **b,** Lipid peroxidation was also measured as cytosolic levels of 8-isoprostanes (for details see Materials and Methods). The reported values (means ± SD) are representative of three independent experiments carried out in triplicate and are expressed as % with respect to untreated cells. *Significant difference ($p \leq 0.05$) *vs* relative untreated cells.

High membrane cholesterol prevents Aβ aggregate cytotoxicity

Next we investigated whether changes in oxidative markers also resulted in modulation of Aβ aggregate toxicity to exposed cells. As shown in figure 30a, morphological evaluation of healthy and FAD fibroblasts using Hoechst 33342 staining revealed no marked characteristics of apoptosis (i.e. nuclear condensation or DNA fragmentation) in cells enriched in membrane cholesterol after 24 h of exposure to Aβ42 aggregates with respect to similarly exposed control cells with basal cholesterol content.

Accordingly, as revealed by the MTT assay (Fig. 30b), both FAD and wild-type fibroblasts with cholesterol-rich membrane were significantly more resistant to Aβ42 aggregate toxicity with respect to similarly exposed control cells with basal cholesterol content. Conversely, loss in membrane cholesterol, following cell treatment with β-CD, resulted in a significant increase in the number of cells showing nuclear condensation, as revealed by the increase in Hoechst fluorescence (Fig. 30a), and in a significant impairment of cell viability (Fig. 30b) upon exposure to the aggregates. Cell treatment with PEG-cholesterol or β-CD do not affect cell viability (data not shown). Vitamin E and Aβ42-1 reversed sequence peptide were used as negative controls. In particular, the absence of any cytotoxic effect in Aβ42-1 treated cells highlighted the selectivity of the cellular response to Aβ42 peptide aggregates. Moreover, the selectivity of the cytoprotective role of high membrane cholesterol was investigated in cells exposed to different forms of Aβ42 aggregates and to amylin prefibrillar aggregates (Fig. 31). Under our experimental conditions, cholesterol-depleted fibroblasts showed an apparent susceptibility to theAβ42 mature fibrils, but to a lesser extent than to Aβ42 oligomers. In any case, Aβ42 fibrils induced a more evident DNA damage in APP than in PS1 fibroblasts. On the other hand, cholesterol-enriched fibroblasts displayed no significant change of cell viability upon exposure to Aβ42 fibrils, suggesting that membrane cholesterol enrichment also protects cells from perturbation by fibrillar aggregates. Overall, FAD fibroblasts exposed to fibrils displayed variable susceptibility to damage and to apoptotic death, confirming a significant inverse relation to membrane content in cholesterol. A reduced vulnerability to the stress induced by amylin oligomers was also observed in cholesterol-enriched fibroblasts with respect to cells with low cholesterol content, further supporting the generality of these effects. On the other hand, a negligible cytotoxicity after treatment with Aβ42 monomeric peptide further tightly linked previous results to the β-sheet structure found in Aβ42 and amylin aggregates. Thought displaying the typical features of apoptotic cells, FAD and wild-type fibroblasts with basal and reduced mem- brane cholesterol content appeared to be similarly affected by 24 h of Aβ42 aggregate exposure. Then, we investigated whether fibroblasts exposed to Aβ42 prefibrillar aggregates for longer times (48 h) underwent a necrotic, rather then apoptotic, cell death. As shown in figure 30c, a significant release of LDH in the cell culture media was observed in fibroblasts with basal and, to a greater

extent, reduced cholesterol content exposed to Aβ aggregates. Again, cholesterol enriched fibroblasts displayed a higher resistance to amyloid toxicity, compared to relative control cells, as revealed by the significant reduction of LDH release into the culture media.

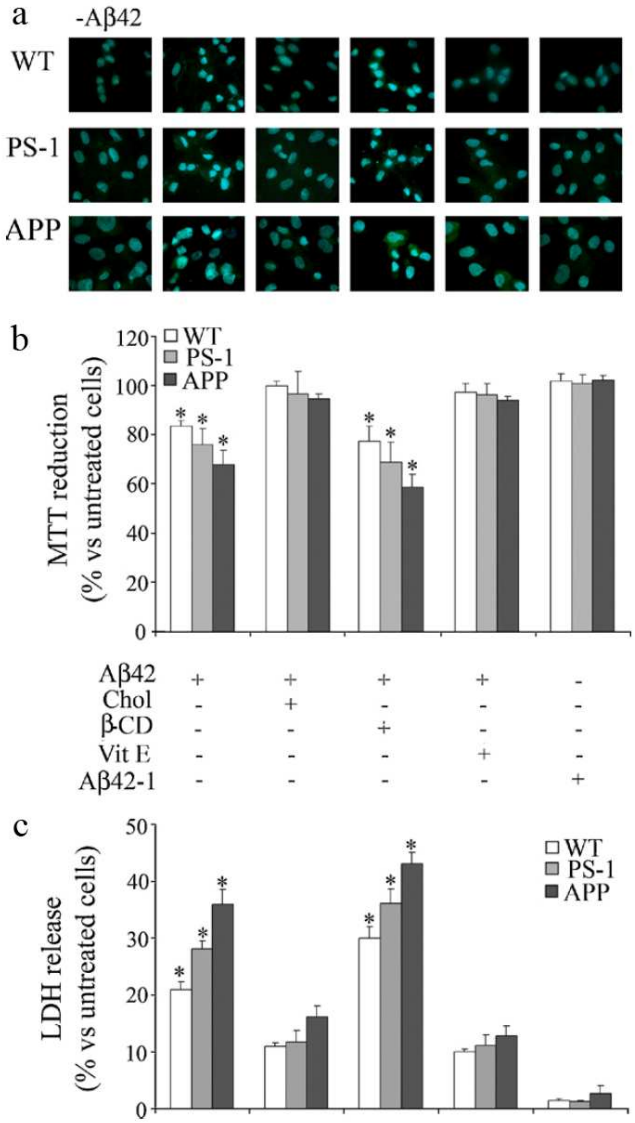

Figure 30. Cholesterol enrichment prevents Aβ aggregate toxicity. **a,** The toxic effect of Aβ42 aggregates on FAD and healthy fibroblast morphology was evaluated using the Hoechst 33342 dye staining. Representative blue fluorescence micrographs of untreated (−Aβ42) or exposed fibroblasts to 1.0μM Aβ42 aggregates for 24 h (for details see Materials and Methods). **b,** Cell viability was checked by the MTT reduction test in cells treated with 1.0 μM Aβ42 aggregates for 24 h. The reported values (means ± SD) are representative of four independent experiments, each performed in triplicate. **c**, Fibroblast viability was checked by LDH release into the culture medium after exposure to 1.0 μM Aβ42 aggregates for 48 h. The values shown are means ± SD of three independent experiments, each performed in triplicate. *Significant difference ($p \leq 0.05$) *vs* relative untreated cells.

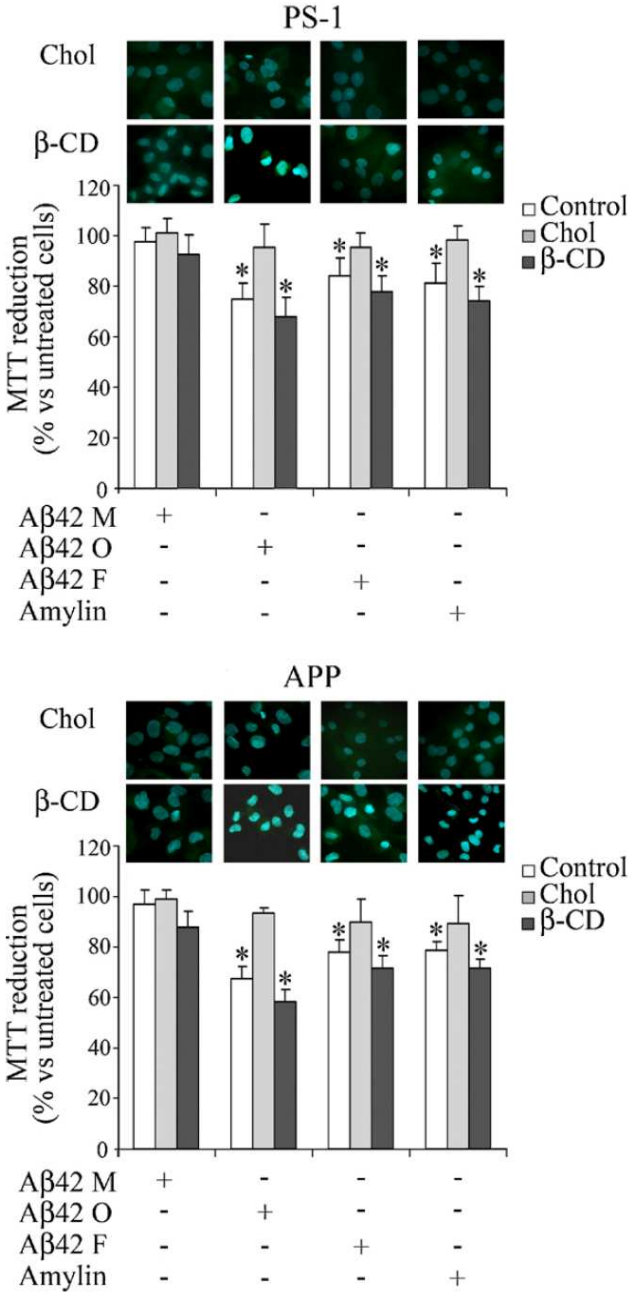

Figure 31. Cholesterol protects against Aβ fibrils and amylin aggregate toxicity. The toxic effect of 1.0 μM Aβ42 monomers (Aβ42 M), Aβ42 oligomers (Aβ42 O), Aβ42 fibrils (Aβ42 F) and amylin aggregates on FAD fibroblasts was evaluated using Hoechst 33342 dye staining. Representative blue fluorescence micrographs of PS-1 and APP fibroblasts exposed to different forms of Aβ42 or amylin prefibrillar aggregates for 24 h. Cell viability was checked by the MTT reduction test in PS-1 and APP fibroblasts exposed to the same aggregates. The reported values are representative of three independent experiments, each performed in duplicate. *Significant difference ($p \leq 0.05$) *vs* relative untreated cells.

-RESULTS III-

LIPID RAFTS ARE PRIMARY TARGETS OF AMYLOID OXIDATIVE ATTACK ON PLASMA MEMBRANE

Increasing evidence indicates that cell surfaces are early interaction sites for Aβ-derived diffusible ligands (ADDLs) and neurons in the pathogenic process of Alzheimer's disease (AD). Previous data showed significant oxidative damage at the plasma membrane in fibroblasts from familial AD patients with enhanced Aβ production. In the third part of the result section, lipid rafts, ordered membrane microdomains rich in cholesterol and sphingolipids, are reported as chronic targets of Aβ-induced lipid peroxidation in SH-SY5Y human neuroblastoma cells overexpressing amyloid precursor protein (APPwt) and APPV717G genes and in fibroblasts bearing the APPV717I gene mutation. Confocal microscope analysis showed that Aβ-oxidized rafts recruit more ADDLs than corresponding domains in control cells, triggering a further increase in raft lipid peroxidation and loss of membrane integrity. Moreover, amyloid pick up at the oxidative-damaged domains was prevented by enhanced cholesterol levels, anti-ganglioside (GM1) antibodies and the B subunit of cholera toxin (CTX-B) binding to GM1. A time- and dose-dependent increase of the structural rigidity of the detergent resistant domains (DRMs), isolated from APPwt and APPV717G cells and exposed to ADDLs, indicates a specific perturbation of raft physicochemical features in cells facing increased amyloid assembly at the membrane surface. This data identifies lipid rafts as key targets of oxidative damage as a result of their ability to recruit aggregates to the cell surface.

Higher lipid peroxidation levels in APPwt and APPV717G overexpressing cells

SH-SY5Y neuroblastoma cells, stably transfected with APPwt and APPV717G constructs expressed higher APP levels (about threefold) compared to cells transfected with an empty pcDNA vector (SY5Y) (Fig. 32a). In particular, APPwt and APPV717G clones showed very similar APP expression levels, providing a useful tool for investigating the dependence of ADDLs binding to neuronal cells on Aβ production level. Indeed, APP undergoes proteolytic β-secretase and γ-secretase activities and generates elevated amounts of Aβ42 peptide both in APPwt and APPV717G neuroblastoma cells and in their culture media (Fig. 32a). However, APPV717G cells produced and released a significant higher level of Aβ42 peptide then APPwt cells. In amyloid diseases, the aggregated species of Aβ peptides interact with the plasma membrane of the affected cells, triggering a free radical-mediated injury that ultimately results in cell degeneration [40, 394]. A confocal microscope analysis showed a higher membrane lipid peroxidation in APPV717G and, to a lesser extent, in APPwt than in SY5Y cells as assessed using the fluorescent probe BODIPY 581/591 (Fig. 32b). By contrast, no difference in the lipid peroxidation levels in the presence of DAPT, a specific γ-secretase inhibitor, was observed among the three clones. These results suggest that the enhanced lipid peroxidation in APP overexpressing clones is predominantly the result of a chronic exposure to increased levels of Aβ42 peptide, rather then to a higher APP content. Accordingly, 8-OH isoprostane levels were significantly higher in APPwt and APPV717G cells compared to SY5Y cells (Fig. 32b), suggesting an oxidative-stressed condition associated with chronic exposure to Aβ in the former. Then, we investigated whether the surface lipid peroxidation enhances the binding process of exogenously added Aβ42 aggregates in APPwt and APPV717G cells. Flow cytometric analysis of the distribution of Aβ42-FAM fluorescent-positive cells showed a curve shift toward higher intensity levels in APPwt and APPV717G cells compared to SY5Y cells exposed to ADDLs for 60 min (Fig. 32c). In particular, the mean fluorescent signal of aggregate-binding cells was significantly higher in APP overexpressing clones than in SY5Y clone.

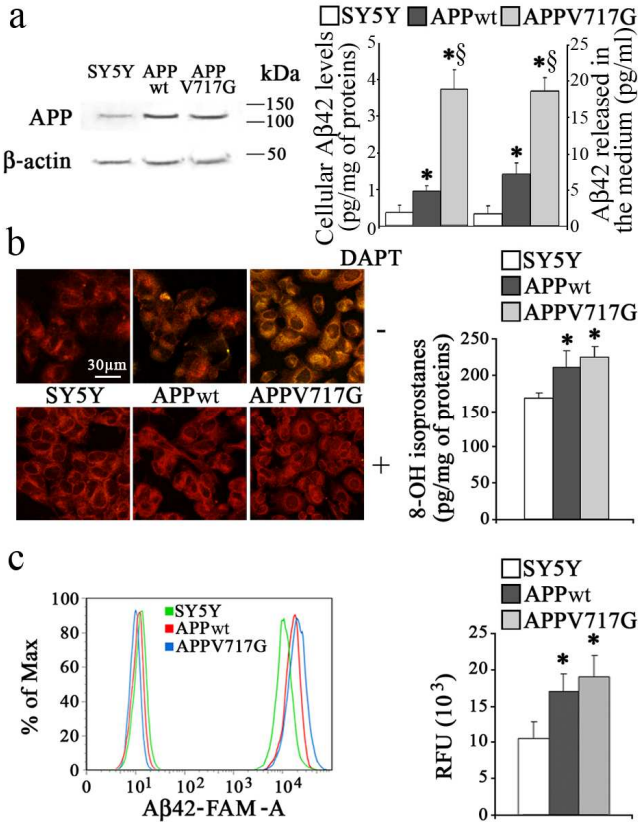

Figure 32. APPwt and APPV717G overexpressing cells show higher lipid peroxidation levels and attract more Aβ42-FAM aggregates to the plasma membrane. **a**, Representative Western blot analysis of total extracts from SH-SY5Y neuroblastoma cells overexpressing wild-type APP gene (APPwt), FAD-like mutant 717 valine-to-glycine APP gene (APPV717G) or mock transfected (SY5Y) was carried out using monoclonal mouse 6E10 antibodies. β-actin expression analysis was used as control loading. Aβ42 levels were measured using an ELISA kit in the cellular extracts and in the conditioned media of the three clones. **b**, Representative confocal microscope images of lipid peroxidation in SY5Y, APPwt and APPV717G cells pre-treated or not with 100 nM DAPT for 24 h, obtained using the fluorescent probe BODIPY 581/591. Lipid peroxidation was quantified by measuring 8-OH isoprostane levels in the three clones. **c**, Representative curves illustrate the flow cytometric analysis of Aβ42-FAM binding to the three clones before and after exposure to ADDLs for 60 min. On the right, in the histograms, the reported values (means ± SD) are representative of three independent experiments carried out in triplicate. *Significant difference ($p \leq 0.05$) *vs* SY5Y cells. § Significant difference ($p \leq 0.05$) *vs* APPwt cells.

Accordingly, confocal microscope analysis showed that when 1.0 μM ADDLs were added to the culture media for 60 min, they accumulate and are internalized mostly in APPwt and APPV717G than in SY5Y cells (Fig. 33). By contrast, DAPT strongly reduced the aggregate-binding to plasma membranes of all three clones exposed to ADDLs, excluding the possibility that amyloid pick up at the cell surfaces is merely

affected by the APP content. Moreover, an increased aggregate-binding capacity was apparent in APPwt and APPV717G clones compared to SY5Y cells also using A11 antibodies, unable to cross-react with the full length human APP (Fig. 33). This evidence let us to rule out the possibility that the differences in 6E10 fluorescence signal were due to different APP expression levels among the three clones. The elevated accumulation of aggregates to the cell surfaces resulted in a sharper increase in membrane oxidative-injury as assessed using the fluorescent probe BODIPY 581/591 (Fig. 33). Indeed, APPwt and APPV717G cells showed a significantly higher shift to green fluorescence signal with respect to their respective change in SY5Y cells, when exposed to ADDLs, confirming an enhanced oxidative insult in cellular surface facing a higher Aβ production.

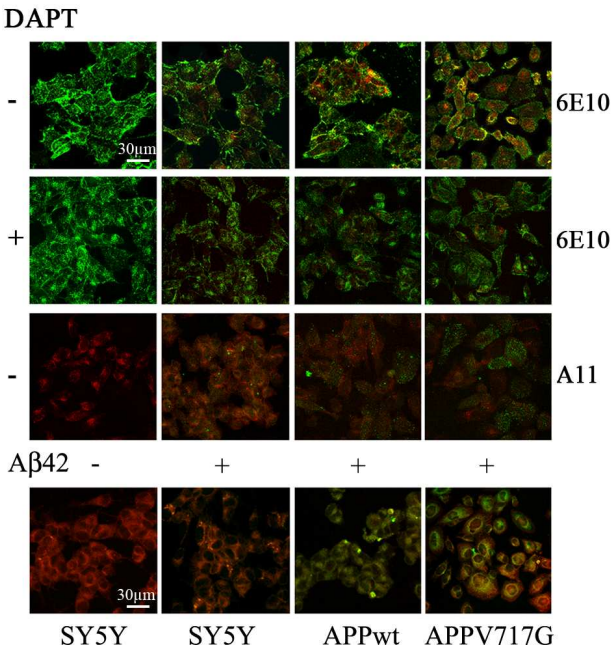

Figure 33. APPwt and APPV717G overexpressing cells show a greater Aβ42 aggregate recruitment to the plasma membrane. Representative confocal microscope images showing aggregates penetrating into the plasma membrane of SY5Y, APPwt and APPV717G neuroblastoma cells exposed to 1.0 μM ADDLs for 60 min (+) compared to untreated cells (–). Cells cultured in the absence (–) or in the presence (+) of 100 nM DAPT for 24 h are compared by labelling Aβ42 aggregates with monoclonal mouse 6E10 antibodies (red). The plasma membrane profile was stained with fluorescein-conjugated wheat germ agglutinin (green). In the third set of images ADDLs were counterstained using polyclonal rabbit A11 anti-oligomer antibodies (green), while the plasma membrane profile was stained with Alexa Fluor 633-conjugated wheat germ agglutinin (red). Bottom, the fourth set of images was obtained using the fluorescent probe BODIPY 581/591 as a marker of lipid peroxidation in SY5Y, APPwt and APPV717G clones before (–) and after (+) Aβ42 exposure.

Membrane cholesterol depletion increases Aβ aggregate binding to the cell surface

Then, the dependence of membrane capacity to bind Aβ42 oligomers on membrane cholesterol content in APPwt and APPV717G clones was investigated. In particular, we induced modifications of membrane cholesterol content by incubating neuroblastoma cells in the presence of either water soluble cholesterol (Chol) or mevastatin (Mev). Quantitative analysis showed a significant increase in membrane cholesterol in SY5Y, APPwt and APPV717G cells (17.01 ± 2.8 µg/mg protein, $p \leq 0.05$) after treatment with soluble cholesterol with respect to untreated control cells (12.93 ± 1.52 µg/mg protein). Conversely, clones treated with mevastatin underwent a significant reduction in membrane cholesterol (8.96 ± 0.91 µg/mg protein, $p \leq 0.05$) vs counterpart cells. Anyway, no significant difference was observed in the cholesterol content among these three clones. The increase in cholesterol content resulted in a reduced membrane capacity to bind amyloid aggregates in APPwt and APPV717G clones with respect to corresponding cells, as assessed by confocal microscope analysis of cells exposed to 1.0 µM ADDLs for 60 min (Fig. 34a). To exclude the contribute of intracellular Aβ, a time-course of aggregate binding to APPwt and APPV717G cells was also performed by a quantitative flow cytometric analysis of cells exposed to fluorescent Aβ42-FAM aggregates. Cell supplementation with cholesterol resulted in a lower membrane ability to bind Aβ42-FAM. Conversely, ADDLs appeared to accumulate more rapidly and to a greater extent at the plasma membrane in mevastatin treated clones, with a reduced content of cholesterol, than in counterpart cells (Fig. 34a). Moreover, amyloid pick up at the membranes was higher in APPV717G than in APPwt cells. Notably, a slight red fluorescence signal is evident in both the analyzed clones without exogenous addition of Aβ42 aggregates, supporting a constant overproduction of Aβ42 in these cells (Fig. 34b). However, APP overexpression could also explain the presence of 6E10 fluorescent signal in the absence of Aβ oligomers [395]. According to the above reported data, a complete absence of red fluorescence signal in the presence of DAPT in both clones occurred (Fig. 34b).

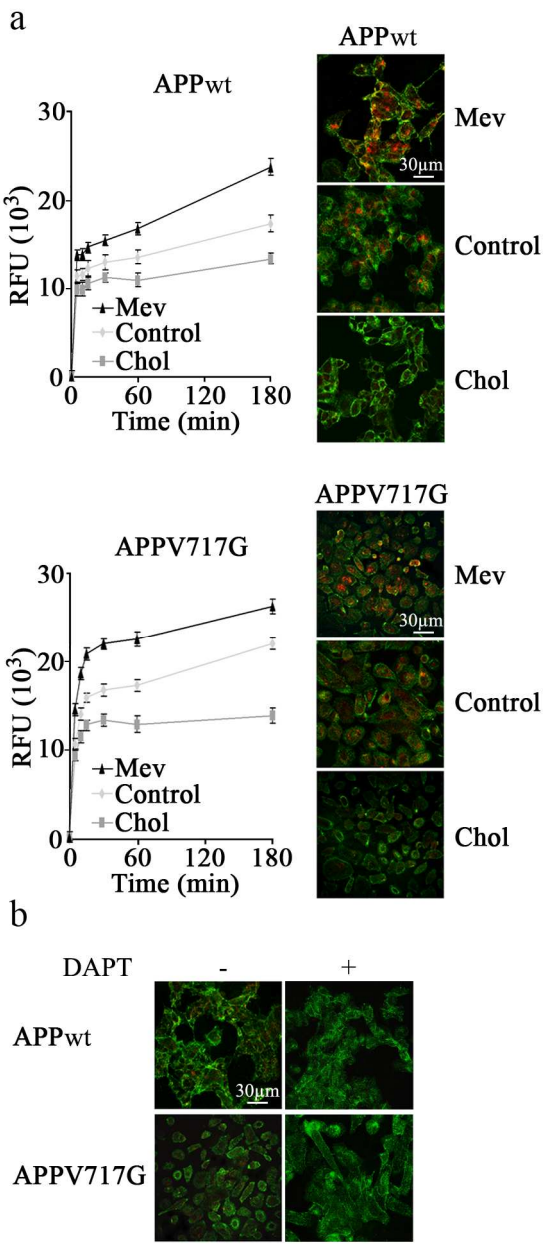

Figure 34. Membrane cholesterol depletion increases Aβ aggregate binding to APPwt and APPV717G cells. **a**, Flow cytometric analysis of Aβ42-FAM binding to the two clones after treatment for differing lengths of time (0, 2, 10, 15, 30, 60 and 180 min) with 3.0 μM Aβ42-FAM aggregates in basal (Control), in cholesterol-enriched (Chol) and in cholesterol-depleted (Mev) conditions. The reported values (mean ± SD) are representative of three independent experiments carried out in duplicate. On the right, representative confocal microscope images showing aggregates penetrating into the plasma membrane of APPwt and APPV717G clones after exposure to 1.0 μM Aβ42 aggregates for 60 min, in basal conditions and after treatment with Chol or Mev. **b**, Representative confocal microscope images showing APPwt and APPV717G clones cultured in the absence (-) or in the presence (+) of 100 nM DAPT for 24 h. The plasma membrane profile was stained with fluorescein-conjugated wheat germ agglutinin (green) and Aβ42 aggregates were labelled with 6E10 antibodies (red).

Lipid rafts are primary recruitment sites and oxidative targets of amyloid aggregates

Recently published research indicates that exogenously applied Aβ in the form of ADDLs can be trafficked on the neuronal membrane and accumulate in lipid rafts, liquid-ordered microdomains rich in cholesterol [241]. Therefore, the role of cholesterol in the modulation of Aβ42 aggregate interaction with these liquid-ordered structures was investigated. Confocal microscope analysis showed a marked colocalization of Aβ42 oligomers with GM1, a well known lipid raft marker, on the plasma membranes (Fig. 35a). When the scatter plots of fluorescence signals were analyzed using the Pearson's correlation coefficient and the overlap coefficient, according to Manders, yielded a colocalization of about 51% between GM1 and Aβ42 aggregates in APPwt and APPV717G cells and 42% in SY5Y cells. A moderate enrichment of membrane cholesterol reduced the interaction of ADDLs with GM1 to about 35% colocalization in APPwt and APPV717G clones and to 25% in SY5Y cells. By contrast, in cholesterol depleted cells an increase in ADDL-GM1 colocalization (about 68%) in APPwt and APPV717G cells and (61%) in SY5Y cells was detected. Then, an APP redistribution in membrane compartments, induced by cholesterol modulation, accounting for the altered membrane ability to bind amyloid aggregates in APP clones was investigated. When APPwt membrane components were separated on a sucrose gradient, no shift in APP immunoreactivity was evident in cholesterol enriched compared to depleted cells, whereas a flotillin-1 transfer to the higher density fractions in the presence of raft reorganization occurred (Fig. 35b). Overall, these data showed that Aβ oligomers interact with the plasma membrane preferentially at the raft domains and that any structural modification induced by cholesterol results in alterations of the aggregate-raft interactions. To make these data more relevant, this study was extended to human primary fibroblasts carrying APPV717I gene mutation, obtained from a FAD patient. A higher lipid peroxidation was evident in APPV717I fibroblasts with respect to wild-type fibroblasts obtained from a healthy subject as assessed by the fluorescent BODIPY 581/591 shift (Fig. 35c), suggesting that cells carrying an altered proteolytic APP process have an increased amyloid assembly at the membrane surface. Then, I investigated whether the more oxidized membranes of APPV717I fibroblast bind more exogenous ADDLs at the lipid raft levels. A higher Aβ42-GM1 colocalization (59%)

was evident in APPV717I than in wild-type fibroblasts (40%) (Fig. 35c). This resulted in a further increase of membrane lipid peroxidation in mutated fibroblasts, when exposed to ADDLs (Fig. 35c). By contrast, wild-type fibroblasts are more resistant to Aβ-oxidative attack with a slight fluorescence shift, likely because of their plasma membrane integrity.

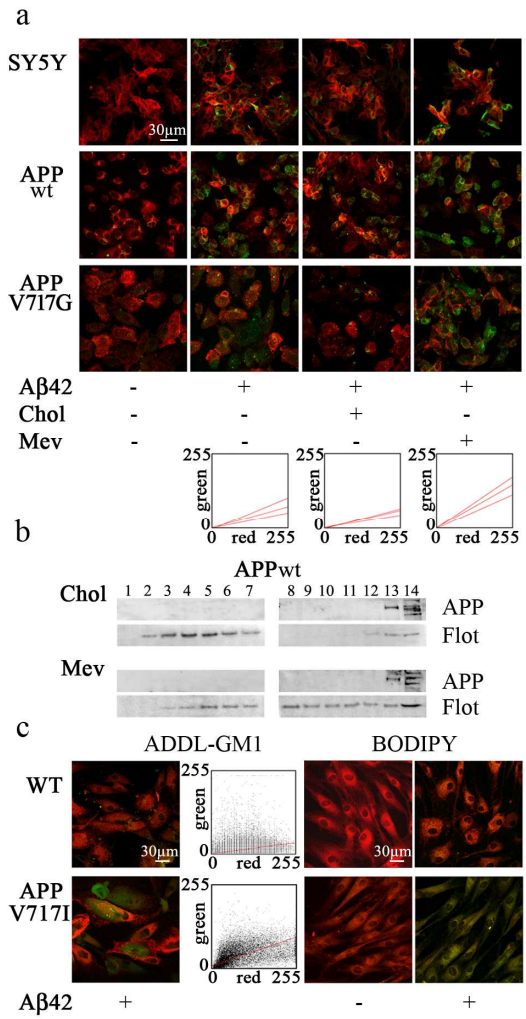

Figure 35. Aβ42 oligomers preferentially colocalize with the raft domains and generate high lipid peroxidation in APPV717I fibroblasts. **a**, Representative confocal microscope images showing Aβ42-GM1 colocalization in SY5Y, APPwt and APPV717G cells exposed to 1.0 μM Aβ42 for 60 min in basal conditions and after treatment with Chol or Mev. Aβ42 aggregates were labelled with 6E10 antibodies (green), while GM1 was stained with Alexa Fluor 647-conjugate CTX-B (red). The scatter plots compare the pattern of Aβ42-GM1 colocalization in the three clones. The sampled pixels are plotted as a function of *red* (*x* axis) and *green* (*y* axis) fluorescence intensity, resulting in partial colocalization (*left panel*), a low degree of colocalization (*middle panel*) and a high degree of colocalization (*right panel*) of Aβ42 aggregates with GM1. **b**, Representative immunoblot analyses of APP and flotillin-1 distributions in 14 sucrose gradient fractions of APPwt cells enriched (Chol) or depleted (Mev) in membrane cholesterol levels. The gradient fractions were collected from the top (low density) to the bottom (high density) of the gradient tube, run on 12% SDS/PAGE and labelled with 6E10 and mouse anti-flotillin-1 monoclonal antibodies. **c**, Representative confocal images showing Aβ42-GM1 colocalization in wild-type (WT) and mutant 717 valine-to-isoleucine APP (APPV717I) fibroblasts are shown on the left-hand side. ADDLs were labelled with 6E10 antibodies (green), while GM1 was stained with Alexa Fluor 647-conjugated CTX-B (red). The scatter plots show the pattern of Aβ42-GM1 colocalization. Representative confocal microscope images of lipid peroxidation in WT and APPV717I fibroblasts exposed (+) or not (–) to 1.0 μM Aβ42 for 60 min using the fluorescent probe BODIPY 581/591 are shown on the right-hand side.

Oxidative effects of Aβ42 oligomers on detergent resistant membranes (DRMs)

To confirm Aβ42 specific interaction with lipid rafts, the biophysical modifications induced by ADDLs in Triton X-100 detergent resistant membranes (DRMs) isolated from SY5Y, APPwt and APPV717G cells at low temperature were investigated. The sucrose gradient fractions rich in flotillin-1 raft marker (fractions from 3 to 5) were pooled and analyzed for the 8-OH isoprostane content and malondialdehyde (MDA) plus 4-hydroxynonenal (4-HNE) levels (Fig. 36a and 36c). A significant higher lipid peroxidation in DRMs from APPwt and APPV717G clones with respect to SY5Y DRMs was evident whereas no APP redistribution in membrane compartments occurred (Fig. 36a and 36c). Moreover, a significant higher level of 8-OH isoprostanes in DRMs from APPV717I fibroblasts with respect to wild-type fibroblasts occurred (Fig. 36b). In particular, the increase in lipid peroxidation levels was higher (about tenfold) in DRM compartments than in the entire membrane, confirming lipid rafts as a preferential site for aggregate binding to cell surface. Then, the effect of Aβ42 oligomers on the structural order of the hydrophobic regions of DRMs was evaluated by measuring the fluorescence anisotropy of DPH dye under steady-state conditions at 37 °C. The relative motion of the DPH molecule within the acyl chain space of the lipid bilayer was determined by polarized fluorescence and expressed as *r*, the anisotropy constant, whose value is inversely proportional to the degree of membrane fluidity. DRMs obtained from APPwt cells displayed a dose dependent anisotropy increase upon exposure to Aβ42 oligomers (Fig. 36c). Then, when the influence of the APP expression levels on the DRM disturbing properties of ADDLs was investigated. DRMs from APPwt and APPV717G cells showed a higher reduction of fluidity with respect to corresponding rafts from SY5Y cells when exposed to ADDLs for different lengths of time (Fig. 36c). Notably, the more ordered structure was reached in less than 10 min of exposure to the oligomers in all cell models. The basal anisotropy level in DRMs from APPwt and APPV717G clones was significantly higher (threefold) than in relatives from SY5Y cells, supporting an increased alteration of membrane structure likely as a result of a chronic exposure to increased levels of Aβ42 peptide.

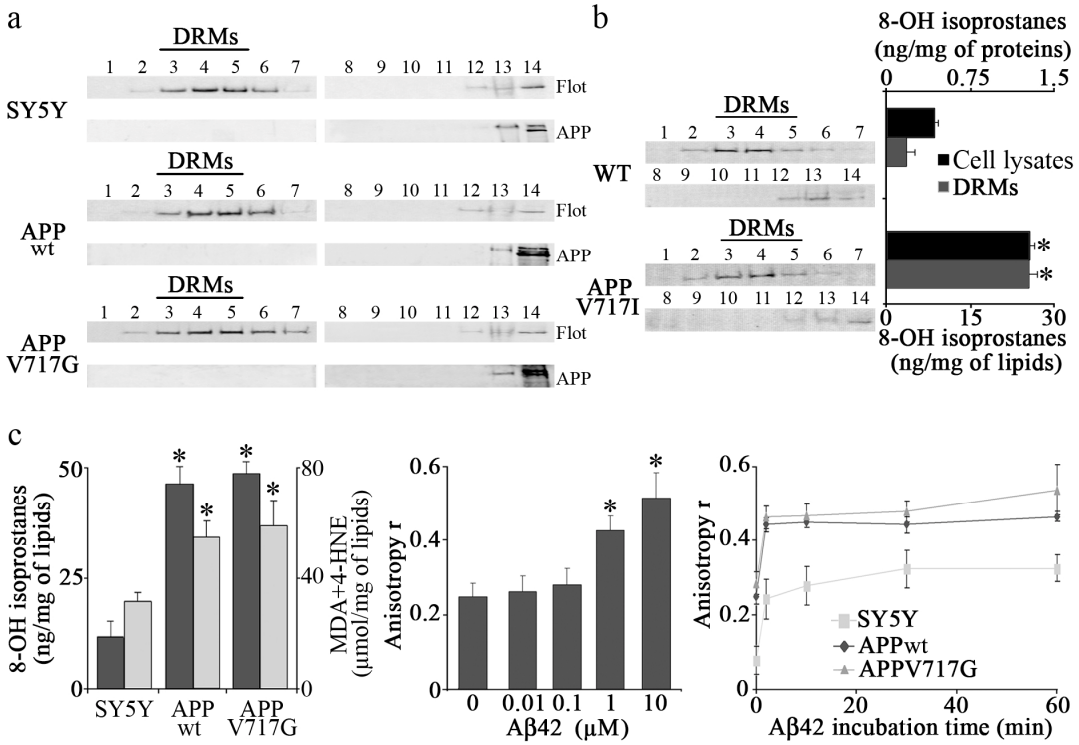

Figure 36. Oxidative effect of Aβ42 aggregates on DRMs. **a**, Representative immunoblot analyses of flotillin-1 and APP distributions in sucrose membrane fractions using specific antibodies. Flotillin-1-rich fractions (from 3 to 5), consisting of detergent resistant membranes (DRMs) were pooled. **b**, Representative immunoblot analysis of flotillin-1 levels in sucrose gradient fractions. 8-OH isoprostane levels were quantified both in cell lysates and in pooled flotillin-1-rich fractions (from 3 to 5) consisting of DRMs purified from WT and APPV717I fibroblasts. The reported values (mean ± SD) are representative of three independent experiments carried out in duplicate. *Significant difference ($p \leq 0.05$) *vs* WT cells. **c**, The amount of 8-OH isoprostanes and MDA plus 4-HNE was quantified in DRMs of the three clones. The reported values (mean ± SD) are representative of three independent experiments carried out in triplicate. *Significant difference ($p \leq 0.05$) *vs* SY5Y cells. DPH fluorescence anisotropy, r, measured by incubating DRMs from APPwt cells with differing concentrations (0.01, 0.1, 1.0 and 10μM) of ADDLs for 30 min. On the right, DRMs from SY5Y, APPwt and APPV717G cells were incubated for 0, 2, 10, 30 and 60 min with 1.0 μM Aβ42 aggregates. The reported values (mean ± SD) are representative of six independent experiments, each performed in duplicate. *$p \leq 0.05$, significant difference *vs* untreated DRMs.

GM1-mediated accumulation of Aβ42 oligomers on plasma membranes

Previous AFM analysis on DRMs, isolated from SY5Y cells, demonstrated an abundant distribution of GM1 granular structures in these membrane compartments [243]. In order to assess whether lipid rafts are specific targets of membrane oxidative injury, APPwt and APPV717G cells were pre-incubated with anti-GM1 antibodies (Ab_{GM1}) or with the B subunit of cholera toxin (CTX-B) before exogenously Aβ42

treatment. The specific binding of anti-GM1 antibodies and of CTX-B to raft monosialoganglioside prevented the BODIPY fluorescence shift both in APPwt and APPV717G cells, suggesting a major role of raft domain GM1 in lipid peroxidation process induced by ADDLs (Fig. 37a). Derangement of ion distribution across the plasma membrane is an early biochemical modification displayed by cells exposed to amyloid aggregates [160, 170]. Accordingly, a sharp calcein leakage in SY5Y, APPwt and APPV717G cells was evident (Fig. 37b), suggesting an extensive alteration of membrane permeability induced by Aβ42 aggregates. Moreover, the lower calcein fluorescence in APPwt and APPV717G cells compared to SY5Y cells, before exogenously addition of ADDLs, indicated a chronic amyloid-induced membrane damage in cell facing a higher Aβ production. In order to assess whether raft ability to bind Aβ42 aggregates triggers the loss of membrane integrity, the cells were pre-incubated with anti-GM1 antibodies (Ab_{GM1}) or with CTX-B and then membrane permeability were analyzed in cells exposed to ADDLs. Anti-GM1 antibodies and CTX-B binding to GM1 reduced the calcein fluorescence decay (Fig. 37b), supporting a major role of lipid rafts in aggregate recruitment to the cell membrane and in the subsequent alterations of surface properties. To confirm lipid rafts as main targets of Aβ42 incorporation, a specific inhibition of GM1 biosynthesis was achieved in SY5Y APPwt, APPV717G clones using the D-threo-1-phenyl-2-decanoylamino-3-morpholino-1-propanol (PDMP) (Fig. 37c), while maintaining cell viability (data not shown). The pharmacological interference with lipid raft structure almost prevented Aβ42 incorporation in all clones exposed to ADDLs.

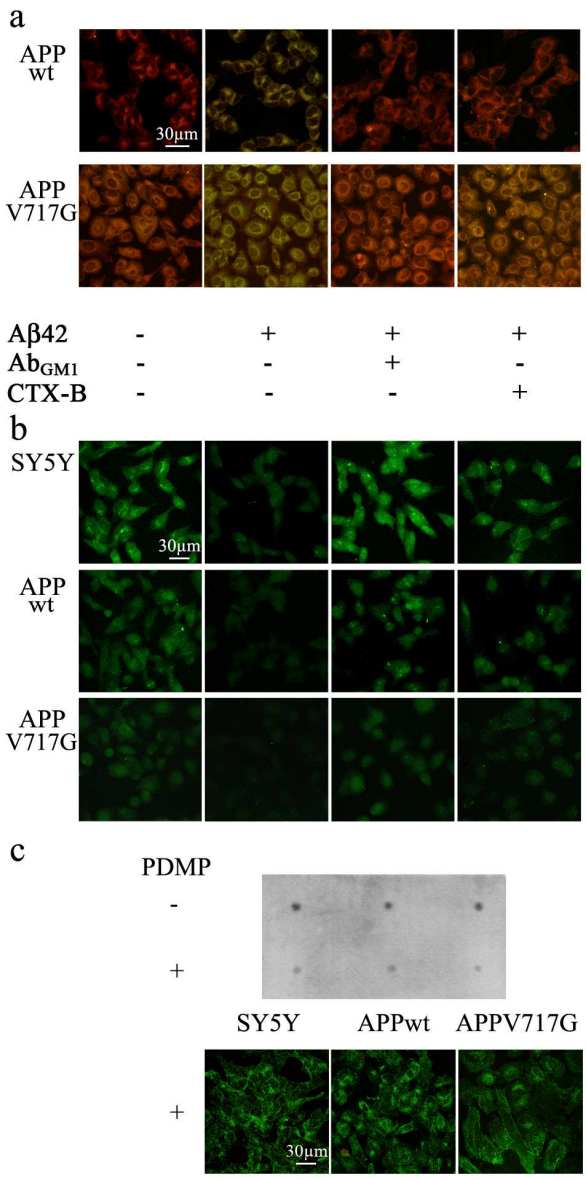

Figure 37. GM1 mediates accumulation of Aβ42 oligomers on plasma membranes. **a**, On the top, representative confocal images of lipid peroxidation in APPwt and APPV717G neuroblastoma cells pre-incubated for 20 min with 1:100 diluted rabbit polyclonal anti-GM1 antibodies (Ab$_{GM1}$) or with 4.5 μg/ml CTX-B and subsequently exposed to Aβ42 aggregates for 60 min as assessed using the fluorescent probe BODIPY581/591. **b**, Representative confocal microscope images of SY5Y, APPwt and APPV717G neuroblastoma cells loaded with 2.0 μM calcein-AM for 20 min. The cells were then incubated for 20 min with or without Ab$_{GM1}$ or CTX-B and subsequently exposed to 1.0 μM ADDLs for 60 min. (c) Representative dot blot analysis of membrane GM1 content in SY5Y, APPwt and APPV717G cells cultured in the absence (-) or in the presence (+) of 25 μM PDMP for 48 h. Bottom, representative confocal images of the three clones pre-treated with PDMP and exposed to 1.0 μM Aβ42 aggregates for 60 min. The plasma membrane profile was stained with fluorescein-conjugated wheat germ agglutinin (green) and Aβ42 aggregates with 6E10 antibodies (red).

-RESULTS IV-

PROTECTIVE EFFECT OF NEW S-ACYL-GLUTATHIONE DERIVATIVES AGAINST AMYLOID-INDUCED OXIDATIVE STRESS

Recent data support the role of oxidative stress in the pathogenesis of Alzheimer disease (AD). In particular, glutathione (GSH) metabolism is altered and its levels are decreased in affected brain regions and peripheral cells from AD patients and in experimental models of AD. In the past decade, interest in the protective effects of various antioxidants aimed at increasing intracellular GSH content has been growing. In this fourth part of the result section the ability of new S-acyl-glutathione (acyl-SG) thioesters to prevent the synaptotoxic and neurodegenerative effects putatively triggered by Aβ accumulation was investigate. Because much experimental evidence suggests a possible protective role of unsaturated fatty acids in age-related diseases, the synthesis of new acyl-SG thioesters was designed. S-lauroyl-glutathione (lauroyl-SG) and S-palmitoleoyl-glutathione (palmitoleoyl-SG) were easily internalized into the cells and they significantly reduced Aβ42-induced oxidative stress in human neurotypic SH-SY5Y cells. In particular, acyl-SG thioesters can prevent the impairment of intracellular ROS scavengers, intracellular ROS accumulation, lipid peroxidation, and apoptotic pathway activation. Palmitoleoyl-SG seemed more effective in cellular protection against Aβ-induced oxidative damage than lauroyl-SG, suggesting a valuable role for the monounsaturated fatty acid. Moreover, acyl-SG derivatives completely avoid the sharp lipoperoxidation in primary fibroblasts from familial AD patients occurring after exposure to Aβ42 aggregates. Hence, these new antioxidant compounds could be excellent candidates for therapeutic treatment of AD and other oxidative stress-related diseases.

Synthesis and analysis of lauroyl-SG and palmitoleoyl-SG thioesters

The GSH acylation by long-chain fatty acids required prior thioesterification to their respective fatty acyl-CoA products, which may then serve as the immediate acylating nucleophiles [396, 397]. Indeed, the activation of fatty acids to their corresponding high-energy acyl-CoA thioester derivatives is a required step before the use of fatty acids for cellular reactions, including fatty acid synthesis [398] and fatty acylation [399], both of which require a reactive carbonyl carbon. The reaction of the carboxylic group of the lauric acid (C12:0) and of the palmitoleic acid (C16:1) of acyl-CoA's with the sulfhydryl group of GSH resulted in a time-dependent synthesis of lauroyl-SG (Fig. 38a) and palmitoleoyl-SG (Fig. 39a) derivatives, reaching a maximum after a 24-h incubation time in sodium phosphate at 37°C (Fig. 38b and 39b). After the purification of glutathione derivatives from reaction mixture by reverse-phase HPLC, the mass spectra of each peak were acquired by MALDI/TOF. Mass peaks distinctive of each conjugate at the expected molecular weights of 490.2 (m/z) for lauroyl-SG (Fig. 38c) and 544.5 (m/z) for palmitoleoyl-SG (Fig. 39c) were revealed. The identity and the purity of the reaction products were also confirmed by ESI–MS/MS analysis (not shown). A quantitative analysis of acyl-SG peaks was performed by Ellman's test, which is based on the conversion of colorless DTNB into yellow TNB in the presence of thiol compounds. A time-dependent increase in the release of GSH after the acid hydrolysis of lauroyl-SG (Fig. 38d) and palmitoleoyl-SG (Fig. 39d) was observed. The amount of synthesized products, after a 48-h complete acid hydrolysis reaction, indicated a purification yield for lauroyl-SG thioester approximately twofold higher (25.8±1.6 nmol GSH) than for palmitoleoyl-SG thioester (9.1±1.3 nmol GSH), starting from 250 nmol of acyl-CoA and 1250 nmol of GSH.

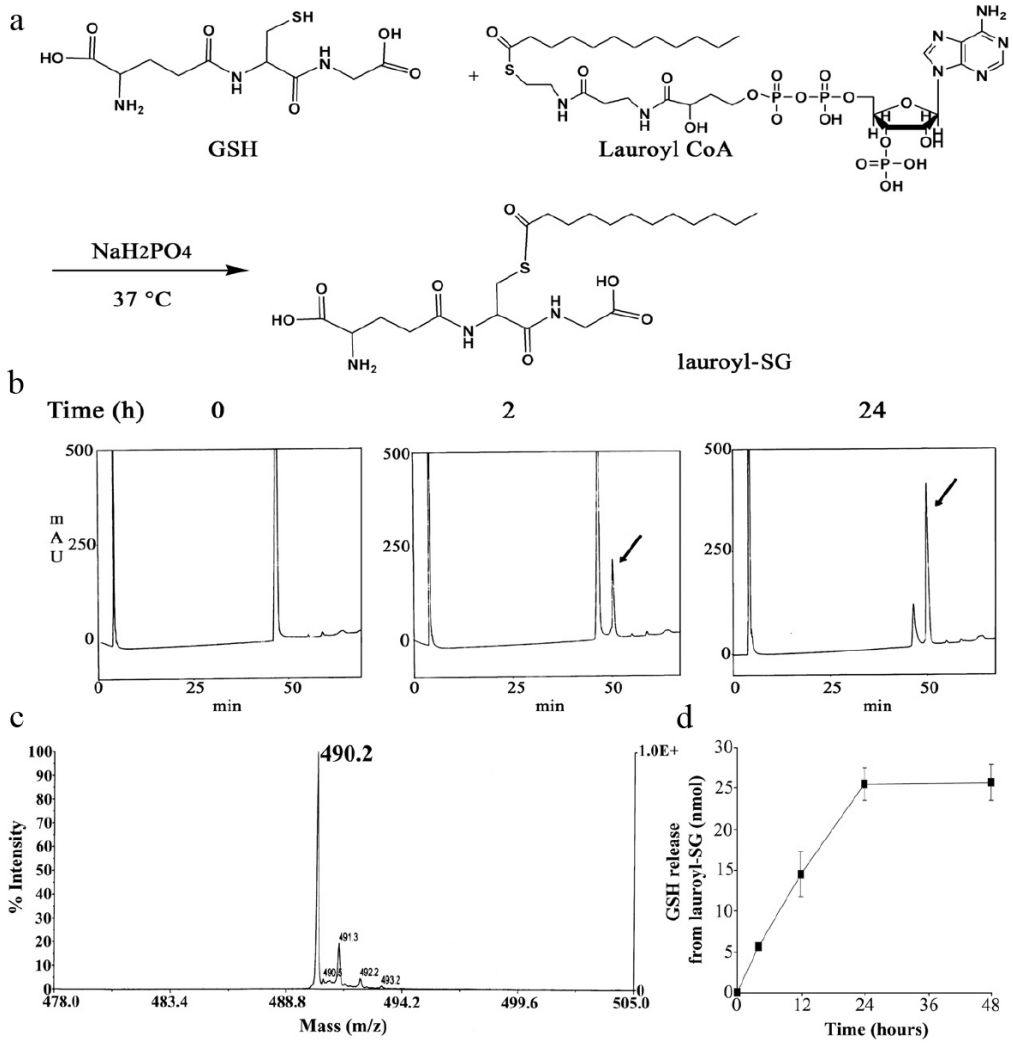

Figure 38. Synthesis, purification, and characterization of lauroyl-SG. **a**, Scheme for chemical synthesis, performed with 25 mM GSH and 5 mM lauroyl-CoA in 50 mM phosphate buffer, pH 7.5, at 37°C. **b,** Representative reverse-phase HPLC chromatograms with UV detection (228 nm) showing the kinetic of lauroyl-SG synthesis after 0, 2, and 24 h of incubation. The arrows indicate the lauroyl-SG peak. **c,** Mass spectrum of product ions obtained by MALDI analysis of the HPLC-purified adduct. For details, see Materials and Methods section. **d,** The amount of lauroyl-SG thioester was indirectly determined by quantitative analysis of the GSH release after acid hydrolysis of HPLC-purified thioester, using a calibration curve with GSH as an internal standard. Values are expressed as means ± SD and are representative of three independent experiments carried out in duplicate.

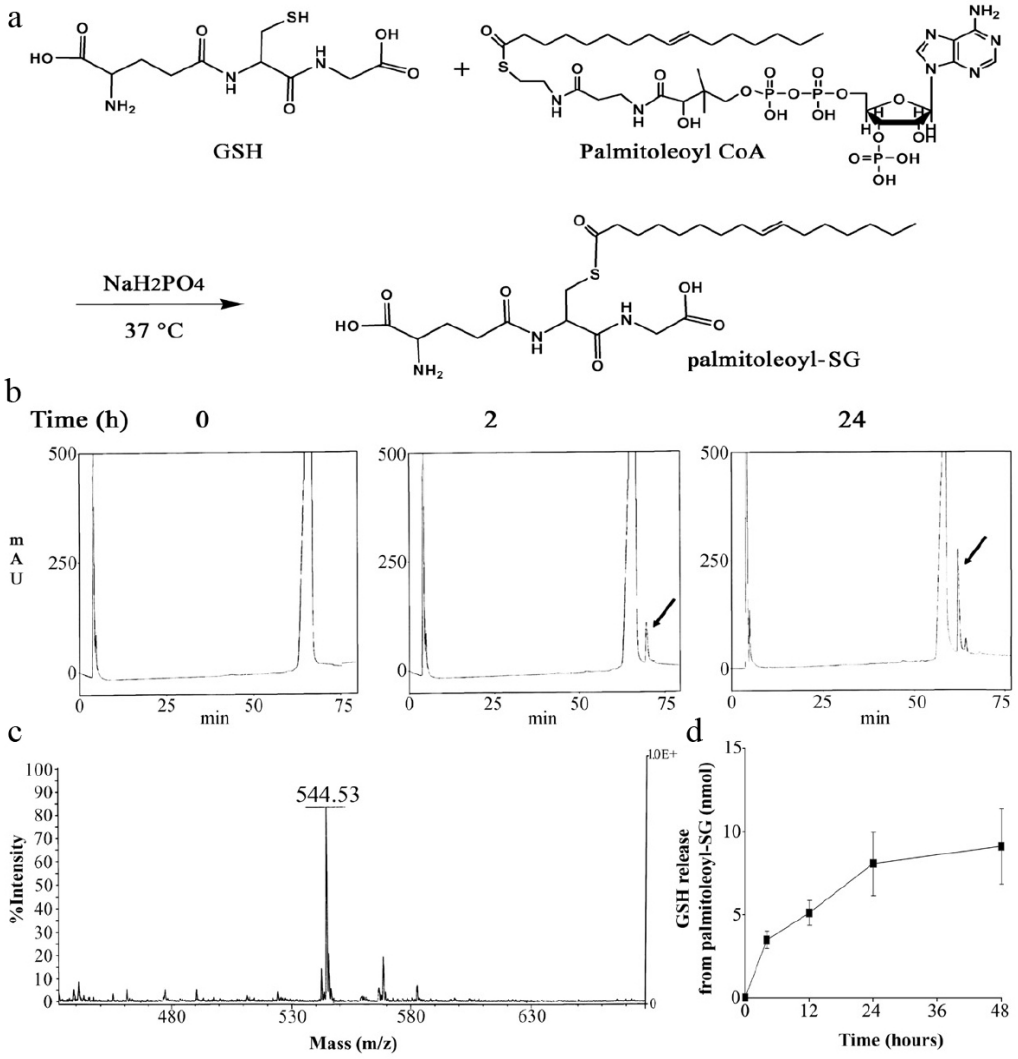

Figure 39. Synthesis, purification, and characterization of palmitoleoyl-SG. **a,** Scheme for chemical synthesis, performed with 25mM GSH and 5 mM palmitoleoyl-CoA in 50 mM phosphate buffer, pH 7.5, at 37°C. **b,** Representative reverse-phase HPLC chromatograms with UV detection (228 nm) showing the kinetic of palmitoleoyl- SG synthesis, after 0, 2, and 24 h of incubation. The arrows indicate palmitoleoyl-SG peak. **c,** Mass spectrum of product ions obtained by MALDI analysis of the HPLC-purified adduct. For details, see Materials and Methods section. **d,** The amount of palmitoleoyl-SG thioester was indirectly determined by quantitative analysis of the GSH release after acid hydrolysis of HPLC-purified thioester. Values are expressed as means ± SD and are representative of three independent experiments carried out in duplicate.

Intracellular GSH increase in SH-SY5Y and FAD cells

Then, I investigated whether exposure to the synthetic compounds can increase intracellular content of free GSH in SH-SY5Y neuroblastoma cells and in skin primary FAD fibroblasts. In particular, the ability of acyl-SG thioesters to cross the plasma membrane and to enter the cells and, once inside, to release free GSH after hydrolysis by cellular thioesterases was evaluated. A time-course analysis showed a significant increase in intracellular GSH levels in SH-SY5Y cells exposed to 1.0 μM lauroyl-SG for 3 and 5 h (Fig. 40a). Accordingly, the more prolonged the palmitoleoyl-SG derivatives treatment time, the higher the increase in intracellular GSH levels. To test whether the acyl-SG derivative uptake was a dose-dependent process, intracellular GSH levels were determined in SH-SY5Ycells exposed to different acyl-SG thioester concentrations. Palmitoleoyl-SG thioester was more effective in increasing intracellular GSH levels than lauroyl-SG thioester at various conjugate concentrations (from 0.2 to 5 μM) (Fig. 40b). Similar experiments carried out on FAD fibroblasts confirmed the internalization process of acyl-SG derivatives. In particular, intracellular GSH levels were significantly raised in fibroblasts treated for 3 h with 1.0 μM palmitoleoyl-SG thioester (29.6± 2.0 nmol/mg of protein, $p<0.01$) or with 1.0 μM lauroyl-SG thioester (25.8±1.5 nmol/mg of protein, $p<0.05$) with respect to untreated cells (21.3±1.6 nmol/mg of protein).

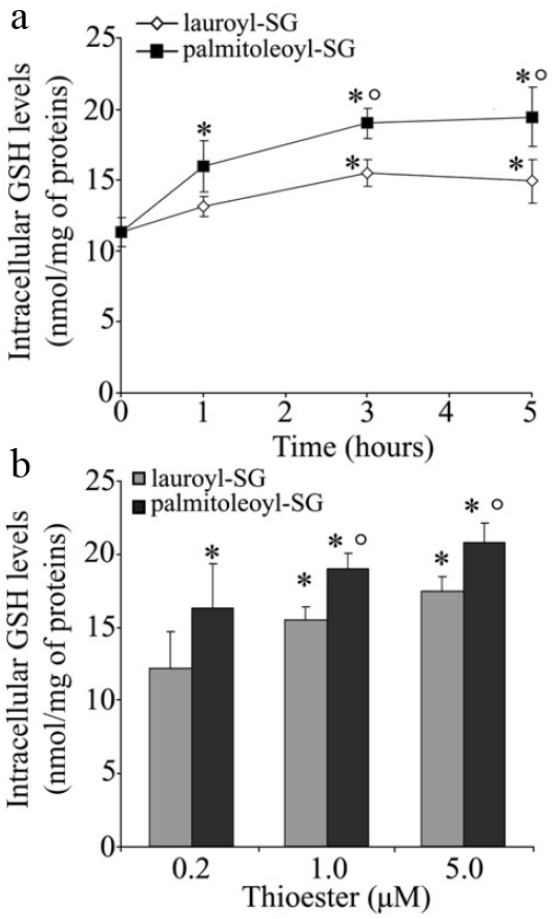

Figure 40. a, Time-course analysis of intracellular GSH levels in SH-SY5Y cells after incubation for 1, 3, and 5 h with 1.0 μM acyl-SG conjugates. **b,** Intracellular GSH content in SH-SY5Y cells after exposure to various final concentrations of acyl-SG thioesters (0.2, 1.0, and 5.0 μM) for 3 h. Values are means ± SD of three independent experiments, each performed in duplicate. *Significant difference ($p \leq 0.05$) vs control cells. °Significant difference ($p \leq 0.05$) vs lauroyl-SG-pretreated cells.

Acyl-SG derivatives counteract amyloid cytotoxicity

Neuronal cells exposed to toxic amyloid assemblies usually exhibit impaired viability, oxidative stress, and mitochondrial dysfunction [195, 196, 400]. A time-course analysis of SH-SY5Y cell viability in the presence of 1.0 μM acyl-SG derivatives, followed by exposure to 5.0 μM Aβ42 prefibrillar aggregates, was performed using the MTT test, taking into account the cautions due to the increase in the cell number in dividing cell samples [401] (Fig. 41). A significant impairment (about 35%) in SH-SY5Y cell viability was evident after exposure to Aβ42 aggregates for 24 h. A significant recovery of cell viability was evident when cells were pretreated with lauroyl-SG and much more

with palmitoleoyl-SG thioesters before exposure to Aβ42 aggregates (Fig. 41a). In particular, the more prolonged the acyl-SG treatment time, the higher the protection against aggregate toxicity. As a result, the following experiments were performed by incubating SH-SY5Y cells with acyl-SG thioesters for 3 h, because at this time the protective effect of such compounds did not significantly differ from that observed at 5 h. On the other hand, no significant increase in cell viability was detected in cells exposed to lauroyl-CoA (about 71.3±3.9%), palmitoleoyl-CoA (about 68.0±2.3%), and GSH (about 63.5±6.8%), compared to control cells (about 65.8±4.4%). The ability of palmitoleoyl-SG thioester to protect SH-SY5Y cells against aggregate cytotoxicity was higher than that of lauroyl-SG thioester at various conjugate concentrations (from 0.2 to 5.0 μM) (Fig. 41b). In particular, at 1.0 μM a significant difference in the protective effect of palmitoleoyl-SG thioester with respect to lauroyl-SG was observed. Similar results were obtained in H_2O_2-exposed cells, in which the ability of palmitoleoyl-SG to counteract H_2O_2 oxidative injury overcame that of lauroyl-SG thioester at all the investigated concentrations (Fig. 41c).

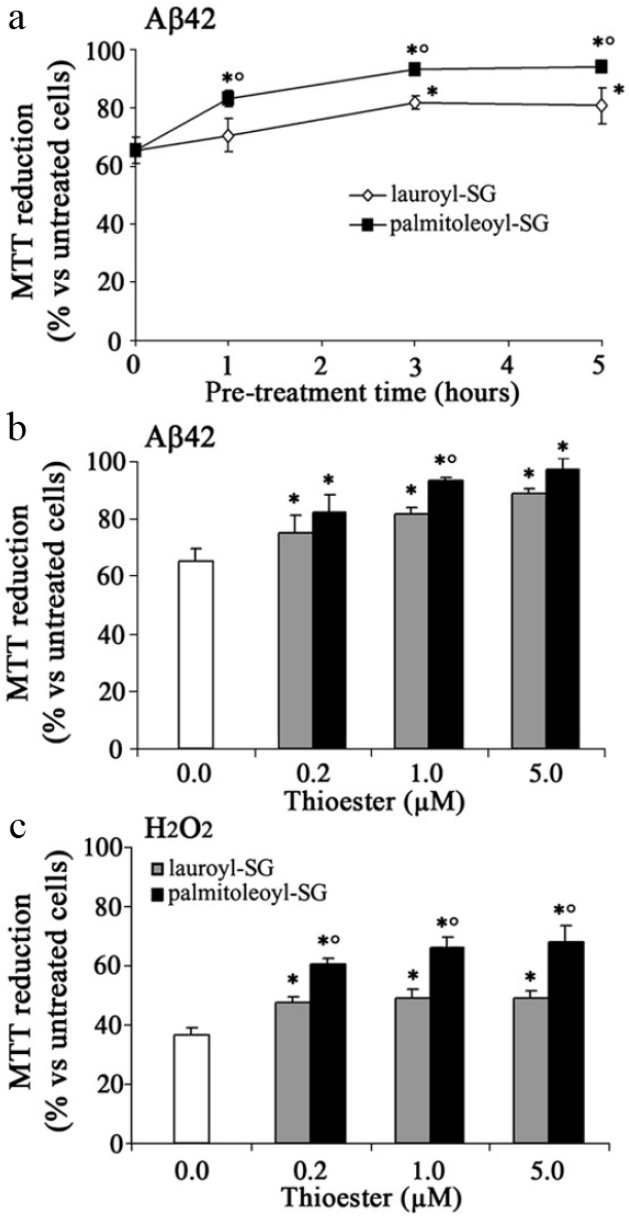

Figure 41. Acyl-SG thioesters improve the viability of SH-SY5Y cells experiencing oxidative damages. **a,** Cell viability was measured by the MTT reduction test in cells treated with 1.0 μM acyl-SG thioesters for various lengths of time (0, 1, 3, and 5 h), before exposure to 5.0 μM Aβ42 aggregates for 24 h. Viability of cells exposed for 3 h to varying amounts of acyl-SG derivatives was checked both in **b**, 5.0 μM Aβ42 prefibrillar aggregates and in **c**, 250 μM H_2O_2 24-h-treated cells. Blank column represents cells treated with Aβ42 or H_2O_2, without thioester pretreatment. The reported values are expressed as percentage of MTT reduction in treated cells with respect to untreated cells (means ± SD) and are representative of three independent experiments carried out in triplicate. *Significant difference ($p \leq 0.05$) vs treated cells. °Significant difference ($p \leq 0.05$) vs lauroyl-SG-pretreated cells.

Antioxidant properties of acyl-SG derivatives

It is well known that oxidative stress can be the effect of either any increased free radical production or the weakening of the cell antioxidant defenses, including antioxidant enzymes, lipophilic, and hydrophilic scavengers. In the present study, the changes in non enzymatic hydrophilic ROS scavengers after exposure to acyl-SG thioesters in SH-SY5Y cells were measured. As shown in figure 42a, cells underwent a significant increase in ROS scavengers in the presence of both 1.0 μM lauroyl-SG and palmitoleoyl-SG thioesters in the cell culture medium, reaching a maximum after 3 h of exposure (1044.39±45.58 and 1174.30±48.63 nmol mg^{-1} of total proteins, respectively), compared to the basal antioxidant defenses of untreated cells (703±33.33 nmol mg^{-1} of total proteins). In particular, a higher palmitoleoyl-SG thioester antioxidant property compared to lauroyl-SG derivative was evident just after 20 min of GSH thioester treatment. These data confirmed that palmitoleoyl-SG permeates neuronal membrane more quickly than lauroyl-SG. Much experimental evidence suggests that oxidative stress is an early biochemical modification in cells facing amyloid aggregates [74, 329]. Therefore, the ability of acyl-SG derivatives to counteract intracellular ROS scavenger impairment after amyloid aggregate or H_2O_2 exposure was investigated. SH-SY5Y cells after Aβ42 aggregate treatment underwent a significant early scavenger decline (30 min), with any recovery at longer times of exposure (Fig. 42b). On the other hand, cells pretreated with both lauroyl-SG and palmitoleoyl-SG derivatives, though displaying a significant decrease in intracellular defense levels during the first 30 min, recovered almost completely at longer times of aggregate exposure. In particular, the palmitoleoyl-SG protective effect against Aβ42-induced antioxidant defense impairment was higher than that of lauroyl-SG. In contrast, after H_2O_2 oxidative injury SY5Y cells can partially preserve their antioxidant capacities, especially in the presence of palmitoleoyl-SG (Fig. 42c).

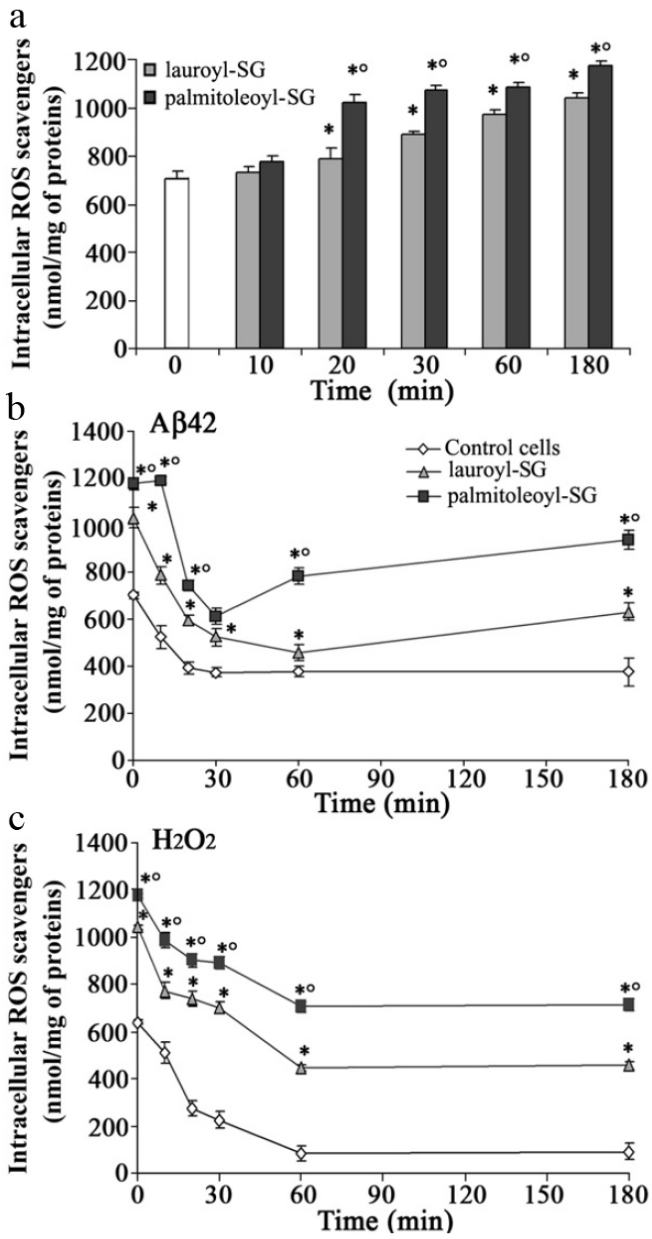

Figure 42. Antioxidant properties of lauroyl-SG and palmitoleoyl-SG thioesters. Intracellular ROS scavengers were measured by a chemiluminescence assay in the cytosolic fractions of cell lysates and expressed in ascorbate-equivalent units. **a,** Time course of intracellular antioxidant defenses measured in SH-SY5Y cells exposed to 1.0 μM acyl-SG thioesters for 10, 20, 30, 60, and 180 min at 37°C. The cells were also incubated with 1.0 μM acyl-SG thioesters for 180 min and then treated with (**b**) 5.0 μM Aβ42 aggregates or (**c**) 250 μM H_2O_2 for 10, 20, 30, 60, and 180 min at 37°C. The reported values (means ± SD) are representative of three independent experiments each carried out in triplicate. *Significant difference ($p \leq 0.05$) vs treated cells. °Significant difference ($p \leq 0.05$) vs lauroyl-SG-pretreated cells.

As a result, GSH thioester-pretreated cells were able to counteract the early rise in intracellular ROS seen in control cells (Fig. 43). In particular, palmitoleoyl-SG was

more effective than lauroyl-SG in facing both aggregate (Fig. 43a) and H_2O_2 (Fig. 43b) oxidative injury.

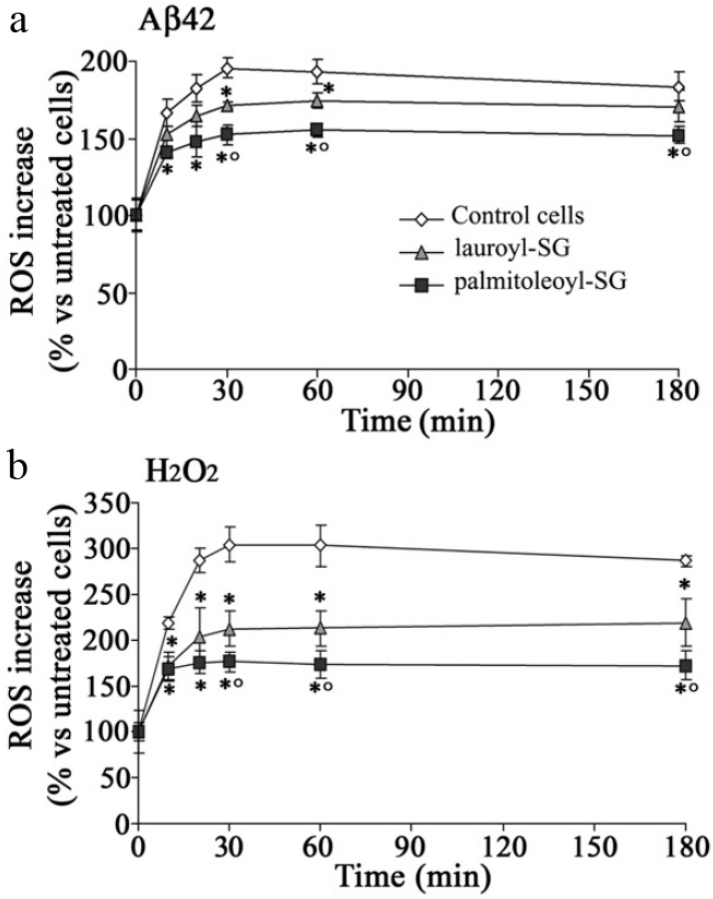

Figure 43. Intracellular ROS production in SH-SY5Y cells. Cells exposed or not to 1.0 μM acyl-SG thioesters were treated with (**a**) 5.0 μM Aβ42 aggregates or (**b**) 250 μM H_2O_2 for 10, 20, 30, 60, and 180 min. CM-H_2DCFDA fluorescence was measured using a spectrofluorimeter. Values are expressed as % with respect to untreated cells. The values shown are means ± SD of three independent experiments, each performed in duplicate. *Significant difference ($p \leq 0.05$) vs treated cells. °Significant difference ($p \leq 0.05$) *vs* lauroyl-SG-pretreated cells.

In addition, the increased ability of SH-SY5Y cells pretreated with acyl-SG thioesters to counteract oxidative stress resulted in an evident reduction in lipoperoxidation. As shown in figure 44a, the BODIPY 581/591 red fluorescence, assessing lipid peroxidation in untreated control cells, shifted to green after 3 h of exposure to the aggregates and, more evidently, to H_2O_2. On the other hand, the fluorescence signals of cells pretreated with both lauroyl-SG and palmitoleoyl-SG thioesters, exposed to Aβ42 aggregates or to H_2O_2, did not notably differ from their counterpart untreated cells.

Accordingly, a significant decrease in lipoperoxidation levels was evident in neuroblastoma cells pretreated with acyl-SG thioesters before exposure to 5.0 μM Aβ42 aggregates, as revealed by the 8-OH isoprostane assay (Fig. 44b).

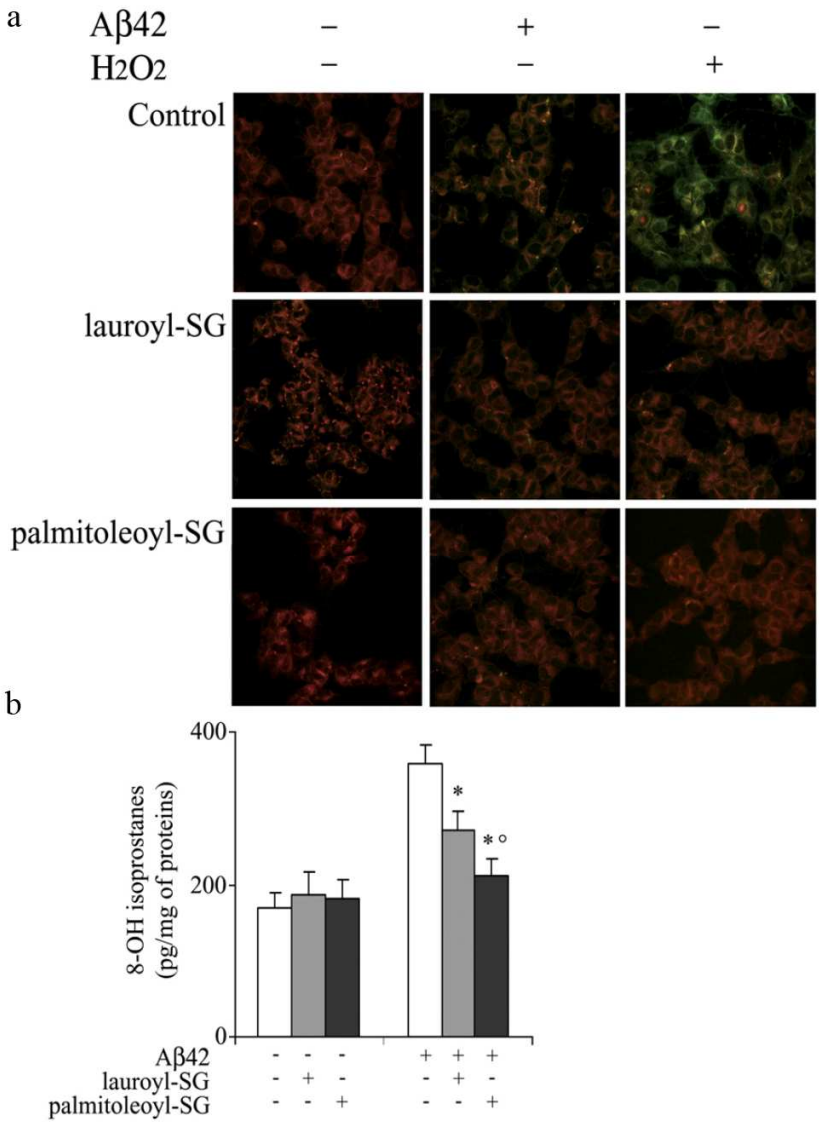

Figure 44. a, Representative confocal microscopy images of BODIPY fluorescence correlated with lipid peroxidation in SH-SY5Y cells. The cells exposed or not to 1.0 μM acyl-SG thioesters were treated with 5.0 μM Aβ42 or 250 μM H_2O_2 for 3 h. **b,** Cytosolic levels of 8-OH isoprostanes in SH-SY5Y cells pretreated or not with 1.0 μM acyl-SG thioesters and then with 5.0 μM Aβ42 aggregates for 3 h. The reported values (means ± SD) are representative of three independent experiments carried out in duplicate. *Significant difference ($p \leq 0.05$) vs Aβ-treated cells. °Significant difference ($p \leq 0.05$) vs lauroyl-SG-pretreated cells.

Previous data on lymphoblasts and fibroblasts carrying APP and PS-1 gene mutations have shown a significant TAC impairment and a marked increase in membrane lipoperoxidation compared to healthy controls [210]. Previous results suggest that Aβ42 aggregates can easily induce a prompt and sharp ROS production in fibroblasts from FAD patients [205]. In the present study, the protective effect of acyl-SG thioesters resulted in an apparent reduction of lipoperoxidation in primary APPV717I mutated fibroblasts as evaluated by a confocal analysis of the fluorescent BODIPY 581/591 reporter (Fig. 45a). Accordingly, as revealed by the 8-OH isoprostane assay reported in figure 45b, a significant decrease in lipoperoxidation levels was induced by a higher ability of fibroblasts pretreated with acyl-SG thioesters to counteract Aβ aggregate oxidative attack. No significant difference with respect to the basal level of controls in cells exposed for 3 h to the acyl-SG derivatives was evident.

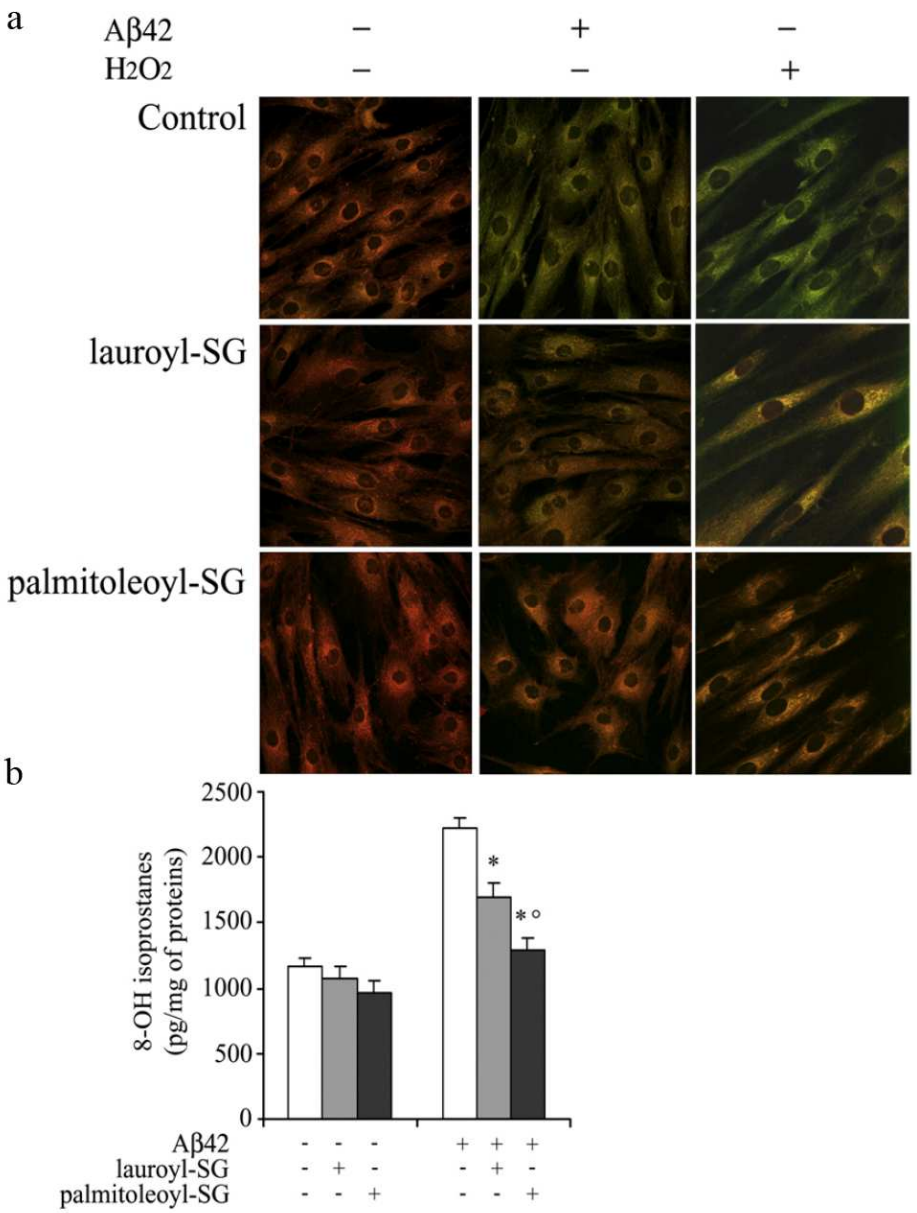

Figure 45. a, Representative confocal microscopy images of BODIPY fluorescence correlated with lipid peroxidation in primary APPV717I mutated fibroblasts. Cells exposed or not to 1.0 μM acyl-SG thioesters were treated with 5.0 μM Aβ42 or 250 μM H_2O_2 for 3 h. **b,** Cytosolic levels of 8-OH isoprostanes in primary APPV717I mutated fibroblasts incubated or not with 1.0 μM acyl-SG thioesters and then with 5.0 μM Aβ42 aggregates for 3 h. The reported values (means ± SD) are representative of three independent experiments carried out in duplicate. *Significant difference ($p \leq 0.05$) vs Aβ-treated cells. °Significant difference ($p \leq 0.05$) vs lauroyl-SG-pretreated cells.

Acyl-SG derivatives prevent aggregate-induced apoptotic cell death

Abundant data indicate that amyloid aggregate toxicity eventually results in apoptotic or, less frequently, necrotic cell death [157, 329, 402]. The extent of the apoptotic program activation in acyl-SG derivative-pretreated cells, exposed or not to Aβ42 aggregates or H_2O_2, was evaluated by confocal microscopy analysis of caspase-3 activity, which is the main effector caspase in apoptosis. According to the above-reported results, the increase in caspase-3 activity was prevented by cell pre-treatment with acyl-SG thioesters (Fig. 46).

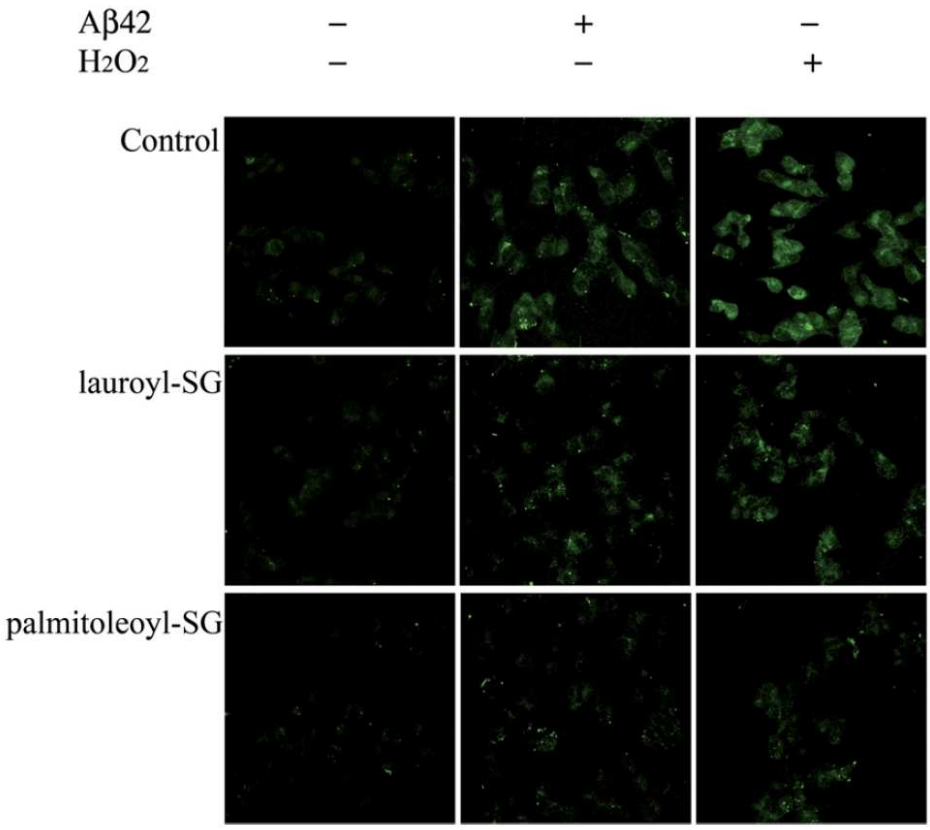

Figure 46. Representative confocal microscopy images of caspase-3 activation. Cells exposed or not to 1.0 μM acyl-SG thioesters were treated with 5.0 μM Aβ42 or 250 μM H_2O_2 for 3 h. Caspase-3 activity was measured using the fluorescent probe FAM-FLICA Caspases 3&7 according to Materials and Methods section.

CHAPTER IV – DISCUSSION

Relationship between cellular impairment and oligomer structure in protein deposition diseases

A number of biochemical modifications eventually leading to cell death have been reported in cells exposed to toxic aggregates of several differing peptides and proteins either in whole animals or in differing cultured cell lines [81, 157, 403-407]. The small (91-residues) globular HypF-N peptide is a valuable model system for investigating the structural basis of the cellular dysfunction caused by misfolded protein oligomers. In fact, HypF-N is able to form amyloid-like fibrils and protofibrils *in vitro* under conditions that promote its partial unfolding [91]. In the present study, the different biological activities, on cells, exerted by two types of HypF-N oligomers, grown under different environmental conditions were explored. These oligomers have a similar hydrophobic core and are sufficiently stable to maintain their structure and properties when transferred to physiological solution such as culture medium and phosphate buffer. To address this issue, the ability of the two different HypF-N oligomers to be cytotoxic to human neurotypic SH-SY5Y cells by modulating aggregate binding to the cell membrane, in most cases a recognized key step in amyloid cytotoxicity was investigated. A close relation between the cytotoxicity and the amount of aggregate inclusion into the membrane of cells exposed to oligomers formed under condition A was found. By contrast, no impairment in cells exposed to differing amount of oligomers grown under condition B was observed, suggesting that the lack of toxicity of this species is not due to an insufficient amount of oligomers being in contact with the cells. These results suggest that the structural differences in HypF-N oligomers, such as the different degrees of packing of the hydrophobic residues within their cores, determine a different ability to permeate the membrane associated with the structural flexibility of such residues. Furthermore, the cytotoxic effect of early aggregates formed in condition A decreased with longer time of aggregate growth, while the aggregates formed in condition B maintained their lack of toxicity after prolonged grown periods. These results are consistent with recent data suggesting that oligomers, rather than mature amyloid fibrils, act as toxins in many protein misfolding pathologies such as

Alzheimer's and Parkinson's diseases [37]. Interestingly, the decline in cytotoxicity is strictly related to a reduced internalization of aggregates into the cells. These findings further confirms the ability of early aggregates with respect to older species to bind and penetrate cell membrane. Moreover, the ability of cell membrane to bind and internalize HypF-N oligomers is influenced by the period of cell exposure to aggregates. The present results indicate that the toxicity is associated with the ability of the oligomeric species to form a more pronounced and disruptive interaction with the cells, stimulating Ca^{2+} influx and leading to cell death. These results also indicate that HypF-N oligomers formed under condition A caused a great modification of membrane permeability, resulting in a sharp increase in cytosolic free Ca^{2+} in SH-SY5Y cells. This increase is inhibited when cells are exposed to oligomers in a free Ca^{2+}-medium, indicating that Ca^{2+} influx from the extracellular medium is responsible for this effect. By contrast, membrane integrity and cytosolic Ca^{2+} homeostasis are maintained when cells are treated with oligomers formed under condition B. ROS accumulation, lipid peroxidation and direct oxidative damage to membranes are also a major outcome of oligomers grown under condition A compared to cells treated with aggregates grown under condition B. Moreover, the increase in oxidative stress is almost completely inhibited when cells are exposed to oligomers formed under condition A in a Ca^{2+}-free medium or after a pre-incubation of cells with vitamin E. Accordingly, caspase 3 levels and LDH release in the cell culture media are markedly increased only in cells exposed to oligomers grown under condition A. Therefore, these results suggest that cell treatment with HypF-N oligomers, showing a low degree of packing of the hydrophobic residues within their cores and a high structural flexibility of such residues, induces oxidative stress, intracellular Ca^{2+} dyshomeostasis and membrane damage, which initially triggers the apoptotic pathway and can ultimately lead to necrosis. In contrast, cell exposure to native or more structurally packed oligomers avoid protein internalization, oxidative attack, membrane damage, cationic influx and ultimately cell dysfunction. In conclusion, these data depict membrane destabilization and the subsequent early derangement of ion balance and intracellular redox status as key events in targeting exposed cells to apoptotic death. These data contribute to the elucidation of the causative link between the molecular structure of aberrant protein oligomers and their ability to cause cell dysfunction. Finally, the conversion of amyloid aggregates into

species unable to damage cell membranes represents a valuable target for therapeutic interventions aimed at preventing the onset of protein deposition diseases.

Membrane cholesterol enrichment prevents Aβ-induced oxidative stress in Alzheimer's fibroblasts

Growing data indicate that changes in membrane cholesterol content, by modulating lipid fluidity, have regulatory consequences for Aβ interactions with the cell plasma membranes and neurotoxicity [186, 221, 242, 256, 266, 408-410]. The present study provides evidence supporting the hypothesis that membrane cholesterol modulation might affect the sensitivity to Aβ42 aggregates of primary fibroblasts carrying APP Val717Ile or PS-1 Leu392Val or Met146Leu gene mutations by modulating Aβ aggregate binding to the cell membrane, recognized as a primary step in amyloid cytotoxicity. In particular, confocal microscopy images, flow cytometric analysis and Congo red assay revealed that Aβ42 assemblies accumulate faster, and are internalized to a greater extent into, the plasma membranes of cholesterol-poor fibroblasts than in cholesterol-enriched cells. Indeed, it seems likely that when the level of cholesterol in the membrane is higher than normal, the insertion process can be prevented by the enhanced stiffness of the membrane. On the other hand, when the Aβ oligomer encounters a membrane with increased fluidity due to a lower cholesterol level, the insertion process can occur [186]. Despite a relatively low number of patient samples employed in our study that limits the statistical power of the results, these findings strongly support the idea that the ability of Aβ42 aggregates to bind to the plasma membrane is significantly affected by its content in cholesterol [94]. Even in human SH-SY5Y neuroblastoma cells, mild cholesterol enrichment appears to prevent Aβ42 aggregate binding to the plasma membrane, corroborating this hypothesis in a neuronal system. However, it cannot be excluded that different APP distribution and/or accessibility in the plasma membranes, likely resulting from lipid raft reorganization at the different experimental conditions used, may contribute to the interaction of the Aβ aggregates with the cell membranes. Indeed, recent evidence suggests that Aβ interacts with the APP present at the cell surface and acts as a ligand of its own precursor, resulting in a cell death-related signal [411].

One leading hypothesis of the molecular basis of amyloid toxicity claims that single misfolded molecules or a subpopulation of prefibrillar aggregates interacts with the cell membrane disassembling the lipid bilayer [242]; the resulting impairment of membrane permeability would then lead to an imbalance of ion homeostasis [390]. In the present study, confocal microscope images with the fluorescent probe calcein show a rapid fluorescence signal decay in FAD fibroblasts, suggesting the presence of a fluorescent dye leakage invoked by an increase in membrane permeability induced by Aβ42 aggregates. Notably, enrichment in membrane cholesterol reduced the calcein fluorescence decay induced by Aβ42, supporting a major role of cholesterol in aggregate recruitment to the cell membrane. Moreover, our confocal images reveal that in FAD fibroblasts exposed to Aβ42 aggregates an early and sharp increase of free cytosolic Ca^{2+} does occur. Actually, our cholesterol-poor fibroblasts displayed a prompt and enhanced Ca^{2+} increase upon aggregate binding to the cell membrane respect to control cells, whereas cholesterol-enriched fibroblasts displayed slower and reduced Aβ42 aggregate binding to the plasma membrane resulting in a delayed and substantially reduced rise of free Ca^{2+} content respect to control cells.

The relevance of these finding is stressed by the well known association between alterations of intracellular free Ca^{2+} and either oxidative stress [412] and cell death [413]. Oxidative stress has largely been implicated as a major cause of neurotoxicity in AD and there is strong evidence linking lipid peroxidation and amyloid plaques within the AD brain [196, 198, 392, 414]. Oxidative damage, possibly induced by Aβ, may further exacerbate Aβ toxicity by modulating the Aβ amyloid pathway [120]. Indeed, Aβ is reported to accumulate faster in membranes containing oxidatively damaged phospholipids than in membranes containing only unoxidized or saturated phospholipids [415]. A previous study showed a marked increase in oxidation levels of lipids and proteins in peripheral cells from FAD patients [210]. Moreover, amyloid oligomers can readily insert into oxidative-damaged APPV717I fibroblasts where the membrane integrity is compromised [205]. The early appearance of amyloid aggregates bounded to fibroblast surfaces therefore suggests that these species are the main source of oxidative stress for cells. Actually, cholesterol poor cells displayed a prompt and enhanced ROS increase upon aggregate binding to the cell membrane with respect to control fibroblasts with basal membrane cholesterol content. Conversely, membrane

cholesterol enrichment resulted in a delayed and significantly reduced rise of ROS production in the affected PS-1 and APP fibroblasts exposed to Aβ aggregates. In these cellular models the protective role of membrane cholesterol against amyloid oxidative damage seem particularly hopeful. This approach allows to study the potential defensive role of a mild membrane cholesterol enrichment against Aβ-induced cytotoxicity in living cells having a genetic drawback in tissues where AD lesions occur. Indeed, mutated fibroblasts displayed a lower level of basal ROS scavengers, thus suggesting that a modified redox status is a common feature of cells carrying these genetic lesions. This evidence could reflect chronic exposure to an oxidizing environment in mutated fibroblasts with a continuous over-production of amyloid peptide. Several studies provide evidence for excess lipoperoxidation and protein oxidation associated with Aβ deposits in APP and PS-1 AD brain and mutant mice [196, 394]. Accordingly, the reported confocal microscopy images and the quantitative analysis of 8-OH isoprostane levels show that Aβ42 aggregates added to the cell culture media induce a more extensive lipoperoxidation and membrane oxidative injury in APP than in PS-1 mutated fibroblasts. Nevertheless, cholesterol-enriched FAD fibroblasts appear more resistant to amyloid oxidative attack with respect to control cells with basal membrane cholesterol. On the other hand, membrane cholesterol depletion strongly exacerbates Aβ-induced lipid peroxidation. These results therefore suggest that membrane cholesterol content negatively correlates with lipoperoxidant effects on polyunsaturated fatty acids in cell membrane phospholipids induced by Aβ42 oligomers. Membrane cholesterol enrichment cannot completely revert Aβ42 oxidative damage in APP mutated fibroblasts, suggesting that other important factors are involved in Aβ42 aggregate binding to cell membranes. Previous findings provided compelling evidence that mutated fibroblasts bearing increased membrane lipoperoxidation are more susceptible to aggregate binding to the plasma membrane and to the resulting amyloid toxicity [205].

This study indicates that membrane cholesterol can readily modulate FAD fibroblast sensitivity to Aβ-induced oxidative attack. In particular, membrane cholesterol enrichment resulted in almost complete recovery of mitochondrial function and in a significant reduction of LDH release into the culture media of exposed FAD fibroblasts according to previous data on SH-SY5Y cells, PC12 cells and rat embryo cortical

neurons [186, 242, 256]. On the other hand, cell sensitivity to the cytotoxic effect of Aβ42 aggregates was significantly enhanced by low cholesterol levels. Remarkably, amylin treatment of low cholesterol fibroblasts affects cell viability resembling Aβ42 outcome. These data suggest that the modification of membrane cholesterol is generally able to modulate the toxic effect of amyloidogenic peptides independently from their amino acid sequence. Moreover, these data are consistent with increasing evidence that oligomeric aggregates, compared to mature fibrils, are likely the more toxic species of amyloid peptides [40, 58, 205]. Therefore, it can be concluded that the presence of β-sheet structure seems to be stringent for the membrane perturbing properties of Aβ oligomers. A moderate, but significant increase of cell resistance to fibril toxicity in fibroblasts with higher membrane cholesterol is likely to be the result of binding inhibition of minute amounts of residual prefibrillar aggregates, although a specific modulation of the toxic effect of the fibrils cannot be ruled out. It has recently been shown that seladin-1 gene, whose proteic product catalyzes the last steps of cholesterol biosynthesis [416], appears to be down-regulated in brain areas affected by AD [265]. Recent findings also indicate that seladin-1-induced membrane cholesterol enrichment protects SH-SY5Y cells against amyloid toxicity by reducing the interaction of Aβ42 oligomer with cell membrane, featuring seladin-1 as a susceptibility gene candidate for sporadic AD [266]. In this view one might propose that, by modulating the membrane fluidity, plasma membrane cholesterol content may specifically influence APP processing and Aβ production as well as the insertion of soluble Aβ in the phospholipid bilayer and its properties to disturb the membrane structure which ultimately trigger cell death.

Lipid rafts are primary targets of amyloid oxidative attack on plasma membrane

Lipid peroxidation is a major outcome of free radical-mediated injury to brain, where it directly damages membranes and generates a number of oxidized products [417]. In the present study, human SH-SY5Y neuroblastoma cells stably expressing about threefold levels of APP and more than threefold levels of Aβ42 showed a higher membrane lipid peroxidation compared to SY5Y control cells, suggesting a chronic oxidative stressed condition associated with enhanced Aβ production. These findings are in agreement with several studies that provide evidence for excess lipid peroxidation associated with Aβ

deposits in APP and PS-1 AD brain and mutant mice [418]. Oxidative damage may further exacerbate Aβ toxicity. Indeed, Aβ is reported to accumulate faster in membranes containing oxidatively damaged phospholipids than in membranes containing only unoxidized or saturated phospholipids [415]. In particular, a marked increase in lipid peroxidation levels and an early amyloid binding to oxidative-damaged membranes in fibroblasts from FAD patients have been previously shown [205]. In the present study, a higher membrane oxidative-damage resulted in an enhanced ADDL binding to the plasma membrane in neuroblastoma cells overexpressing APPwt and APPV717G as compared to control cells. As recent evidence suggests that Aβ interacts with the APP present at the cell surface and acts as a ligand of its own precursor [411], a minor contribute to Aβ binding could be given by APP over-expression. However, amyloid pick up at the plasma membrane was higher in APPV717G than in APPwt cells, suggesting a causative role for APP mutation in cell surface ability to bind ADDLs. Moreover, DAPT, a specific γ-secretase inhibitor, strongly reduced both the lipid peroxidation levels and the aggregate-binding to plasma membranes of all three clones exposed to ADDLs, excluding the possibility that amyloid pick up at the cell surfaces is merely affected by the APP content. Anyway, the early appearance of amyloid aggregates bounded to cell surfaces suggests a main role for these species in oxidative stress process. Indeed, when Aβ42 aggregates were added to cell culture media, they induced a quick membrane lipid peroxidation in APPwt and APPV717G neuroblastoma clones as well as in APPV717I mutated fibroblasts.

There is a growing consensus that cell surfaces are patchworks of domains, local concentrations of membrane proteins, and lipids quite different from the average for an entire membrane. Cholesterol is likely important in organising some types of domains, usually termed lipid rafts [419]. Increasing data indicate that changes in membrane cholesterol content have regulatory consequences for Aβ interactions with the cell plasma membranes and neurotoxicity [158, 186, 266]. Confocal and cytofluorimetric evidence on neuroblastoma cells, carrying wild-type and V717G mutated APP, supports this hypothesis. Indeed, when ADDLs were added to the culture medium of cells depleted in membrane cholesterol following treatment with mevastatin, the Aβ42 oligomers appeared to accumulate earlier and to a greater extent at the cell plasma membrane. Recent data suggest that cholesterol depletion, dispersing phosphatidylinositol 4,5-bisphosphate from

sites of functional interaction with cell proteins, can alter cell actin organization and inhibit lateral diffusion of membrane proteins [420]. However, it can be excluded that different APP distribution in plasma membrane compartments, likely resulting from lipid raft reorganization in the present experimental conditions, may contribute to Aβ42 binding to the cell membrane. It has recently been reported that Aβ binding and aggregation occurs in lipid raft domains where it is mediated by clusters of the ganglioside GM1 [241, 245]. Confocal laser microscope analysis showed a marked Aβ42-GM1 colocalization on membrane rafts in APPV717I mutated fibroblasts obtained from a FAD patient. Moreover, lipid peroxidation and 8-OH isoprostane quantitative analysis at the raft levels showed that ADDLs induced a more extensive membrane oxidative-injury in APPV717I fibroblasts than in control fibroblasts from a healthy subject. These data are also supported by the evidence that lipid composition can influence ADDL recruitment to raft microdomains on neuroblastoma cells. In particular, cholesterol-depleted membranes displayed enhanced ADDL-GM1 colocalization with respect to control cells, whereas a lower Aβ42 binding to cholesterol-enriched lipid rafts compared to control cells occurred in SY5Y, APPwt and APPV717G cells. Furthermore, the pharmacological interference with lipid raft structure achieved by PDMP, a specific inhibitor of GM1 biosynthesis, prevented Aβ42 incorporation in all clones exposed to ADDLs. Moreover, the anti-GM1 antibody or CTX-B binding to the raft GM1 prevented the amyloid lipid peroxidation process on plasma membrane, suggesting that lipid rafts are specific targets of membrane oxidative injury in APPwt and APPV717G neuroblastoma cells exposed to Aβ42 aggregates. Interestingly, membrane lipid peroxidation positively correlates with the perturbing effects of Aβ42 oligomers on DRMs. Indeed, DRMs purified from APP overexpressing cells were more susceptible to the decrease of fluidity produced by ADDL exposure as compared to rafts purified from control cells. As a consequence, APPwt and APPV717G overexpressing cells were more unsuccessful than SY5Y cells in facing aggregate oxidative injury, resulting in a more significant increase in DRM lipid peroxidation. Moreover, the higher increase in lipid peroxidation levels in DRM compartments than in entire membrane of Alzheimer fibroblasts defines lipid rafts as a preferential site for Aβ aggregate binding to cell surface. These results suggest that the more oxidized the DRMs, the greater its ability to bind specifically ADDLs.

Recent evidence suggest that DRMs differ substantially from lipid rafts [421]. Moreover, membrane microdomains can arrange themselves into larger detergent-resistant membrane during triton treatment. Taking into account these limitations, the present data are consistent with previous reports indicating that ADDLs affect membrane physical features such as fluidity and density of lipid packing, hindering both membrane oxidation and permeabilization [222, 224, 239]. Recent AFM data also showed that treatment of DRMs with ADDLs induced the formation of large steps reflecting differences between the thickness of a standard bilayer and that of a thinner phase [243]. A leading theory on the molecular basis of amyloid toxicity is that pore-like aggregates interact with the cell membranes leading to membrane permeabilization and free Ca^{2+} imbalance [40, 58, 170]. In the present study, confocal microscope images with the fluorescent probe calcein suggest that DRM disturbing properties of ADDLs were associated to the loss of membrane integrity in SY5Y, APP overexpressing cells. The lower calcein loading in APPwt and APPV717G cells compared to SY5Y cells, before exogenously addition of ADDLs, suggests a chronic amyloid-induced membrane damage with a loss of surface integrity and a constant calcein leakage in cell facing a higher Aβ production. Notably, anti-GM1 antibodies and CTX-B binding to raft GM1 reduced the calcein fluorescence decay induced by ADDLs, supporting a major role of lipid rafts in aggregate recruitment to the cell membrane. This finding suggests that these two ligands can prevent raft structure alteration by decreasing the ADDL binding to GM1 amphipathic targets and subsequently disfavouring Aβ42 incorporation into the membrane. Indeed, the partial lipophilic nature of raft GM1 can account for Aβ42 intracellular uptake. We did not investigate in depth, in our cell system, any direct inhibition of GM1 redistribution by CTX-B and anti-GM1 antibodies. However, the addition of stoichiometric amounts of cholera toxin to samples containing ganglioside GM1 seems to produce only a small decrease in the measured diffusion coefficient [422]. This pattern relies on a progressive amplification mechanism of the early reactive free radicals by repeated chain reaction processes in raft lipids consistent with the age dependence of AD. This data identifies lipid rafts as key targets of oxidative damage as a result of their ability to recruit Aβ42 aggregates to the cell surface. Finally, an altered APP processing in Alzheimer's fibroblasts strengthens the claim that the changes

observed could be the direct outcome of the chronic presence of an increased grade of cellular oxidising environment induced by Aβ.

Protective effect of new S-acylglutathione derivatives against amyloid-induced oxidative stress

Reduced levels of GSH in specific regions of the central nervous system and in peripheral cells from AD patients carrying mutations in the APP and PS-1 genes have been described [195, 209, 423]. The alteration of GSH homeostasis impairs neuronal viability, leaving neurons vulnerable to oxidative stress injury. Therefore, therapeutic strategies based on intracellular increase in GSH levels by dietary or pharmacological intake of GSH precursors or substrates for GSH synthesis to protect the brain against oxidative stress have been developed [195]. Because GSH itself poorly penetrates the blood–brain barrier and does not freely cross cellular membranes, other treatment options to increase the brain concentration of GSH, including GSH carriers, analogs, mimetics, or precursors, have been used in patients or animal models [195, 348, 424-426]. Taking into account these considerations, the synthesis of new acyl-SG derivatives able to cross neuronal plasma membranes was designed. In particular, the synthesis of GSH thioesters was performed by reacting the electrophilic species of two active acyl-CoA's (lauroyl-CoA and palmitoleoyl-CoA) with GSH, to form the respective acyl-SG products. According to previously published results, our data show that lauroyl-CoA and palmitoleoyl-CoA, reactive thioester derivatives of lauric and palmitoleic acids, are able to acylate a thiol-containing nucleophile as the free cysteine sulfhydryl group of GSH in vitro [370, 427]. After the one-step procedure of reverse-phase HPLC, the purification yield of acyl-SG was about 10% as indirectly determined by quantitative analysis of the respective GSH release after subjecting these thioesters to acid hydrolysis. No difference in the absorbance values between sample and background readings were observed at time 0 of the hydrolysis reaction, indicating that, under our experimental conditions, the formation of GSH derivatives involves the free thiol group of the GSH cysteine, and not the free amino group of glutamine. The identity and the purity of acyl-SG thioesters were validated by MALDI/TOF analysis. As expected, GSH reacts with lauroyl CoA or palmitoleoyl CoA in a 1:1 ratio. In particular, the molecular weights of conjugates totally match with the hypothesized one,

ruling out the possibility that two equivalent molecules of S-acyl-CoA have reacted simultaneously with the same molecule of GSH, one with the cysteine sulfhydryl group and the other with the glutamyl amino group.

The addition of fatty acyl CoA's at the free thiol group of GSH cysteine represents a useful approach in the production of potential diffusible drugs because of the hydrophobic properties of the aliphatic chains. Here, these compounds acting as GSH carriers allowed GSH to enter the cell and, once internalized in the cytoplasm, to be converted back to the corresponding free fatty acid and GSH by cellular thioesterases. Moreover, the results showed that these compounds possessing long hydrocarbon chains, with or without the presence of a double bond in the structure, do not show exactly the same biological aptitude. Indeed, an increase in antioxidant and neuroprotective effects with the presence of the double bond and the lengthening of the chain occurred. This finding suggests that the double-bond portion and the hydrophobic backbone might be important to this series of compounds for the activity expression, increasing the lipophilicity of the molecules, facilitating diffusibility of these compounds into the cells and allowing the increase of intracellular GSH. Indeed, the partial lipophilic nature of such compounds can account for their intracellular uptake. We did not investigate in depth, in our cell system, whether the direct antioxidant properties of the GSH conjugate's fatty acid counterpart were involved. However, fatty acids could play a key role in maintaining the structural integrity and fluidity of neuronal membranes, which account for neuronal transmission [365].

In the present study, cell culture supplementation with the newly synthesized acyl-SG derivatives protects human SH-SY5Y neuroblastoma cells against Aβ42 aggregate-induced oxidative stress, as shown by a significant increase in cell viability. In particular, pre-treatment of the cells with acyl-SG thioesters caused a significant decrease in intracellular ROS accumulation and in lipid peroxidation by the enhancement of the intracellular antioxidant scavengers. Moreover, the severe oxidative stress in cells after exposure to H_2O_2 was partially reversed by the pre-treatment with acyl-SG thioesters. In particular, cells pre-treated with palmitoleoyl-SG displayed milder and almost completely reversible oxidative stress after exposure to the aggregates and to H_2O_2 than cells pre-treated with lauroyl-SG, which also partially recovered the ability to counteract redox status alteration. Moreover, when Aβ42

aggregates were added to cellular culture media, they induced a quick lipoperoxidation and membrane oxidative injury in APPV717I mutated fibroblasts. These findings on peripheral cells are in agreement with several studies that provide evidence for excess lipoperoxidation and protein oxidation associated with Aβ deposits in APP and PS-1 AD brain and mutant mice [195, 268]. These findings imply a systemic abnormality in FAD that could be important for the use of peripheral cells in preclinical trials of antioxidant drugs. Indeed, Alzheimer fibroblasts seem more resistant to amyloid oxidative attack after pre-treatment with acyl-SG thioesters, as a result of their increase in GSH intracellular levels. In particular, the addition of palmitoleoyl-SG to the APPV717I fibroblast culture medium triggers more extensive and powerful protective effect against lipid peroxidation than lauroyl-SG. These findings provide compelling evidence that cells bearing increased powerful antioxidant capacity are more resistant to aggregate toxicity as a result of their increased ability to counteract amyloid oligomeric attack. We have previously shown that familial Alzheimer fibroblasts exhibited lower levels of GSH and TAC than fibroblasts from healthy subjects [209, 210]. TAC impairment could reflect chronic exposure to an oxidizing environment in mutated fibroblasts with a continuous over-production of amyloid peptide. The daily intake of such thioesters in AD patients could therefore minimize the cytotoxic effects of oxidative stress after neuronal exposure to extracellular amyloid plaques. GSH was found in eukaryotic cells at millimolar concentrations. A moderate increase in intracellular GSH levels in pre-treated Alzheimer fibroblasts strengthens the claim that the changes observed could be the direct outcome of the chronic presence of a reduced grade of cellular oxidizing environment induced by micromolar concentrations of acyl-SG thioesters. This encourages to provide for further studies aimed at addressing the potential role of acyl-SG thioesters versus amyloid aggregates in other experimental in vivo models.

Several studies suggest that cell death associated with protein aggregates begins with stimulation of the apoptotic response, although recent data show necrotic rather than apoptotic death in some cases [157, 402]. Because the involvement of caspases has been proposed in amyloid-induced apoptosis in cultured neurons [428], I also investigated the activation of caspase-3/CPP32. Accordingly, caspase-3 levels were significantly increased in Aβ42-treated cells. On the other hand, cells pre-treated with acyl-SG

thioesters underwent a significant reduction in caspase-3 activity. Based on these observations, a mechanism was proposed by which acyl-SG thioesters can offer neuronal protection against Aβ42 aggregate toxic insult by increasing the intracellular levels of GSH. Further studies are required to gain insight into the potential use of such acyl-SG thioesters as modulators of Aβ42 cytotoxicity. The trial of these compounds in *in vivo* models could be useful to design therapeutic strategies for AD and other oxidative stress-related diseases.

CONCLUDING REMARKS

Taken together, these results provide information useful to depict a mechanism of cell impairment and death that can be common to prefibrillar aggregates of most peptides and proteins. It apparently starts with aggregate binding to the cell membrane resulting in membrane destabilization and the subsequent early derangement of ion balance and intracellular redox status as key events in targeting exposed cells to apoptotic death.

These results implement the recently published data on the role of a moderate reduction of membrane cholesterol in AD pathogenesis. In particular, they suggest that the extent of amyloid aggregate cytotoxicity depends, among others, by the amount of cholesterol in plasma membrane. By affecting the physical properties of the membrane, at the lipid raft level, cholesterol modulates the interaction and the uptake of the amyloid aggregates into the cell membrane. Therefore, neuronal integrity appears to require the maintenance of a proper steady-state level of brain cholesterol and its reduction can result in severe impairment of cell viability. Indeed, a mild loss of neuronal membrane cholesterol results in a quicker and increased binding of Aβ oligomers to the neuronal membrane with subsequent alteration of Ca^{2+} distribution and cellular redox status eventually leading to cell death. In particular, these data identifies lipid rafts as specific targets of oxidative damage and membrane degeneration as a result of their ability to recruit amyloid aggregates to the cell surface.

Moreover, these results put forward new acyl-SG derivatives as new antioxidants with neuroprotective effect against amyloid-induced oxidative injury. The novel findings propose a useful approach in the production of potential diffusible drugs because of the hydrophobic properties of the acyl-SG thioesters, which can cross the plasmalemma and be trapped intracellularly following hydrolysis, thus releasing the parent carboxylic acid and free GSH. In this view, this study introduce substantial innovations in biochemical analysis and pharmaceutical sector research, with new antioxidant compounds, which could be excellent candidates for therapeutic treatment of AD and other oxidative stress-related diseases.

ABBREVIATIONS

Aβ	Amyloid-β peptide	**Fluo3-AM**	Fluo3-acetoxymethyl ester
Aβ42-FAM	Aβ42 amine-reactive succinimidyl esters of carboxyfluorescein	**G418**	Geneticin
Acyl-SG	S-acyl-glutathione	**GM1**	Monosialotetrahexosylganglioside
AD	Alzheimer's Disease	**GSH**	Glutathione
ADDLs	Amyloid β-Derived Diffusible Ligands	**HBSS**	Hank's Balanced Saline Solution
AFM	Atomic Force Microscopy	**HEPES**	N-(2-hydroxyethyl)piperazine-N'-(2-ethanesulfonic acid)
APOE	Apolipoprotein E	**HFIP**	Hexafluoro-2-isopropanol
APP	Amyloid Precursor Protein	**HPLC**	High-Pressure Liquid Chromatography
β-CD	methyl-β-cyclodextrin	**HypF-N**	N-terminal domain of the prokaryotic hydrogenase maturation factor HypF
BACE	Beta site APP Cleaving Enzyme or β-secretase	**HRP**	Horseradish Peroxidase
BBB	Blood Brain Barrier	**4-HNE**	4-hydroxyalkenals
BODIPY	4,4-difluoro-3',4adiaza-s-indacene	**IAPP**	Islet Amyloid Polypeptide
BSA	Bovine Serum Albumin	**LDH**	Lactate Dehydrogenase
BSTFA	N,O-bis(trimethylsilyl)-trifluoroacetamide	**MALDI/TOF**	Matrix-Assisted Laser Desorption/Ionization Time-Of-Flight
calcein-AM	calcein-acetoxymethyl	**MDA**	Malonaldehyde
CM-H_2, DCFDA	2'-7' dichlorodihydrofluorescein diacetate, acetyl ester	**MTT**	3-(4,5-dimethylthiazol-2-yl)-2,5-diphenyltetrazolium bromide
CNS	Central Nervous System	**MUFA**	Monounsaturated Fatty Acids
CR	Congo Red	**PBS**	Phosphate Buffer Saline
CSF	Cerebro Spinal Fluid	**PDMP**	D-Threo-1-phenyl-2-decanoylamino-3-morpholino-1-propanol
CTX-B	Cholera Toxin subunit B	**PMSF**	Phenylmethylsulphonylfluoride
DAPT	N-[N-(3,5-difluorophenacetyl)-l-alanyl]-S-phenylglycine t-buthyl ester	**PI3-SH3**	SH3 domain from bovine phosphatidyl-inositol-3' –kinase
DMEM	Dulbecco's modified Eagle's medium	**PS-1**	Presenilin-1
DMSO	Dimethylsulfoxide	**PS-2**	Presenilin-2
DPH	1,6-diphenyl-1,3,5-hexatriene	**PUFA**	Polyunsaturated Fatty Acids
DRMs	Detergent-Resistant Membranes	**PVDF**	Polyvinylidene difluoride
ECL	Enhanced Chemiluminescence	**RNS**	Reactive Nitrogen Species
EDTA	Ethylenediaminetetraacetc acid	**ROS**	Reactive Oxygen Species
EGTA	Ethylene glycol-bis(β aminoethylether) N,N,N',N'-tetraacetc acid	**SDS-PAGE**	Sodiumdodecylsulfate Polyacrylamide Gel Electrophoresis
ELISA	Enzyme-linked immunosorbent assay	**SFA**	Saturated Fatty Acids
FAD	Familial Alzheimer's Disease	**TAC**	Total Antioxidant Capacity
FBS	Foetal Bovine Serum	**TEM**	Transmission Electron Microscopy

TFA	Trifluoroacetic acid
TFE	Trifluoroethanol
ThT	Thioflavin T
Vit E	Vitamin E

REFERENCES

1. Dobson, C.M., *Experimental investigation of protein folding and misfolding.* Methods, 2004. **34**(1): p. 4-14.
2. Dobson, C.M., *Protein folding and misfolding.* Nature, 2003. **426**(6968): p. 884-90.
3. Dobson, C.M., Sali, A. and M. Karplus, *Protein folding: A perspective from theory and experiment.* Angew. Chem. Int. Ed. Engl., 1998. **37**: p. 868-893.
4. Plaxco, K.W. and C.M. Dobson, *Time-resolved biophysical methods in the study of protein folding.* Curr Opin Struct Biol, 1996. **6**(5): p. 630-6.
5. Schaeffer, R.D., A. Fersht, and V. Daggett, *Combining experiment and simulation in protein folding: closing the gap for small model systems.* Curr Opin Struct Biol, 2008. **18**(1): p. 4-9.
6. Levinthal, C.J., *Are there pathways for protein folding?* . J. Chem. Phys. , 1968. **65**: p. 44-45.
7. Dobson, C.M., *Principles of protein folding, misfolding and aggregation.* Semin Cell Dev Biol, 2004. **15**(1): p. 3-16.
8. Wolynes, P.G., J.N. Onuchic, and D. Thirumalai, *Navigating the folding routes.* Science, 1995. **267**(5204): p. 1619-20.
9. Dinner, A.R., *et al*., *Understanding protein folding via free-energy surfaces from theory and experiment.* Trends Biochem Sci, 2000. **25**(7): p. 331-9.
10. Fersht, A.R., *Transition-state structure as a unifying basis in protein-folding mechanisms: contact order, chain topology, stability, and the extended nucleus mechanism*. Proc Natl Acad Sci U S A, 2000. **97**(4): p. 1525-9.
11. Jahn, T.R. and S.E. Radford, *The Yin and Yang of protein folding.* FEBS J, 2005. **272**(23): p. 5962-70.
12. Watters, A.L., *et al*., *The highly cooperative folding of small naturally occurring proteins is likely the result of natural selection.* Cell, 2007. **128**(3): p. 613-24.
13. Vendruscolo, M., *et al*., *Structures and relative free energies of partially folded states of proteins.* Proc Natl Acad Sci U S A, 2003. **100**(25): p. 14817-21.
14. Vendruscolo, M., *et al*., *Three key residues form a critical contact network in a protein folding transition state.* Nature, 2001. **409**(6820): p. 641-5.
15. Shea, J.E. and C.L. Brooks, 3rd, *From folding theories to folding proteins: a review and assessment of simulation studies of protein folding and unfolding.* Annu Rev Phys Chem, 2001. **52**: p. 499-535.

16. Makarov, D.E. and K.W. Plaxco, *The topomer search model: A simple, quantitative theory of two-state protein folding kinetics.* Protein Sci, 2003. **12**(1): p. 17-26.
17. Plaxco, K.W., K.T. Simons, and D. Baker, Contact order, transition state placement and the refolding rates of single domain proteins. J Mol Biol, 1998. **277**(4): p. 985-94.
18. Schuler, B., E.A. Lipman, and W.A. Eaton, *Probing the free-energy surface for protein folding with single-molecule fluorescence spectroscopy.* Nature, 2002. **419**(6908): p. 743-7.
19. Cheung, M.S., A.E. Garcia, and J.N. Onuchic, *Protein folding mediated by solvation: water expulsion and formation of the hydrophobic core occur after the structural collapse.* Proc Natl Acad Sci U S A, 2002. **99**(2): p. 685-90.
20. Hardesty, B. and G. Kramer, *Folding of a nascent peptide on the ribosome.* Prog Nucleic Acid Res Mol Biol, 2001. **66**: p. 41-66.
21. Bukau, B. and A.L. Horwich, *The Hsp70 and Hsp60 chaperone machines.* Cell, 1998. **92**(3): p. 351-66.
22. Hartl, F.U. and M. Hayer-Hartl, *Molecular chaperones in the cytosol: from nascent chain to folded protein.* Science, 2002. **295**(5561): p. 1852-8.
23. Schiene, C. and G. Fischer, *Enzymes that catalyse the restructuring of proteins.* Curr Opin Struct Biol, 2000. **10**(1): p. 40-5.
24. Hammond, C. and A. Helenius, *Quality control in the secretory pathway.* Curr Opin Cell Biol, 1995. **7**(4): p. 523-9.
25. Herczenik, E. and M.F. Gebbink, *Molecular and cellular aspects of protein misfolding and disease.* FASEB J, 2008. **22**(7): p. 2115-33.
26. Richardson, J.S. and D.C. Richardson, *Natural beta-sheet proteins use negative design to avoid edge-to-edge aggregation.* Proc Natl Acad Sci U S A, 2002. **99**(5): p. 2754-9.
27. Kelly, J.W., *The alternative conformations of amyloidogenic proteins and their multi-step assembly pathways.* Curr Opin Struct Biol, 1998. **8**(1): p. 101-6.
28. Dobson, C.M., *Protein misfolding, evolution and disease.* Trends Biochem Sci, 1999. **24**(9): p. 329-32.
29. Prakash, S. and A. Matouschek, *Protein unfolding in the cell.* Trends Biochem Sci, 2004. **29**(11): p. 593-600.
30. Horwich, A., *Protein aggregation in disease: a role for folding intermediates forming specific multimeric interactions.* J Clin Invest, 2002. **110**(9): p. 1221-32.
31. Bullock, A.N. and A.R. Fersht, *Rescuing the function of mutant p53.* Nat Rev Cancer, 2001. **1**(1): p. 68-76.

32. Parsell, D.A., *et al*., *Protein disaggregation mediated by heat-shock protein Hsp104.* Nature, 1994. **372**(6505): p. 475-8.
33. Thomas, P.J., B.H. Qu, and P.L. Pedersen, *Defective protein folding as a basis of human disease.* Trends Biochem Sci, 1995. **20**(11): p. 456-9.
34. Dobson, C.M., *The structural basis of protein folding and its links with human disease.* Philos Trans R Soc Lond B Biol Sci, 2001. **356**(1406): p. 133-45.
35. Dobson, C.M., *Getting out of shape.* Nature, 2002. **418**(6899): p. 729-30.
36. Balch, W.E., *et al*., *Adapting proteostasis for disease intervention.* Science, 2008. **319**(5865): p. 916-9.
37. Chiti, F. and C.M. Dobson, *Protein misfolding, functional amyloid, and human disease.* Annu Rev Biochem, 2006. **75**: p. 333-66.
38. Rousseau, F., J. Schymkowitz, and L. Serrano, *Protein aggregation and amyloidosis: confusion of the kinds?* Curr Opin Struct Biol, 2006. **16**(1): p. 118-26.
39. Huang, T.H., *et al*., *Alternate aggregation pathways of the Alzheimer beta-amyloid peptide. An in vitro model of preamyloid.* J Biol Chem, 2000. **275**(46): p. 36436-40
40. Stefani, M. and C.M. Dobson, *Protein aggregation and aggregate toxicity: new insights into protein folding, misfolding diseases and biological evolution.* J Mol Med, 2003. **81**(11): p. 678-99.
41. Westermark, P., *et al*., *Amyloid: toward terminology clarification. Report from the Nomenclature Committee of the International Society of Amyloidosis.* Amyloid, 2005. **12**(1): p. 1-4.
42. Sunde, M. and C. Blake, *The structure of amyloid fibrils by electron microscopy and X-ray diffraction.* Adv Protein Chem, 1997. **50**: p. 123-59.
43. Serpell, L.C., *et al*., *The protofilament substructure of amyloid fibrils.* J Mol Biol, 2000. **300**(5): p. 1033-9.
44. Bauer, H.H., *et al*., *Architecture and polymorphism of fibrillar supramolecular assemblies produced by in vitro aggregation of human calcitonin.* J Struct Biol, 1995. **115**(1): p. 1-15.
45. Saiki, M., *et al*., *Higher-order molecular packing in amyloid-like fibrils constructed with linear arrangements of hydrophobic and hydrogen-bonding side-chains.* J Mol Biol, 2005. **348**(4): p. 983-98.
46. Jimenez, J.L., *et al*., *Cryo-electron microscopy structure of an SH3 amyloid fibril and model of the molecular packing.* EMBO J, 1999. **18**(4): p. 815-21.
47. Bousset, L., *et al*., *Structural characterization of the fibrillar form of the yeast Saccharomyces cerevisiae prion Ure2p.* Biochemistry, 2004. **43**(17): p. 5022-32.

48. Chamberlain, A.K., *et al*., *Ultrastructural organization of amyloid fibrils by atomic force microscopy*. Biophys J, 2000. **79**(6): p. 3282-93.
49. Jimenez, J.L., *et al*., *The protofilament structure of insulin amyloid fibrils.* Proc Natl Acad Sci U S A, 2002. **99**(14): p. 9196-201.
50. Fandrich, M. and C.M. Dobson, *The behaviour of polyamino acids reveals an inverse side chain effect in amyloid structure formation.* EMBO J, 2002. **21**(21): p. 5682-90.
51. Baldwin, R.L., *Protein folding. Matching speed and stability.* Nature, 1994. **369**(6477): p. 183-4.
52. Chayen, N.E., *Methods for separating nucleation and growth in protein crystallisation.* Prog Biophys Mol Biol, 2005. **88**(3): p. 329-37.
53. Bitan, G., *et al*., *Amyloid beta -protein (Abeta) assembly: Abeta 40 and Abeta 42 oligomerize through distinct pathways.* Proc Natl Acad Sci U S A, 2003. **100**(1): p. 330-5.
54. Lambert, M.P., *et al*., *Diffusible, nonfibrillar ligands derived from Abeta1-42 are potent central nervous system neurotoxins.* Proc Natl Acad Sci U S A, 1998. **95**(11): p. 6448-53.
55. Walsh, D.M., *et al*., *Amyloid beta-protein fibrillogenesis. Structure and biological activity of protofibrillar intermediates.* J Biol Chem, 1999. **274**(36): p. 25945-52.
56. Kayed, R., *et al*., *Common structure of soluble amyloid oligomers implies common mechanism of pathogenesis.* Science, 2003. **300**(5618): p. 486-9.
57. Conway, K.A., *et al*., *Acceleration of oligomerization, not fibrillization, is a shared property of both alpha-synuclein mutations linked to early-onset Parkinson's disease: implications for pathogenesis and therapy.* Proc Natl Acad Sci U S A, 2000. **97**(2): p. 571-6.
58. Kayed, R., *et al*., *Permeabilization of lipid bilayers is a common conformation-dependent activity of soluble amyloid oligomers in protein misfolding diseases.* J Biol Chem, 2004. **279**(45): p. 46363-6.
59. Ionescu-Zanetti, C., *et al*., *Monitoring the assembly of Ig light-chain amyloid fibrils by atomic force microscopy.* Proc Natl Acad Sci U S A, 1999. **96**(23): p. 13175-9.
60. Quintas, A., *et al*., *Tetramer dissociation and monomer partial unfolding precedes protofibril formation in amyloidogenic transthyretin variants.* J Biol Chem, 2001. **276**(29): p. 27207-13.
61. Relini, A., *et al*., *Monitoring the process of HypF fibrillization and liposome permeabilization by protofibrils.* J Mol Biol, 2004. **338**(5): p. 943-57.

62. Campioni, S., *et al*., *Conformational properties of the aggregation precursor state of HypF-N.* J Mol Biol, 2008. **379**(3): p. 554-67.
63. Plakoutsi, G., *et al*., *Aggregation of the Acylphosphatase from Sulfolobus solfataricus: the folded and partially unfolded states can both be precursors for amyloid formation.* J Biol Chem, 2004. **279**(14): p. 14111-9.
64. Bader, R., *et al*., *Probing the mechanism of amyloidogenesis through a tandem repeat of the PI3-SH3 domain suggests a generic model for protein aggregation and fibril formation.* J Mol Biol, 2006. **356**(1): p. 189-208.
65. Guijarro, J.I., *et al*., *Amyloid fibril formation by an SH3 domain.* Proc Natl Acad Sci U S A, 1998. **95**(8): p. 4224-8.
66. Chiti, F., *et al*., *Solution conditions can promote formation of either amyloid protofilaments or mature fibrils from the HypF N-terminal domain.* Protein Sci, 2001. **10**(12): p. 2541-7.
67. Pedersen, J.S., *et al*., *Sulfates dramatically stabilize a salt-dependent type of glucagon fibrils.* Biophys J, 2006. **90**(11): p. 4181-94.
68. Tjernberg, L., *et al*., *Charge attraction and beta propensity are necessary for amyloid fibril formation from tetrapeptides.* J Biol Chem, 2002. **277**(45): p. 43243-6.
69. Bucciantini, M., *et al*., *Inherent toxicity of aggregates implies a common mechanism for protein misfolding diseases.* Nature, 2002. **416**(6880): p. 507-11.
70. Jahn, T.R. and S.E. Radford, *Folding versus aggregation: polypeptide conformations on competing pathways.* Arch Biochem Biophys, 2008. **469**(1): p. 100-17.
71. Chiti, F. and C.M. Dobson, *Amyloid formation by globular proteins under native conditions.* Nat Chem Biol, 2009. **5**(1): p. 15-22.
72. Chiti, F., *et al*., *Rationalization of the effects of mutations on peptide and protein aggregation rates.* Nature, 2003. **424**(6950): p. 805-8.
73. McLean, C.A., *et al*., *Soluble pool of Abeta amyloid as a determinant of severity of neurodegeneration in Alzheimer's disease.* Ann Neurol, 1999. **46**(6): p. 860-6.
74. Butterfield, D.A., *Proteomics: a new approach to investigate oxidative stress in Alzheimer's disease brain.* Brain Res, 2004. **1000**(1-2): p. 1-7.
75. Sousa, M.M., *et al*., *Deposition of transthyretin in early stages of familial amyloidotic polyneuropathy: evidence for toxicity of nonfibrillar aggregates.* Am J Pathol, 2001. **159**(6): p. 1993-2000.
76. Hartley, D.M., *et al*., *Protofibrillar intermediates of amyloid beta-protein induce acute electrophysiological changes and progressive neurotoxicity in cortical neurons.* J Neurosci, 1999. **19**(20): p. 8876-84.

77. Larson, J., *et al*., *Alterations in synaptic transmission and long-term potentiation in hippocampal slices from young and aged PDAPP mice.* Brain Res, 1999. **840**(1-2): p. 23-35.
78. Lin, H., R. Bhatia, and R. Lal, *Amyloid beta protein forms ion channels: implications for Alzheimer's disease pathophysiology.* FASEB J, 2001. **15**(13): p. 2433-44.
79. Ding, T.T., *et al*., *Annular alpha-synuclein protofibrils are produced when spherical protofibrils are incubated in solution or bound to brain-derived membranes.* Biochemistry, 2002. **41**(32): p. 10209-17.
80. Zhu, Y.J., H. Lin, and R. Lal, *Fresh and nonfibrillar amyloid beta protein(1-40) induces rapid cellular degeneration in aged human fibroblasts: evidence for AbetaP-channel-mediated cellular toxicity.* FASEB J, 2000. **14**(9): p. 1244-54.
81. Morishima, Y., *et al*., *Beta-amyloid induces neuronal apoptosis via a mechanism that involves the c-Jun N-terminal kinase pathway and the induction of Fas ligand.* J Neurosci, 2001. **21**(19): p. 7551-60.
82. Goldberg, A.L., *Protein degradation and protection against misfolded or damaged proteins.* Nature, 2003. **426**(6968): p. 895-9.
83. Colbeau, A., *et al*., *Rhodobacter capsulatus HypF is involved in regulation of hydrogenase synthesis through the HupUV proteins.* Eur J Biochem, 1998. **251**(1-2): p. 65-71.
84. Nicolet, Y., *et al*., *Desulfovibrio desulfuricans iron hydrogenase: the structure shows unusual coordination to an active site Fe binuclear center.* Structure, 1999. **7**(1): p. 13-23.
85. Paschos, A., R.S. Glass, and A. Bock, *Carbamoylphosphate requirement for synthesis of the active center of [NiFe]-hydrogenases.* FEBS Lett, 2001. **488**(1-2): p. 9-12.
86. Casalot, L. and M. Rousset, *Maturation of the [NiFe] hydrogenases.* Trends Microbiol, 2001. **9**(5): p. 228-37.
87. Stefani, M., N. Taddei, and G. Ramponi, *Insights into acylphosphatase structure and catalytic mechanism.* Cell Mol Life Sci, 1997. **53**(2): p. 141-51.
88. Reissmann, S., *et al*., *Taming of a poison: biosynthesis of the NiFe-hydrogenase cyanide ligands.* Science, 2003. **299**(5609): p. 1067-70.
89. Rosano, C., *et al*., *Crystal structure and anion binding in the prokaryotic hydrogenase maturation factor HypF acylphosphatase-like domain.* J Mol Biol, 2002. **321**(5): p. 785-96.
90. Marcon, G., *et al*., *Amyloid formation from HypF-N under conditions in which the protein is initially in its native state.* J Mol Biol, 2005. **347**(2): p. 323-35.

91. Campioni, S., *et al*., *A causative link between the structure of aberrant protein oligomers and their toxicity.* Nat. Chem. Biol., Published online: 10 January 2010, doi:10.1038/nchembio.283.
92. Canale, C., *et al*., *Natively folded HypF-N and its early amyloid aggregates interact with phospholipid monolayers and destabilize supported phospholipid bilayers.* Biophys J, 2006. **91**(12): p. 4575-88.
93. Bucciantini, M., *et al*., *Patterns of cell death triggered in two different cell lines by HypF-N prefibrillar aggregates.* FASEB J, 2005. **19**(3): p. 437-9.
94. Cecchi, C., *et al*., *Insights into the molecular basis of the differing susceptibility of varying cell types to the toxicity of amyloid aggregates.* J Cell Sci, 2005. **118**(Pt 15): p. 3459-70.
95. Cecchi, C., *et al*., *Differing molecular mechanisms appear to underlie early toxicity of prefibrillar HypF-N aggregates to different cell types.* FEBS J, 2006. **273**(10): p. 2206-22.
96. Cecchi, C., *et al*., *Differentiation increases the resistance of neuronal cells to amyloid toxicity.* Neurochem Res, 2008. **33**(12): p. 2516-31.
97. Pellistri, F., *et al*., *Nonspecific interaction of prefibrillar amyloid aggregates with glutamatergic receptors results in Ca2+ increase in primary neuronal cells.* J Biol Chem, 2008. **283**(44): p. 29950-60.
98. Baglioni, S., *et al*., *Prefibrillar amyloid aggregates could be generic toxins in higher organisms.* J Neurosci, 2006. **26**(31): p. 8160-7.
99. Petkova, A.T., *et al*., *Self-propagating, molecular-level polymorphism in Alzheimer's beta-amyloid fibrils.* Science, 2005. **307**(5707): p. 262-5.
100. Lee, S., E.J. Fernandez, and T.A. Good, *Role of aggregation conditions in structure, stability, and toxicity of intermediates in the Abeta fibril formation pathway.* Protein Sci, 2007. **16**(4): p. 723-32.
101. Kayed, R., *et al*., *Annular protofibrils are a structurally and functionally distinct type of amyloid oligomer.* J Biol Chem, 2009. **284**(7): p. 4230-7.
102. Hung, L.W., *et al*., *Amyloid-beta peptide (Abeta) neurotoxicity is modulated by the rate of peptide aggregation: Abeta dimers and trimers correlate with neurotoxicity.* J Neurosci, 2008. **28**(46): p. 11950-8.
103. Kremer, J.J., *et al*., *Correlation of beta-amyloid aggregate size and hydrophobicity with decreased bilayer fluidity of model membranes.* Biochemistry, 2000. **39**(33): p. 10309-18.

104. Oma, Y., *et al*., *Comparative analysis of the cytotoxicity of homopolymeric amino acids.* Biochim Biophys Acta, 2005. **1748**(2): p. 174-9.
105. Cheon, M., *et al*., *Structural reorganisation and potential toxicity of oligomeric species formed during the assembly of amyloid fibrils.* PLoS Comput Biol, 2007. **3**(9): p. 1727-38.
106. Katzman, R., *Alzheimer's disease.* N Engl J Med, 1986. **314**(15): p. 964-73.
107. Sheng, J.G., R.E. Mrak, and W.S. Griffin, *Neuritic plaque evolution in Alzheimer's disease is accompanied by transition of activated microglia from primed to enlarged to phagocytic forms.* Acta Neuropathol, 1997. **94**(1): p. 1-5.
108. Metuzals, J., V. Montpetit, and D.F. Clapin, *Organization of the neurofilamentous network.* Cell Tissue Res, 1981. **214**(3): p. 455-82.
109. Kosik, K.S., C.L. Joachim, and D.J. Selkoe, *Microtubule-associated protein tau (tau) is a major antigenic component of paired helical filaments in Alzheimer disease.* Proc Natl Acad Sci U S A, 1986. **83**(11): p. 4044-8.
110. Iqbal, K., *et al*., *Alzheimer paired helical filaments. Restoration of the biological activity by dephosphorylation.* FEBS Lett, 1994. **349**(1): p. 104-8.
111. Patrick, G.N., *et al*., *Conversion of p35 to p25 deregulates Cdk5 activity and promotes neurodegeneration.* Nature, 1999. **402**(6762): p. 615-22.
112. Vincent, I., *et al*., *Aberrant expression of mitotic cdc2/cyclin B1 kinase in degenerating neurons of Alzheimer's disease brain.* J Neurosci, 1997. **17**(10): p. 3588-98.
113. Cruz, J.C., *et al*., *Aberrant Cdk5 activation by p25 triggers pathological events leading to neurodegeneration and neurofibrillary tangles.* Neuron, 2003. **40**(3): p. 471-83.
114. Braak, E., H. Braak, and E.M. Mandelkow, *A sequence of cytoskeleton changes related to the formation of neurofibrillary tangles and neuropil threads.* Acta Neuropathol, 1994. **87**(6): p. 554-67.
115. Goedert, M., *Filamentous nerve cell inclusions in neurodegenerative diseases: tauopathies and alpha-synucleinopathies.* Philos Trans R Soc Lond B Biol Sci, 1999. **354**(1386): p. 1101-18.
116. Nunan, J. and D.H. Small, *Proteolytic processing of the amyloid-beta protein precursor of Alzheimer's disease.* Essays Biochem, 2002. **38**: p. 37-49.
117. Hardy, J. and D.J. Selkoe, *The amyloid hypothesis of Alzheimer's disease: progress and problems on the road to therapeutics.* Science, 2002. **297**(5580): p. 353-6.
118. Tomic, J.L., *et al*., *Soluble fibrillar oligomer levels are elevated in Alzheimer's disease brain and correlate with cognitive dysfunction.* Neurobiol Dis, 2009. **35**(3): p. 352-8.

119. Selkoe, D.J., *Cell biology of the amyloid beta-protein precursor and the mechanism of Alzheimer's disease.* Annu Rev Cell Biol, 1994. **10**: p. 373-403.
120. Crouch, P.J., *et al.*, *Mechanisms of A beta mediated neurodegeneration in Alzheimer's disease.* Int J Biochem Cell Biol, 2008. **40**(2): p. 181-98.
121. Takeda, K., W. Araki, and T. Tabira, *Enhanced generation of intracellular Abeta42 amyloid peptide by mutation of presenilins PS1 and PS2.* Eur J Neurosci, 2004. **19**(2): p. 258-264.
122. Hardy, J., *Amyloid, the presenilins and Alzheimer's disease.* Trends Neurosci, 1997. **20**(4): p. 154-9.
123. De Strooper, B., *et al.*, *Deficiency of presenilin-1 inhibits the normal cleavage of amyloid precursor protein.* Nature, 1998. **391**(6665): p. 387-90.
124. Cruts, M. and C. Van Broeckhoven, *Molecular genetics of Alzheimer's disease.* Ann Med, 1998. **30**(6): p. 560-5.
125. Steiner, H., *et al.*, *Genes and mechanisms involved in beta-amyloid generation and Alzheimer's disease.* Eur Arch Psychiatry Clin Neurosci, 1999. **249**(6): p. 266-70.
126. Sherrington, R., *et al.*, *Cloning of a gene bearing missense mutations in early-onset familial Alzheimer's disease.* Nature, 1995. **375**(6534): p. 754-60.
127. Mattson, M.P., *Cellular actions of beta-amyloid precursor protein and its soluble and fibrillogenic derivatives.* Physiol Rev, 1997. **77**(4): p. 1081-132.
128. Abad-Rodriguez, J., *et al.*, *Neuronal membrane cholesterol loss enhances amyloid peptide generation.* J Cell Biol, 2004. **167**(5): p. 953-60.
129. Crameri, A., *et al.*, *The role of seladin-1/DHCR24 in cholesterol biosynthesis, APP processing and Abeta generation in vivo.* EMBO J, 2006. **25**(2): p. 432-43.
130. Gandhi, S., L.M. Refolo, and K. Sambamurti, *Amyloid precursor protein compartmentalization restricts beta-amyloid production: therapeutic targets based on BACE compartmentalization.* J Mol Neurosci, 2004. **24**(1): p. 137-43.
131. Kojro, E., *et al.*, *Low cholesterol stimulates the nonamyloidogenic pathway by its effect on the alpha -secretase ADAM 10.* Proc Natl Acad Sci U S A, 2001. **98**(10): p. 5815-20.
132. Ehehalt, R., *et al.*, *Amyloidogenic processing of the Alzheimer beta-amyloid precursor protein depends on lipid rafts.* J Cell Biol, 2003. **160**(1): p. 113-23.
133. Kracun, I., *et al.*, *Brain gangliosides in Alzheimer's disease.* J Hirnforsch, 1990. **31**(6): p. 789-93.
134. Zha, Q., *et al.*, *GM1 ganglioside regulates the proteolysis of amyloid precursor protein.* Mol Psychiatry, 2004. **9**(10): p. 946-52.

135. Lorenzo, A., *et al*., *Amyloid beta interacts with the amyloid precursor protein: a potential toxic mechanism in Alzheimer's disease.* Nat Neurosci, 2000. **3**(5): p. 460-4.
136. Davis-Salinas, J., *et al*., *Amyloid beta-protein induces its own production in cultured degenerating cerebrovascular smooth muscle cells.* J Neurochem, 1995. **65**(2): p. 931-4.
137. Yang, A.J., *et al*., *Intracellular accumulation of insoluble, newly synthesized abetan-42 in amyloid precursor protein-transfected cells that have been treated with Abeta1-42.* J Biol Chem, 1999. **274**(29): p. 20650-6.
138. Nishimura, I., *et al*., *Degeneration in vivo of rat hippocampal neurons by wild-type Alzheimer amyloid precursor protein overexpressed by adenovirus-mediated gene transfer.* J Neurosci, 1998. **18**(7): p. 2387-98.
139. Bursztajn, S., *et al*., *Overexpression in neurons of human presenilin-1 or a presenilin-1 familial Alzheimer disease mutant does not enhance apoptosis.* J Neurosci, 1998. **18**(23): p. 9790-9.
140. Uetsuki, T., *et al*., *Activation of neuronal caspase-3 by intracellular accumulation of wild-type Alzheimer amyloid precursor protein.* J Neurosci, 1999. **19**(16): p. 6955-64.
141. Yamatsuji, T., *et al*., *G protein-mediated neuronal DNA fragmentation induced by familial Alzheimer's disease-associated mutants of APP.* Science, 1996. **272**(5266): p. 1349-52.
142. Esposito, L., *et al*., *Intracellularly generated amyloid-beta peptide counteracts the antiapoptotic function of its precursor protein and primes proapoptotic pathways for activation by other insults in neuroblastoma cells.* J Neurochem, 2004. **91**(6): p. 1260-74.
143. Xu, X., *et al*., *Wild-type but not Alzheimer-mutant amyloid precursor protein confers resistance against p53-mediated apoptosis.* Proc Natl Acad Sci U S A, 1999. **96**(13): p. 7547-52.
144. Gasparini, L., *et al*., *Peripheral markers in testing pathophysiological hypotheses and diagnosing Alzheimer's disease.* FASEB J, 1998. **12**(1): p. 17-34.
145. Steimberg, D., *The Metabolic Basis of Inherited Disease.* McGraw Hill, New York, 1983. **73**: p. 1-747.
146. Peterson, C. and J.E. Goldman, *Alterations in calcium content and biochemical processes in cultured skin fibroblasts from aged and Alzheimer donors.* Proc Natl Acad Sci U S A, 1986. **83**(8): p. 2758-62.

147. Van Huynh, T., *et al*., *Reduced protein kinase C immunoreactivity and altered protein phosphorylation in Alzheimer's disease fibroblasts.* Arch Neurol, 1989. **46**(11): p. 1195-9.
148. Bruel, A., *et al*., *Reduced protein kinase C activity in sporadic Alzheimer's disease fibroblasts.* Neurosci Lett, 1991. **133**(1): p. 89-92.
149. Kim, C.S., *et al*., *Alzheimer and beta-amyloid-treated fibroblasts demonstrate a decrease in a memory-associated GTP-binding protein, Cp20.* Proc Natl Acad Sci U S A, 1995. **92**(7): p. 3060-4.
150. Joachim, C.L., H. Mori, and D.J. Selkoe, *Amyloid beta-protein deposition in tissues other than brain in Alzheimer's disease.* Nature, 1989. **341**(6239): p. 226-30.
151. Rittling, S.R., *et al*., *Expression of cell cycle-dependent genes in young and senescent WI-38 fibroblasts.* Proc Natl Acad Sci U S A, 1986. **83**(10): p. 3316-20.
152. Tesco, G., *et al*., *Growth properties of familial Alzheimer skin fibroblasts during in vitro aging.* Exp Gerontol, 1993. **28**(1): p. 51-8.
153. Adler, M.J., *et al*., *Increased gene expression of Alzheimer disease beta-amyloid precursor protein in senescent cultured fibroblasts.* Proc Natl Acad Sci U S A, 1991. **88**(1): p. 16-20.
154. Ito, E., *et al*., *Internal Ca2+ mobilization is altered in fibroblasts from patients with Alzheimer disease.* Proc Natl Acad Sci U S A, 1994. **91**(2): p. 534-8.
155. Stefani, M., *What the use of disease-unrelated model proteins can tell us about the molecular basis of amyloid aggregation and toxicity.* Ital J Biochem, 2003. **52**(4): p. 162-76.
156. Svanborg, C., *et al*., *HAMLET kills tumor cells by an apoptosis-like mechanism--cellular, molecular, and therapeutic aspects.* Adv Cancer Res, 2003. **88**: p. 1-29.
157. Bucciantini, M., *et al*., *Prefibrillar amyloid protein aggregates share common features of cytotoxicity.* J Biol Chem, 2004. **279**(30): p. 31374-82.
158. Yip, C.M. and J. McLaurin, *Amyloid-beta peptide assembly: a critical step in fibrillogenesis and membrane disruption.* Biophys J, 2001. **80**(3): p. 1359-71.
159. Deshpande, A., *et al*., *Different conformations of amyloid beta induce neurotoxicity by distinct mechanisms in human cortical neurons.* J Neurosci, 2006. **26**(22): p. 6011-8.
160. Demuro, A., *et al*., *Calcium dysregulation and membrane disruption as a ubiquitous neurotoxic mechanism of soluble amyloid oligomers.* J Biol Chem, 2005. **280**(17): p. 17294-300.

161. Glabe, C.G. and R. Kayed, *Common structure and toxic function of amyloid oligomers implies a common mechanism of pathogenesis.* Neurology, 2006. **66**(2 Suppl 1): p. S74-8.
162. Sparr, E., *et al*., *Islet amyloid polypeptide-induced membrane leakage involves uptake of lipids by forming amyloid fibers.* FEBS Lett, 2004. **577**(1-2): p. 117-20.
163. Arispe, N., H.B. Pollard, and E. Rojas, *Giant multilevel cation channels formed by Alzheimer disease amyloid beta-protein [A beta P-(1-40)] in bilayer membranes.* Proc Natl Acad Sci U S A, 1993. **90**(22): p. 10573-7.
164. Eckert, G.P., *et al*., *Cholesterol modulates the membrane-disordering effects of beta-amyloid peptides in the hippocampus: specific changes in Alzheimer's disease.* Dement Geriatr Cogn Disord, 2000. **11**(4): p. 181-6.
165. Walter, M.F., P.E. Mason, and R.P. Mason, *Alzheimer's disease amyloid beta peptide 25-35 inhibits lipid peroxidation as a result of its membrane interactions.* Biochem Biophys Res Commun, 1997. **233**(3): p. 760-4.
166. Martinez-Senac, M.M., Villalaın, J., and Gomez-Fernandez, J. C., Eur. J. Biochem., 1999. **265**: p. 744-753.
167. Ji, S.R., Y. Wu, and S.F. Sui, *Cholesterol is an important factor affecting the membrane insertion of beta-amyloid peptide (A beta 1-40), which may potentially inhibit the fibril formation.* J Biol Chem, 2002. **277**(8): p. 6273-9.
168. McLaurin, J. and A. Chakrabartty, *Characterization of the interactions of Alzheimer beta-amyloid peptides with phospholipid membranes.* Eur J Biochem, 1997. **245**(2): p. 355-63.
169. Wakabayashi, M., *et al*., *GM1 ganglioside-mediated accumulation of amyloid beta-protein on cell membranes.* Biochem Biophys Res Commun, 2005. **328**(4): p. 1019-23.
170. Lal, R., H. Lin, and A.P. Quist, *Amyloid beta ion channel: 3D structure and relevance to amyloid channel paradigm.* Biochim Biophys Acta, 2007. **1768**(8): p. 1966-75.
171. Mattson, M.P., *et al*., *beta-Amyloid peptides destabilize calcium homeostasis and render human cortical neurons vulnerable to excitotoxicity.* J Neurosci, 1992. **12**(2): p. 376-89.
172. Butterfield, D.A., *et al*., *beta-Amyloid peptide free radical fragments initiate synaptosomal lipoperoxidation in a sequence-specific fashion: implications to Alzheimer's disease.* Biochem Biophys Res Commun, 1994. **200**(2): p. 710-5.
173. Mattson, M.P., *Pathways towards and away from Alzheimer's disease.* Nature, 2004. **430**(7000): p. 631-9.

174. Morgan, D., *et al*., *A beta peptide vaccination prevents memory loss in an animal model of Alzheimer's disease.* Nature, 2000. **408**(6815): p. 982-5.
175. Kuchibhotla, K.V., *et al*., *Abeta plaques lead to aberrant regulation of calcium homeostasis in vivo resulting in structural and functional disruption of neuronal networks.* Neuron, 2008. **59**(2): p. 214-25.
176. Lashuel, H.A., *et al*., *Neurodegenerative disease: amyloid pores from pathogenic mutations.* Nature, 2002. **418**(6895): p. 291.
177. Sokolov, Y., *et al*., *Soluble amyloid oligomers increase bilayer conductance by altering dielectric structure.* J Gen Physiol, 2006. **128**(6): p. 637-47.
178. Domingues, A., *et al*., *Toxicity of beta-amyloid in HEK293 cells expressing NR1/NR2A or NR1/NR2B N-methyl-D-aspartate receptor subunits.* Neurochem Int, 2007. **50**(6): p. 872-80.
179. Snyder, E.M., *et al*., *Regulation of NMDA receptor trafficking by amyloid-beta.* Nat Neurosci, 2005. **8**(8): p. 1051-8.
180. Good, T.A., D.O. Smith, and R.M. Murphy, *Beta-amyloid peptide blocks the fast-inactivating K+ current in rat hippocampal neurons.* Biophys J, 1996. **70**(1): p. 296-304.
181. Silei, V., *et al*., *Activation of microglial cells by PrP and beta-amyloid fragments raises intracellular calcium through L-type voltage sensitive calcium channels.* Brain Res, 1999. **818**(1): p. 168-70.
182. Hou, X., *et al*., *Transthyretin oligomers induce calcium influx via voltage-gated calcium channels.* J Neurochem, 2007. **100**(2): p. 446-57.
183. Ye, C., *et al*., *Amyloid-beta proteins activate Ca(2+)-permeable channels through calcium-sensing receptors.* J Neurosci Res, 1997. **47**(5): p. 547-54.
184. Mirzabekov, T.A., M.C. Lin, and B.L. Kagan, *Pore formation by the cytotoxic islet amyloid peptide amylin.* J Biol Chem, 1996. **271**(4): p. 1988-92.
185. Lin, M.C. and B.L. Kagan, *Electrophysiologic properties of channels induced by Abeta25-35 in planar lipid bilayers.* Peptides, 2002. **23**(7): p. 1215-28.
186. Arispe, N. and M. Doh, *Plasma membrane cholesterol controls the cytotoxicity of Alzheimer's disease AbetaP (1-40) and (1-42) peptides.* FASEB J, 2002. **16**(12): p. 1526-36.
187. Larner, A.J. and M. Doran, *Clinical phenotypic heterogeneity of Alzheimer's disease associated with mutations of the presenilin-1 gene.* J Neurol, 2006. **253**(2): p. 139-58.

188. Chan, S.L., *et al*., *Presenilin-1 mutations increase levels of ryanodine receptors and calcium release in PC12 cells and cortical neurons.* J Biol Chem, 2000. **275**(24): p. 18195-200.
189. Green, K.N., *et al*., *SERCA pump activity is physiologically regulated by presenilin and regulates amyloid beta production.* J Cell Biol, 2008. **181**(7): p. 1107-16.
190. Dreses-Werringloer, U., *et al*., *A polymorphism in CALHM1 influences Ca2+ homeostasis, Abeta levels, and Alzheimer's disease risk.* Cell, 2008. **133**(7): p. 1149-61.
191. Chance, B., H. Sies, and A. Boveris, *Hydroperoxide metabolism in mammalian organs.* Physiol Rev, 1979. **59**(3): p. 527-605.
192. Halliwell, B., J.M. Gutteridge, and C.E. Cross, *Free radicals, antioxidants, and human disease: where are we now?* J Lab Clin Med, 1992. **119**(6): p. 598-620
193. Butterfield, D.A., *et al*., *Evidence of oxidative damage in Alzheimer's disease brain: central role for amyloid beta-peptide.* Trends Mol Med, 2001. **7**(12): p. 548-54.
194. Butterfield, D.A. and C.M. Lauderback, *Lipid peroxidation and protein oxidation in Alzheimer's disease brain: potential causes and consequences involving amyloid beta-peptide-associated free radical oxidative stress.* Free Radic Biol Med, 2002. **32**(11): p. 1050-60.
195. Butterfield, D.A., *Amyloid beta-peptide (1-42)-induced oxidative stress and neurotoxicity: implications for neurodegeneration in Alzheimer's disease brain. A review.* Free Radic Res, 2002. **36**(12): p. 1307-13.
196. Canevari, L., A.Y. Abramov, and M.R. Duchen, *Toxicity of amyloid beta peptide: tales of calcium, mitochondria, and oxidative stress.* Neurochem Res, 2004. **29**(3): p. 637-50.
197. Markesbery, W.R. and M.A. Lovell, *Four-hydroxynonenal, a product of lipid peroxidation, is increased in the brain in Alzheimer's disease.* Neurobiol Aging, 1998. **19**(1): p. 33-6.
198. Subbarao, K.V., J.S. Richardson, and L.C. Ang, *Autopsy samples of Alzheimer's cortex show increased peroxidation in vitro.* J Neurochem, 1990. **55**(1): p. 342-5.
199. Hensley, K., *et al*., *A model for beta-amyloid aggregation and neurotoxicity based on free radical generation by the peptide: relevance to Alzheimer disease.* Proc Natl Acad Sci U S A, 1994. **91**(8): p. 3270-4.
200. Smith, M.A., *et al*., *Carbonyl-related posttranslational modification of neurofilament protein in the neurofibrillary pathology of Alzheimer's disease.* J Neurochem, 1995. **64**(6): p. 2660-6.
201. Montine, T.J., *et al*., *Lipid peroxidation in aging brain and Alzheimer's disease.* Free Radic Biol Med, 2002. **33**(5): p. 620-6.

202. Floyd, R.A. and K. Hensley, *Oxidative stress in brain aging. Implications for therapeutics of neurodegenerative diseases.* Neurobiol Aging, 2002. **23**(5): p. 795-807.
203. Mason, R.P., *et al.*, *Alzheimer's disease amyloid beta peptide 25-35 is localized in the membrane hydrocarbon core: x-ray diffraction analysis.* Biochem Biophys Res Commun, 1996. **222**(1): p. 78-82.
204. Mattson, M.P., *et al.*, *beta-Amyloid precursor protein metabolites and loss of neuronal Ca2+ homeostasis in Alzheimer's disease.* Trends Neurosci, 1993. **16**(10): p. 409-14.
205. Cecchi, C., *et al.*, *Increased susceptibility to amyloid toxicity in familial Alzheimer's fibroblasts.* Neurobiol Aging, 2007. **28**(6): p. 863-76.
206. Varadarajan, S., *et al.*, *Review: Alzheimer's amyloid beta-peptide-associated free radical oxidative stress and neurotoxicity.* J Struct Biol, 2000. **130**(2-3): p. 184-208.
207. Butterfield, D.A. and A.I. Bush, *Alzheimer's amyloid beta-peptide (1-42): involvement of methionine residue 35 in the oxidative stress and neurotoxicity properties of this peptide.* Neurobiol Aging, 2004. **25**(5): p. 563-8.
208. Mattson, M.P., *et al.*, *Presenilins, the endoplasmic reticulum, and neuronal apoptosis in Alzheimer's disease.* J Neurochem, 1998. **70**(1): p. 1-14.
209. Cecchi, C., *et al.*, *Gluthatione level is altered in lymphoblasts from patients with familial Alzheimer's disease.* Neurosci Lett, 1999. **275**(2): p. 152-4.
210. Cecchi, C., *et al.*, *Oxidative stress and reduced antioxidant defenses in peripheral cells from familial Alzheimer's patients.* Free Radic Biol Med, 2002. **33**(10): p. 1372-9.
211. Bloch, K.E., *Sterol structure and membrane function.* CRC Crit Rev Biochem, 1983. **14**(1): p. 47-92.
212. Spector, A.A. and M.A. Yorek, *Membrane lipid composition and cellular function.* J Lipid Res, 1985. **26**(9): p. 1015-35.
213. Bastiaanse, E.M., K.M. Hold, and A. Van der Laarse, *The effect of membrane cholesterol content on ion transport processes in plasma membranes.* Cardiovasc Res, 1997. **33**(2): p. 272-83.
214. Herman, G.E., *Disorders of cholesterol biosynthesis: prototypic metabolic malformation syndromes.* Hum Mol Genet, 2003. **12 Spec No 1**: p. R75-88.
215. Pfrieger, F.W., *Cholesterol homeostasis and function in neurons of the central nervous system.* Cell Mol Life Sci, 2003. **60**(6): p. 1158-71.
216. Turley, S.D., *et al.*, *Brain does not utilize low density lipoprotein-cholesterol during fetal and neonatal development in the sheep.* J Lipid Res, 1996. **37**(9): p. 1953-61.
217. Jurevics, H. and P. Morell, *Cholesterol for synthesis of myelin is made locally, not imported into brain.* J Neurochem, 1995. **64**(2): p. 895-901.

218. Mahley, R.W., *Apolipoprotein E: cholesterol transport protein with expanding role in cell biology.* Science, 1988. **240**(4852): p. 622-30.
219. Poirier, J., *Apolipoprotein E and cholesterol metabolism in the pathogenesis and treatment of Alzheimer's disease.* Trends Mol Med, 2003. **9**(3): p. 94-101.
220. Haines, T.H., *Do sterols reduce proton and sodium leaks through lipid bilayers?* Prog Lipid Res, 2001. **40**(4): p. 299-324.
221. Ledesma, M.D. and C.G. Dotti, *Amyloid excess in Alzheimer's disease: what is cholesterol to be blamed for?* FEBS Lett, 2006. **580**(23): p. 5525-32.
222. Allen, J.A., R.A. Halverson-Tamboli, and M.M. Rasenick, *Lipid raft microdomains and neurotransmitter signalling.* Nat Rev Neurosci, 2007. **8**(2): p. 128-40.
223. Morgan, M.J., Y.S. Kim, and Z. Liu, *Lipid rafts and oxidative stress-induced cell death.* Antioxid Redox Signal, 2007. **9**(9): p. 1471-83.
224. Kusumi, A. and K. Suzuki, *Toward understanding the dynamics of membrane-raft-based molecular interactions.* Biochim Biophys Acta, 2005. **1746**(3): p. 234-51.
225. Stefani, M. and G. Liguri, *Cholesterol in Alzheimer's disease: unresolved questions.* Curr Alzheimer Res, 2009. **6**(1): p. 15-29.
226. Kirsch, C., *et al.*, *Brain cholesterol, statins and Alzheimer's Disease.* Pharmacopsychiatry, 2003. **36 Suppl 2**: p. S113-9.
227. Parton, R.G. and A.A. Richards, *Lipid rafts and caveolae as portals for endocytosis: new insights and common mechanisms.* Traffic, 2003. **4**(11): p. 724-38.
228. Mauch, D.H., *et al.*, *CNS synaptogenesis promoted by glia-derived cholesterol.* Science, 2001. **294**(5545): p. 1354-7.
229. Dietschy, J.M. and S.D. Turley, *Thematic review series: brain Lipids. Cholesterol metabolism in the central nervous system during early development and in the mature animal.* J Lipid Res, 2004. **45**(8): p. 1375-97.
230. Yoon, I.S., *et al.*, *Low-density lipoprotein receptor-related protein promotes amyloid precursor protein trafficking to lipid rafts in the endocytic pathway.* FASEB J, 2007. **21**(11): p. 2742-52.
231. Taylor, D.R. and N.M. Hooper, *The prion protein and lipid rafts.* Mol Membr Biol, 2006. **23**(1): p. 89-99.
232. Harris, D.A., *Cellular biology of prion diseases.* Clin Microbiol Rev, 1999. **12**(3): p. 429-44.
233. Sarnataro, D., *et al.*, *PrP(C) association with lipid rafts in the early secretory pathway stabilizes its cellular conformation.* Mol Biol Cell, 2004. **15**(9): p. 4031-42.

234. Kawarabayashi, T., *et al*., *Dimeric amyloid beta protein rapidly accumulates in lipid rafts followed by apolipoprotein E and phosphorylated tau accumulation in the Tg2576 mouse model of Alzheimer's disease.* J Neurosci, 2004. **24**(15): p. 3801-9.
235. Kakio, A., *et al*., *Formation of a membrane-active form of amyloid beta-protein in raft-like model membranes.* Biochem Biophys Res Commun, 2003. **303**(2): p. 514-8.
236. Suzuki, T., *et al*., *Biochemical evidence for localization of AMPA-type glutamate receptor subunits in the dendritic raft.* Brain Res Mol Brain Res, 2001. **89**(1-2): p. 20-8.
237. Besshoh, S., *et al*., *Increased phosphorylation and redistribution of NMDA receptors between synaptic lipid rafts and post-synaptic densities following transient global ischemia in the rat brain.* J Neurochem, 2005. **93**(1): p. 186-94.
238. De Felice, F.G., *et al*., *Abeta oligomers induce neuronal oxidative stress through an N-methyl-D-aspartate receptor-dependent mechanism that is blocked by the Alzheimer drug memantine.* J Biol Chem, 2007. **282**(15): p. 11590-601.
239. Kim, S.I., J.S. Yi, and Y.G. Ko, *Amyloid beta oligomerization is induced by brain lipid rafts.* J Cell Biochem, 2006. **99**(3): p. 878-89.
240. Saavedra, L., *et al*., *Internalization of beta-amyloid peptide by primary neurons in the absence of apolipoprotein E.* J Biol Chem, 2007. **282**(49): p. 35722-32.
241. Williamson, R., *et al., Membrane-bound beta-amyloid oligomers are recruited into lipid rafts by a fyn-dependent mechanism.* FASEB J, 2008. **22**(5): p. 1552-9.
242. Yip, C.M., *et al*., *Cholesterol, a modulator of membrane-associated Abeta-fibrillogenesis and neurotoxicity.* J Mol Biol, 2001. **311**(4): p. 723-34.
243. Cecchi, C., *et al*., *A protective role for lipid raft cholesterol against amyloid-induced membrane damage in human neuroblastoma cells.* Biochim Biophys Acta, 2009. **1788**(10): p. 2204-16.
244. Yanagisawa, K., *Role of gangliosides in Alzheimer's disease.* Biochim Biophys Acta, 2007. **1768**(8): p. 1943-51.
245. Fujita, A., *et al*., *Gangliosides GM1 and GM3 in the living cell membrane form clusters susceptible to cholesterol depletion and chilling.* Mol Biol Cell, 2007. **18**(6): p. 2112-22.
246. Lentz, B.R., *Use of fluorescent probes to monitor molecular order and motions within liposome bilayers.* Chem Phys Lipids, 1993. **64**(1-3): p. 99-116.
247. Lentz, B.R., *Membrane "fluidity" as detected by diphenylhexatriene probes.* Chem Phys Lipids, 1989. **50**: p. 171–190.

248. Kaiser, R.D. and E. London, *Location of diphenylhexatriene (DPH) and its derivatives within membranes: comparison of different fluorescence quenching analyses of membrane depth.* Biochemistry, 1998. **37**(22): p. 8180-90.
249. Eckert, G.P., W.G. Wood, and W.E. Muller, *Membrane disordering effects of beta-amyloid peptides.* Subcell Biochem, 2005. **38**: p. 319-37.
250. Rinia, H.A., *et al.*, *Visualization of highly ordered striated domains induced by transmembrane peptides in supported phosphatidylcholine bilayers.* Biochemistry, 2000. **39**(19): p. 5852-8.
251. Teller, H.V., Waring, A.J., Lehrer, R.I., Harroun, T.A., Weiss, T.M., Yang, L., Huang, H.W., *Membrane thinning effect of the β-sheet antimicrobial peptide protegrin.* Biochemistry, 2000. **39**: p. 139-145.
252. Wolozin, B., *Cholesterol and the biology of Alzheimer's disease.* Neuron, 2004. **41**(1): p. 7-10.
253. Corder, E.H., *et al.*, *Gene dose of apolipoprotein E type 4 allele and the risk of Alzheimer's disease in late onset families.* Science, 1993. **261**(5123): p. 921-3.
254. Tanzi, R.E. and L. Bertram, *New frontiers in Alzheimer's disease genetics.* Neuron, 2001. **32**(2): p. 181-4.
255. Kawahara, M. and Y. Kuroda, *Intracellular calcium changes in neuronal cells induced by Alzheimer's beta-amyloid protein are blocked by estradiol and cholesterol.* Cell Mol Neurobiol, 2001. **21**(1): p. 1-13.
256. Sponne, I., *et al.*, *Membrane cholesterol interferes with neuronal apoptosis induced by soluble oligomers but not fibrils of amyloid-beta peptide.* FASEB J, 2004. **18**(7): p. 836-8.
257. Simons, M., *et al.*, *Cholesterol depletion inhibits the generation of beta-amyloid in hippocampal neurons.* Proc Natl Acad Sci U S A, 1998. **95**(11): p. 6460-4.
258. Fassbender, K., *et al.*, *Simvastatin strongly reduces levels of Alzheimer's disease beta - amyloid peptides Abeta 42 and Abeta 40 in vitro and in vivo.* Proc Natl Acad Sci U S A, 2001. **98**(10): p. 5856-61.
259. Austen, B., G. Christodoulou, and J.E. Terry, *Relation between cholesterol levels, statins and Alzheimer's disease in the human population.* J Nutr Health Aging, 2002. **6**(6): p. 377-82.
260. Shobab, L.A., G.Y. Hsiung, and H.H. Feldman, *Cholesterol in Alzheimer's disease.* Lancet Neurol, 2005. **4**(12): p. 841-52.
261. Vance, J.E., H. Hayashi, and B. Karten, *Cholesterol homeostasis in neurons and glial cells.* Semin Cell Dev Biol, 2005. **16**(2): p. 193-212.

262. Svennerholm, L., *et al*., *Membrane lipids of adult human brain: lipid composition of frontal and temporal lobe in subjects of age 20 to 100 years.* J Neurochem, 1994. **63**(5): p. 1802-11.
263. Svennerholm, L. and C.G. Gottfries, *Membrane lipids, selectively diminished in Alzheimer brains, suggest synapse loss as a primary event in early-onset form (type I) and demyelination in late-onset form (type II).* J Neurochem, 1994. **62**(3): p. 1039-47.
264. Ledesma, M.D. and C.G. Dotti, *The conflicting role of brain cholesterol in Alzheimer's disease: lessons from the brain plasminogen system.* Biochem Soc Symp, 2005(72): p. 129-38.
265. Greeve, I., *et al*., *The human DIMINUTO/DWARF1 homolog seladin-1 confers resistance to Alzheimer's disease-associated neurodegeneration and oxidative stress.* J Neurosci, 2000. **20**(19): p. 7345-52.
266. Cecchi, C., *et al*., *Seladin-1/DHCR24 protects neuroblastoma cells against Abeta toxicity by increasing membrane cholesterol content.* J Cell Mol Med, 2008. **12**(5B): p. 1990-2002.
267. Gutteridge, J.M. and B. Halliwell, *Free radicals and antioxidants in the year 2000. A historical look to the future.* Ann N Y Acad Sci, 2000. **899**: p. 136-47.
268. Schulz, J.B., *et al*., *Glutathione, oxidative stress and neurodegeneration.* Eur J Biochem, 2000. **267**(16): p. 4904-11.
269. DeLeve, L.D. and N. Kaplowitz, *Glutathione metabolism and its role in hepatotoxicity.* Pharmacol Ther, 1991. **52**(3): p. 287-305.
270. Meister, A. and S.S. Tate, *Glutathione and related gamma-glutamyl compounds: biosynthesis and utilization.* Annu Rev Biochem, 1976. **45**: p. 559-604.
271. Meister, A. and M.E. Anderson, *Glutathione.* Annu Rev Biochem, 1983. **52**: p. 711-60.
272. Hinchman, C.A. and N. Ballatori, *Glutathione conjugation and conversion to mercapturic acids can occur as an intrahepatic process.* J Toxicol Environ Health, 1994. **41**(4): p. 387-409.
273. Fridovich, I., *Superoxide dismutases. An adaptation to a paramagnetic gas.* J Biol Chem, 1989. **264**(14): p. 7761-4.
274. Sundquist, A.R. and R.C. Fahey, *Evolution of antioxidant mechanisms: thiol-dependent peroxidases and thioltransferase among procaryotes.* J Mol Evol, 1989. **29**(5): p. 429-35.
275. Wang, W. and N. Ballatori, *Endogenous glutathione conjugates: occurrence and biological functions.* Pharmacol Rev, 1998. **50**(3): p. 335-56.

276. Olney, J.W., *et al*., *L-cysteine, a bicarbonate-sensitive endogenous excitotoxin.* Science, 1990. **248**(4955): p. 596-9.
277. Jakoby, W.B., *The glutathione S-transferases: a group of multifunctional detoxification proteins.* Adv Enzymol Relat Areas Mol Biol, 1978. **46**: p. 383-414.
278. Mannervik, B., *The isoenzymes of glutathione transferase.* Adv Enzymol Relat Areas Mol Biol, 1985. **57**: p. 357-417.
279. Douglas, K.T., *Reactivity of glutathione in model systems for glutathione Stransferases and related enzymes.* In Glutathione Conjugation: Mechanisms and Biological Significance (Sies H and Ketterer B Eds) Academic Press, New York, 1988. p. 1–41.
280. Armstrong, R.N., *Enzyme-catalyzed detoxication reactions: mechanisms and stereochemistry.* CRC Crit Rev Biochem, 1987. **22**(1): p. 39-88.
281. Ballatori, N., *Glutathione mercaptides as transport forms of metals.* Adv Pharmacol, 1994. **27**: p. 271-98.
282. Rannug, U., *Genotoxic effects of 1,2-dibromoethane and 1,2-dichloroethane.* Mutat Res, 1980. **76**(3): p. 269-95.
283. Anders, M.W., A.A. Elfarra, and L.H. Lash, *Cellular effects of reactive intermediates: nephrotoxicity of S-conjugates of amino acids.* Arch Toxicol, 1987. **60**(1-3): p. 103-8.
284. Koob, M. and W. Dekant, *Bioactivation of xenobiotics by formation of toxic glutathione conjugates.* Chem Biol Interact, 1991. **77**(2): p. 107-36.
285. Bains, J.S. and C.A. Shaw, *Neurodegenerative disorders in humans: the role of glutathione in oxidative stress-mediated neuronal death.* Brain Res Brain Res Rev, 1997. **25**(3): p. 335-58.
286. Sohal, R.S. and R. Weindruch, *Oxidative stress, caloric restriction, and aging.* Science, 1996. **273**(5271): p. 59-63.
287. Halliwell, B., *Reactive oxygen species and the central nervous system.* J Neurochem, 1992. **59**(5): p. 1609-23.
288. Mecocci, P., *et al*., *Oxidative damage to mitochondrial DNA shows marked age-dependent increases in human brain.* Ann Neurol, 1993. **34**(4): p. 609-16.
289. Mitchell, J.R., *et al*., *Acetaminophen-induced hepatic necrosis. IV. Protective role of glutathione.* J Pharmacol Exp Ther, 1973. **187**(1): p. 211-7.
290. Ketterer, B., *Protective role of glutathione and glutathione transferases in mutagenesis and carcinogenesis.* Mutat Res, 1988. **202**(2): p. 343-61.
291. Cudkowicz, M.E., *et al*., *The pharmacokinetics and pharmaco-dynamics of Procysteine in amyotrophic lateral sclerosis.* Neurology, 1999. **52**(7): p. 1492-4.

292. Coyle, J.T. and P. Puttfarcken, *Oxidative stress, glutamate, and neurodegenerative disorders.* Science, 1993. **262**(5134): p. 689-95.
293. Meister, A., *On the biochemistry of glutathione.* In: N. Taniguchi, T. Higashi, Y. Sakamoto, A. Meister Eds., Glutathione Centennial: Molecular Perspectives and Clinical Implications, Academic Press, San Diego, 1989. p. 3–21.
294. Lomaestro, B.M. and M. Malone, *Glutathione in health and disease: pharmacotherapeutic issues.* Ann Pharmacother, 1995. **29**(12): p. 1263-73.
295. Varga, V., *et al*., *Glutathione is an endogenous ligand of rat brain N-methyl-D-aspartate (NMDA) and 2-amino-3-hydroxy-5-methyl-4-isoxazolepropionate (AMPA) receptors.* Neurochem Res, 1997. **22**(9): p. 1165-71.
296. Shaw, C.A., B.A. Pasqualotto, and K. Curry, *Glutathione-induced sodium currents in neocortex.* Neuroreport, 1996. **7**(6): p. 1149-52.
297. Harding, J.J., *Free and protein-bound glutathione in normal and cataractous human lenses.* Biochem J, 1970. **117**(5): p. 957-60.
298. Lang, C.A., *et al*., *Low blood glutathione levels in healthy aging adults.* J Lab Clin Med, 1992. **120**(5): p. 720-5.
299. Li, Y., P. Maher, and D. Schubert, *A role for 12-lipoxygenase in nerve cell death caused by glutathione depletion.* Neuron, 1997. **19**(2): p. 453-63.
300. Peuchen, S., *et al*., *Interrelationships between astrocyte function, oxidative stress and antioxidant status within the central nervous system.* Prog Neurobiol, 1997. **52**(4): p. 261-81.
301. Bolanos, J.P., *et al*., *Effect of peroxynitrite on the mitochondrial respiratory chain: differential susceptibility of neurones and astrocytes in primary culture.* J Neurochem, 1995. **64**(5): p. 1965-72.
302. Cooper, A.J.L., *Role of astrocytes in maintaining cerebral glutathione homeostasis and in protecting the brain against xenobiotics and oxidative stress.* In: C.A. Shaw Ed., The Role of Glutathione in the Nervous System, Taylor and Francis, Washington, DC, 1998. p. 91-115.
303. Janaky, R., *et al*., *Glutathione and glutathione derivatives: possible modulators of ionotropic glutamate receptors.* In: C.A. Shaw Ed., Glutathione in the Nervous System, Taylor and Francis, Washington, DC, 1998. p. 163-196.
304. Reed, D.J., *Glutathione: toxicological implications.* Annu Rev Pharmacol Toxicol, 1990. **30**: p. 603-31.

305. Sandri, G., E. Panfili, and L. Ernster, *Hydrogen peroxide production by monoamine oxidase in isolated rat-brain mitochondria: its effect on glutathione levels and Ca2+ efflux.* Biochim Biophys Acta, 1990. **1035**(3): p. 300-5.
306. Heales, S.J., *et al.*, *Depletion of brain glutathione is accompanied by impaired mitochondrial function and decreased N-acetyl aspartate concentration.* Neurochem Res, 1995. **20**(1): p. 31-8.
307. Hjelle, O.P., *et al.*, *Antibodies to glutathione: production, characterization and immunocytochemical application to the central nervous system.* In: C.A. Shaw Ed., Glutathione in the Nervous System, Taylor and Francis, Washington, DC, 1998. p.25-43.
308. Kane, D.J., *et al.*, *Bcl-2 inhibition of neural death: decreased generation of reactive oxygen species.* Science, 1993. **262**(5137): p. 1274-7.
309. Beaver, J.P. and P. Waring, *A decrease in intracellular glutathione concentration precedes the onset of apoptosis in murine thymocytes.* Eur J Cell Biol, 1995. **68**(1): p. 47-54.
310. Wullner, U., *et al.*, *Glutathione depletion and neuronal cell death: the role of reactive oxygen intermediates and mitochondrial function.* Brain Res, 1999. **826**(1): p. 53-62.
311. Meister, A., *Glutathione-ascorbic acid antioxidant system in animals.* J Biol Chem, 1994. **269**(13): p. 9397-400.
312. Jain, A., *et al.*, *Glutathione deficiency leads to mitochondrial damage in brain.* Proc Natl Acad Sci U S A, 1991. **88**(5): p. 1913-7.
313. Aksenov, M.Y. and W.R. Markesbery, *Changes in thiol content and expression of glutathione redox system genes in the hippocampus and cerebellum in Alzheimer's disease.* Neurosci Lett, 2001. **302**(2-3): p. 141-5.
314. Apelt, J., *et al.*, *Aging-related increase in oxidative stress correlates with developmental pattern of beta-secretase activity and beta-amyloid plaque formation in transgenic Tg2576 mice with Alzheimer-like pathology.* Int J Dev Neurosci, 2004. **22**(7): p. 475-84.
315. White, A.R., *et al.*, *Exacerbation of copper toxicity in primary neuronal cultures depleted of cellular glutathione.* J Neurochem, 1999. **72**(5): p. 2092-8.
316. Woltjer, R.L., *et al.*, *Role of glutathione in intracellular amyloid-alpha precursor protein/carboxy-terminal fragment aggregation and associated cytotoxicity.* J Neurochem, 2005. **93**(4): p. 1047-56.
317. Harding, J.J., R. Blakytny, and E. Ganea, *Glutathione in disease.* Biochem Soc Trans, 1996. **24**(3): p. 881-4.

318. Sechi, G., *et al*., *Reduced intravenous glutathione in the treatment of early Parkinson's disease.* Prog Neuropsychopharmacol Biol Psychiatry, 1996. **20**(7): p. 1159-70.
319. Yamamoto, M., *et al*., *Protective actions of YM737, a new glutathione analog, against cerebral ischemia in rats.* Res Commun Chem Pathol Pharmacol, 1993. **81**(2): p. 221-32.
320. Butterfield, D.A., and Stadtman, E.R., *Protein oxidation processes in aging brain.* Adv. Cell Aging Gerontol, 1997. **2**: p.161–191.
321. Butterfield, D.A., *et al*., *Free radical oxidation of brain proteins in accelerated senescence and its modulation by N-tert-butyl-alpha-phenylnitrone.* Proc Natl Acad Sci U S A, 1997. **94**(2): p. 674-8.
322. Sano, M., *et al*., *A controlled trial of selegiline, alpha-tocopherol, or both as treatment for Alzheimer's disease. The Alzheimer's Disease Cooperative Study.* N Engl J Med, 1997. **336**(17): p. 1216-22.
323. Lovell, M.A., *et al*., *Elevated thiobarbituric acid-reactive substances and antioxidant enzyme activity in the brain in Alzheimer's disease.* Neurology, 1995. **45**(8): p. 1594-601.
324. Perry, T.L., *et al*., *Amino acids, glutathione, and glutathione transferase activity in the brains of patients with Alzheimer's disease.* Ann Neurol, 1987. **21**(4): p. 331-6.
325. Aksenov, M.Y., *et al*., *The expression of key oxidative stress-handling genes in different brain regions in Alzheimer's disease.* J Mol Neurosci, 1998. **11**(2): p. 151-64.
326. Benzi, G. and A. Moretti, *Age- and peroxidative stress-related modifications of the cerebral enzymatic activities linked to mitochondria and the glutathione system.* Free Radic Biol Med, 1995. **19**(1): p. 77-101.
327. Lovell, M.A., C. Xie, and W.R. Markesbery, *Decreased glutathione transferase activity in brain and ventricular fluid in Alzheimer's disease.* Neurology, 1998. **51**(6): p. 1562-6.
328. Markesbery, W.R., *Oxidative stress hypothesis in Alzheimer's disease.* Free Radic Biol Med, 1997. **23**(1): p. 134-47.
329. Lesne, S., *et al*., *A specific amyloid-beta protein assembly in the brain impairs memory.* Nature, 2006. **440**(7082): p. 352-7.
330. Sayre, L.M., *et al*., *4-Hydroxynonenal-derived advanced lipid peroxidation end products are increased in Alzheimer's disease.* J Neurochem, 1997. **68**(5): p. 2092-7.
331. Lovell, M.A., C. Xie, and W.R. Markesbery, *Acrolein is increased in Alzheimer's disease brain and is toxic to primary hippocampal cultures.* Neurobiol Aging, 2001. **22**(2): p. 187-94.

332. Montine, T.J., *et al*., *Cerebrospinal fluid F2-isoprostane levels are increased in Alzheimer's disease.* Ann Neurol, 1998. **44**(3): p. 410-3.
333. Mark, R.J., *et al*., *A role for 4-hydroxynonenal, an aldehydic product of lipid peroxidation, in disruption of ion homeostasis and neuronal death induced by amyloid beta-peptide.* J Neurochem, 1997. **68**(1): p. 255-64.
334. Mark, R.J., *et al*., *Amyloid beta-peptide impairs glucose transport in hippocampal and cortical neurons: involvement of membrane lipid peroxidation.* J Neurosci, 1997. **17**(3): p. 1046-54.
335. Hensley, K., *et al*., *Brain regional correspondence between Alzheimer's disease histopathology and biomarkers of protein oxidation.* J Neurochem, 1995. **65**(5): p. 2146-56.
336. Milchak, L.M. and J. Douglas Bricker, *The effects of glutathione and vitamin E on iron toxicity in isolated rat hepatocytes.* Toxicol Lett, 2002. **126**(3): p. 169-77.
337. Deibel, M.A., W.D. Ehmann, and W.R. Markesbery, *Copper, iron, and zinc imbalances in severely degenerated brain regions in Alzheimer's disease: possible relation to oxidative stress.* J Neurol Sci, 1996. **143**(1-2): p. 137-42.
338. Lovell, M.A., *et al*., *Copper, iron and zinc in Alzheimer's disease senile plaques.* J Neurol Sci, 1998. **158**(1): p. 47-52.
339. Cooper, A.J. and B.S. Kristal, *Multiple roles of glutathione in the central nervous system.* Biol Chem, 1997. **378**(8): p. 793-802.
340. Dringen, R., J.M. Gutterer, and J. Hirrlinger, *Glutathione metabolism in brain metabolic interaction between astrocytes and neurons in the defense against reactive oxygen species.* Eur J Biochem, 2000. **267**(16): p. 4912-6.
341. Good, P.F., *et al*., *Evidence of neuronal oxidative damage in Alzheimer's disease.* Am J Pathol, 1996. **149**(1): p. 21-8.
342. Moreira, P.I., *et al*., *Oxidative stress and neurodegeneration.* Ann N Y Acad Sci, 2005. **1043**: p. 545-52.
343. Behl, C., *et al*., *Vitamin E protects nerve cells from amyloid beta protein toxicity.* Biochem Biophys Res Commun, 1992. **186**(2): p. 944-50.
344. Pappolla, M.A., *et al*., *Melatonin prevents death of neuroblastoma cells exposed to the Alzheimer amyloid peptide.* J Neurosci, 1997. **17**(5): p. 1683-90.
345. Smith, J.V. and Y. Luo, *Elevation of oxidative free radicals in Alzheimer's disease models can be attenuated by Ginkgo biloba extract EGb 761.* J Alzheimers Dis, 2003. **5**(4): p. 287-300.

346. Behl, C., *et al*., *Neuroprotection against oxidative stress by estrogens: structure-activity relationship.* Mol Pharmacol, 1997. **51**(4): p. 535-41.
347. Adair, J.C., J.E. Knoefel, and N. Morgan, *Controlled trial of N-acetylcysteine for patients with probable Alzheimer's disease.* Neurology, 2001. **57**(8): p. 1515-7.
348. Halliwell, B., *Role of free radicals in the neurodegenerative diseases: therapeutic implications for antioxidant treatment.* Drugs Aging, 2001. **18**(9): p. 685-716.
349. Butterfield, D., *et al*., *Nutritional approaches to combat oxidative stress in Alzheimer's disease.* J Nutr Biochem, 2002. **13**(8): p. 444.
350. Perluigi, M., *et al*., *In vivo protection by the xanthate tricyclodecan-9-yl-xanthogenate against amyloid beta-peptide (1-42)-induced oxidative stress.* Neuroscience, 2006. **138**(4): p. 1161-70.
351. Henderson, J.T., *et al*., *Reduction of lower motor neuron degeneration in wobbler mice by N-acetyl-L-cysteine.* J Neurosci, 1996. **16**(23): p. 7574-82.
352. Jain, A., *et al*., *L-2-oxothiazolidine-4-carboxylate, a cysteine precursor, stimulates growth and normalizes tissue glutathione concentrations in rats fed a sulfur amino acid-deficient diet.* J Nutr, 1995. **125**(4): p. 851-6.
353. Pileblad, E. and T. Magnusson, *Increase in rat brain glutathione following intracerebroventricular administration of gamma-glutamylcysteine.* Biochem Pharmacol, 1992. **44**(5): p. 895-903.
354. Dringen, R., B. Pfeiffer, and B. Hamprecht, *Synthesis of the antioxidant glutathione in neurons: supply by astrocytes of CysGly as precursor for neuronal glutathione.* J Neurosci, 1999. **19**(2): p. 562-9.
355. Anderson, M.E., *et al*., *Glutathione monoethyl ester: preparation, uptake by tissues, and conversion to glutathione.* Arch Biochem Biophys, 1985. **239**(2): p. 538-48.
356. Anderson, M.F., M. Nilsson, and N.R. Sims, *Glutathione monoethylester prevents mitochondrial glutathione depletion during focal cerebral ischemia.* Neurochem Int, 2004. **44**(3): p. 153-9.
357. Lauderback, C.M., *et al*., *Derivatives of xanthic acid are novel antioxidants: application to synaptosomes.* Free Radic Res, 2003. **37**(4): p. 355-65.
358. Sultana, R., *et al*., *Protective effect of the xanthate, D609, on Alzheimer's amyloid beta-peptide (1-42)-induced oxidative stress in primary neuronal cells.* Free Radic Res, 2004. **38**(5): p. 449-58.
359. Joshi, G., *et al*., *In vivo protection of synaptosomes from oxidative stress mediated by Fe2+/H2O2 or 2,2-azobis-(2-amidinopropane) dihydrochloride by the glutathione*

mimetic tricyclodecan-9-yl-xanthogenate. Free Radic Biol Med, 2005. **38**(8): p. 1023-31.

360. Butterfield, D.A., C.B. Pocernich., and J. Drake, *Elevated Gutathione as a Therapeutic Strategy in Alzheimer's Disease.* Drug Development Research , 2002. **56** p: 428-437.
361. Solfrizzi, V., *et al*., *Dietary fatty acids intake: possible role in cognitive decline and dementia.* Exp Gerontol, 2005. **40**(4): p. 257-70.
362. Kalmijn, S., *et al*., *Dietary intake of fatty acids and fish in relation to cognitive performance at middle age.* Neurology, 2004. **62**(2): p. 275-80.
363. Morris, M.C., *et al*., *Dietary fats and the risk of incident Alzheimer disease.* Arch Neurol, 2003. **60**(2): p. 194-200.
364. Morris, M.C., *et al*., *Consumption of fish and n-3 fatty acids and risk of incident Alzheimer disease.* Arch Neurol, 2003. **60**(7): p. 940-6.
365. Solfrizzi, V., F. Panza, and A. Capurso, *The role of diet in cognitive decline.* J Neural Transm, 2003. **110**(1): p. 95-110.
366. Panza, F., *et al*., *Mediterranean diet and cognitive decline.* Public Health Nutr, 2004. **7**(7): p. 959-63.
367. Favrelere, S., *et al*., *Age-related changes in ethanolamine glycerophospholipid fatty acid levels in rat frontal cortex and hippocampus.* Neurobiol Aging, 2000. **21**(5): p. 653-60.
368. Bourre, J.M., *Roles of unsaturated fatty acids (especially omega-3 fatty acids) in the brain at various ages and during ageing.* J Nutr Health Aging, 2004. **8**(3): p. 163-74.
369. Bourre, J.M., *et al*., *Endogenous synthesis cannot compensate for absence of dietary oleic acid in rats.* J Nutr, 1997. **127**(3): p. 488-93.
370. Shore, L.J., *et al*., *Characterization and formation of the glutathione conjugate of clofibric acid.* Drug Metab Dispos, 1995. **23**(1): p. 119-23.
371. Ellman, G.L., *Tissue sulfhydryl groups.* Arch Biochem Biophys, 1959. **82**(1): p. 70-7.
372. Bulaj, G., T. Kortemme, and D.P. Goldenberg, *Ionization-reactivity relationships for cysteine thiols in polypeptides.* Biochemistry, 1998. **37**(25): p. 8965-72.
373. Simakova, O. and N.J. Arispe, *The cell-selective neurotoxicity of the Alzheimer's Abeta peptide is determined by surface phosphatidylserine and cytosolic ATP levels. Membrane binding is required for Abeta toxicity.* J Neurosci, 2007. **27**(50): p. 13719-29.
374. Lambert, M.P., *et al*., *Vaccination with soluble Abeta oligomers generates toxicity-neutralizing antibodies.* J Neurochem, 2001. **79**(3): p. 595-605.

375. Dahlgren, K.N., *et al*., *Oligomeric and fibrillar species of amyloid-beta peptides differentially affect neuronal viability.* J Biol Chem, 2002. **277**(35): p. 32046-53.
376. American Psychiatric Association, *Diagnostic and Statistical Manual of Mental Disorders*, 4th Ed., Washington DC., 1994.
377. The Dementia Study Group of the Italian Neurological Society, *Guidelines for the diagnosis of dementia and Alzheimer's disease.* Ital. J. Neurol. Sci. 2000. **21**: p. 87–194.
378. Wirths, O., *et al*., *Altered cholesterol metabolism in APP695-transfected neuroblastoma cells.* Brain Res, 2007. **1152**: p. 209-14.
379. Tamboli, I.Y., *et al*., *Inhibition of glycosphingolipid biosynthesis reduces secretion of the beta-amyloid precursor protein and amyloid beta-peptide.* J Biol Chem, 2005. **280**(30): p. 28110-7.
380. Bradford, M.M., *A rapid and sensitive method for the quantitation of microgram quantities of protein utilizing the principle of protein-dye binding.* Anal Biochem, 1976. **72**: p. 248-54.
381. Romiti, E., *et al*., *Localization of neutral ceramidase in caveolin-enriched light membranes of murine endothelial cells.* FEBS Lett, 2001. **506**(2): p. 163-8.
382. Hojjati, M.R. and X.C. Jiang, *Rapid, specific, and sensitive measurements of plasma sphingomyelin and phosphatidylcholine.* J Lipid Res, 2006. **47**(3): p. 673-6.
383. Mohanty, J.G., *et al*., *A highly sensitive fluorescent micro-assay of H2O2 release from activated human leukocytes using a dihydroxyphenoxazine derivative.* J Immunol Methods, 1997. **202**(2): p. 133-41.
384. Amundson, D.M. and M. Zhou, *Fluorometric method for the enzymatic determination of cholesterol.* J Biochem Biophys Methods, 1999. **38**(1): p. 43-52.
385. Datki, Z., *et al*., *In vitro model of neurotoxicity of Abeta 1-42 and neuroprotection by a pentapeptide: irreversible events during the first hour.* Neurobiol Dis, 2004. **17**(3): p. 507-15.
386. Rasband, W.S., *ImageJ*, U. S. National Institutes of Health, Bethesda, Maryland, USA, http://rsb.info.nih.gov/ij/, 1997-2008.
387. Esterbauer, H., R.J. Schaur, and H. Zollner, *Chemistry and biochemistry of 4-hydroxynonenal, malonaldehyde and related aldehydes.* Free Radic Biol Med, 1991. **11**(1): p. 81-128.
388. Naguib, Y.M., *A fluorometric method for measurement of peroxyl radical scavenging activities of lipophilic antioxidants.* Anal Biochem, 1998. **265**(2): p. 290-8.

389. Drummen, G.P., *et al*., *Mass spectrometric characterization of the oxidation of the fluorescent lipid peroxidation reporter molecule C11-BODIPY(581/591).* Free Radic Biol Med, 2004. **36**(12): p. 1635-44.
390. Orrenius, S., B. Zhivotovsky, and P. Nicotera, *Regulation of cell death: the calcium-apoptosis link.* Nat Rev Mol Cell Biol, 2003. **4**(7): p. 552-65.
391. Bojarski, L., J. Herms, and J. Kuznicki, *Calcium dysregulation in Alzheimer's disease.* Neurochem Int, 2008. **52**(4-5): p. 621-33.
392. Lovell, M.A. and W.R. Markesbery, *Amyloid beta peptide, 4-hydroxynonenal and apoptosis.* Curr Alzheimer Res, 2006. **3**(4): p. 359-64.
393. Bokvist, M., *et al*., *Two types of Alzheimer's beta-amyloid (1-40) peptide membrane interactions: aggregation preventing transmembrane anchoring versus accelerated surface fibril formation.* J Mol Biol, 2004. **335**(4): p. 1039-49.
394. Butterfield, D.A., *et al*., *Roles of amyloid beta-peptide-associated oxidative stress and brain protein modifications in the pathogenesis of Alzheimer's disease and mild cognitive impairment.* Free Radic Biol Med, 2007. **43**(5): p. 658-77.
395. Tampellini, D., *et al*., *Internalized antibodies to the Abeta domain of APP reduce neuronal Abeta and protect against synaptic alterations.* J Biol Chem, 2007. **282**(26): p. 18895-906.
396. Riendeau, D. and D. Guertin, *ATP- and coenzyme A-dependent fatty acid incorporation into proteins of cell-free extracts from mouse tissues.* J Biol Chem, 1986. **261**(2): p. 976-81.
397. Bizzozero, O.A., J.F. McGarry, and M.B. Lees, *Autoacylation of myelin proteolipid protein with acyl coenzyme A.* J Biol Chem, 1987. **262**(28): p. 13550-7.
398. Brophy, P.J. and D.E. Vance, *The synthesis and hydrolysis of long-chain fatty acyl-coenzyme A thioesters by soluble and microsomal fractions from the brain of the developing rat.* Biochem J, 1976. **160**(2): p. 247-51.
399. Grand, R.J., *Acylation of viral and eukaryotic proteins.* Biochem J, 1989. **258**(3): p. 625-38.
400. Cotman, C.W., *Apoptosis decision cascades and neuronal degeneration in Alzheimer's disease.* Neurobiol Aging, 1998. **19**(1 Suppl): p. S29-32.
401. Datki, Z., *et al*., *Method for measuring neurotoxicity of aggregating polypeptides with the MTT assay on differentiated neuroblastoma cells.* Brain Res Bull, 2003. **62**(3): p. 223-9.
402. Loo, D.T., *et al*., *Apoptosis is induced by beta-amyloid in cultured central nervous system neurons.* Proc Natl Acad Sci U S A, 1993. **90**(17): p. 7951-5.

403. Velez-Pardo, C., *et al*., *Ultrastructure evidence of necrotic neural cell death in familial Alzheimer's disease brains bearing presenilin-1 E280A mutation.* J Alzheimers Dis, 2001. **3**(4): p. 409-415.
404. Zhang, Y., *et al*., *Selective cytotoxicity of intracellular amyloid beta peptide1-42 through p53 and Bax in cultured primary human neurons.* J Cell Biol, 2002. **156**(3): p. 519-29.
405. Bhagat, Y.A., *et al*., *Evolution of beta-amyloid induced neuropathology: magnetic resonance imaging and anatomical comparisons in the rodent hippocampus.* MAGMA, 2002. **14**(3): p. 223-32.
406. Kranenburg, O., *et al*., *Recombinant endostatin forms amyloid fibrils that bind and are cytotoxic to murine neuroblastoma cells in vitro.* FEBS Lett, 2003. **539**(1-3): p. 149-55.
407. Iijima, K., *et al*., *Dissecting the pathological effects of human Abeta40 and Abeta42 in Drosophila: a potential model for Alzheimer's disease.* Proc Natl Acad Sci U S A, 2004. **101**(17): p. 6623-8.
408. Mazziotti, M. and D.H. Perlmutter, *Resistance to the apoptotic effect of aggregated amyloid-beta peptide in several different cell types including neuronal- and hepatoma-derived cell lines.* Biochem J, 1998. **332 (Pt 2)**: p. 517-24.
409. Zhou, Y. and J.S. Richardson, *Cholesterol protects PC12 cells from beta-amyloid induced calcium disordering and cytotoxicity.* Neuroreport, 1996. **7**(15-17): p. 2487-90.
410. Chochina, S.V., *et al*., *Amyloid beta-peptide1-40 increases neuronal membrane fluidity: role of cholesterol and brain region.* J Lipid Res, 2001. **42**(8): p. 1292-7.
411. Shaked, G.M., *et al*., *Abeta induces cell death by direct interaction with its cognate extracellular domain on APP (APP 597-624).* FASEB J, 2006. **20**(8): p. 1254-6.
412. Ermak, G. and K.J. Davies, *Calcium and oxidative stress: from cell signaling to cell death.* Mol Immunol, 2002. **38**(10): p. 713-21.
413. Mattson, M.P. and S.L. Chan, *Calcium orchestrates apoptosis.* Nat Cell Biol, 2003. **5**(12): p. 1041-3.
414. Squier, T.C., *Oxidative stress and protein aggregation during biological aging.* Exp Gerontol, 2001. **36**(9): p. 1539-50.
415. Murray, I.V., *et al*., *Membrane-mediated amyloidogenesis and the promotion of oxidative lipid damage by amyloid beta proteins.* J Biol Chem, 2007. **282**(13): p. 9335-45.
416. Waterham, H.R., *et al*., *Mutations in the 3beta-hydroxysterol Delta24-reductase gene cause desmosterolosis, an autosomal recessive disorder of cholesterol biosynthesis.* Am J Hum Genet, 2001. **69**(4): p. 685-94.

417. Montine, K.S., *et al.*, *Isoprostanes and related products of lipid peroxidation in neurodegenerative diseases.* Chem Phys Lipids, 2004. **128**(1-2): p. 117-24.
418. Abdul, H.M., *et al.*, *Oxidative damage in brain from human mutant APP/PS-1 double knock-in mice as a function of age.* Free Radic Biol Med, 2008. **45**(10): p. 1420-5.
419. Simons, K. and D. Toomre, *Lipid rafts and signal transduction.* Nat Rev Mol Cell Biol, 2000. **1**(1): p. 31-9.
420. Kwik, J., *et al.*, *Membrane cholesterol, lateral mobility, and the phosphatidylinositol 4,5-bisphosphate-dependent organization of cell actin.* Proc Natl Acad Sci U S A, 2003. **100**(24): p. 13964-9.
421. Lichtenberg, D., F.M. Goni, and H. Heerklotz, *Detergent-resistant membranes should not be identified with membrane rafts.* Trends Biochem Sci, 2005. **30**(8): p. 430-6.
422. Goins, B., *et al.*, *Lateral diffusion of ganglioside GM1 in phospholipid bilayer membranes.* Biophys J, 1986. **49**(4): p. 849-56.
423. Abramov, A.Y., L. Canevari, and M.R. Duchen, *Changes in intracellular calcium and glutathione in astrocytes as the primary mechanism of amyloid neurotoxicity.* J Neurosci, 2003. **23**(12): p. 5088-95.
424. Anderson, M.E. and J.L. Luo, *Glutathione therapy: from prodrugs to genes.* Semin Liver Dis, 1998. **18**(4): p. 415-24.
425. Pocernich, C.B., M. La Fontaine, and D.A. Butterfield, *In-vivo glutathione elevation protects against hydroxyl free radical-induced protein oxidation in rat brain.* Neurochem Int, 2000. **36**(3): p. 185-91.
426. Drake, J., *et al.*, *Elevation of brain glutathione by gamma-glutamylcysteine ethyl ester protects against peroxynitrite-induced oxidative stress.* J Neurosci Res, 2002. **68**(6): p. 776-84.
427. Grillo, M.P. and L.Z. Benet, *Studies on the reactivity of clofibryl-S-acyl-CoA thioester with glutathione in vitro.* Drug Metab Dispos, 2002. **30**(1): p. 55-62.
428. Harada, J. and M. Sugimoto, *Activation of caspase-3 in beta-amyloid-induced apoptosis of cultured rat cortical neurons.* Brain Res, 1999. **842**(2): p. 311-23.